

YGOR JACQUES AGRA BEZERRA DA SILVA

**INFLUENCE OF GEOCHEMICAL SIGNATURE AND MINERALOGY OF
GRANITES ON THE PEDOGENESIS AND GEOCHEMISTRY OF SOILS
ACROSS A CLIMOSEQUENCE**

**Recife-PE
June – 2016**

YGOR JACQUES AGRA BEZERRA DA SILVA

**INFLUENCE OF GEOCHEMICAL SIGNATURE AND MINERALOGY OF
GRANITES ON THE PEDOGENESIS AND GEOCHEMISTRY OF SOILS
ACROSS A CLIMOSEQUENCE**

Adviser: Dr. Clístenes Williams Araújo do Nascimento

Co-advisors: Dr.^a Caroline Miranda Biondi

Dr. Peter Van Straaten

Thesis presented to the Graduate Program in
Soil Science of the Federal Rural University of
Pernambuco, as part of the requirements to
obtain the Doctor Scientiae degree.

Recife-PE

June – 2016

Ficha catalográfica

S586i Silva, Ygor Jacques Agra Bezerra da
Influence of geochemical signature and mineralogy of granites on
the pedogenesis and geochemistry of soils across a climosequence /
Ygor Jacques Agra Bezerra da Silva. – Recife, 2016.
187 f. : il.

Orientador: Clístenes Williams Araújo do Nascimento.
Tese (Doutorado em Ciências do Solo) – Universidade
Federal Rural de Pernambuco. Departamento de Agronomia,
Recife, 2016.

Inclui referências.

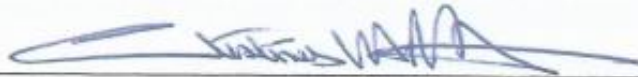
1. Granitic rocks 2. I-type granite 3. S-type granite 4. Chemical
weathering 5. Rare earth elements 6. Soil geochemical
I. Nascimento, Clístenes Williams Araújo do, orientador II. Título

CDD 631.4

YGOR JACQUES AGRA BEZERRA DA SILVA

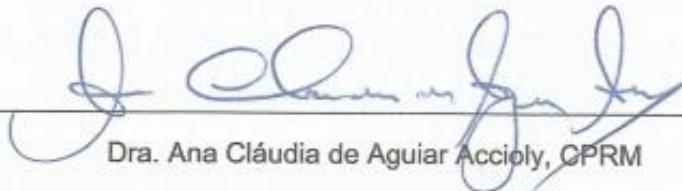
Title **"INFLUENCE OF GEOCHEMICAL SIGNATURE AND MINERALOGY OF GRANITES ON THE PEDOGENESIS AND GEOCHEMISTRY OF SOILS ACROSS A CLIMOSEQUENCE"** a thesis submitted in partial fulfillment of the requirements for the degree of Doctor of Philosophy (Soil Science) at the Federal Rural University of Pernambuco, and approved on June 16, 2016.

Adviser:



Dr. Clístenes Williams Araújo do Nascimento, UFRPE

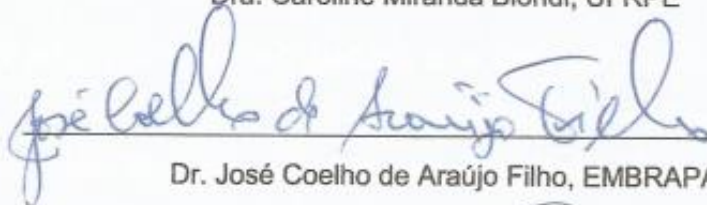
Examiners:



Dra. Ana Cláudia de Aguiar Accioly, CPRM



Dra. Caroline Miranda Biondi, UFRPE



Dr. José Coelho de Araújo Filho, EMBRAPA



Dr. Valdomiro Severino de Souza Júnior, UFRPE

Dear God,

Why do you love me so much? How could I not realize your help from the first day of my thesis? I started as a child that runs without the slightest idea of where he is going, but devoid of any fear, because he felt the presence of his loving and gracious Father very closely! Impossible not to realize that you have prepared someone to help me in all my doubts. Your love is so pure that I feel unworthy of it. None book teaches me as much as your holy scriptures. None of them are resistant to time, and became obsolete, however your words remain forever. Nowadays, I feel a little more prepared and ready to teach your young children.

"If I speak in the tongues of men or of angels, but do not have love, I am only a resounding gong or a clanging cymbal. If I have the gift of prophecy and can fathom all mysteries and all knowledge, and if I have a faith that can move mountains, but do not have love, I am nothing. If I give all I possess to the poor and give over my body to hardship that I may boast, but do not have love, I gain nothing.

Love is patient, love is kind. It does not envy, it does not boast, it is not proud. It does not dishonour others, it is not self-seeking, it is not easily angered, it keeps no record of wrongs. Love does not delight in evil but rejoices with the truth. It always protects, always trusts, always hopes, always perseveres".

1 Corinthians, chapter 13, verses 1 to 8

God, creator of all things

My blessed parents Roberto Jacques and Vilma Agra, for the dedication and
love that taught me to have principles;

To my brothers, Yuri and Rayanna Jacques, for always being by my side
at all times of my life;

My beloved wife, Iracema Jacques, for completing the half that
missing me;

My dear grandmother Zene dos Anjos and aunt Angela Jacques for teaching
me the importance of taking care of our family;

My mother in law Rivânia de Jesus, my father in law Jânio Almeida, and brother
in law Jânio Almeida Filho, for the love that always treated me.

With all my love,

DEDICATE

ACKNOWLEDGEMENTS

It would not have been possible to write this doctoral thesis without the help and protection of God that put kind people around me. It is only possible to mention some of them here.

Thanks to Federal Rural University of Pernambuco by the opportunity of obtaining the Doctor Scientiae degree in the soil science program.

I am very grateful to CNPq, for providing the doctoral scholarship.

I would like to express my special love to my family for the support and encouragement.

I am especially grateful to my adviser Dr. Clistenes Williams Araújo do Nascimento for his supervision, friendship, education and patience. Without his guidance and the foundation laid by their research this thesis would not have been possible.

I wish to extend my sincere appreciation to my co-advisors Dra. Caroline Miranda Biondi and Dr. Peter Van Straaten for the guidance, valuable assistance in the field and help throughout the research.

I am very grateful to Dr. Valdomiro for the valuable time, suggestions and comments to improve my thesis.

I would like to thank Dr. José Coelho for their valuable assistance in the field.

Thanks to Dr. Tiago Osório and Dr. Antônio Carlos for the support in Esalq/USP and valuable suggestions.

I am especially grateful to Prof. José Fernando Wanderley Fernandes Lima (Zeca) for his valuable field support and friendship.

I would like to express gratitude to Dra. Ana Cláudia Aguiar Accioly, Adeilson Alves Wanderley, Dr. Carlos Alberto dos Santos, Dr. Roberto Gusmão de Oliveira, Dra. Vanja Coelho Alcantara and Dr. Vanildo Almeida Mendes from Resources Research Company (CPRM/Brazil), Geological Survey of Brazil, in

Recife- PE for supporting fieldworks and petrographic analysis.

I would like to acknowledge Dr. José Ramon Barros Cantalice for the first internship opportunity and friendship.

I am very grateful to Dra. Sheila Maria Bretas Bittar Schulze for the precious guidance during my graduation and friendship.

Thanks to Professors in the PPGCS represented by Brivaldo Gomes de Almeida, Edivan Rodrigues de Souza, Emídio Cantídio Almeida de Oliveira, Fernando José Freire, Giselle Gomes Monteiro Fracetto, Izabel Cristina de Luna Galindo, Maria Betânia Galvão dos Santos Freire, Mário de Andrade Lira Júnior, Mateus Rosas Ribeiro Filho.

For their friendship, guidance, devotion and patience, I would like to thank Maria do Socorro Santana and Josué Camilo de Melo.

I am especially grateful to Franklone Lima, Rebbeka Galvão and Talmo Henrique for the assistance in the laboratory analyzes and friendship.

My sincere appreciation to Josângela Trezena for the support throughout my thesis

I would like to acknowledge the members of the Environmental Soil Chemistry Group for friendship, constructive discussions and comments.

Thanks to Carina Soares do Nascimento for the support in the scanning electron microscope analyses.

I would like to thank Dr. Jean Cheyson for assistance in the identification of minerals by scanning electron microscope

Last but not least, special thanks go to my friends of the church for the support along the way, especially for your prayers.

Finally, I would like to extend my acknowledgment for all who contributed in several ways toward the success of this Thesis.

Thank you!

CONTENTS

1. GENERAL INTRODUCTION.....	24
2. LITERATURE REVIEW.....	26
2.1. General characterization of physical environment.....	26
2.1.1. Pernambuco State.....	26
2.1.2. Borborema Province.....	27
2.2. Granitic rocks.....	30
2.3. Soil geochemistry of major, trace and rare earth elements.....	31
2.4. Influence of granites on pedogenesis and soil geochemistry.....	34
3. References.....	35
CHAPTER I – WEATHERING RATES AND CARBON STORAGE ALONG A CLIMOSEQUENCE OF SOILS DEVELOPED FROM CONTRASTING GRANITES IN NORTHEAST BRAZIL.....	46
Abstract.....	47
1. Introduction.....	48
2. Materials and methods.....	49
2.1. Study area.....	49
2.2. Soil and rock sampling.....	50
2.3. Rock analysis.....	52
2.4. Soil analysis.....	52
2.4.1. Physical and chemical analysis.....	52
2.4.2. Selective dissolution.....	53
2.4.3. Redness rating index.....	53
2.4.4. Mineralogical analysis.....	53
2.5. Chemical weathering.....	54
3. Results and Discussion.....	54
3.1. Mineralogy of the I- and S-type granites.....	54
3.2. Soil properties.....	58

3.2.1. Morphological, physical and chemical attributes.....	58
3.2.2. Selective dissolution.....	66
3.2.3. Mineralogy.....	66
3.2.3.1. Fine sand and silt fraction.....	66
3.2.3.2. Clay fraction.....	66
3.2.4. Weathering and mineral transformation.....	70
4. Conclusion.....	72
5. References.....	73
 CHAPTER II - GEOCHEMISTRY OF MAJOR AND TRACE ELEMENTS IN SOILS DEVELOPED FROM I- AND S-TYPE GRANITES ACROSS A CLIMOSEQUENCE	
	82
Abstract.....	83
1. Introduction.....	84
2. Materials and methods.....	85
2.1. Study area.....	85
2.2. Soil and rock sampling.....	86
2.3. Analytical methods.....	88
2.3.1. Whole-rock geochemistry analyses.....	88
2.3.2. Soil analyses.....	88
2.3.2.1. Physical and chemical analyses.....	88
2.3.2.2. Major element analyses.....	90
2.3.2.3. Trace element analyses.....	90
2.4. Chemical weathering.....	91
2.5. Enrichment factor.....	91
2.6. Statistical analysis.....	92
3. Results and Discussion.....	93
3.1. Mineralogy of I- and S- type granites.....	93

3.2. Geochemistry of major elements.....	97
3.3. Geochemistry of trace elements.....	101
3.4. Enrichment factor of major elements.....	104
3.5. Enrichment factor of trace elements.....	107
3.6. Geochemistry of soil derived from I- and S-type granites: a multivariate approach	110
4. Conclusions.....	114
5. References.....	115
CHAPTER III - GEOCHEMISTRY OF REE IN I- AND S-TYPE GRANITES	
AND DERIVED SOILS IN THREE CLIMATE ZONES OF NORTHEAST BRAZIL.....	121
Abstract.....	122
1. Introduction.....	123
2. Materials and methods.....	124
2.1. Study area.....	124
2.2. Soil and rock sampling.....	125
2.3. Analytical methods.....	127
2.3.1. Granite analysis.....	127
2.3.2. Soil analyses.....	127
2.3.2.1. Physical and chemical analyses.....	127
2.3.2.2. Rare earth elements analyses.....	129
2.3.2.3. Clay mineralogy analysis.....	130
2.4. Measurements of chemical weathering.....	131
2.5. Statistical analysis.....	131
3. Results.....	131
3.1. Mineralogy of S- and I-type granites.....	131
3.2. Clay mineralogy.....	134
3.3. Geochemistry of REEs in soil profiles.....	137
4. Discussion.....	141
4.1. Geochemistry of REEs in I- and S-type granites.....	141
4.2. Enrichment/depletion of REEs during granite weathering.....	145

4.3. Geochemical signatures of REEs: Climate vs. Parent material.....	148
4.4. REEs as indicator of weathering intensity.....	150
5. Conclusions.....	152
6. References.....	153
CHAPTER IV - EFFECT OF I- AND S-TYPE GRANITE PARENT MATERIAL	
MINERALOGY AND GEOCHEMISTRY ON SOIL FERTILITY: A MULTIVARIATE	
STATISTICAL AND GIS-BASED APPROACH.....	
	161
Abstract.....	162
1. Introduction.....	163
2. Materials and methods.....	164
2.1. Site setting and sampling.....	164
2.2. Granite analysis.....	165
2.3. Soil analysis.....	166
2.4. Quality assurance and quality control.....	167
2.5. Statistical and geographic information system.....	167
3. Results and discussion.....	168
3.1. Mineralogy of S- and I-type granites.....	168
3.2. Geochemistry of I- and S-type granites and corresponding topsoils.....	171
3.3. Physico-chemical properties and soil fertility.....	174
3.4. Multivariate statistical analyses.....	178
3.5. Spatial distribution patterns of soil fertility.....	180
4. Conclusions.....	182
5. References.....	183

LIST OF FIGURES

LITERATURE REVIEW	26
Figure 1. Generalized geological map of western Gondwana showing the distribution of main cratons and Pan-African/Brasiliano belts. Dashed lines are approximate contours of cratons. Cratons are as follows: AM, Amazonian; CC, Congo; SF, São Francisco; and WA, West African. Belts are as follows: AB, Araguaia belt; BB, Brasília belt. Provinces are as follows: BP, Borborema Province; CA, Cameroon province; EN, East Nigerian province; and WN, West Nigerian province. TS is Tuareg shield (Neves, 2003).....	28
Figure 2. Borborema Province major domains according to Van Schmus et al. (2008) and terranes of the Transversal Zone domain: Ceará domain (CE); Médio Coreaú domain (MCD); Pernambuco–Alagoas domain (PEAL); Rio Grande do Norte domain (RGND), (São José do Campestre Archaean nucleus - SJC); Seridó fold belt (SFB); Riacho do Pontal domain (RPD); Sergipano domain (SD), [Macururé (M), Canindé (C), Marancó-Poço Redondo (MPR), Vasa Barris (VB), Estancia (E) - Oliveira et al. (2010); São Francisco craton (SFC), São Luís craton (SLC), Transversal Zone domain(DZT) [Alto Pajeú terrane (APT), Alto Moxoto terrane (AMT), Piancó Alto Brígida terrane(PABT), Cariris Velhos belt (CV), Rio Capibaribe terrane (RCT), São José do Caino terrane (SJCT)]. Faults and shear zones: Patos shear zone (PaSZ), Pernambuco shear zone (PeSZ), São Miguel do Aleixo shear zone (SMASZ); GG-01, location of the sample analysed by SHRIMP from the Transversal Zone domain. Cities and towns: Fortaleza (Fo), Natal (Na), Recife (Re), Salvador (Sa). Inset: general distribution of Brasiliano granites (Silva Filho et al. 2014)	29
CHAPTER I – WEATHERING RATES AND CARBON STORAGE ALONG A CLIMOSEQUENCE OF SOILS DEVELOPED FROM CONTRASTING GRANITES IN NORTHEAST BRAZIL	46
Figure 1. Location of the studied granites, and soil profiles over I-type and S-type granites in three climatic zones of Pernambuco State, Borborema Province, Northeast Brazil.....	51
Figure 2. Macro-photograph (a) and selected petrographic characteristics of S-type granites. (b) General aspect; (c) Biotite and Allanite; (d) Muscovite; (e) Opaque mineral; (f) Orthoclase; (g) Plagioclase; (h) Microcline. Qz– Quartz; Micr – Microcline; Ort – Orthoclase; Bt– Biotite; Pl – Plagioclase; Ms – Muscovite; Al – Allanite.....	55
Figure 3. Macro-photograph (a) and selected petrographic characteristics of I-type granites. (b) General aspect; (c) Mafic minerals; (d) Amphibole; (e) Biotite, apatite and opaque minerals; (f) Titanite, apatite and opaque minerals; (g) Typical section, overview; (h) Allanite. Qz – Quartz; Kfs – K-feldspar; Bt– Biotite; Pl – Plagioclase; Op – Opaque mineral; Al – Allanite.....	57
Figure 4. Relationship between RI and total iron in soils derived from I-type	

granites from the dry to humid zones of Pernambuco State, Northeast Brazil..... 61

Figure 5. Scanning electron microscope (SEM) images captured from minerals in I-type granite and their respective elemental composition by energy dispersive X-ray spectrum (EDS). (a) Chemical composition of magnetite (Spectrum 12: Fe – 97%, Si – 2%, Al – 0.8, K – 0.2%), and biotite (Spectrum 13: Fe – 21%, Si – 38%, Al, K – 15%, Mg – 8%, Ti – 2%, Na – 1%). (b) Chemical composition of biotite (Spectrum 56: Si - 34%, Fe – 24%, Al - 15%, K – 14%, Mg – 9%, Ti – 3%, Na – 1%), biotite (Spectrum 57: Si - 48%, Fe – 21%, Al – 17%, K – 7%, Na – 6%, Ca – 1%), biotite (Spectrum 58: Si – 31%, Fe – 29%, Al, K – 14%, Mg – 8%, Ti – 3%, Na – 1%), ilmenite (Spectrum 60: Ti – 44%, Fe – 41.6%, Mn – 11%, Si – 1.6%, Al - 1%, Na, K – 0.4%) (c) Semiquantitative Fe map from a cross-section of biotite with inclusion of bastnaesite using scanning electron microscope with energy-dispersive X-ray spectroscopy attached facilities (SEM-EDS). Bastnaesite (Spectrum 34: Ce - 32%, La – 20%, F – 13%, Nd – 9%, Ca – 8%, Si, Fe – 5%, Pr – 3%, Al, K – 2%, Mg – 1%), biotite (Spectrum 35: Si – 32%, Fe – 29%, Al – 15%, K – 13%, Mg – 8%, Ti – 2%, Mn – 1%), biotite (Spectrum 36: Si – 33%, Fe – 28%, Al – 16%, K – 13%, Mg – 8%, Ti – 2%)..... 62

Figure 6. Figure 6. X-ray diffraction patterns for fine sand, silt, clay and various clay treatments obtained from diagnostic horizons of soil profiles derived from I-type granites in different climatic zones of Pernambuco State, Northeast Brazil. Diagnostic horizon of the Lixisols (Bt₄) under humid zone (a, b, c, d); Diagnostic horizon of the Regosols (C₂) under sub-humid zone (e, f, g, h); Diagnostic horizon of the Regosols (C₃) under Dry zone (i, j, k, l). Q – Quartz; F – Feldspar; Amp – Amphibole; K – Kaolinite; Gt – Goethite; I – Illite; I / V – Interstratified illite-vermiculite..... 68

Figure 7. X-ray diffraction patterns for fine sand, silt, clay and various clay treatments obtained from diagnostic horizons of soil profiles derived from S-type granites in different climatic zones of Pernambuco State, Northeast Brazil. Diagnostic horizon of the Ferralsols (Bw₂) under humid zone (a, b, c, d); Diagnostic horizon of the Regosols (C₃) under sub-humid zone (e, f, g, h); Diagnostic horizon of the Regosols (C₂) under dry zone (i, j, k, l). Q – Quartz; F – Feldspar; K – Kaolinite; Gb – Gibbsite; I – Illite..... 69

CHAPTER II - GEOCHEMISTRY OF MAJOR AND TRACE ELEMENTS IN SOILS DEVELOPED FROM I- AND S-TYPE GRANITES ACROSS A CLIMOSEQUENCE..... 82

Figure 1. Location of the studied granites, and soil profiles over I-type and S-type granites in three climatic zones of Pernambuco State, Borborema Province, Northeast Brazil..... 87

Figure 2. Petrographic characteristics of I-type granites. (a) General aspect; (b) K-feldspar; (c) Typical section, overview; (d) Amphibole; (e) Opaque mineral; (f) Titanite, apatite and opaque minerals; (g) Quartz; (h) Mafic phase minerals; (i) Apatites associated with mafic minerals; (j) Titanite; (k) Allanite..... 94

Figure 3. Petrographic characteristics of S-type granites. (a) General aspect; (b) Plagioclase; (c) Orthoclase; (d) Microcline; (e) Biotite; (f) Muscovite; (g) Opaque mineral; (h) Allanite; (i) Opaque minerals associated with chlorite; (j) Perthite; (k) Typical section, overview.....	96
---	----

Figure 4. Concentration of major elements in soils derived from I- and S-type granites in three climatic zones of Pernambuco State, Northeast Brazil.....	98
--	----

Figure 5. Scanning electron microscope (SEM) images captured from minerals in I-type granite and their respective elemental composition by energy dispersive X-ray spectrum (EDS). (a) Chemical composition of K-feldspar (Spectrum 9: Si – 56%, K – 23%, Al – 17%, Fe – 2%, Na – 1%, Ba – 1%), magnetite (Spectrum 10: Fe – 97%, Si – 2%, Al – 1%), and Zircon (Spectrum 11: Zr – 41%, Au – 23%, O – 17%, Si – 12%, C – 6.7%, Al – 0.3%), (b) Chemical composition of magnetite (Spectrum 4: Fe – 95%, Si – 3%, Al – 1%, K – 1%), plagioclase (Spectrum 5: Si – 60%, Al – 23%, Na – 10%, Ca – 7%), biotite (Spectrum 6: Si – 30%, Fe – 19%, Al – 14%, Mg – 13%, K – 12%, Au – 10%, Ti – 2%), and quartz (Spectrum 7: Si – 100%).....	99
--	----

Figure 6. Concentration of trace elements in soils derived from I- and S-type granites in three climatic zones of Pernambuco State.....	102
--	-----

Figure 7. Scanning electron microscope (SEM) images captured from minerals in I-type granites and their respective elemental composition by energy dispersive X-ray spectrum (EDS). (a) Chemical composition of Ilmenite: spectrum 52 (Ti – 41%, Fe – 44%, Mn – 7%; Si – 4%, Ca – 2%, Al – 1.5%, K – 0.5%) and spectrum 55 (Fe – 48%, Ti – 43%, Mn – 7%, Si – 1%, Al – 1%) (b) Chemical composition of Plagioclase: spectrum 46 (Si – 57%, Al – 21%, Na – 9%, Ca – 8%, Fe – 3%, K – 2%), and magnetite: spectrum 47 (Fe – 96%, Al – 2%, Si – 2%) and spectrum 48 (Fe – 91%, Si – 4%, Al – 3%, Ti – 1%, Ca – 0.5%, K – 0.5%).....	103
---	-----

Figure 8. Discriminant analysis based on geochemistry of major and trace elements in soils developed on I- and S-type granites from dry to humid zones of Pernambuco State.....	110
--	-----

Figure 9. Loadings of major and trace elements on significant factors for soils derived from I-type granites in three climatic zones of Pernambuco State.....	112
--	-----

Figure 10. Loadings of major and trace elements on significant factors for soils derived from S-type granites in three climatic zones of Pernambuco State.....	113
---	-----

CHAPTER III - GEOCHEMISTRY OF REE IN I- AND S-TYPE GRANITES AND DERIVED SOILS IN THREE CLIMATE ZONES OF NORTHEAST BRAZIL..... 121

Figure 1. Location of the studied granites, and soil profiles over I-type and S-type granites in three climatic zones of Pernambuco State, Borborema Province, Northeast Brazil.....	126
---	-----

Figure 2. Macro-photograph of I- and S-type granites (a, c, respectively) and selected petrographic characteristics. General aspects (b, d, respectively). Mafic	
---	--

minerals of I- and S-type granites (e, f, respectively). Titanite, apatite and opaque minerals (g). Allanite (h). Amphibole (i) Qz – Quartz. Micr – Microcline; Ort – Orthoclase; Bt – Biotite; Pl – Plagioclase; Ms – Muscovite; Om – Opaque minerals Ti – Titanite. Al – Allanite; Amp – Amphibole..... 133

Figure 3. X-ray diffraction patterns for clays obtained from diagnostic horizons of soil profiles derived from I- and S-type granites in different climatic zones of Pernambuco State. Humid zone (a, d); Sub-humid zone (b, e); Dry zone (c, f). Ka – Kaolinite; Gt – Goethite; Il – Illite; Qz – Quartz..... 135

Figure 4. X-ray diffraction patterns for various clay treatments obtained from diagnostic horizons of soil profiles derived from I- and S-type granites in different climatic zones of Pernambuco State. Humid zone (a and d); Sub-humid zone (b and e); Dry zone (c and f). Ka – Kaolinite; Gb – Gibbsite; Il – Illite; Qz – Quartz; Il / Vm - Interstratified illite-vermiculite..... 136

Figure 5. Concentration of REEs in soils derived from I-type granites in three climatic zones of Pernambuco State..... 138

Figure 6. Concentrations of REEs in soils derived from S-type granites in three climatic zones of Pernambuco State..... 140

Figure 7. Rare earth elements in I- and S-type granites normalized to Upper Continental Crust (UCC). UCC values used (Taylor and McLennan 1985) (mg kg⁻¹) La: 30; Ce: 64; Pr: 7.1; Nd: 26; Sm: 4.5; Eu:0.88; Gd: 3.8; Yb: 2.2; Lu: 0.32; Dy: 3.5; Er: 2.3; Ho: 0.8; Tb: 0.64; Tm: 0.33; Y: 22; Sc: 11..... 142

Figure 8. Cross-section of biotite with inclusion of bastnaesite using scanning electron microscope with energy-dispersive X-ray spectroscopy (SEM-EDS) (a): Spectrum 34 (Bastnaesite, Ce – 32%, La – 20%, F – 13%, Nd – 9%, Ca – 8%, Si, Fe – 5%, Pr – 3%, Al, K – 2%, Mg – 1%), spectrum 35 (Biotite, Si – 32%, Fe – 29%, Al – 15%, K – 14%, Mg – 8%, Ti – 1.8%, Mn – 0.2%), spectrum 36 (Biotite, Si – 33%, Fe – 28%, Al – 16%, K – 13%, Mg – 8%, Ti – 2%). Semiquantitative elemental map (b, c, d) from a cross-section of biotite with inclusion of bastnaesite using scanning electron microscope with energy-dispersive X-ray spectroscopy (SEM-EDS) 143

Figure 9. Scanning electron microscope (SEM) image captured from apatite with inclusion of monazite in S-type granite (a) and respective elemental composition by energy dispersive X-ray spectrum (EDS). (b) Cross-section of apatite with inclusion of monazite: spectrum 90 (apatite plus monazite, Ca – 28%, P – 20%, Ce – 15%, Si – 11%, La – 7%, Nd – 5%, Al, K, Th – 4%, Pr – 2%), spectrum 91 (Monazite Ce – 35%, Nd – 19%, La – 15%, Si – 7%, Pr – 6%, Sm – 5%, Al – 3%, K -2%, Ca, Cd - 1%), spectrum 92 (Apatite, Ca – 54%, P – 31%, Ce – 5%, Si, La, Nd – 3%, Al – 1%), spectrum 93 (Monazite, Ce – 33%, Nd – 19%, La – 13%, Si – 9%, Sm, Gd – 7%, Pr – 6%, Al – 3%, K,Th – 2%) (b). Quantitative Ce (c), Nd (d) and P (e) maps from a cross-section of apatite with inclusion of monazite using scanning electron microscope with energy-dispersive X-ray spectroscopy (SEM-EDS) 144

Figure 10. Concentration of REEs in soils profiles derived from I- and S-type granites in three climatic zones of Pernambuco State relative to the concentration of the upper continental crust. UCC values used (Taylor and McLennan 1985) (mg kg-1) La: 30; Ce: 64; Pr: 7.1; Nd: 26; Sm: 4.5; Eu: 0.88; Gd: 3.8; Yb: 2.2; Lu: 0.32; Dy: 3.5; Er: 2.3; Ho: 0.8; Tb: 0.64; Tm: 0.33; Y: 22; Sc: 11..... 146

CHAPTER IV - EFFECT OF I- AND S-TYPE GRANITE PARENT MATERIAL MINERALOGY AND GEOCHEMISTRY ON SOIL FERTILITY: A MULTIVARIATE STATISTICAL AND GIS-BASED APPROACH..... 161

Figure 1. Distribution of soil sampling location over I- and S-type granites from the Borborema Province, Pernambuco State, northeastern Brazil..... 165

Figure 2. (a) Macrophotograph (b) and microphotographs of a typical S-type granite, (c) inclusion of allanite in biotite, (d) microcline, (e) flame perthites, (f) opaque mineral. Bt – Biotite; Qz – Quartz; Micr – Microcline; Ort – Orthoclase; Pl – Plagioclase; Ms – Muscovite; Alb – Albite..... 169

Figure 3. (a) Macrophotograph and (b) Microphotographs of a typical I-type granite. (c) Mafic phase minerals (d) Apatites associated with mafic minerals. (e) Titanite, apatite and opaque mineral phases, (f) typical section, overview. Bt – Biotite; Qz – Quartz; Pl – Plagioclase; Ms – Muscovite; Kfs - K-feldspar; Ep - Epidote..... 171

Figure 4. Scanning electron microscope (SEM) image captured from I-type granites and their respective elemental composition by energy dispersive X-ray spectrum (EDS). (a) Chemical composition of apatite (Spectrum 20: Ca – 67%, P – 29%, Fe – 1%, Si – 1%, Al – 1% K – 1%), magnetite (Spectrum 21: Fe – 98%, Si, Al, Ca – 1%), and zircon (Spectrum 22: Zr – 78%, Si – 20%, Fe – 2%). (b) Chemical composition of magnetite: spectrum 28 (Fe – 98%, Si, Al – 1%) and spectrum 29 (Fe – 98%, Si, Al – 1%); and biotite (Spectrum 30 Si – 33%, Fe – 25%, Al – 16%, K – 13%, Mg - 11%, Ti – 2%)..... 173

Figure 5. Representative X-ray diffraction patterns (Cu K α -radiation) obtained from the two soil types: (a) Topsoil derived from I-type granite, (b) Topsoil derived from S-type granite. Il: illite; Ka: kaolinite. Qz: quartz; Mg gly: Mg glyconated..... 174

Figure 6. Cluster analyses of soils derived from I- and S-type granites in similar climatic zone of Pernambuco State..... 179

Figure 7. Discriminant analysis of the groups formed in cluster analysis..... 180

Figure 8. Digital Terrain Model for available contents of Ca (a), Mg (b), P (c), Mn (d), Ni (f) and Co (g) in soils derived from I- and S-type granites in similar climatic zone of Pernambuco State..... 181

LIST OF TABLES

CHAPTER I – WEATHERING RATES AND CARBON STORAGE ALONG A CLIMOSEQUENCE OF SOILS DEVELOPED FROM CONTRASTING GRANITES IN NORTHEAST BRAZIL.....	46
Table 1. Mineralogical composition (%) of I- and S-type granites in Pernambuco State, Northeast Brazil.....	56
Table 2. Selected macro-morphological and physical characteristics of soil profiles derived from I-type granites in different climatic zones of Pernambuco State, Northeast Brazil.....	59
Table 3. Selected macro-morphological and physical characteristics of soil profiles derived from S-type granites in different climatic zones of Pernambuco State, Northeast Brazil.....	60
Table 4. Chemical characterization, iron selective dissolution analysis and weathering index of soil profiles derived from I-type granites in different climatic zones of Pernambuco State, Northeast Brazil.....	64
Table 5. Chemical characterization, iron selective dissolution analysis and weathering index of soil profiles derived from S-type granites in different climatic zones of Pernambuco State, Northeast Brazil.....	65
CHAPTER II - GEOCHEMISTRY OF MAJOR AND TRACE ELEMENTS IN SOILS DEVELOPED FROM I- AND S-TYPE GRANITES ACROSS A CLIMOSEQUENCE.....	82
Table 1. Selected chemical and physical characteristics of soil profiles derived from I-type granites along a climosequence in Pernambuco state, Brazil Borborema Province.....	89
Table 2. Selected chemical and physical characteristics of soil profiles derived from S-type granites along a climosequence in Pernambuco State, Brazil.....	90
Table 3. Mineralogical composition (%) of I- and S-type granites in Pernambuco State.....	95
Table 4. Enrichment factor (EF) of major and trace elements with respect to the soils derived from I-type granites along a climosequence in Pernambuco State, Brazil.....	106
Table 5. Enrichment factor (EF) of major and trace elements with respect to the soils derived from S-type granites along a climosequence in Pernambuco State, Brazil.....	109

CHAPTER III - GEOCHEMISTRY OF REE IN I- AND S-TYPE GRANITES AND DERIVED SOILS IN THREE CLIMATE ZONES OF NORTHEAST BRAZIL..... 121

Table 1. Selected chemical and physical attributes of soil profiles derived from I-type granites along a climosequence in Pernambuco State, Brazil..... 128

Table 2. Selected chemical and physical attributes of soil profiles derived from S-type granites along a climosequence in Pernambuco State, Brazil..... 129

Table 3. Mineralogical composition (%) of I- and S-type granites in Pernambuco State..... 134

Table 4. Mean Σ LREE, Σ HREE and Σ REE concentrations (mg kg^{-1}) in soil profiles derived from I- and S-type granites in different climatic zones of Pernambuco State, Brazil..... 139

Table 5. Geochemistry of REEs in I- and S-type granites in Pernambuco State, Brazil..... 141

Table 6. Factors controlling REEs behavior during weathering process in three climatic zones of Pernambuco, Brazil..... 149

CHAPTER IV - EFFECT OF I- AND S-TYPE GRANITE PARENT MATERIAL MINERALOGY AND GEOCHEMISTRY ON SOIL FERTILITY: A MULTIVARIATE STATISTICAL AND GIS-BASED APPROACH..... 161

Table 1. Total chemical composition of I- and S-type granites and topsoils overlying both granite types in sub-humid zone of Pernambuco State, Brazil..... 172

Table 2. Mean, maximum and minimum nutrient concentrations, and standard deviation of selected chemical and physical characteristics of soils derived from I- and S-type granites in sub-humid zone of Pernambuco, Brazil..... 177

LIST OF ABBREVIATIONS AND ACRONYMS

ABNT	Associação Brasileira de Normas Técnicas
BD	Bulk Density
BS	Base saturation
CA	Cluster Analysis
CEC	Cation-Exchange Capacity
CIA	Chemical Index of Alteration
CIE	Comission Internationale de I-Eclairage
CPRM	Mineral Resources Research Company
C stocks	Carbon stocks
DA	Discriminant Analysis
DCB	Dithionite-Citrate-Bicarbonate
EDS	Energy Dispersive X-ray Spectrum
EF	Enrichment fator
Embrapa	Empresa Brasileira de Pesquisa Agropecuária
FA	Factor Analysis
Fe _d	Dithionite extractable iron
Fe _o	Oxalate extractable iron
Fe _t	Total iron
GIS	Geographic Information Systems
HCl	Hydrochloric acid
HF	Hydrofluoric acid
HNO ₃	Nitric acid
HREE	Heavy Rare Earth Elements
ICP-OES	Inductively Coupled Plasma Optical Emission Spectroscopy

IDW	Inverse Distance Weighted
INMET	Instituto Nacional de Meteorologia
IPA	Instituto Agronômico de Pernambuco
IUSS	International Union of Soil Sciences
KCl	Potassium chloride
KW	Kilowatt
LREE	Light Rare Earth Elements
NE	Northeast
NIST	National Institute of Standards and
PCA	Principal Component Analysis
pH	Potential hydrogen
r^2	Coefficient of Determination
REE	Rare Earth Elements
RI	Redness Index
SE	Southeast
SEM	Scanning Electron Microscope
SRM	Standard Reference Material
SSSA	Soil Science Society of America
TOC	Total Organic Carbon
UCC	Upper Continental Crust
WDXRF	Wavelength Dispersive X-ray Fluorescence
WRB	World Reference Base for Soil Resources
XRD	X-ray Diffraction
XRF	X-ray fluorescence

ABSTRACT

Ygor Jacques Agra Bezerra da Silva, D. Sc. Federal Rural University of Pernambuco, Recife, June, 2016. Influence of geochemical signature and mineralogy of granites on the pedogenesis and geochemistry of soils across a climosequence. Adviser: Clístenes Williams Araújo do Nascimento.

Granites underlie large land areas and play a key role in global weathering patterns. This study provides insights into the effects of I- and S-type granites on weathering, pedogenesis, mineralogy and soil geochemistry of major, trace and rare earth elements across a climosequence in a tropical environment. We hypothesized that soils derived from I-type granites lead to huge differences in weathering, pedogenesis, mineralogical and geochemical patterns in comparison to those derived from S-type granites. The study was carried out in Borborema Province, NE Brazil, using petrological, mineralogical, geochemical and soil standard analyses; multivariate analysis and geographic information system approaches were used to evaluate such data. In general, results showed that the highest major, trace and rare earth element concentrations in soils derived from I-type granites are related to their higher proportion of accessory minerals: allanite, titanite, apatite, amphibole and opaque minerals. Bastnaesite and monazite seems to be the major sources of rare earth elements in soils derived from I- and S-type granites, respectively. Geophysical field measurements show different magnetic susceptibilities, whereby I-type granites have substantial higher magnetic properties than S-type granites. Soils originated from I-type granites are quantitatively more significant carbon pools. Multivariate statistical techniques are useful to guide and support environmental management decisions not only to understand soils variability but also to contribute to agriculture production and soil-related environmental issues. Spatial distribution maps are suitable for supporting soil fertility management and crop specific fertilization. These results highlight the following issues: i) The importance of detailed characterization of granite types to understand the weathering patterns and carbon stocks in tropical settings; ii) Granitic composition and climate-related weathering processes are soil formation key factors to understanding major, trace and rare earth element distributions in soils; iii) The geologic factor on soil formation cannot be neglected in

climosequence studies aiming to allow the understanding of environmental issues such as pedogenesis, soil geochemistry and carbon stocks. In addition, our findings provide wider implications in large parts of the tropics (S-America, sub-Saharan Africa, India, SE and East Asia, Australia) which are underlying by igneous rock types including I- and S-type granites and where effective management tools are needed to increase nutrient use efficiencies for increased productivity of food, fodder and energy crops.

1. GENERAL INTRODUCTION

Granites are among the most common rock types of the continental crust (Frost et al., 2001). These rocks can present different compositions and originate from diverse petrogenetic processes (Chappell and White, 1974, 1984, 2001). As a result, distinct mineralogical and geochemical rock characteristics have been observed (Clemens, 2003). In order to simplify the subcategories of granites, Chappell and White (1974, 2001) proposed the distinction between I (igneous source) and S (sedimentary source) type granites. This classification scheme has been widely adopted (Almeida et al., 2007; Zhao et al., 2008 ; Antunes et al., 2009 ; Clemens et al., 2011; Chappell et al., 2012; Guani et al., 2013; Guan et al., 2014; Foden et al., 2015; Wang et al., 2015; Yu et al., 2016).

Several studies have addressed the I- and S-type granites genesis, geochemistry and mineralogy (Clemens, 2002; Healy et al., 2004; Farahat et al., 2007; Antunes et al., 2008 ; Canosa et al., 2012; Chappel et al., 2012; Guani et al., 2013; Guan et al., 2014; Foden et al., 2015; Robinson et al., 2015). However few studies have dealt with weathering and pedogenesis from both granite types over the last decades (Gontier et al., 2015; Marechal et al., 2015; Yousefifard et al., 2015). To our knowledge no attempt has been made to elucidate the comparative influence of I- and S-type granites on soil chemical weathering, pedogenesis and soil geochemistry of major, trace and rare earth elements along an environmental gradient.

The Borborema Province, northeastern Brazil, comprises an area of around 380,000 km² (Ferreira et al., 1998), and represents the Western portion of the extensive geologic Brasiliano-Pan African orogenic system formed by a convergence of the West Africa/São Luis and San Francisco-Congo Cratons (Brito Neves, 1975). This strategic position characterizes our studies as transcontinental, with wide implications in large parts of the tropics (S-America, sub-Saharan Africa, India, SE and East Asia, Australia) which underly soils derived from I- and S-type granites. Thus, this study poses relevant data for environmental quality issues in tropical climates, such as weathering patterns, pedogenesis, geochemical cycles, water quality, and carbon storage.

The specific objectives of this work were: (i) to describe the petrography and mineralogy of I- and S-type granites of the Borborema Province, Northeast Brazil; (ii) to address the effect of petrography and mineralogy of I- and S-type granites on weathering and pedogenesis across a climosequence; (iii) to study the effects of granite types and climate on carbon stocks. (IV) to investigate the source and geochemical behavior of major, trace and rare earth elements, and the controlling factors for their soil profile distribution; (V) to evaluate the climosequence influence on soil geochemistry of major, trace and rare earth elements; (VI) to assess the use of multivariate statistical techniques and geographic information system as a tool to support environmental management decisions.

The three climatic zones occurring in Pernambuco State provides an ideal setting to understanding mineral transformations, translocations, and pathways of elements during pedogenesis of soils derived from I- and S-type granites. The geochemical signatures are useful reference values for major, trace and rare earth elements in soils developed from different granite types in a tropical environment, and will provide the basis for practical land use recommendations with regards to micronutrient fertilization and soil fertility management as well as an assessment of the distribution of potentially harmful elements in soils derived from I- and S-type granites.

2. LITERATURE REVIEW

2.1. General characterization of physical environment

2.1.1. Pernambuco State

Pernambuco covers three major physiographic regions named as: Mata, Agreste and Sertão. The Mata zone is located in coastal humid zone, comprising an area of 11,776 km². The Agreste is situated in sub-humid zone. It is a transition zone between Mata and Sertão, covering an area of 17,970 km². Sertão is the largest physiographic region of Pernambuco State, with about 68,535 km² (Brazil, 1973).

The study region is divided into three climatic zones according to Koppen classification (Koppen, 1931). The dry zone presents a semiarid climate (Bsh), characterized by negative water balance, which results from high annual evaporation (2,000 mm year⁻¹) and low precipitation rates (< 800 mm). The mean insolation is 2800 h year⁻¹, and the means annual temperature ranges from 23 to 27 °C (Brito et al., 2007). The sub-humid zone presents a climate classified as Aw, characterized by mean air temperature of about 24 °C, with the annual rainfall ranging from 800 to 1,000 mm. The humid zone presents a tropical climate (Am), characterized by precipitations between 1,000-2,000 mm year⁻¹ (INMET, 2015) and annual average air temperature of 27 °C.

In response to climatic contrasts, vegetation patterns vary with the following units: (i) Dry Zone - Dry deciduous forest (Caatinga); the unique Brazilian biome, equivalent to 11% of the national territory, characterized as being xeric shrubland and thorn forest, which consists primarily of small, thorny trees that shed their leaves seasonally (Souza et al., 2012); (ii) Sub-humid Zone - Semideciduous forest characterized by predominance of hipoxerophilic Caatinga (Drumond et al., 2004); (iii) Humid Zone - Primary evergreen forest (Atlantic rainforest), one of the richest biomes in biodiversity of the world (Thomas et al., 1998).

The geology in Pernambuco is composed dominantly by Precambrian rocks, which comprise 90% of its territory and to a lesser extent by sedimentary basins Paleo/Mesozoic interior and coastal basins Meso/Cenozoic (Brazil, 2001).

The Pernambuco relief presents sedimentary coastal belt, crystalline levels that precede the Borborema highlands, Borborema highlands, peripheral depression of São Francisco River, Jatobá Basin and other sedimentary areas, besides Araripe Plateau (Brazil, 2000).

All soil orders of the Brazilian system of soil classification can be observed in Pernambuco (Santos et al., 2013); this takes place owing to the state wide range in the east-west direction (nearly 700 km), from the most humid regions in the east up to the dry climates in the west. The geomorphology and parent material variations throughout the territory, coupled with climatic contrasts, play a fundamental role in modelling the high soil variability of Pernambuco State (IPA, 2008).

2.1.2. Borborema Province

The Borborema Province (northeastern Brazil), north of the São Francisco craton, comprises an area of around 380,000 km² (Ferreira et al., 1998). This province is surrounded by paleogeographical reconstructions of the western Gondwana supercontinent; it also represents the Western portion of the extensive geologic Brasiliano-Pan African orogenic system formed by a convergence of the West Africa/São Luis and San Francisco-Congo Cratons (Figure 1) (Brito Neves, 1975; Neves et al., 2003). The strategic position of Borborema Province characterizes studies developed in this region as transcontinental with wide implications in large parts of the tropics and sub-tropics.

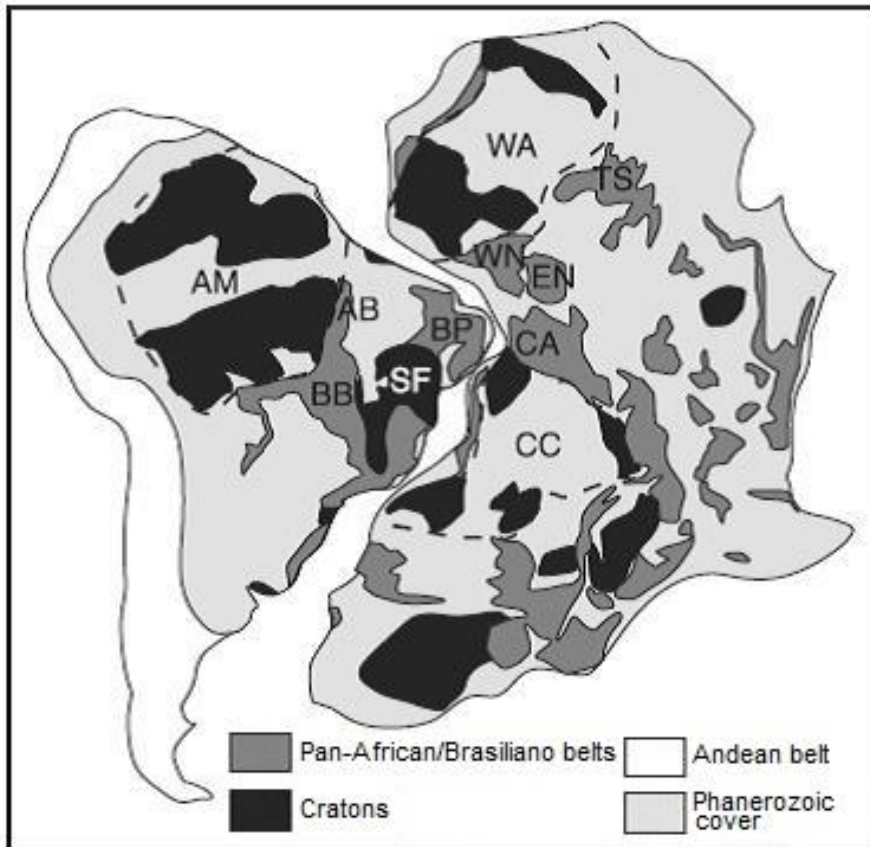


Figure 1. Generalized geological map of western Gondwana showing the distribution of main cratons and Pan-African/Brasiliano belts. Dashed lines are approximate contours of cratons. Cratons are as follows: AM, Amazonian; CC, Congo; SF, São Francisco; and WA, West African. Belts are as follows: AB, Araguaia belt; BB, Brasília belt. Provinces are as follows: BP, Borborema Province; CA, Cameroon province; EN, East Nigerian province; and WN, West Nigerian province. TS is Tuareg shield (Neves, 2003).

The Borborema Province is traditionally subdivided into four tectonic domains (Van Schmus et al., 2008): Northern, Transversal Zone, Pernambuco–Alagoas (PEAL), and Sergipano domains (Figure 2).

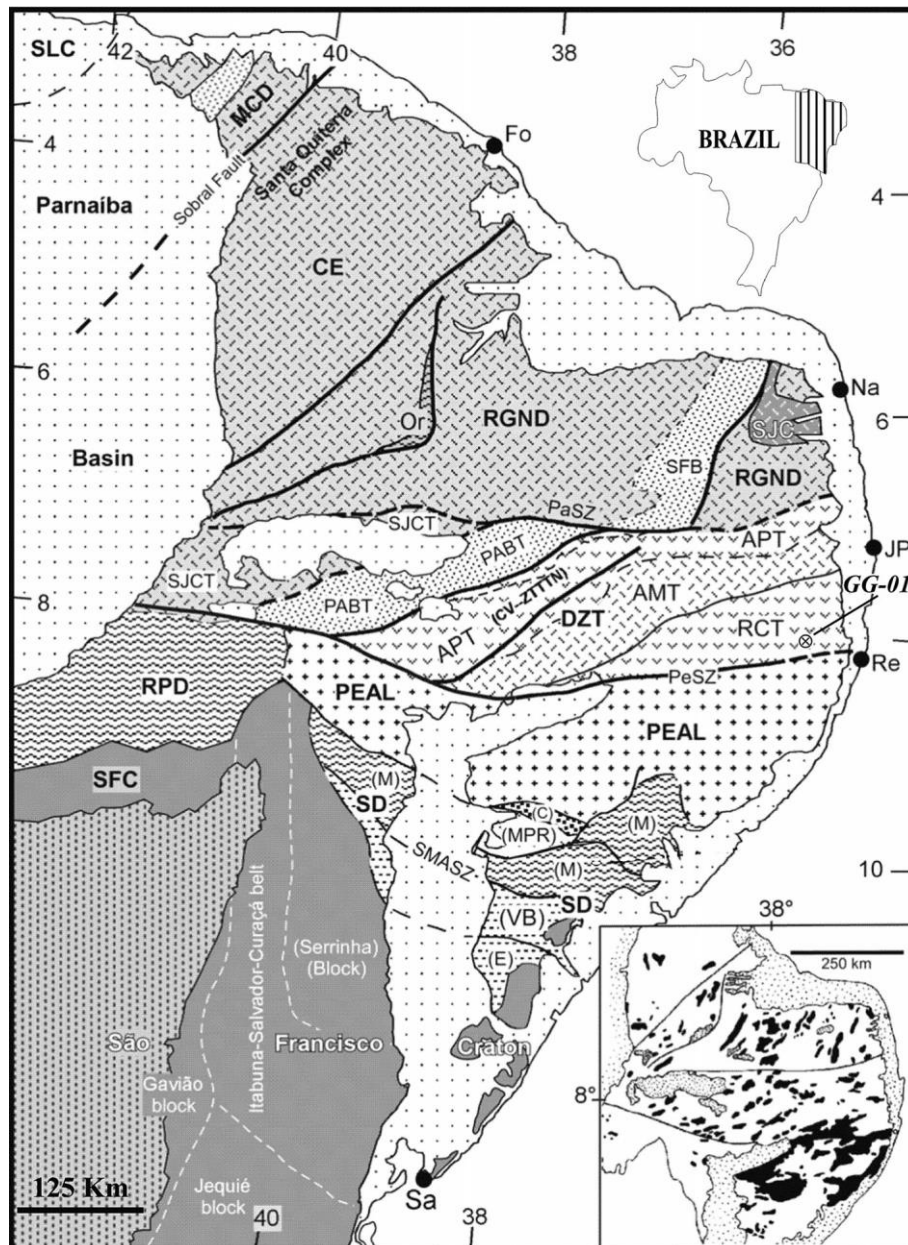


Figure 2. Borborema Province major domains according to Van Schmus et al. (2008) and terranes of the Transversal Zone domain: Ceará domain (CE); Médio Coreaú domain (MCD); Pernambuco–Alagoas domain (PEAL); Rio Grande do Norte domain (RGND), (São José do Campestre Archaean nucleus - SJC); Seridó fold belt (SFB); Riacho do Pontal domain (RPD); Sergipano domain (SD), [Macururé (M), Canindé (C), Marancó-Poço Redondo (MPR), Vasa Barris (VB), Estância (E)] - Oliveira et al. (2010); São Francisco craton (SFC), São Luís craton (SLC), Transversal Zone domain (DZT) [Alto Pajeú terrane (APT), Alto Moxoto terrane (AMT), Piancó Alto Brígida terrane (PABT), Cariris Velhos belt (CV), Rio Capibaribe terrane (RCT), São José do Caino terrane (SJCT)]. Faults and shear zones: Patos shear zone (PaSZ),

Pernambuco shear zone (PeSZ), São Miguel do Aleixo shear zone (SMASZ); GG-01, location of the sample analysed by SHRIMP from the Transversal Zone domain. Cities and towns: Fortaleza (Fo), Natal (Na), Recife (Re), Salvador (Sa). Inset: general distribution of Brasiliano granites (Silva Filho et al., 2014).

From a lithological perspective, the Borborema Province comprises a mosaic of tectonic terrains including Paleoproterozoic basement and scattered Archean nuclei, Meso to Neoproterozoic supracrustal rocks, and large intrusions of granites (Brito et al., 2000; Van Schmus et al., 2008). The Pernambuco-Alagoas domain occurs across the Sergipe part of the Borborema Province and contains the largest granitic batholiths (Silva et al., 2014). Silva et al. (1997) identified various late tectonic granitic intrusions in the eastern part of the Pernambuco-Alagoas domain, with compositions ranging from high-K, calc-alkaline, shoshonitic, mildly alkaline to peraluminous (\pm garnet bearing) granites.

2.2. Granitic rocks

Granite rocks can present different compositions and originate from diverse petrogenetic processes (Chappell and White, 1974, 1984, 2001). As a result of this complexity, petrologists have relied upon geochemical classifications to distinguish between various granitoid types. There are more than 20 different schemes involving granite classifications [see Barbarin (1990, 1999) for a summary thereof].

Granite formation is the result of the interaction of a range of processes including partial melting, fractional crystallization, crustal assimilation, magma mixing and melt-residue segregation on various source materials (mafic mantle melts, meta-igneous and meta-sedimentary crustal sources) in a number of different tectonic settings (Frost, 2001).

In order to simplify the subcategories of granites, Chappell and White (1974) proposed the subdivision into I- and S-type granites. This classification was initially developed in southeastern Australia, where they emphasized the importance of source rock composition and the concept of separation of melt and refractory residue during production of felsic magmas. The scheme

considers I-type granites as the melt products of meta-igneous source rocks mainly through high-temperature hornblende breakdown, whereas S-type granites result from melting of meta-sedimentary source material mainly through muscovite or biotite dehydration reactions.

The concept has been developed by Chappell and White and their co-workers in a series of papers (e.g. Chappell and White, 1984, 1992, 2001; White and Chappell, 1988; Chappell and Stephens, 1988; Chappell, 1999, 2004; Chappell and Wyborn, 2012; Chappell et al., 2012), and has been adopted worldwide (Guani et al., 2013; Guan et al., 2014; Wang et al., 2014; Foden et al., 2015; Wang et al., 2015).

In general, I-type granites are derived from igneous protolith (or infracrustal material), whereas S-type granites are formed from sedimentary rocks (or supracrustal material) (Chappell and White, 1984). As a result, distinct mineralogical and geochemical characteristics are observed in both types (Clemens, 2003). I-type granites exhibited a broad spectrum of compositions from felsic to mafic, with relatively high sodium ($\text{Na}_2\text{O} > 3.2\%$) in felsic varieties decreasing in more mafic types (2.2%), and presence of hornblende and titanite. S-type granites are relatively restricted in composition due to high SiO_2 , with relatively low sodium ($\text{Na}_2\text{O} < 3.2\%$) and approximately 5% of K_2O (Chappell and White, 2001).

2.3. Soil geochemistry of major, trace and rare earth elements

Geochemistry studies are mainly focused on origin, concentration, distribution and migration of chemical elements on the terrestrial globe, aiming to discover the principles that govern their distribution and migration (Mason and Moore, 1982). According to Hancock and Skinner (2000) chemical elements are classified in accordance with their abundance in the earth's crust as major elements - concentration is higher than 1.0%; minor elements - concentration between 1.0 and 0.1%; and trace elements - with a concentration below 0.1%.

Soil, one of the essential life support systems of our planet earth, is formed from common rocks on the earth's surface by various processes (Van Straaten, 2007). The distribution and abundance of elements in soils are largely

controlled by chemical and mineralogical composition of parent materials and various pedogenic processes involved during pedogenesis. Thus, acquisitions of geology, mineralogy and geochemistry results of soils derived from different geo-pedological environments are fundamental to evaluate the influence of pedogenic processes on element distribution in soil profiles (Palumbo et al., 2000). Soils developed on different parent materials have different geochemical signatures (Van Straaten, 2007, 2009).

The influence of parent material on element distribution tends to decrease with soil development (Zhang et al., 2002). The most important pedogenesis aspects related to element dynamics are those that affect release of elements from parent material by weathering, and translocation and accumulation of sorbents, such as clay minerals, oxides and organic matter, which are controlled by leaching, eluviation, salinization, calcification, podzolization, ferralitization, gleization and organic matter accumulation (Alloway, 1995). These geo-pedological factors not only determine the total content, but also the chemical speciation and bioavailability of elements.

In the last decades, new research methods, tools and optimization of old practices have refined the soil geochemical studies, allowing the understanding of complex issues as discrimination between natural and anthropogenic sources of elements in soils (Blaser et al., 2000; Reiman and Caritat, 2005; Nael et al., 2009) and the use of elements as tracers of pedogenic processes (Laveuf et al., 2008).

Classically, soil scientists explore the major elements and mineralogy data as pedogenic processes tracers. However, as several of these processes mobilize the same major elements in the soil, they become difficult to quantify (Laveuf and Cornu, 2009). As a result, other tracers must be used, for example rare earth elements (REEs).

The International Union of Pure and Applied Chemistry (IUPAC: Connely et al., 2005) defines REEs as a group of 17 chemically similar metallic elements (Lanthanide series, plus scandium and yttrium). The latter two elements (Sc and Y) are included as REEs because they are chemically similar to the lanthanides (Jaireth et al., 2014). These elements have been commonly divided into two groups: light rare earth elements (LREEs: La-Eu) and heavy rare earth

elements (HREEs: Gd-Lu) (Hu et al., 2006; Long et al., 2010; Walters et al., 2010; Sadeghi et al., 2013).

The REEs are not as rare in nature as the name suggests. LREEs are not rare in the Earth's crust (Σ LREE = 152 mg kg⁻¹); however, HREEs are less common (Σ HREE = 51 mg kg⁻¹) (Tyler and Olsson, 2002). These elements are found in more than 200 minerals, mainly phosphates, carbonates, silicates, and iron and manganese oxides (Kanazawa and Hamitani, 2006). Cerium, 25th most abundant element in the crust, exhibits higher concentration in Earth's crust than copper and similar to Zn (Tyler, 2004).

Rare earth elements have become strategically critical for developed and developing economies around the world owing to the wide application for multiple purposes, such as industrial key technologies (Gandois et al., 2014; Mihajlovic et al., 2014; Pagano et al., 2015) and agricultural fertilizers (Pang et al., 2002; Kobayashi et al., 2007). The increasing exploitation and disposal of products containing REEs over the last decades has drawn attention to REEs leaking into the soil. Thus, their accumulation in soil can become an environmental concern in the future (d'Aquino et al., 2009). For instance, adverse effects on biota have been observed (Chen et al., 2001; Oral et al., 2010).

The large variations of total REE contents in soils are highly dependent on the soil type and of their parent material (Liu, 1988; Hu et al., 2006). The mineralogical composition of parent materials controls their REE content (Yamasaki et al., 2001).

The behaviour of REEs during weathering has been extensively studied (Loell et al., 2011; Sadeghi et al., 2013; Yusoff et al., 2013; Liang et al., 2014; Mihajlovic et al., 2014). The REE redistribution during weathering is a function of: i) the nature primary phase, i.e. its mineralogical composition and relative mineral stability (Tyler, 2004); ii) the properties of the different REEs in the solution (Condie et al., 1995); iii) the degree of weathering (Walter, 1991; Huang and Gong, 2001).

The REE stock generally decreases with an increasing weathering degree (Öhlander et al., 1996). The upper part of weathering profiles is frequently depleted in REEs compared to the bottom part that may even be enriched following possible reprecipitation (Nesbitt and Markovics, 1997). In

most cases, weathering results in a relative enrichment of LREEs over HREEs in the weathering profile (Compton et al., 2003).

As a conclusion, REE concentrations in soils are determined to a significant extent by processes occurring during chemical weathering (Taunton et al., 2000). A careful characterization of the initial REE distribution in primary minerals is essential to understand the redistribution of REEs from their release during primary mineral dissolution to their fixation onto secondary minerals.

Nevertheless, the pedological behavior of REEs remains poorly understood (Chen et al., 2014). Recently, Laveuf and Cornu (2009) and Laveuf et al. (2012) recommended further study of the REEs behavior in different pedological environments in order to quantify different geochemical behavior of REEs.

2.4. Influence of granites on pedogênese and soil geochemistry

Granitic rocks are abundant in the Earth's upper continental crust underlying large areas of agricultural land in the tropics and temperate climates. In Pernambuco State alone, granites cover approximately 1/3 of the whole land area (Brazil, 2001). The influence of granites in soil geochemistry of major and trace elements has been extensively studied by many researchers, including REEs (Panahi et al., 2000; Yusoff et al., 2013; Sanematzu et al., 2015). These studies have provided new knowledge on soil geochemistry during pedogenesis in different climates.

In spite of the large amount of researches related to granites, studies regarding the granite types according to chemical and mineralogical composition under tropical environments as well as on the cause-effect relationship with the genesis and geochemistry of their soils are scarce. In this study, soil profiles were sampled based on granite types (I- and S-types) under three climatic zones (humid, sub-humid and dry) from tropical to semiarid region of the Borborema Province.

These granite types underly large areas in the tropics and play a key role for the most tropical ecosystems in terms of environmental quality issues, such as geochemical cycles, global weathering patterns and carbon storage. Thus, understanding the relationship between major, trace and rare earth elements of

soils derived from different granites (I- and S-types) and climate conditions is essential to understand the variability among soils developed from these parent materials.

3. References

Almeida, M.E., Macambira, M.J.B., Oliveira, E.C. 2007. Geochemistry and zircon geochronology of the I-type high-K calc-alkaline and S-type granitoid rocks from southeastern Roraima, Brazil: Orosirian collisional magmatism evidence (1.97–1.96 Ga) in central portion of Guyana Shield. *Precambrian Research* 155: 69–97.

Alloway, B.J. 1995. The origins of heavy metals in soils. In: Alloway, B.J. (Ed.), *Heavy Metals in Soils*. Johns Wiley & Sons, Inc., New York, p. 29–39.

Antunes, I.M.H.R., Neiva, A.M.R., Silva, M.M.V.G., Corfu F. 2009. The genesis of I- and S-type granitoid rocks of the Early Ordovician Oledo pluton, Central Iberian Zone (central Portugal). *Lithos* 111: 168–185.

Antunes, I.M.H.R., Neiva, A.M.R., Silva, M.M.V.G., Corfu, F. 2008. Geochemistry of S-type granitic rocks from the reversely zoned Castelo Branco pluton (central Portugal). *Lithos* 103: 445–465.

Barbarin, B. 1990. Granitoids: main petrogenetic classification in relation to origin and tectonic setting. *Geological Journal* 25, 227-238.

Barbarin, B. 1999. A review of the relationships between granitoid types, their origins and their geodynamic environments. *Lithos* 46, 605-626.

Blaser, P., Zimmermann, S., Luster, J., Shotyk W. 2000. Critical examination of trace element enrichments and depletions in soils: As, Cr, Cu, Ni, Pb, and Zn in Swiss forest soils. *Science of the Total Environment* 249: 257-280.

Brazil.1973. Ministério da Agricultura, Levantamento exploratório – Reconhecimento de solos do Estado de Pernambuco. Boletim Técnico n.º 26, Volume I.

Brazil. 2000. Ministério da Agricultura; Levantamento de Reconhecimento de Baixa e Média Intensidade dos Solos do Estado de Pernambuco. Boletim de Pesquisa n. 11.

Brazil. 2001. Ministry of Mines and Energy. Geology and mineral resources of Pernambuco State. Geological Survey of Brazil, Pernambuco State, Recife, CPRM.

Brito, L.T.L., Moura M.S.B., Gama, G.F.B. 2007. Potencialidades da água de chuva no Semiárido brasileiro. Petrolina: Embrapa Semi-Árido. 181p.

Brito Neves, B.B. 1975. Regionalização geotectônica do Pré-cambriano nordestino. São Paulo. Tese de Doutorado. Instituto de Geociências, Universidade de São Paulo, Tese de Livre Docência. 198p.

Canosa, F., Izard, A.M., Fuente, M.F. 2012. Evolved granitic systems as a source of rare-element deposits: The Ponte Segade case (Galicia, NW Spain). *Lithos* 153: 165–176.

Chappell, B.W., White, A.J.R. 1974. Two contrasting granite types. *Pacific Geology* 8:173–174.

Chappell, B.W., White, A.J.R. 1984. I- and S- type granites in the Lachlan Fold Belt. southeastern Australia. In: Keqin. Xu.. Guangchi. Tu. (Eds.). *Geology of Granites and their Metallogenic Relation*: Beijing Science Press. pp.87–101.

Chappell, B.W., Stephens, W.E. 1988. Origin of infracrustal (I-type) granite magmas. *Transactions of the Royal Society of Edinburgh: Earth Sciences* 79: 71–86.

Chappell, B.W., White, A.J.R. 1992. I- and S-type granites in the Lachlan Fold Belt. *Transactions of the Royal Society of Edinburgh: Earth Sciences* 83: 1–26.

Chappell, B.W. 1999. Aluminium saturation in I- and S-type granites and the characterization of fractionated haplogranites. *Lithos* 46: 535–551.

Chappell, B.W., White, A.J.R. 2001. Two contrasting granite types: 25 years later. *Australian Journal of Earth Sciences* 48: 489–499.

Chappell, B.W. 2004. Towards a unified model for granite genesis. *Transactions of the Royal Society of Edinburgh: Earth Sciences* 95: 1–10.

Chappell, B.W., Wyborn, D. 2012. Origin of enclaves in S-type granites of the Lachlan Fold Belt. *Lithos* 154: 235–247.

Chappell, B.W., Bryant, C.J., Wyborn, D. 2012. Peraluminous I-type granites. *Lithos* 153: 142–153.

Chen, W.J., Tao, Y., Gu, Y.H., Zhao, G.W. 2001. Effect of lanthanide chloride on photosynthesis and dry matter accumulation in tobacco seedlings. *Biological Trace Element Research* 79: 169–176.

Chen, L.M., Zhang, G.L., Jin, Z.D. 2014. Rare earth elements of a 1000-year paddy soil chronosequence: Implications for sediment provenances. Parent material uniformity and pedological changes. *Geoderma* 230–231:274–279.

Clemens, J.D. 2002. Melting of the continental crust I: fluid regimes, melting reactions and source-rock fertility. In: Brown, M., Rushmer, T. (Eds.), *Evolution and Differentiation of the Continental Crust*. Cambridge University Press (in press).

Clemens, J.D. 2003. S-type granitic magmas – petrogenetic issues, models and evidence. *Earth Sciences* 61: 1–18.

Clemens J.D., Stevens G., Farina F. 2011. The enigmatic sources of I-type granites: The peritectic connexion. *Lithos* 126: 174–181.

Compton, J.S., White, R.A., Smith, M. 2003. Rare earth element behavior in soils and salt pan sediments of a semiarid granitic terrain in the Western Cape, South Africa. *Chemical Geology* 201 (3–4):239–255.

Condie, K.C., Dengate, J., Cullers, R.L. 1995. Behavior of rare earth elements in a paleoweathering profile on granodiorite in the Front Range, Colorado, USA. *Geochimica et Cosmochimica Acta* 59 (2): 279–294.

Connelly, N.G., Damhus, T., Hartshorn, R.M., Hutton, A.T. 2005. Nomenclature of Inorganic Chemistry: IUPAC Recommendations 2005, RSC Publishing, Cambridge. 366p.

d'Aquino, L., Pinto, M.C., Nardi, L., Morgana, M., Tommasi, F. 2009. Effect of some light rare earth elements on seed germination, seedling growth and antioxidante metabolism in *Triticum durum*. *Chemosphere* 75: 900–905.

Drumond, M.A., Santana, A.C., Antoniole, A. 2004. Recomendações para o uso sustentável da biodiversidade no biomacaatinga. In: Biodiversidade da Caatinga: Áreas e ações prioritárias para a conservação. Brasília: MMA-UFRPE; Brasília, DF: 47-90pp.

INMET. 2015. Instituto Nacional de Meteorologia. Available in <http://www.inmet.gov.br/portal/index.php?r=clima/normaisclimatologicas>. Accessed in: 16 de nov. de 2015.

IPA - Instituto Agrônomo de Pernambuco. 2008. Recomendações de adubação para o Estado de Pernambuco; 2º aproximação. 3. ed. Revisada/ coordenado por Francisco José e Albuquerque Cavalcanti – Recife. 212p.

Farahat, E.S., Mohamed, H.A., Ahmed, A.F., El Mahallawi, M.M. 2007. Origin of I- and A-type granitoids from the Eastern Desert of Egypt: Implications for crustal growth in the northern Arabian–Nubian Shield. *Journal of African Earth Sciences* 49: 43–58.

Ferreira, V.P., Sial, A.N., Sá, E.F.J. 1998. Geochemical and isotopic signatures of Proterozoic granitoids in terranes of the Borborema structural province, northeastern Brazil. *Journal South American Earth Sciences* 5: 439-455.

Foden, J., Sossi, P.A., Wawryk, C.M. 2015. Fe isotopes and the contrasting petrogenesis of A-, I- and S-type granite. *Lithos* 212-215: 32-44.

Frost, B.R., Barnes, C.G., Collins, W.J., Arculus, R.J., Ellis, D.J., Frost, C.D. 2001. A geochemical classification for granitic rocks. *Journal of Petrology* 42: 2033–2048.

- Gandois, L., Agnan, Y., Leblond, S., Delmas, N.S., Roux, G.L., Probst, A. 2014. Use of geochemical signatures, including rare earth elements in mosses and lichens to assess spatial integration and the influence of forest environment. *Atmospheric Environment* 95:96-104.
- Gontier, A., Rihs, S., Chabaux, F., Lemarchand, D., Pelt, E., Turpault, M.P. 2015. Lack of bedrock grain size influence on the soil production rate. *Geochimica et Cosmochimica Acta* 166: 146–164.
- Guan, Y., Yuan, C., Sun, M., Wilde, S., Long, X., Huang, X., Wang, Q. 2014. I-type granitoids in the eastern Yangtze Block: implications for the Early Paleozoic intracontinental orogeny in South China. *Lithos* 206-207: 34-51.
- Guani, A.A., Searle, M., Robb, L., Chung, S.L. 2013. Transitional I S type characteristic in the Main Range Granite. Peninsular Malaysia. *Journal of Asian Earth Sciences*. 76: 225-240.
- Hancock, P. L., Skinner, B.J. 2000. *The Oxford Companion to the Earth*. Oxford, New York: Oxford University Press. 1174pp.
- Healy, B., Collins, W.J., Richards, S.W. 2004. A hybrid origin for Lachlan S-type granites: the Murrumbidgee Batholith example. *Lithos* 78: 197– 216.
- Hu, Z., Haneklaus, S., Sparovek, G., Schnug, E. 2006. Rare earth elements in soils. *Communications in Soil Science Plant Analysis* 37:1381–1420.
- Jaireth, S., Hoatson, D.M., Mieзитis, Y. 2014. Geological setting and resources of the major rare-earth-element deposits in Australia. *Ore Geology Reviews* 62: 72–128.
- Kanazawa, Y., Kamitani, M. 2006. Rare earth minerals and resources in the world. *Journal of Alloys and Compounds* 408–412: 1339–1343.
- Kobayashi, Y., Ikka, T., Kimura, K., Yasuda, O., Koyama, H. 2007. Characterisation of lanthanum toxicity for root growth of *Arabidopsis thaliana* from the aspect of natural genetic variation. *Functional Plant Biology* 34: 984–994.

- Koppen, W.P., 1931. Grundriss der Klimakunde. 2nd ed. Berlin: Walter de Gruyter. 388p.
- Laveuf C., Cornu S., Juillot F. 2008. Rare earth elements as tracers of pedogenetic processes. *Comptes Rendus Geoscience* 340: 523-532.
- Laveuf, C., Cornu, S. A. 2009. Review on the potentiality of rare earth elements to trace pedogenetic processes. *Geoderma* 154: 1-12.
- Laveuf, C., Cornu, S., Guillerme, L.R.G., Juillot, F. 2012. The impact of redox conditions on the rare earth element signature of redoximorphic features in a soil sequence developed from limestone. *Geoderma* 170:25-38.
- Liang, T., Li, K., Wang, L. 2014. State of rare earth elements in different environmental components in mining areas of China. *Environmental Monitoring and Assessment* 186:1499–1513.
- Liew, T.C. 1983. Petrogenesis of the Peninsular Malaysia granitoid batholith. PhD thesis. Australia National University. Canberra. 291pp.
- Liu, Z. 1988. Rare earth elements in soil. In: Guo, B.S., Zhu, W.M., Xiong, B.K., Ji, Y.J., Liu, Z., Wu, Z.M. (Eds.), *Rare Earth Elements in Agriculture* (in Chinese). China Agricultural Science and Technology Press, Beijing, 22–44pp.
- Loell, M., Albrecht, C., Henningsen, P.F. 2011. Rare earth elements and relation between their potential bioavailability and soil properties, Nidda catchment (Central Germany) *Plant and Soil* 349:303–317.
- Long, K.R., Van Gosen, B.S., Foley, N.K., Cordier, D. 2010. The principal rare earth deposits of the United States—a summary of domestic deposits and a global perspective. United States Geological Survey Scientific Investigations Report 2010-5220, 96 p.
- Mareschal, L., Turpault, M.P., Ranger, J. 2015. Effect of granite crystal grain size on soil properties and pedogenic processes along a lithosequence. *Geoderma* 249–250: 12–20.

Mason, B., Moore, C.B. 1982. Principles of Geochemistry, 4th ed., New York, John Wiley & Sons.

Mihajlovic, J., Stärk, H.J., Rinklebe, J. 2014. Geochemical fractions of rare earth elements in two floodplain soil profiles at the Wupper River, Germany. *Geoderma* 228–229:160–172.

Nael, M., Khademi, H., Jalalian, A., Schulin, R., Kalbasi, M., Sotohian, F. 2009. Effect of geo-pedological conditions on the distribution and chemical speciation of selected trace elements in forest soils of western Alborz, Iran. *Geoderma* 152:157–170.

Nesbitt, H.W., Markovics, G. 1997. Weathering of granodioritic crust, long-term storage of elements in weathering profiles, and petrogenesis of siliciclastic sediments. *Geochimica et Cosmochimica Acta* 61 (8): 1653–1670.

Neves, S.P. 2003. Proterozoic history of the Borborema Province (NE Brazil): Correlations with neighboring cratons and Pan-African belts and implications for the evolution of western Gondwana. *Tectonics* 22 (4): 1031p.

Öhlander, B., Land, M., Ingri, J., Widerlund, A. 1996. Mobility of rare earth elements during weathering of till in northern Sweden. *Applied Geochemistry* 11: 93–99.

Oliveira, E.P., Windley, B., Araújo, M.N.C. 2010. The Neoproterozoic Sergipano orogenic belt, NE Brazil: a complete plate tectonic cycle in western Gondwana. *Precambrian Research* 181:64–84.

Oral, R., Bustamante, P., Warnau, M., D'Ambra, A., Guida, M., Pagano, G. 2010. Cytogenetic and developmental toxicity of cerium and lanthanum to search in embryos. *Chemosphere* 81: 194–198.

Pagano, G., Guida, M., Tommasi, F., Oral, R. 2015. Health effects and toxicity mechanisms of rare Earth elements—Knowledge gaps and research prospects. *Ecotoxicology and Environmental Safety* 115:40–48.

Palumbo, B., Angelone, M., Bellanca, A., Dazzi, C., Hauser, S., Neri, R., Wilson, J. 2000. Influence of inheritance and pedogenesis on heavy metal distribution in soils of Sicily, Italy. *Geoderma* 95: 247-266.

Panahi, A., Young, G.M., Rainbird, R.H. 2000. Behavior of major and trace elements (including REE) during Paleoproterozoic pedogenesis and diagenetic alteration of an Archaean granite near Ville Marie, Quebec, Canada. *Geochimica Cosmochimica Acta* 64 (13): 2199–2220.

Pang, X., Li, D., Peng, A. 2002. Application of rare-earth elements in the agriculture of China and its environmental behaviour in soil. *Environmental Science and Pollution Research* 9:143–148.

Reimann, C., Caritat, P. 2005. Distinguishing between natural and anthropogenic sources for elements in the environment: regional geochemical surveys versus enrichment factors. *Science of the Total Environment* 337: 91-107.

Robinson, F.A., Foden, J.D., Collins, A.S. 2015. Geochemical and isotopic constraints on island arc, synorogenic, post-orogenic and anorogenic granitoids in the Arabian Shield, Saudi Arabia. *Lithos* 220–223: 97–115.

Sadeghi, M., Morris, G.A., Carranza, E.J.M., Ladenberger, A., Andersson, M. 2013. Rare earth element distribution and mineralization in Sweden: An application of principal component analysis to FOREGS soil geochemistry. *Journal of Geochemical Exploration* 133:160–175.

Sanematsu, K., Kon, Y., Imai, A. 2015. Influence of phosphate on mobility and adsorption of REEs during weathering of granites in Thailand. *Journal of Asian Earth Sciences* 111:14–30.

Santos, H.G., Jacomine, P.K.T., Anjos, L.H.C., Oliveira, V.Á., Lumbreiras, J.F., Coelho, M.R., Almeida, J.A., Cunha, T.J.F., Oliveira, J.B. 2013. Sistema brasileiro de classificação de solos. 3. ed. Brasília: Embrapa, 353p.

Silva, A.F.F., Guimarães, I.P., Brito, M.F.L., Pimentel, M.M. 1997. Geochemical signatures of the main Neoproterozoic late tectonic granitoids from the

Proterozoic Sergipano fold belt, NE Brazil and its significance for the Brasiliano orogeny. *International Geology Review* 39: 639–659.

Silva, A.F.F., Guimarães, I.P., Van Schmus, W.R., Armstrong, R.A., Rangel da Silva, J.M., Osako, L.S., Cocentino, L.M. 2014. Shrimp U–Pb zircon geochronology and Nd signatures of supracrustal sequences and orthogneisses constrain the Neoproterozoic evolution of the Pernambuco–Alagoas domain, southern part of Borborema Province, NE Brazil. *International Journal of Earth Sciences* 103: 2155–2190.

Souza, F.P., Ferreira, T.O., Mendonça, E.S., Romero, R.E., Oliveira, J.G.B. 2012. Carbon and nitrogen in degraded Brazilian semiarid soils undergoing desertification. *Agriculture Ecosystems & Environment* 148:11–21.

Taunton, A.E., Welch, S.A., Banfield, J.F. 2000. Geomicrobiological controls on light rare earth element, Y and Ba distributions during granite weathering and soil formation. *Journal of Alloys and Compounds* 303–304: 30–36.

Thomas, W.W., Carvalho, A.M.V., Amorim, A.M.A., Arbelaez, A.L. 1998. Plant endemism in two forests in southern Bahia, Brazil. *Biodiversity and Conservation* 7 (3): 311–322.

Tyler, G., Olsson, T. 2002. Conditions related to solubility of rare and minor elements in forest soils. *Journal of Plant Nutrition and Soil Science* 165:594–601.

Tyler, G. 2004. Rare earth elements in soil and plant systems—a review. *Plant and Soil* 267 (1–2):191–206.

Van Schmus, W.R., Oliveira, E.P., Silva, A.F.F., Toteu, S.F., Penaye, J., Guimarães, I.P. 2008. Proterozoic links between the Borborema Province, NE Brazil, and the Central African Fold Belt. *Geological Society of London*, 294: 69–99.

Van Straaten, P. 2007. *Agrogeology: The use of rocks for crops*. Enviroquest, Cambridge, Ontario, Canadá. 426p.

Van Straaten, P. 2009. Agrogeology: geological soil rejuvenation processes and agromineral resources. In: Ribeiro M.R., do Nascimento C.W., Ribeiro Filho M.R., Cantalice J.R.B. (eds) *Topicos em ciencia do solo*. Sociedade Brasileira de Ciencia do Solo. 319-412pp.

Walters, A., Lusty, P., Chetwyn, C., Hill, A. 2010. Rare earth elements. Mineral Profile Series British Geological Survey. United Kingdom. 45p.

Wang, Z., Wang, J., Deng, Q., Du, Q., Zhou, X., Yang, F., Liu, H. 2015. Paleoproterozoic I-type granites and their implications for the Yangtze block position in the Columbia supercontinent: Evidence from the Lengshui Complex, South China. *Precambrian Research* 263:157-173.

Wang, X.S., Hu, R.Z., Bi, X.W., Leng, C.B., Panl, C., Zhu, J.J., Chen, Y.W. 2014. Petrogenesis of Late Cretaceous I-type granites in the southern Yidun Terrane: New constraints on the Late Mesozoic tectonic evolution of the eastern Tibetan Plateau. *Lithos* 208-209, 202-219.

White, A.J.R., Chappell, B.W. 1988. Some supracrustal (S-type) granites of the Lachlan Fold Belt. *Transactions of the Royal Society of Edinburgh: Earth Sciences* 79:169–181.

Yamasaki, S.I., Takeda, A., Nanzyo, M., Taniyama, I., Nakai, M. 2001. Background levels of trace and ultra-trace elements in soils of Japan. *Soil Science and Plant Nutrition* 47 (4): 755–765.

Yousefifard, M., Ayoubi, S., Poch, R.M., Jalalian, A., Khademi, H., Khormali, F. 2015. Clay transformation and pedogenic calcite formation on a lithosequence of igneous rocks in northwestern Iran. *Catena* 133: 186–197.

Yu, Y., Huang, X.L., He, P.L., Li, J. 2016. I-type granitoids associated with the early Paleozoic intracontinental orogenic collapse along pre-existing block boundary in South China. *Lithos* 248–251: 353–365.

Yusoff, Z.M., Ngwenya, B.T., Parsons, I. 2013. Mobility and fractionation of REEs during deep weathering of geochemically contrasting granites in a tropical setting, Malaysia. *Chemical Geology* 349:71–86.

Zhang, C., Wang, L., Li, G., Dong, S., Yang, J., Wang, X. 2002. Grain size effect on multi-element concentrations in sediments from intertidal flats of Bohai Bay, India. *Applied Geochemistry* 17: 59–68.

Zhao, X.F., Zhou, M.F., Li, J.W., Wu, F.Y. 2008. Association of Neoproterozoic A- and I-type granites in South China: Implications for generation of A-type granites in a subduction-related environment. *Chemical Geology* 257 (1): 1–15.

CHAPTER I

WEATHERING RATES AND CARBON STORAGE ALONG A
CLIMOSEQUENCE OF SOILS DEVELOPED FROM CONTRASTING
GRANITES IN NORTHEAST BRAZIL

Weathering rates and carbon storage along a climosequence of soils developed from contrasting granites in northeast Brazil

Abstract

I- and S-type granites comprise large areas and play a key role in global soil weathering patterns. I-type granites are originated from melting of igneous source rocks, whereas S-type granites result from melting of sedimentary sources. This gives rise to differences in mineralogical and geochemical characteristics of the rocks. The objective of this study was to address the effect of petrology and mineralogy of I- and S-type granites on weathering, pedogenesis and total organic carbon stocks across a climosequence. Significant differences in morphological, physical and chemical properties of soils derived from I- and S-type granites were observed and directly linked to petrological, mineralogical and geochemical signatures of the underlying granites, e.g., presence of more mafic minerals in the I-type granite, and therefore a higher clay and iron content in their derived soils. In addition, this higher iron content favored the hematite pathway and, thus, the red soil development. Despite the influence of the climate on weathering patterns, i.e., higher soil development in humid areas, parent material seems to play a decisive role in determining soils characteristics in the studied area. The type of parent material also governed the rates of carbon accumulation in soils. I-type granites originated soils with higher TOC stocks than soil profiles developed from S-type granites. This carbon accumulation is mainly due to soil chemical and physical characteristics driven by the type of granite, notably soil fertility and clay content.

Keywords: Granitic rocks; I-type granite; S-type granite; pedogenesis; tropical soils; carbon sequestration.

1. Introduction

Granites are among the most common rock types occurring at the continental crust (Frost et al., 2001). In Brazil, granitic terrains extend through vast areas and function as the foundation for a great variety of tropical ecosystems ranging from caatinga vegetation in the dry lands to rain forests. Therefore, soils developed from these materials influence a plethora of ecosystem services such as water quality control, carbon sequestration, nutrient cycling, provision of natural habitat, and contaminants retention (Blum et al., 2006). For instance, large amounts of carbon can be stocked in soil profiles thereby mitigating global warming and improving soil fertility status.

Granitic rocks vary in their mineralogical and chemical compositions as they originate from different petrogenetic processes (Chappell and White, 1974, 1984, 2001). In order to simplify the subcategories of granites, the I- and S-type classification, along with the use of A-type granites have been widely adopted (Chappell, 1999; Foden et al., 2015; Guani et al., 2013; Guan et al., 2014; Litvinovsky et al., 2015; Vilalva et al., 2016; Wang et al., 2014; Wang et al., 2015).

In general, I-types are derived from igneous protolith (or infracrustal material), whereas S-types are formed from sedimentary rocks (or supracrustal material) (Chappell and White, 1984). As a result, distinct mineralogical and geochemical characteristics are observed in both types (Clemens, 2003; Ghani, 2000). I-types usually exhibit a broad spectrum of compositions from felsic to mafic, with relatively high sodium ($\text{Na}_2\text{O} > 3.2\%$) concentrations in the felsic varieties which decreases in the mafic types ($\text{Na}_2\text{O} \sim 2.2\%$). On the other hand, S-type granites present a less diverse composition due to their high SiO_2 content, with relatively low sodium concentrations ($\text{Na}_2\text{O} < 3.2\%$) and approximately 5% of K_2O (Chappell and White, 2001).

Several studies have addressed the petrogenesis of I- and S-type granites, their chemistry and mineralogy (Almeida et al., 2007; Antunes et al., 2008, 2009; Canosa et al., 2012; Chappel et al., 2012; Clemens et al., 2011; Farahat et al., 2007; Foden et al., 2015; Guani et al., 2013; Guan et al., 2014; Healy et al., 2004; Robinson et al., 2015). On the other hand, only few studies have dealt with both the weathering and the pedogenesis processes taking

place according to granite types (Gontier et al., 2015; Marechal et al., 2015). The present work studied soil profiles originated from I- and S-type granites under three contrasting climatic zone (humid, sub-humid and dry) at the Borborema Province, northeastern Brazil.

The Borborema Province comprises an area of around 380,000 km² (Ferreira et al., 1998) and represents the Western portion of the extensive geologic Brasiliano-Pan African orogenic system formed by a convergence of the West Africa/São Luis and San Francisco-Congo Cratons (Brito Neves, 1975). This geological setting represents parts of the Gondwana continent found in large tropical areas such as: South America, sub-Saharan Africa, India, Asia (SE and East) and Australia.

Due to the abundance of I- and S-type granites in the Earth's upper continental crust, as evidenced in Australia (Chappell et al., 2012; Foden et al., 2015), China (Guan et al., 2014), Saudi Arabia (Robinson et al., 2015), Spain (Canosa et al., 2012), and Brazil (Almeida et al., 2007), as well as the scarcity of information about the influence of granite types on rock weathering and carbon storage, the objectives of this work were: (i) to describe the petrography and mineralogy of I- and S-type granites of the Borborema Province; (ii) to address the effect of petrography and mineralogy of I- and S-type granites on weathering across a climosequence; (iii) to study the effect of granite types and climosequence on different properties and organic carbon stocks of soil profiles.

2. Materials and methods

2.1. Study area

The study area lies in the Borborema Province (Pernambuco State), northeastern Brazil. From a lithological perspective, the Borborema Province comprises a mosaic of tectonic blocks including Paleoproterozoic basement and scattered Archean nuclei, Meso to Neoproterozoic supracrustal rocks, and large intrusions of granites (Van Schmus et al., 2008). Neoproterozoic magmatism in this province produced voluminous S- and I-type granites.

The region of study is divided into three climatic zones according to Koppen classification (Koppen, 1931). In response to this sharp climatic

contrast, vegetation demonstrates a distinct zonation. The coastal humid zone is located in the eastern part of Pernambuco. The region is characterized by a tropical humid climate, with mean precipitation of 1,800 mm. The vegetation is an evergreen broad-leaf tropical forest. The sub-humid zone can be considered a transition between the humid and dry zones, presenting a large dry season and a relatively small rainfall (600-900 mm). The vegetation is a deciduous forest, locally classified as hypoxerophilous caatinga. The dry zone, in its turn, presents a semiarid climate with an annual precipitation of 500 mm and mean annual temperature of 28 °C. This region is characterized by dense tree-shrub deciduous vegetation, classified as hyperxerophilic caatinga, somewhat similar to a dry season deciduous thorn bush savannah (Nascimento et al., 2006).

2.2. Soil and Rock samplings

Three soil profiles and the underlying rocks (from both I- and S-type granites) were sampled under native vegetation in the three climatic zones; sampling locations were based on analysis of geological maps and field confirmation in order to guarantee that the soils actually formed over the granites that they overlie. The soil profiles did not present any of the diagnostic criteria for lithic discontinuity described in WRB (2014). All sampling sites (Figure 1) were selected in relatively undisturbed environments in order to guarantee minimal anthropic influence and similar topographic conditions (gently sloping sites).

according to the World Reference Base for Soil Resources (IUSS Working Group WRB, 2014).

2.3. *Rock analysis*

The I- and S-type granites and their modal mineralogical compositions were determined in the fresh rock samples collected from outcrops nearby the soil profiles. A petrographic microscope was used to minerals identification in polished thin sections prepared according to Murphy (1986).

Granite samples were also coated with a 20 nm gold layer (model Q150R - Quorum Technologies). Then fine-grained minerals and textures were observed using a TESCAN (model: VEGA-3 LMU) field emission scanning electron microscopy (SEM) at an accelerating voltage of 15 kV. Afterwards, an energy dispersive X-ray spectrum (EDS; Oxford Instrument, model: 51-AD0007) coupled with SEM was used to semiquantitatively analyze the mineral assemblage.

2.4. *Soil analysis*

2.4.1. *Physical and chemical analysis*

The particle size distribution was determined according to Gee and Or (2002), using Calgon for chemical dispersion. Prior to analysis, all samples were pre-treated to eliminate organic matter (30% v/v H₂O₂). The pH values were measured in H₂O (1:2.5 soil:solution ratio). Potential acidity (H⁺ + Al³⁺) was determined by the calcium acetate method (0.5 mol L⁻¹, pH 7.0), and total organic carbon (TOC) according to Yeomans and Bremner (1988).

Potassium and Na⁺ were extracted with Mehlich⁻¹, while Ca²⁺, Mg²⁺ and Al³⁺ were measured after extraction with 1 mol L⁻¹ KCl. These cations were determined by optical emission spectrometry (ICP-OES/Optima 7000, Perkin Elmer). Cations concentrations were used to calculate base saturation, cation exchange capacity, and aluminum saturation percentage.

The bulk density (volumetric ring method) was determined according to Embrapa (2011). The TOC stocks were calculated according to Weissert et al. (2016), using Eq. (1),

$$\text{TOC stocks} = \text{TOC} \times \text{BD} \times \text{D} \quad (1)$$

where TOC (%) is the soil organic carbon concentration, BD (g cm^{-3}) dry bulk density and D (m) the sampling depth.

2.4.2. *Selective dissolution*

Free iron oxides (Fed) was determined using sodium dithionite-citrate-bicarbonate (DCB), following a sequence of three successive extractions every 15 min ($80\text{ }^{\circ}\text{C}$) (Mehra and Jackson, 1960). An ammonium oxalate ($(\text{NH}_4)_2\text{C}_2\text{O}_4\cdot\text{H}_2\text{O}$ at pH 3.0) extraction was used to obtain the low-crystallinity iron forms (Feo) (Mckeague and Day, 1966). Iron concentrations were determined by ICP-OES.

2.4.3. *Redness rating index*

The redness rating index (RI) suggested by Torrent et al. (1980) was used. It is defined as follows:

$$\text{RR} = \frac{(10 - H) \times C}{V}$$

Where C and V are the numerical values of the Munsell chroma and value, respectively, and H is the figure preceding YR in the Munsell hue, so that for 10YR "H" is 10 and for 10R "H" is 0.

2.4.4. *Mineralogical analysis*

X-ray diffraction (XRD) was used to identify minerals in clay ($< 2\text{ }\mu\text{m}$), silt ($2\text{-}53\text{ }\mu\text{m}$) and fine sand ($53\text{-}2000\text{ }\mu\text{m}$) fractions from every diagnostic soil horizons. The different soil fractions were separated by dispersion with calgon and sedimentation in water. Diffraction patterns were obtained in a Shimadzu 6000 diffractometer fitted with a graphite monochromator set to select Cu K α radiation (30mA/40 kV). Prior to analysis, all clay samples were submitted to the following treatments: elimination of organic matter (15% hydrogen peroxide)

and iron oxides (dithionite-citrate-bicarbonate method) (Mehra and Jackson, 1960).

The following clay treatments were performed: Mg saturation, glycerol solvation, K saturation, followed by heating for three hours at 350 and 550 °C (Brown and Brindley, 1980). Silt and fine sand fractions were scanned from 5° to 70°2θ with steps of 0.02°2θ at 0.8 s/step while the XRD of clays were obtained from 3 to 35°2θ with steps of 0.02°2θ at 1.2 s/step, except for the glycerol solvation treatment (3-15°2θ). The mineral identification were based on the criteria proposed by Jackson (1975), Brown and Brindley (1980), and Moore Jr and Reynolds (1997).

2.4.5. Chemical weathering

Sample powders were mechanically compressed to make pellets for X-ray fluorescence (XRF) analysis. Molecular proportions of the major element (expressed as oxides) were determined by XRF spectrometry (S8 TIGER ECO - WDXRF). Loss on ignition was determined at 1,000 °C. Data were used to calculate the chemical index of alteration (CIA), according to Nesbitt and Young (1982):

$$\text{CIA} = [\text{Al}_2\text{O}_3 / (\text{Al}_2\text{O}_3 + \text{Na}_2\text{O} + \text{CaO} + \text{K}_2\text{O})] \times 100.$$

The results were verified using the international geochemical standard SRM 2709, San Joaquin soil (NIST, 2002). The recovery rates for major elements (%) were as follows: Al (106) > Ca (105) > Fe (100) > K (98) > Mg (96) > Na (72).

3. Results and discussion

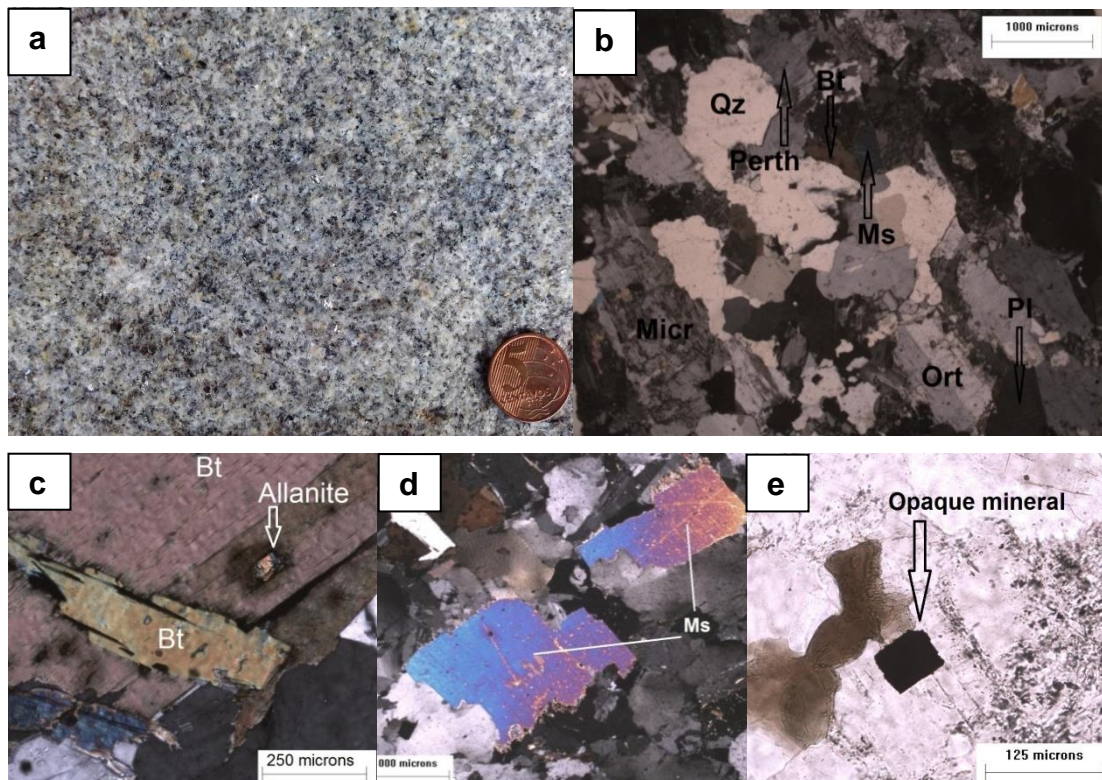
3.1. Mineralogy of the I- and S-type granites

Overall, S-type granites presented fine to medium grains, with light gray color (Figure 2a). They were mainly composed of quartz (ranging from 23 to 34%), feldspars (plagioclase ranging from 5 to 28%, microcline ranging from 11 to 33% and orthoclase ranging from 7 to 12%), muscovite (ranging from 3 to

6%) and biotite (ranging from 8 to 14%) evenly distributed and absence of magnetic minerals. These rock types showed gentle foliations outlined by mafic minerals.

I-type granites were inequigranular, porphyritic texture, with medium to coarse K-feldspars, small amounts of gray quartz and black mafic minerals, mostly biotite (Figure 3a). I-type granites presented magnetic minerals, mainly magnetite. K-feldspar, quartz, plagioclase and biotite were the dominant components of both granites types (Table 1).

Quartz and plagioclase were more abundant in S-type granites whilst K-feldspars and opaque minerals dominated I-type granites. Muscovite was present only in S-type granites, ranging from 3 to 6% and exhibiting some degree of alteration, chiefly being replaced by sericite. Amphibole, apatite and titanite were visualized only in I-type granites (Table 1). Magnetic minerals and minor amounts of chlorite predominated in I-type granites.



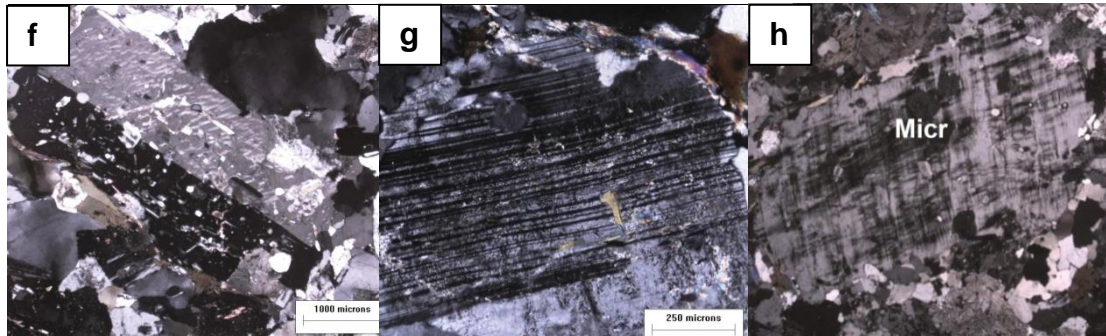


Figure 2. Macro-photograph (a) and selected petrographic characteristics of S-type granites. (b) General aspect; (c) Biotite and allanite; (d) Muscovite; (e) Opaque mineral; (f) Orthoclase; (g) Plagioclase; (h) Microcline. Qz– Quartz; Micr – Microcline; Ort – Orthoclase; Bt– Biotite; Pl – Plagioclase; Ms – Muscovite; Al – Allanite.

Biotites in I- and S-type granites were at an early alteration stage to chlorite. Plagioclases were slightly altered to sericites. K-feldspars were found as microcline and orthoclase. The phosphate mineral apatite occurred in small crystals and often associated with mafic minerals (Figure 3e). Allanite and titanite tend to occur in I-type rather than in S-type granites (Bea, 1992). Apatite inclusions are commonly found in biotites of I-type granites whereas in S-type granites they occur in larger discrete crystals, confirming the findings of Chappell and White (2001).

Table 1. Mineralogical composition (%) of I- and S-type granites sampled in Pernambuco State, Northeast Brazil

Mineral	I-type granites			S-type granites		
	Humid	Sub-humid	Dry	Humid	Sub-humid	Dry
K-feldspar	61	55	65	45	37	23
Quartz	12	7	8	23	26	34
Plagioclase	7	12	7	5	22	28
Biotite	10	11	5	14	12	8
Amphibole	4	4	7	nd	nd	nd
Sericite / Muscovite	nd	nd	nd	6	3	6
Opaque mineral	2	4	4	4	<1	1
Allanite	3	2	< 1	3	<1	< 1
Apatite	1	2	3	nd	nd	nd
Titanite	nd	2	1	nd	nd	nd
Chlorite	< 1	< 1	nd	nd	nd	< 1

Total	100	100	100	100	100	100
Ratio felsic/mafic minerals	4.0	2.9	4.0	3.7	6.8	9.1

Small inclusions of allanite were found in biotite (Figure 2c). The disintegration of allanite is responsible for biotite spot formations. Plagioclases were sericitized usually forming lamellae of muscovite/sericite.

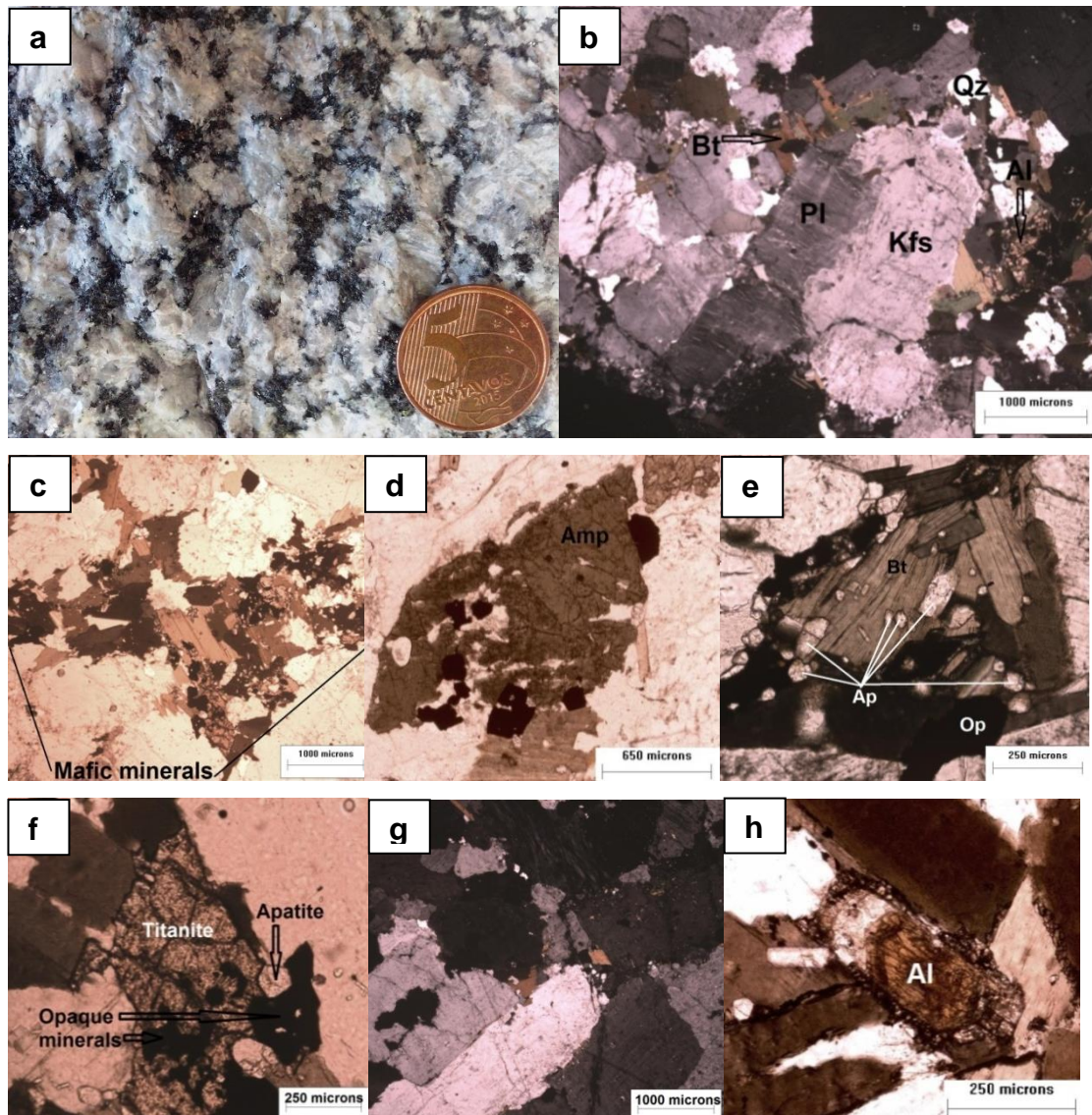


Figure 3. Macro-photograph (a) and selected petrographic characteristics of I-type granites. (b) General aspect; (c) Mafic minerals; (d) Amphibole; (e) Biotite, apatite and opaque minerals; (f) Titanite, apatite and opaque minerals; (g) Typical section, overview; (h) Allanite; Qz – Quartz; Kfs – K-feldspar; Bt– Biotite; PI – Plagioclase; Op – Opaque mineral; AI – Allanite.

3.2. Soil properties

3.2.1. Morphological, physical and chemical attributes

According to WRB (2014), lithic discontinuities are defined as significant differences in particle-size distribution or mineralogy that represent differences in parent material within a soil. Thus, the homogeneity of the depth distribution of soil particle sizes (Tables 2 and 3) as well as similar primary minerals between fine sand, silt and clay fractions (Figures 6 and 7) and granites (Figures 2 and 3) indicate that there was no interference of other parental materials.

Soil profiles developed from I- and S-type granites showed distinguished differences in morphological, physical and chemical properties (Tables 2 and 3). Soil profiles developed from I-type granites presented the highest mean silt and clay contents, especially in the humid climate (Tables 2 and 3). For both granite types, the highest clay contents were found in the humid zones (mean value of 24% and 22% for I- and S-type granite, respectively). Conversely, soils originating from S-type granites were sandiest irrespectively to climate zones with mean values of 45%, 80% and 86% for humid, sub-humid and dry zones.

The higher proportion of easily weathereable minerals in I-type granites favored the genesis of soils with higher clay contents. Soils developed from fine-grained granite exhibited higher clay contents (Mareschal et al. 2015). This texture influence results in a greater water retention potential, which in turn can enhance weathering reactions.

Despite similar climatic and topographic conditions in humid and sub-humid zone, soil colors of subsurface horizons from I- and S-type granites were clearly distinguishable (Tables 2 and 3). Soil horizons from I-type granite presented were redder than S-type granites. The dominance of red colors is further corroborated by the significantly higher values of the redness index found for I-type granite soils (mean RR values for subsurface horizons= 7.15 and hues from 2.5YR to 10YR); on the contrary, S-type granite soils present mean RR value of 1.61 and hues from 7.5 to 10YR.

Table 2. Selected macro-morphological and physical characteristics of soil profiles derived from I-type granites in different climatic zones of Pernambuco State, Northeast Brazil

Horizon/depth (cm)	Color (Moist)	Clay (g kg ⁻¹)	Silt	Sand	BD (g cm ⁻³)	Textural classes ^a	Structure ^b
Humid zone (537 m) – (Hypereutric Chromic Lixisols)							
A ₁ (0-8)	7.5YR 3/1	150	379	471	1.2	l	vf f gr (1); f m sbk (2)
A ₂ (8-18)	10YR 3/2	170	383	447	1.2	l	f m co sbk (2)
AB (18-30)	7.5YR 4/4	180	414	406	1.2	l	f m co sbk (2)
BA (30-46)	5YR 5/8	250	440	310	1.1	l	f m co sbk (2)
Bt ₁ (46-64)	2.5YR 4/8	300	507	193	1.0	scl	vf f m co sbk (2,3)
Bt ₂ (64-84)	2.5YR 4/8	310	506	184	0.9	scl	vf f m co sbk (2,3)
Bt ₃ (84-135)	2.5YR 4/8	300	522	178	1.0	scl	vf f m co sbk (3)
BC (135-175)	2.5YR 4/8	260	569	171	1.0	scl	f m co sbk (3)
C (175-195)	2.5YR 4/8	270	558	172	1.1	scl	f m co sbk (3)
Sub-humid zone (695 m) – (Eutric Regosols)							
A (0-11)	10YR 3/1	50	290	660	1.4	sdl	vf f gr (2); f sbk (2)
CA (11-17)	10YR 4/1	60	282	658	1.5	sdl	f m sbk (1)
C ₁ (17-46)	10YR 5/2	50	280	670	1.5	sdl	f m sbk (1)
C ₂ (46-70)	10YR 5/3	50	300	650	1.6	sdl	f m sbk (1)
C ₃ (70-78)	10YR 6/3	50	240	710	1.7	sdl	f sbk (1)
Cr ₁ (78-148)	-	-	-	-	-	-	-
Cr ₂ (148-185)	-	-	-	-	-	-	-
Cr ₃ (185-200)	-	-	-	-	-	-	-
Dry zone (473 m) – (Eutric Regosols)							
A (0-3)	10YR 2/2	50	195	755	1.1	sdl	f gr (1)
CA (3-9)	10YR3/2	80	304	616	1.4	sdl	f m sbk (1)
C ₁ (9-17)	10YR3/4	100	321	579	1.5	l	f m sbk (1)
C ₂ (17-27)	5YR3/3	110	308	582	1.4	l	f m sbk (1)
C ₃ (27-39)	5YR3/3	120	326	554	1.4	l	f m sbk (1)
Cr ₁ (39-53)	-	-	-	-	-	-	-
Cr ₂ (53-63)	-	-	-	-	-	-	-

^a Textural classes: loam (l); sandy clay loam (scl); sandy loam (sdl); silt loam (stl)

^b Structure (type/size/grade): subangular blocky (sbk); granular (gr); very fine (vf); fine (f); medium (m); coarse (co); prismatic (pr); weak (1); moderate (2); strong (3)

Table 3. Selected macro-morphological and physical characteristics of soil profiles derived from S-type granites in different climatic zones of Pernambuco State, Northeast Brazil

Horizon/depth (cm)	Color (Moist)	Clay (g kg ⁻¹)	Silt	Sand	BD (g cm ⁻³)	Textural classes	Structure
--------------------	---------------	----------------------------	------	------	--------------------------	------------------	-----------

Humid zone (348 m) – (Dystric Xanthic Ferralsols)							
A ₁ (0-9)	10YR3/1	200	244	556	1.3	scl	vf f m co gr (3)
A ₂ (9-20)	10YR4/1	200	263	547	1.2	scl	vf f gr(2); f m sbk (2)
AB (20-37)	10YR4/3	200	361	439	1.2	l	f m sbk (2)
BA (37-50)	10YR4/6	230	385	385	1.1	l	m; c; vf f sbk (2)
Bo ₁ (50-69)	10YR5/6	230	364	406	1.1	l	m; c; vf f sbk (1)
Bo ₂ (69-89)	7.5YR5/8	220	350	430	1.2	l	vf gr; vf f sbk (2)
Bo ₃ (89-109)	7.5YR5/8	200	362	438	1.2	l	vf gr; f m co sbk (1)
Bo ₄ (109-147)	7.5YR5/8	230	348	422	1.2	l	vf gr; f m co sbk (1)
Bo ₅ (147-165+)	7.5YR5/8	250	365	385	1.2	i	vf gr; f m sbk (1)
Sub-humid zone (738 m) – (Dystric Regosols)							
A (0-16)	7.5YR4/2	50	90	860	1.6	ls	g; vf f sbk (1)
AC (16-34)	7.5YR3/2	30	126	844	1.5	ls	g; vf f sbk (1)
CA (34-56)	7.5YR4/2	60	139	801	1.5	sl	m; f m sbk (1)
C ₁ (56-93)	7.5YR4/2	70	139	791	1.6	sl	m; f m sbk (1)
C ₂ (93-111)	7.5YR4/2	80	137	783	1.5	sl	m; f m sbk (1)
C ₃ (111-136)	7.5YR5/3	70	166	764	1.6	sl	m; f m sbk (1)
C ₄ (136-152)	7.5YR4/3	60	161	779	1.5	sl	m; f m sbk (1)
C ₅ (152-195)	7.5YR4/3	70	183	747	1.6	sl	m; f m sbk (1)
Cr (195-205+)	-	-	-	-	-	-	-
Dry zone (389 m) – (Eutric Regosols)							
Ap (0-5)	10YR7/2	40	51	909	1.7	ls	g; m co l (1); f m sbk (1)
CA (5-17)	10YR5/3	50	80	870	1.8	ls	g; f m sbk (1)
C ₁ (17-26)	10YR5/3	50	97	853	1.7	ls	m; vf f sbk (1)
C ₂ (26-40)	10YR5/3	50	113	837	1.7	ls	m; vf f sbk (1)
C ₃ (40-48)	10YR6/2	40	120	840	1.7	ls	m; vf f sbk (1)
Cr (48-59)	-	-	-	-	-	-	-

a Textural classes: sandy clay loam (scl); loam (l); loamy sand (ls); sandy loam (sl)

b Structure (type/size/grade): grain (g); laminar (l); subangular blocky (sbk); granular (gr); massive (m); cohesion (c) very fine (vf); fine (f); medium (m); coarse (co); prismatic (pr); weak (1); moderate (2); strong (3)

The contrasting results for soil color can be explained by the higher proportions of mafic, opaque and accessory minerals (Table 1). Upon weathering, these minerals release relatively large amounts of Fe (Table 4) that likely exceed the solubility product of ferrihydrite and favor the hematite pathway (Kampf and Schwertmann, 1983). The positive and highly significant correlation ($r= 0.874$; $n= 19$; $p < 0.0001$) between RR values and Fe_t for the I-granite soils (Figure 4) corroborates this hypothesis. Such correlation was not observed for soil profiles originated from S-type granites. The chemical

compositions of some of these opaque and mafic minerals are shown in Figure 5. Subsurface horizons derived from S-type granites showed predominance of yellowish colors (7.5YR and 10YR) resulting from the probable preferential formation of goethite; this iron oxide is readily bound to organic compounds, giving the soil brownish colors (Chen et al., 2010). Additionally, the lower proportions of Fe-bearing minerals in soils derived from S-type granites would preclude the hematite pathway (Table 4).

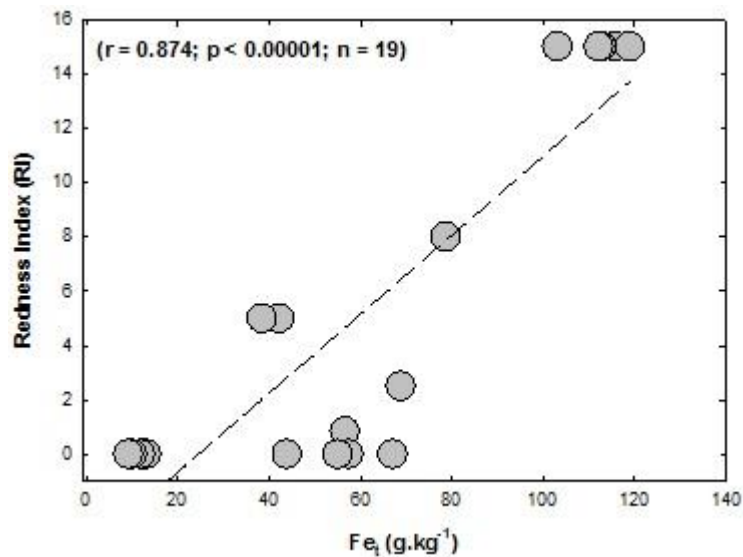


Figure 4. Relationship between redness index and total iron in a climosequence of soils derived from I-type granites in Northeast Brazil.

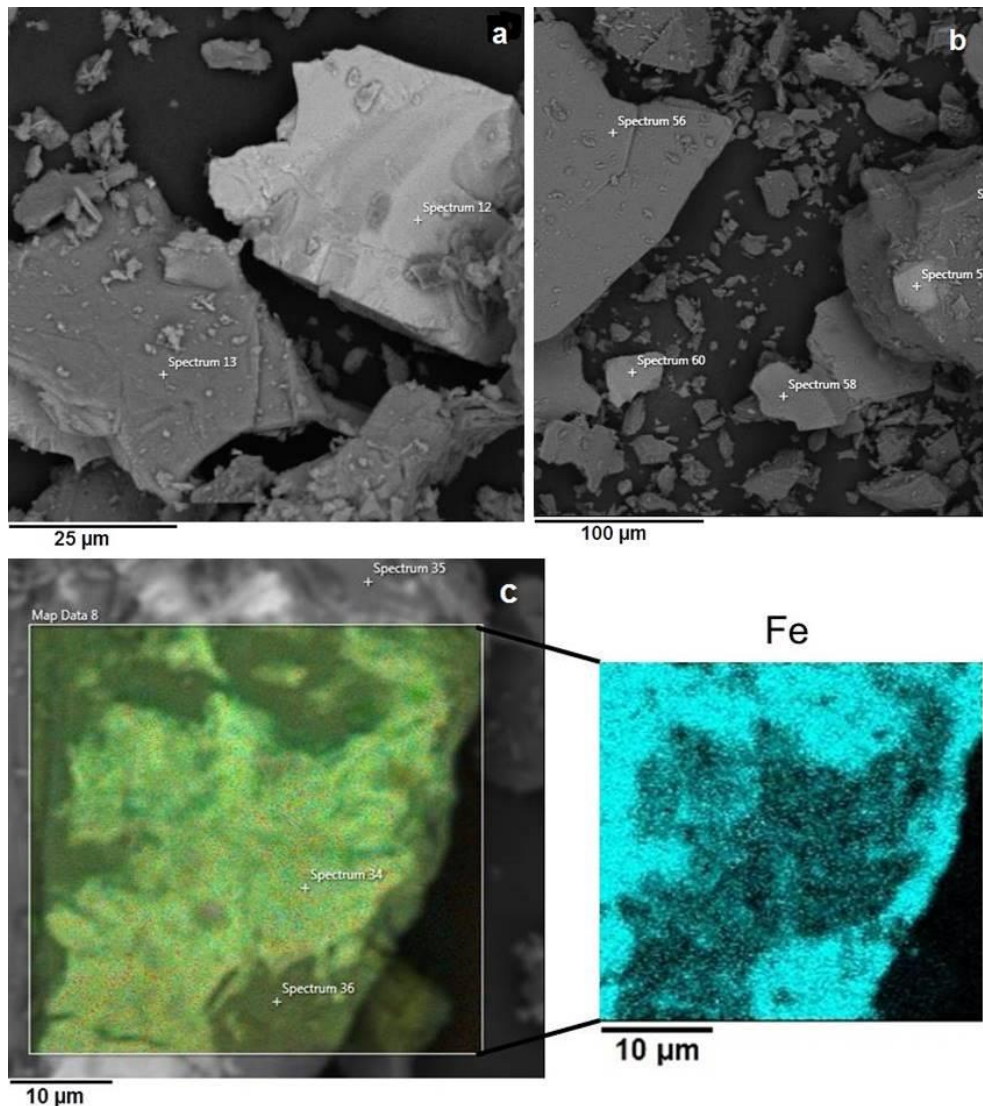


Figure 5. Scanning electron microscope (SEM) images captured from minerals in I-type granite and their respective elemental composition by energy dispersive X-ray spectrum (EDS). (a) Chemical composition of magnetite (Spectrum 12: Fe – 97%, Si – 2%, Al – 0.8, K – 0.2%), and biotite (Spectrum 13: Fe – 21%, Si – 38%, Al, K – 15%, Mg – 8%, Ti – 2%, Na – 1%). (b) Chemical composition of biotite (Spectrum 56: Si - 34%, Fe – 24%, Al - 15%, K – 14%, Mg – 9%, Ti – 3%, Na – 1%), biotite (Spectrum 57: Si - 48%, Fe – 21%, Al – 17%, K – 7%, Na – 6%, Ca – 1%), biotite (Spectrum 58: Si – 31%, Fe – 29%, Al, K – 14%, Mg – 8%, Ti – 3%, Na – 1%), ilmenite (Spectrum 60: Ti – 44%, Fe – 41.6%, Mn – 11%, Si – 1.6%, Al -1%, Na, K – 0.4%) (c) Semiquantitative Fe map from a cross-section of biotite with inclusion of bastnaesite using scanning electron microscope with energy-dispersive X-ray spectroscopy attached facilities (SEM-EDS). Bastnaesite (Spectrum 34: Ce -

32%, La – 20%, F – 13%, Nd – 9%, Ca – 8%, Si, Fe – 5%, Pr – 3%, Al, K – 2%, Mg – 1%), biotite (Spectrum 35: Si – 32%, Fe – 29%, Al – 15%, K – 13%, Mg – 8%, Ti – 2%, Mn – 1%), biotite (Spectrum 36: Si – 33%, Fe – 28%, Al – 16%, K – 13%, Mg – 8%, Ti – 2%).

Regarding chemical properties, soils from I- and S-type granites showed contrasting results as well. Soils developed from I-type granites showed higher soil fertility than those deriving from S-type granites (Table 4). There are clear differences with regards to base saturation (BS > 50%) levels and Al saturation (< 50%) in all climatic zones. These results can be explained by the greater proportion of mafic, opaque and accessory minerals (Table 1). On the other hand, soils derived from S-type granites only exhibit high BS levels and low Al saturation under the dry pedo-environment (Table 5). The effect of granite types on soil fertility was discussed elsewhere (Silva et al., 2016).

The mean TOC contents were always higher in soil profiles developed on I-type granites (Table 4 and 5). These soil profiles showed mean TOC values of 17.2, 12.0, 13.4 g kg⁻¹ for humid, sub-humid and dry zones. On the other hand, the mean TOC values for S-type granite soils were only 10.2, 2.6, 2.8 g kg⁻¹. As a result, TOC stocks in the I- and S-granite soils showed a clear climatic zonation with increasing values from the dry zone to the humid zone. It is important to highlight that, regardless climate, the highest TOC stocks were recorded in soil profiles developed from I-type granite soils (46 to 207 Mg ha⁻¹); S-type granite soils presented TOC stocks ranging from 23 to 150 Mg ha⁻¹ (Table 4).

This finding demonstrates that the parent material rather than the climate plays the most significant role on determining the soil carbon stocks. This outcome can result from both the natural higher soil fertility that allows biomass increasing and the higher clay contents in I-type soils. Additionally, the large surface area of clay minerals stabilizes soil organic carbon by forming stable organic-mineral complexes that protect C against microbial decomposition (Six et al., 2000; Six et al., 2002; Lehmann and Kleber, 2015).

Table 4. Chemical characterization, iron selective dissolution analysis and weathering index of soil profiles derived from I-type granites in different climatic zones of Pernambuco State, Northeast Brazil

Horizon/depth (cm)	TOC ^a (g kg ⁻¹)	TOC stock ^b Mg ha ⁻¹	pH (H ₂ O)	Na ⁺	Ca ²⁺	Mg ²⁺	K ⁺	H+Al	Al ³⁺ cmolc kg ⁻¹	CEC ^c	BS ^d	Sat. Al ^{3+e}	Fe _t ^f	Fe _o ^g	Fe _d ^h	Fe _d /Fe _o	CIA ⁱ (%)
Humid zone (537 m) – (Hypereutric Chromic Lixisols)																	
A ₁ (0-8)	59.6	59.1	5.5	0.1	3.4	1.2	0.7	3.2	0.0	8.5	63	0.5	56.6	2.2	3.6	1.6	90
A ₂ (8-18)	58.4	71.9	5.0	0.1	2.5	1.0	0.4	3.2	0.1	7.2	56	1.4	57.4	2.5	7.3	2.9	91
AB (18-30)	12.0	17.1	4.7	0.0	2.0	0.7	0.3	2.4	0.2	5.5	56	4.7	68.8	1.8	8.9	4.9	93
BA (30-46)	6.4	11.0	4.8	0.0	1.6	0.9	0.2	1.9	0.1	4.6	59	3.5	78.7	1.9	11.4	6.0	94
Bt ₁ (46-64)	5.7	11.1	5.2	0.1	2.1	0.5	0.1	1.5	0.0	4.2	64	0.0	103.1	1.8	18.0	10.0	97
Bt ₂ (64-84)	4.2	7.8	5.0	0.1	1.7	0.8	0.1	1.6	0.1	4.2	62	1.9	115.8	1.3	18.0	18.8	98
Bt ₃ (84-135)	1.5	7.7	5.0	0.1	0.9	1.6	0.1	1.4	0.1	4.0	65	1.9	119.0	1.6	17.8	11.1	98
BC (135-175)	3.7	15.3	5.0	0.2	0.4	1.9	0.1	1.3	0.0	3.8	65	0.0	112.8	1.3	17.2	13.2	98
C (175-195+)	3.1	6.6	4.8	0.1	0.7	1.4	0.1	1.3	0.3	3.6	64	10.6	112.2	1.6	14.4	9.0	98
Sub-humid zone (695 m) – (Eutric Regosols)																	
A (0-11)	45.3	67.4	5.2	0.1	4.7	1.3	0.2	2.9	0.1	9.1	68	1.6	12.3	1.7	9.2	5.4	70
CA (11-17)	7.0	6.3	5.2	0.1	3.0	0.9	0.1	1.7	0.1	5.8	70	1.2	13.1	1.8	9.5	5.2	71
C ₁ (17-46)	3.9	18.0	5.1	0.1	2.3	0.6	0.1	1.5	0.1	4.5	67	3.2	11.8	1.1	8.5	7.7	70
C ₂ (46-70)	2.1	8.3	5.5	0.1	1.9	0.5	0.0	0.9	0.1	3.4	73	3.9	10.0	1.4	10.9	7.8	68
C ₃ (70-78)	1.6	2.3	5.7	0.1	0.9	0.8	0.0	0.7	0.1	2.5	70	5.5	9.2	1.6	12.4	7.7	64
Cr ₁ (78-148)	-	-	-	-	-	-	-	-	-	-	-	-	-	-	-	-	93
Cr ₂ (148-185)	-	-	-	-	-	-	-	-	-	-	-	-	-	-	-	-	87
Cr ₃ (185-200)	-	-	-	-	-	-	-	-	-	-	-	-	-	-	-	-	79
Dry zone (473 m) – (Eutric Regosols)																	
A (0-3)	39.6	13.5	7.1	0.0	7.3	2.7	0.5	1.0	0.0	10.6	100	0.0	67.0	1.4	2.0	1.4	56
CA (3-9)	11.3	9.7	6.9	0.1	4.6	5.8	0.4	1.1	0.0	10.8	100	0.0	55.0	1.7	4.6	2.7	70
C ₁ (9-17)	7.1	8.3	6.0	0.1	6.1	1.1	0.2	1.3	0.1	7.5	100	0.7	43.9	1.6	4.7	2.9	74
C ₂ (17-27)	5.0	7.1	5.5	0.1	5.6	2.3	0.2	1.6	0.1	8.2	100	0.9	42.2	1.5	4.8	3.2	76
C ₃ (27-39)	4.1	7.0	5.1	0.2	7.3	0.4	0.1	1.9	0.2	8.0	100	1.8	38.4	1.6	4.9	3.1	78
Cr ₁ (39-53)	-	-	-	-	-	-	-	-	-	-	-	-	-	-	-	-	83
Cr ₂ (53-63+)	-	-	-	-	-	-	-	-	-	-	-	-	-	-	-	-	75

^a Total organic carbon; ^b Carbon stock; ^c Cation Exchange capacity; ^d Base saturation; ^e Aluminum saturation; ^f Total iron; ^g oxalate extractable iron; ^h

Dithionite extractable iron; ⁱ Chemical index of alteration.

Table 5. Chemical characterization, iron selective dissolution analysis and weathering index of soil profiles developed from S-type granites in different climatic zones in three climatic zones of Pernambuco State, Northeast Brazil

Horizon/depth (cm)	TOC ^a (g kg ⁻¹)	TOC stock ^b Mg ha ⁻¹	pH (H ₂ O)	Na ⁺	Ca ²⁺	Mg ²⁺	K ⁺	H+Al (cmol _c kg ⁻¹)	Al ³⁺	CEC ^c	BS ^d	Sat. Al ^{3+e}	Fe _t ^f	Fe _o ^g	Fe _d ^h (g kg ⁻¹)	Fe _d /Fe _o	CIA ⁱ (%)
Humid zone (348 m) – (Dystric Xanthic Ferralsols)																	
A ₁ (0-9)	39.7	45.8	4.6	0.1	1.7	0.9	0.2	4.3	0.7	7.1	39	20.7	20.6	1.9	3.1	1.6	91
A ₂ (9-20)	14.8	15.8	4.3	0.0	0.7	0.8	0.1	4.2	1.3	5.8	28	44.0	24.8	2.0	5.9	2.9	94
AB (20-37)	9.0	17.6	4.2	0.0	0.7	0.5	0.1	3.4	1.6	4.6	26	56.5	29.9	1.7	5.3	3.1	95
BA (37-50)	7.0	10.2	4.1	0.0	0.9	0.6	0.0	2.7	1.1	4.3	37	39.8	32.3	1.3	5.9	4.5	95
Bo ₁ (50-69)	4.2	9.1	4.2	0.0	0.5	0.6	0.0	1.9	1.2	3.0	38	51.1	35.0	0.7	6.2	8.8	96
Bo ₂ (69-89)	3.9	9.1	4.1	0.0	0.6	0.3	0.0	1.8	1.1	2.7	33	55.8	33.3	0.6	5.4	9.0	95
Bo ₃ (89-109)	3.6	8.3	4.1	0.0	0.6	0.2	0.0	1.7	1.1	2.5	33	55.5	32.4	0.7	4.6	6.6	95
Bo ₄ (109-147)	5.5	25.7	4.2	0.0	0.5	0.5	0.0	1.6	1.1	2.5	38	52.3	36.8	0.9	4.2	4.7	96
Bo ₅ (147-165)	4.0	8.4	4.1	0.0	0.3	0.6	0.0	1.7	1.1	2.6	38	51.8	41.3	0.8	3.7	4.6	96
Sub-humid zone (738 m) – (Dystric Regosols)																	
A (0-16)	4.4	11.1	4.3	0.0	1.1	1.2	0.1	1.7	0.0	4.1	58	1.4	5.0	0.3	4.1	13.7	79
AC (16-34)	2.8	7.7	4.1	0.0	0.4	0.3	0.2	2.0	0.4	2.8	28	35.0	8.5	0.4	3.8	9.5	83
CA (34-56)	3.3	11.2	3.8	0.0	0.3	0.2	0.1	2.2	1.0	2.8	21	62.3	10.2	0.6	5.6	9.3	83
C ₁ (56-930)	3.6	21.3	3.7	0.0	0.2	0.5	0.0	2.2	1.1	3.0	25	59.4	12.1	0.8	4.3	5.3	85
C ₂ (93-111)	2.6	7.2	3.9	0.2	0.2	0.4	0.0	2.4	1.1	3.2	25	58.4	8.2	0.7	3.8	5.4	84
C ₃ (111-136)	1.3	5.2	3.8	0.1	0.3	0.3	0.1	2.0	1.2	2.8	28	59.7	8.9	0.5	3.8	7.6	84
C ₄ (136-152)	1.4	3.5	4.0	0.1	0.3	0.2	0.1	1.7	1.2	2.3	25	66.6	10.8	0.3	3.8	12.7	82
C ₅ (152-195)	1.2	8.1	4.2	0.1	0.6	0.5	0.1	1.1	0.9	2.3	53	41.4	9.9	0.2	4.1	20.5	82
Cr (95-205)	-	-	-	-	-	-	-	-	-	-	-	-	-	-	-	-	72
Dry zone (389 m) – (Eutric Regosols)																	
Ap (0-5)	4.6	4.0	6.0	0.0	1.0	1.3	0.2	0.3	0.0	2.8	88	0.0	4.7	0.0	0.3	0.0	58
CA (5-17)	3.2	6.8	5.3	0.0	0.4	1.2	0.1	0.5	0.2	2.2	75	8.2	4.4	0.0	0.3	0.0	61
C ₁ (17-26)	2.0	3.1	5.2	0.0	0.7	0.7	0.2	0.7	0.3	2.2	70	16.0	4.9	0.0	0.3	0.0	62
C ₂ (26-46)	2.6	6.2	4.8	0.0	0.5	1.2	0.1	0.6	0.3	2.4	74	14.6	5.3	0.0	0.3	0.0	62
C ₃ (40-48)	1.8	2.5	5.2	0.0	0.8	1.1	0.1	0.5	0.2	2.4	81	7.0	5.4	0.0	0.3	0.0	61
Cr (48-59)	-	-	-	-	-	-	-	-	-	-	-	-	-	-	-	-	62

^a Total organic carbon; ^b Carbon stock; ^c Cation Exchange capacity; ^d Base saturation; ^e Aluminum saturation; ^f Total iron; ^g oxalate extractable iron; ^h Dithionite extractable iron; ⁱ Chemical index of alteration.

3.2.2. Selective dissolution

The Fe_d and Fe_o contents in I-type were always higher than in S-type granite soils (Table 4 and 5) and varied from 2.0 to 18.0 $g\ kg^{-1}$ and 1.4 to 2.5 $g\ kg^{-1}$, respectively, from dry to humid zone. The Fe_t values followed a similar pattern with highest values in I-type granite soils. Soil samples from both humid zones exhibited the highest Fe_d and Fe_o contents (Table 4). In opposite, lower Fe_d and Fe_o contents were found in soils derived from S-type granites (Table 5); these values ranged from 0.3 to 6.2 $g\ kg^{-1}$ and 0.0 to 2.0 $g\ kg^{-1}$, respectively, from the dry to the humid zone. Irrespective to the granite type, Fe_d values increased with depth whereas the Fe_o contents decreased. It occurs due to the organic matters are concentrated on the soil surface.

3.2.3. Mineralogy

3.2.3.1. Fine sand and silt fraction

According to the XRD patterns of fine sand and silt, there were visible changes in the mineral assemblages of soils developed from both granites (Figures 6 and 7). Fine sand and silt fractions from I-types showed greater diversity of primary most weatherable minerals (i.e. presence of amphiboles - 0.84 nm) when compared to soils from S-type granite (Figure 6i). Soil samples from S-type granites showed a mineral assemblage mostly dominated by least weatherable minerals, such as quartz (0.42 and 0.33 nm) and feldspars (e.g. 0.64, 0.38, 0.32, 0.31 nm) (Figure 4i). Regardless granite types, the highest quantities of primary minerals were found in the driest climate. Higher relative weathering intensities for both granite types were observed in the humid zone; additionally, in the humid climate, the diversity of feldspars decreased (Figure 6a, b) while no amphiboles were detected (Figure 6a, e).

3.2.3.2. Clay fraction

The presence of kaolinite, illite, an interstratified illite-vermiculite and gibbsite was observed in the XRD of oriented aggregates (Figures 6d, 6h, 6i and 7d, 7h, 7i). Kaolinite was recognized by its characteristic (001) and (002)

peak reflections at 0.71 and 0.35 nm, respectively. The disappearance of these peaks upon heating (550 °C) confirmed the presence of kaolinite and the absence of chlorite in all samples. Peaks at 1.0 nm after ethylene glycol solvation treatment confirm the presence of mica.

Powder XRD of the clay fraction from soils of I- and S-type granites revealed kaolinite as the dominant mineral (peaks at 0.71 and 0.35 nm), with minor amounts of quartz and feldspar (Figures 6 and 7). Greater proportions of primary minerals were identified in the dry zone, mainly in soils developed from S-type granites (Figure 7k). The more humid zones seemed to have favored kaolinitic soils (Figures 6c, 7c). The main contrasting mineralogical pattern between granites was the identification of goethite (peak at 0.41 nm) in soils derived from I-type granites (Figure 6c).

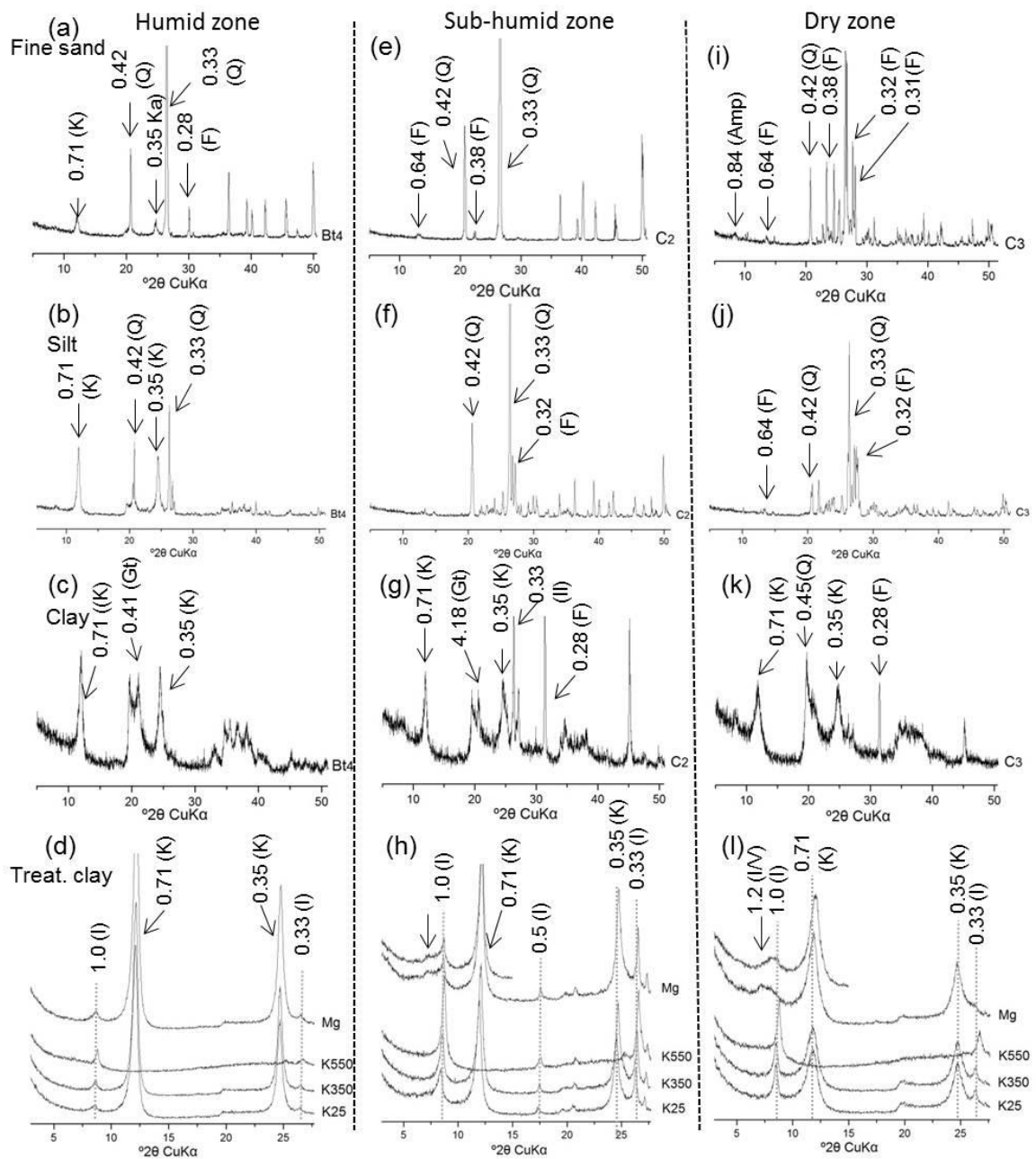


Figure 6. X-ray diffraction patterns for fine sand, silt, clay and various clay treatments obtained from diagnostic horizons of soil profiles derived from I-type granites in different climatic zones of Pernambuco State, Northeast Brazil. Diagnostic horizon of the Lixisols (Bt₄) under humid zone (a, b, c, d); Diagnostic horizon of the Regosols (C₂) under sub-humid zone (e, f, g, h); Diagnostic horizon of the Regosols (C₃) under Dry zone (i, j, k, l). Q – Quartz; F – Feldspar; Amp – Amphibole; K – Kaolinite; Gt – Goethite; I – Illite; I / V – Interstratified illite-vermiculite.

Peaks at 1.2 nm (Figure 6l) were identified in I-type granite soils from the dry zone and are probably related to an interstratified illite-vermiculite mineral. This mineral is commonly formed from the initial alteration of biotite. In contrast, the S-type samples showed no evidence of a mixed-layered illite-vermiculite (Figure 7l). The two granite types, from both the dry and the humid zones formed typical kaolinitic soils, with minor amounts of illites (Figures 6d, 7d). Gibbsite (peak 0.48 nm) was only found in soils derived from S-type granite from the humid zone (Figure 5d).

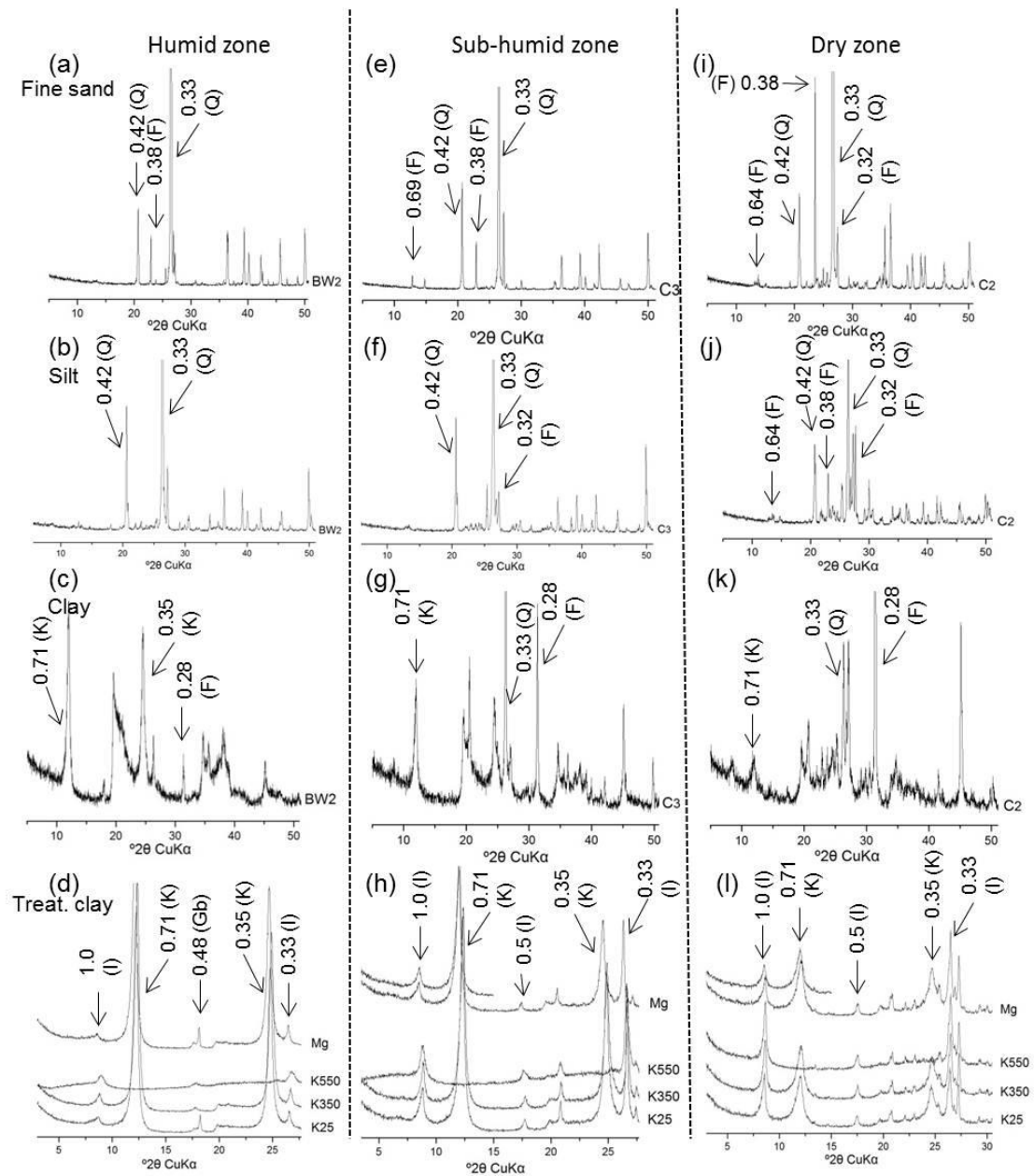


Figure 7. X-ray diffraction patterns for fine sand, silt, clay and various clay treatments obtained from diagnostic horizons of soil profiles derived from S-type granites in different climatic zones of Pernambuco State, Northeast Brazil. Diagnostic horizon of the Ferralsols (Bw_2) under humid zone (a, b, c, d); Diagnostic horizon of the Regosols (C_3) under sub-humid zone (e, f, g, h); Diagnostic horizon of the Regosols (C_2) under dry zone (i, j, k, l). Q – Quartz; F – Feldspar; K – Kaolinite; Gb – Gibbsite; I – Illite.

3.2.4. Weathering and mineral transformation

The degree of weathering of soils originating from I- and S-type granites varied systematically in the different climatic zones (Tables 4 and 5). Overall, the weathering intensity decreased in the following order: humid zone > sub-humid zone > dry zone. The chemical indexes of alteration (CIA) values in humid zones were higher than 90%. In the sub-humid zone, the mean CIA values were 75% and 81% for soils derived from I- and S-type granites, respectively. The lowest CIA values were found in the dry zone, with mean values of 73% and 61% for soils derived from I- and S-type granites, respectively.

The climate effect was clearly expressed on the soil properties regardless the parent material, i.e., soils from the humid zones were subjected to more intensive weathering (mean CIA values of 95%). The higher clay contents (15-31% and 20-25%, for I- and S-types, respectively), higher chroma colors in subsurface horizons (yellowish in S-type and reddish in I-type), lower BS, lower pH values and higher Al saturation percentages also indicate the more intensive weathering process. Several studies on climosequence (Barbosa et al., 2015; Egli et al., 2003) found significant similar climate effects in soil properties.

Weathering intensity and mineral transformations changed significantly along the climosequence. Weathering intensities were highest in soil profiles located in the humid zone. The mineral assemblage in the humid zones is dominated by kaolinites and crystalline Fe-oxyhydroxides (Figures 6d and 7d) and CIA values are close to 100% (Table 4 and 5). This finding demonstrates strong feldspar weathering and loss of cations (Rasmussen et al., 2010).

Several authors observed the prevalence of secondary minerals, i.e. kaolinite and Al–Fe (hydro)oxides, under warm, wet and tropical conditions, with increase in annual rainfall and a large rate of desilication (Kleber et al., 2007).

The Regosols in the sub-humid and dry zones exhibited good drainage that facilitated the monosialitization process owing to easily promote loss of alkali and alkaline earth metals. This makes possible the formation and predominance of kaolinite in the clay fraction (Figures 6 and 7). In Brazilian semiarid region is very common the predominance of kaolinite in well-drained soils derived from Regosols (Santos et al., 2012).

4. Conclusion

This study assessed the weathering processes and organic carbon stocks of soils developed on I- and S-type granites along a climosequence ranging from semiarid lands to humid zones. Significant differences in morphological, physical and chemical properties of soils derived from I- and S-type granites were observed and directly linked to petrological, mineralogical and geochemical signatures of the underlying granites. Despite the influence of the climate on weathering patterns, i.e., higher soil development in humid areas, parent material seems to play a more decisive role in determining soil characteristics in the studied region. For instance, owing to the higher concentration of Fe leading to hematite formation, soils developed from I-type granites are more reddish while S-type granite soils pose yellowish colors related to goethite. The type of parent material also governed the rates of carbon accumulation in soils. I-type granites originated soils with higher TOC stocks than soil profiles developed from S-type granites. This carbon accumulation is mainly due to soil chemical and physical characteristics driven by the type of granite, notably soil fertility and clay content that boost both the biomass production and the carbon protection against biodegradation. Thus, soil developed from I-type granites can, regardless the climate of the region where they lie, play a more important role in ecosystems services such as regulation of watersheds, forestry and agriculture production, carbon sequestration and mitigation of soil degradation than soils originating from S-types granites. Our data highlight the importance of the mineralogy and chemistry of granite types in order to understand the relationship between parent materials and climate conditions. However, the hypothesis that the difference between soil properties can be attributed to the difference of the types of granite needs further validation. Such knowledge is important not only to assess the variables governing the weathering processes and soil characteristics but also the soil functioning in the environment as a whole.

5. References

- Akpa, S.I.C., Odeh, I.O.A., Bishop, T.F.A., Hartemint, A.E., Amapu, I.Y., 2016. Total soil organic carbon and carbon sequestration potential in Nigeria. *Geoderma*. 271, 202–215.
- Almeida, M.E., Moacir, J.B., Macambira, B., Elma, C.O., 2007. Geochemistry and zircon geochronology of the I-type high-K calc-alkaline and S-type granitoid rocks from southeastern Roraima, Brazil: Orosirian collisional magmatism evidence (1.97–1.96 Ga) in central portion of Guyana Shield. *Precambrian Research*. 155, 69–97.
- Antunes, I.M.H.R., Neiva, A.M.R., Silva, M.M.V.G., Corfu, F., 2008. Geochemistry of S-type granitic rocks from the reversely zoned Castelo Branco pluton (central Portugal). *Lithos*. 103, 445–465.
- Antunes, I.M.H.R., Neiva, A.M.R., Silva, M.M.V.G., Corfu, F., 2009. The genesis of I- and S-type granitoid rocks of the Early Ordovician Oledo pluton, Central Iberian Zone (central Portugal). *Lithos*. 111, 168–185.
- Barbosa, W.R., Romero, R.E., Souza Júnior, V.S., Cooper, M., Sartor, L.R., Partiti, C.S.M., Jorge, F.O., Cohen, R., Jesus, S.L., Ferreira, T.O., 2015. Effects of slope orientation on pedogenesis of altimontane soils from the Brazilian semiarid region (Baturité massif, Ceará). *Environ Earth Sciences* 73, 3731–3743.
- Bea, F., Fershtater, G., Corretge, L.G., 1992. The geochemistry of phosphorus in granite rocks and the effect of aluminium. *Lithos* 29, 43–56.
- Bird, M.I., Veenedal, E.M., Moyo, C., Frost, Lloyd J., 2000. Effect of fire and soil texture on soil carbon in sub-humid savanna (Matopos, Zimbabwe). *Geoderma* 94, 71–90.
- Birkeland, P.W., 1999. *Soils and Geomorphology*. Oxford University Press, New York.

Blum, W.E.H., Warkentin, B.P., Frossard, E., 2006. Soil, human society and the environmental. Geological Society, London, Special Publication 266, 1-8.

Brazil. 2001. Mistério de Minas e Energia. Geologia e recursos minerais do Estado de Pernambuco. Serviço Geológico do Brasil e do Estado de Pernambuco, Recife, CPRM.

Brito, L.T.L., Moura, M.S.B., Gama, G.F.B., 2007. Potencialidades da água de chuva no Semiárido brasileiro. Petrolina: Embrapa Semi-Árido. 181p.

Brito Neves, B. B. de. 1975. Regionalização geotectônica do Pré-cambriano nordestino. São Paulo. Tese de Doutorado. Instituto de Geociências, Universidade de São Paulo, Tese de Livre Docência 198p.

Brown, G., Brindley, G.W., 1980. X-ray diffraction procedures for clay mineral identification. In: Brindley, G.W., Brown, G. (Eds.), Crystal Structures of Clay Minerals and their X-ray Identification. Mineralogical Society. 305– 360pp.

Brye, K., Kucharik, C.J., 2003. Carbon and nitrogen sequestration in two prairie topochronosequences on contrasting soils in southern Wisconsin. American Midland Naturalist Journal 149, 90–103.

Burke, I.C., Yonker, C.M., Parton, W.J., Cole, C.V., Flach, K., Schimel, D.S., 1989. Texture, climate, and cultivation effects on soil organic matter in U.S. grassland soils. Soil Science Society of America Journal 53, 800–805.

Canosa, F., Izard, A.M., Fuente, M.F., 2012. Evolved granitic systems as a source of rare-element deposits: The Ponte Segade case (Galicia, NW Spain). Lithos 153, 165–176.

Chappell, B.W., 1999. Aluminium saturation in I- and S-type granites and the characterization of fractionated haplogranites. Lithos 46, 535–551.

Chappell B.W., White A.J.R., 1974. Two contrasting granite types. Pacific Geology 8, 173–174

Chappell B.W., White A.J.R. 2001. Two contrasting granite types: 25 years later. Australian Journal of Earth Sciences 48, 489–499.

- Chappell, B.W., White, A.J.R., 1984. I- and S- type granites in the Lachlan Fold Belt. southeastern Australia. In: Keqin. Xu..Guangchi. Tu. (Eds.). *Geology of Granites and their Metallogenic Relation*. Beijing Science Press. pp. 87–101.
- Chappell, B.W., Bryant, C.J., Wyborn, D., 2012. Peraluminous I-type granites. *Lithos* 153,142–153.
- Chen, T., Xie, Q., Xu, H., Chen, J., Ji, J., Lu, H., Balsam, W., 2010. Characteristics and formation mechanism of pedogenic hematite in Quaternary Chinese loess and paleosols. *Catena* 81, 217–225.
- Clemens, J.D., 2003. S-type granitic magmas – petrogenetic issues, models and evidence. *Earth Science Reviews* 61,1–18.
- Clemens, J.D., Stevens, G., Farina, F., 2011. The enigmatic sources of I-type granites: The peritectic connexion. *Lithos* 126, 174–181.
- De Deyn, G.B., Cornelissen, J.H.C., Bardgett, R.D., 2008. Plant functional traits and soil carbon sequestration. *Ecology Letters* 11, 516–531.
- Dlamini, P., Chivenge, P., Chaplot, V., 2016. Overgrazing decreases soil organic carbon stocks the most under dry climates and low soil pH: A meta-analysis shows. *Agriculture, Ecosystems and Environment* 221, 258–269.
- Drumond, M.A., Santana, A.C., Antoniole, A., 2004. Recomendações para o usosustentável da biodiversidade no biomacaatinga. In: *Biodiversidade da Caatinga: Áreas e ações prioritárias para a conservação*. Brasília: MMA-UFRPE; Brasília, DF: p. 47-90.
- Egli, M., Mirabella, A., Sartori, G., Fitze, P., 2003. Weathering rates as a function of climate: results from a climosequence of the Val Genova (Trentino, Italian Alps). *Geoderma* 111, 99–121.
- Egli, M., Mirabella, A., Sartori, G., Giaccari, D., Zanelli, R., Plötze, M., 2007. Effect of slope aspect on transformation of clay minerals in Alpine soils. *Clay Minerals* 42, 375–401.

Embrapa—Brazilian Agricultural Research Corporation, 2011. Manual de Métodos de Análise de Solo. Embrapa, Rio de Janeiro.

Farahat, E.S., Mohamed, H.A., Ahmed, A.F., El Mahallawi, M.M., 2007. Origin of I- and A-type granitoids from the Eastern Desert of Egypt: Implications for crustal growth in the northern Arabian–Nubian Shield. *Journal of African Earth Science* 49, 43–58.

Ferreira, V.P., Sial, A.N., Sá, E.F.J., 1998. Geochemical and isotopic signatures of Proterozoic granitoids in terranes of the Borborema structural province, northeastern Brazil. *Journal South American Earth Sciences* 5, 439-455.

Foden, J., Sossi, P.A., Wawryk, C.M., 2015. Fe isotopes and the contrasting petrogenesis of A-, I- and S-type granite. *Lithos* 32 (44), 212-215.

Frost B.R., Barnes C.G., Collins W.J., Arculus R.J., Ellis D.J., Frost C.D. 2001. A geochemical classification for granitic rocks. *Journal of Petrology* 42, 2033–2048.

Gee, G.W., Or, D., 2002. Particle size analysis. In: Dane, J.H., Topp, C.T. *Methods of soil analysis: physical methods*. Cap II, p.255-289, SSSA, Madison, 866p.

Ghani, A.A., 2000. The Western Belt granite of Peninsular Malaysia: some emergent problems on granite classification and its implication. *Geosciences Journal* 4 (4), 283–293.

Gontier, A., Rihs, S., Chabaux, F., Lemarchand, D., Pelt, E., Turpault, M.P., 2015. Lack of bedrock grain size influence on the soil production rate. *Geochimica et Cosmochimica Acta* 166,146–164.

Guan, Y., Yuan, C., Sun, M., Wilde, S., Long, X., Huang, X., Wang, Q., 2014. I-type granitoids in the eastern Yangtze Block: implications for the Early Paleozoic intracontinental orogeny in South China. *Lithos* 206 (207), 34-51.

Guani, A.A., Searle, M., Robb, L., Chung, S., 2013. L. Transitional I S type characteristic in the Main Range Granite. Peninsular Malaysia. *Journal of Asian Earth Sciences* 76, 225-240.

Healy, B., Collins, W.J., Richards, S.W., 2004. A hybrid origin for Lachlan S-type granites: the Murrumbidgee Batholith example. *Lithos* 78, 197– 216.

INMET. 2015. Instituto Nacional de Meteorologia. Available in <http://www.inmet.gov.br/portal/index.php?r=clima/normaisclimatologicas>.

Accessed in: 16 de nov. de 2015.

IUSS Working Group WRB., 2014. World Reference Base for Soil Resources. World Soil Resources Report No. 106, FAO, Rome.

Jackson, M.L., 1975. Soil chemical analysis: advanced course. 29ed. Madison, University of Wisconsin, 895p.

Kahle, M., Kleber, M., Torn, M. S., and Jahn, R., 2012. Carbon storage in coarse and fine clay fractions of illitic soils, *Soil Science Society of America Journal* 67, 1732–1739.

Kaiser, K., Guggenberger, G., 2007. Sorptive stabilization of organic matter by microporous goethite: sorption into small pores vs. surface complexation. *European Journal of Soil Science* 58, 45–59.

Kampf, N., Schwertmann, U., 1983. Goethite and hematite in a climosequence in southern Brazil and their application in classification of kaolinitic soils. *Geoderma* 29, 27-39.

Kleber, M., Schwendenmann, L., Veldkamp, E., Rossner, J., Jahn, R., 2007. Halloysite versus gibbsite: silicon cycling as a pedogenetic process in two lowland neotropical rain forest soils of La Selva, Costa Rica. *Geoderma* 138 (1–2), 1–11.

Koppen, W.P., 1931. *Grundriss der Klimakunde*. 2nd ed. Berlin: Walter de Gruyter. 388p.

Lehmann, J., Kleber, M., 2015. The contentious nature of soil organic matter. *Nature* 528(7580), 60-68.

Litvinovsky, B.A., Jahn, B.M., Eyal, M., 2015. Mantle-derived sources of syenites from the A-type igneous suites — New approach to the provenance of alkaline silicic magmas. *Lithos* 232, 242–265.

Mareschal, L., Turpault, M.P., Ranger, J., 2015. Effect of granite crystal grain size on soil properties and pedogenic processes along a lithosequence. *Geoderma* 249 (250), 12–20.

Mckeague, J.A., Day, J.H., 1966. Dithionite- and oxalate-extractable Fe and Al as aids in differentiating various classes of soils. *Can. J. Soil Sci.* 46(1), 13-22.

Mehra, O.P., Jackson, M.L., 1960. Iron oxide removal from soils and clays by a dithionite-citrate system buffered with sodium bicarbonate. *Clays Clay Minerals* 7, 317-327.

Moore, D.M., Reynolds, R.C., 1997. X-ray diffraction and the identification and analysis of clay minerals. Oxford University Press, Oxford

Murphy, C.P., 1986. Thin section preparation of soils and sediments. Berkhamsterd: Academic Publis. 145p.

Nascimento, C.W.A., Oliveira, A.B., Ribeiro, M.R., Melo, É.E.C., 2006. Distribution and availability of zinc and copper in benchmark soils of Brazil. *Commun. Soil Sci. and Plan. Anal.*, Athens 37(1-2), 109-125.

NIST - National Institute of Standards and Technology. Standard Reference Materials -SRM 2709, 2710 and 2711 Addendum Issue Date: 18 January 2002.

Nesbitt, H.W., Young, G.M., 1982. Early Proterozoic climates and plate motions inferred from major element chemistry of lutites. *Nature* 299 (5885), 715–717.

Rasmussen, C., Dahlgren, R.A., Southard, R.J., 2010. Basalt weathering and pedogenesis across an environmental gradient in the Southern Cascade Range, California, USA. *Geoderma* 154, 473–485.

Robinson, F.A., Foden, J.D., Collins, A.S., 2015. Geochemical and isotopic constraints on island arc, synorogenic, post-orogenic and anorogenic granitoids in the Arabian Shield, Saudi Arabia. *Lithos* 220 (223), 97–115.

Santos, J.C.B., de Souza Jr., V.S., Correa, M. M., de Almeida, M. C., Borges, L.E.P., 2012. Characterization of regosols in the Semiarid region of Pernambuco, Brazil. *Braz. J. Soil Sci.* 36, 683-695.

Schoeneberger, P.J., 2002. Field book for describing and sampling soils. Government Printing Office.

Schmidt, M.W., Torn, M.S., Abiven, S., Dittmar, T., Guggenberger, G., Janssens, I.A. et al., 2011. Persistence of soil organic matter as an ecosystem property. *Nature* 478(7367), 49-56.

Silva, Y.J.A.B., Nascimento, C.W.A., Van Straaten, P., Biondi, C.M., Souza Júnior, V.S., Silva, Y.J.A.B., 2016. Effect of I and S type granite parent material mineralogy and geochemistry on soil fertility: a multivariate statistical and gis-based approach. *Catena* (Accepted for publication).

Six, J., Elliot, E.T., Paustian, K., 2000. Soil macroaggregate turnover and microaggregate formation: a mechanism for C sequestration under no-tillage agriculture. *Soil Biology and Biochemistry* 32, 2099–2103.

Six, J., Conant, R.T., Paul, E.A., Paustian, K., 2002. Stabilization mechanisms of organic matter: implications for C-saturation of soils. *Plant and Soil* 241, 155–176.

Skjemstad, J.O., Clarke, P., Taylor, J.A., Oades, J.M., McClure, S.G., 1996. The chemistry and nature of protected carbon in soil. *Australian Journal of Soil Research* 34, 251–271.

Sorensen, L.H., 1981. Carbon-nitrogen relationships during the humification of cellulose in soils containing different amounts of clay. *Soil Biology and Biochemistry* 13(4), 313-321.

Souza, F.P., Ferreira, T.O., Mendonça, E.S., Romero, R.E., Oliveira, J.G.B., 2012. Carbon and nitrogen in degraded Brazilian semiarid soils undergoing desertification. *Agriculture, Ecosystems and Environment* 148, 11–21.

Rasmussen, C., Southard, R.J., Horwath, W.R., 2008. Litter type and soil minerals control temperate forest soil carbon response to climate change. *Global Change Biology* 14 (9), 2064–2080.

Thomas, W.W., Carvalho, A.M.V., Amorim, A.M.A., Arbelaez, A.L., 1998. Plant endemism in two forests in southern Bahia, Brazil. *Biodiversity and Conservation* 7 (3), 311-322.

Torrent, J., Schwertmann, U., Fechter, H., Alferez, F., 1983. Quantitative relationships between soil color and hematite content. *Soil Science* 136(6), 354-358.

Van Schmus, W.R., Oliveira E.P., Silva A.F.F., Toteu S.F., Penaye J., Guimarães I.P., 2008. Proterozoic links between the Borborema Province, NE Brazil, and the Central African Fold Belt. *Geological Society of London* 294, 69–99.

Vilalva, F.C.J., Vlach, S.R.F., Simonetti, A., 2016. Chemical and O-isotope compositions of amphiboles and clinopyroxenes from A-type granites of the Papanduva Pluton, South Brazil: Insights into late- to post-magmatic evolution of peralkaline systems. *Chemical Geology* 420, 186–199.

Wang, X.S., Hu, R.Z., Bi, X.W., Leng, C.B., Panl, C., Zhu, J.J., Chen, Y.W., 2014. Petrogenesis of Late Cretaceous I-type granites in the southern Yidun Terrane: New constraints on the Late Mesozoic tectonic evolution of the eastern Tibetan Plateau. *Lithos* 208-209, 202-219.

Wang, Z., Wang, J., Deng, Q., Du, Q., Zhou, X., Yang, F., Liu, H., 2015. Paleoproterozoic I-type granites and their implications for the Yangtze block position in the Columbia supercontinent: Evidence from the Lengshui Complex, South China. *Precambrian Research* 263, 157-173.

Weissert, L.F., Salmond, J.A., Schwendenmann, L., 2016. Variability of soil organic carbon stocks and soil CO₂ efflux across urban land use and soil cover types. *Geoderma* 271: 80–90.

Yeomans, J.C., Bremner, J.M., 1988. A rapid and precise method for routine determination of organic carbon in soil. *Communications in Soil Science and Plant Analysis* 19, 1467–1476.

Yousefifard, M., Ayoubi, S., Poch, R. M., Jalalian, A., Khademi, H., Khormali, F., 2015. Clay transformation and pedogenic calcite formation on a lithosequence of igneous rocks in northwestern Iran. *Catena* 133, 186–197.

CHAPTER II

GEOCHEMISTRY OF MAJOR AND TRACE ELEMENTS IN SOILS
DEVELOPED FROM I- AND S-TYPE GRANITES ACROSS A
CLIMOSEQUENCE

Geochemistry of major and trace elements in soils developed from I- and S-type granites across a climosequence

Abstract

Soils derived from I- and S-type granites are widely distributed in tropical environments; however, studies regarding their comparative soil geochemistry in tropical settings are scarce. This paper reports a geochemical study on major and trace elements as related to I- and S-type granites weathering across a climosequence using standard mineralogical, geochemical and soil analyses. In general, I-type granites originated soils with higher major and trace element concentrations owing to their richness in mafic and accessory minerals. The enrichment factor (EF) was a useful tool to observe enrichment signatures of soils derived from I- and S-type granites. Clearly, soils derived from S-types present V enrichment increasing from dry to humid zones while opposite enrichment pattern was observed for Pb. The highest EF values observed in soils derived from I-type granites are mostly explained by its mineral composition which originates soils with higher clay contents and CEC values. Major elements were easier leached than trace elements during weathering processes of both granite types. The applications of multivariate statistical techniques are suitable tools to guide and support soil geochemistry management decisions not only to understand soils variability derived from different granite types but also to contribute to agriculture production and soil-related environmental issues. The data obtained are useful as reference values of major and trace elements derived from granites in tropical environments. Additionally, this study clearly highlights the complex interactive control of granite types and climate on soil geochemistry. The geologic factor of soil formation cannot be neglected in climosequence studies to warrant the understanding of important environmental issues such as soil geochemistry.

Keywords: Soil geochemical; chemical weathering; granitoid rocks; tropical settings

1. Introduction

Granites are among the most common rock types of the continental crust (Frost et al. 2001). These rocks can present different compositions and originate from diverse petrogenetic processes (Chappell and White, 1974, 1984, 2001). As a result, distinct mineralogical and geochemical characteristics have been observed (Clemens, 2003; Ghani, 2000). In order to simplify the subcategories of granites, Chappell and White (1974, 2001) proposed the distinction between I (igneous source) and S (sedimentary source) types of granites. This classification, along with the use of A-type granites have been widely adopted (Almeida et al. 2007; Canosa et al. 2012; Chappell et al. 2012; Foden et al. 2015; Guan et al. 2014; Guani et al. 2013; Robinson et al. 2015; Vilalva et al. 2016; Wang et al. 2015; Zhao et al. 2008).

These granite types underlie large areas in tropical and temperate climates. Brazil shows a large extension of soils derived from granites that play a key role for crops, geochemical cycles, water quality, and carbon storage in tropical ecosystems. Thus, knowing the concentrations and relationships between major and trace elements in soils derived from different granite types and climate conditions is essential not only to understand soils variability but also to contribute to agriculture production and soil-related environmental issues.

Pernambuco State, Brazil, poses a strategic settlement for geochemical studies across environments. Along the state, I- and S-type granites cover approximately 1/3 of the whole land area (Brazil, 2001), and can be sampled from tropical to semiarid region of the Borborema Province together with the soil that they originate. The Borborema Province, NE Brazil, represents the Western portion of the extensive geologic Brasiliano-Pan African orogenic system formed by a convergence of the West Africa/São Luis and San Francisco-Congo Cratons (Brito Neves, 1975). This province comprises an area of around 380,000 km² (Ferreira et al., 1998), and it is characterized by voluminous S- and I-type granites.

The study addressed the question of how geochemical and mineralogical signatures of major and trace elements differ from soils developed over I- and S-type granites along a climosequence. In this regard, our objectives were (a) to

describe the petrography and mineralogy of I- and S-type granites of the Borborema Province; (b) to investigate the source and geochemical behavior of major and trace elements as well as the factors controlling their distribution in soil profiles; (c) to evaluate the climosequence influence on the geochemistry of major and trace elements in soils; (d) to assess the use of multivariate statistical techniques as a tool to support soil geochemistry management decisions. Our results can hopefully be used to understand the geochemistry of major and trace elements in large parts of the tropics (S-America, sub-Saharan Africa, India, SE and East Asia, Australia) which are underlined by S- and I-type granites.

2. Materials and methods

2.1. Study area

The study was carried out in the Borborema Province, Pernambuco State, northeastern Brazil. The Borborema Province represents the Western portion of the extensive Brasiliano-Pan African orogenic system formed by convergence of the West Africa/São Luis and San Francisco-Congo Cratons (Brito Neves, 1975). Geologically speaking, the Borborema Province comprises a mosaic of tectonic blocks including Paleoproterozoic basement and scattered Archean nuclei, Meso to Neoproterozoic supracrustal rocks, and large intrusions of granites (Van Schmus et al. 2008).

The study region is divided into three climatic zones according to Koppen classification (Koppen, 1931). The dry zone shows a semiarid climate (Bhs), characterized by negative water balance, as a result of the annual rainfall (< 800 mm) lower than evaporation (2.000 mm year⁻¹). Annual average air temperature ranges from 23 to 27 °C and relative humidity is about 50% (Brito et al. 2007). The sub-humid zone shows a climate classified as Aw, characterized by average air temperature equal to 24 °C, with annual rainfall ranging from 800 to 1000 mm, situated over the Borborema highlands (400-800m). The humid zone shows a tropical climate (Am), known as warm and humid with annual rainfall ranging from 1.000 to 2.000 mm year⁻¹ (INMET, 2015). The annual average air temperature equal to 27 °C shows thermal amplitude of about 5 °C and high relative humidity, higher than 50%.

In accordance with climatic contrasts, the vegetation demonstrated a clear zonation, with the following units: (i) Dry deciduous forest known as Caatinga in dry zone – an exclusively Brazilian biome and one of the most vulnerable sites to desertification (Souza et al. 2012). It is characterized as being xeric shrubland and thorn forest, which consists primarily of small, thorny trees that shed their leaves seasonally (Souza et al., 2012); (ii) Semideciduous forest in sub-humid zone, characterized by predominance of hipoxerophilic Caatinga (Drumond et al., 2004); (iii) Primary evergreen forest (Atlantic rainforest) in humid zone, characterized as one of the richest biomes in biodiversity of the world (Thomas et al., 1998).

2.2. Soil and Rock sampling

Soil profiles developed on I- and S-type granites from three climatic zones under native vegetation or with minimal anthropic influence were chosen based on geological maps and field local observation (Figure 1).

were classified according to the World Reference Base for Soil Resources (IUSS Working Group WRB 2014).

2.3. *Analytical methods*

2.3.1. *Whole-rock geochemistry analyses*

The I- and S-type granites and their modal mineral compositions were determined from fresh rock samples which were collected from an outcrop beside the soil profiles. The mineralogical identification was made from polished thin sections according to Murphy (1986) using petrographic microscope.

Powder samples were mechanically compressed to pellets for X-ray fluorescence analysis and the molecular proportions of major element oxides (SiO_2 , TiO_2 , Al_2O_3 , Fe_2O_3 , MgO , CaO , MnO , Na_2O , K_2O , and P_2O_5) were determined using an XRF spectrometry (S8 TIGER ECO – WDXRF-1KW). Loss on ignition was determined at 1.000 °C. The results were verified using an international geochemical standard SRM 2709, San Joaquin soil (NIST, 2002). The two granite types were also analyzed for their magnetic properties, using a handheld magnetic susceptibility meter (KT-10, Terraplus).

After optic microscope observation, granite samples were coated with a 20 nm gold layer (model Q150R - Quorum Technologie). Fine-grained minerals and their textures were observed using a TESCAN (model: VEGA-3 LMU) field emission SEM at an accelerating voltage of 15 kV. Afterwards, the energy dispersive X-ray spectrum (EDS; Oxford Instrument, model: 51-AD0007) coupled with SEM were used to analyze the semiquantitative characteristics of the mineral compositions.

2.3.2. *Soil analyses*

2.3.2.1. *Physical and chemical analyses*

The particle size distribution was obtained according to Gee and Or (2002), using Calgon as chemical dispersion. All samples were submitted to pre-treatment to eliminate organic matter (H_2O_2). Soil pH was determined using distilled water (1:2.5 soil:solution ratio). Exchangeable K and Na were extracted with Mehlich-1 procedures (1:10 soil:solution ratio). Calcium, Mg and Al were

extracted with 1 mol L⁻¹ KCl (1:10 soil:solution ratio). All elements were determined by optical emission spectrometry (ICP-OES/Optima 7000, Perkin Elmer). Potential acidity (H⁺ + Al³⁺) was determined by calcium acetate method (0.5 mol L⁻¹, pH 7.0), and total organic carbon (TOC) according to Yeomans and Bremner (1988). The cation-exchange capacity (CEC) was calculated from the sum of the exchangeable cations and the total acidity. Physical and chemical analyses (Tables 1, 2) reflect the large differences between soils derived from I- and S-type granites and climates.

Table 1. Selected chemical and physical characteristics of soil profiles derived from I-type granites along a climosequence in Pernambuco state, Brazil

Horizon/depth (cm)	Clay	Silt	Sand	TOC ^a (g kg ⁻¹)	pH (H ₂ O)	CEC ^b (cmol _c kg ⁻¹)	Fe _t ^c (g kg ⁻¹)	Ti (mg kg ⁻¹)	CIA ^d (%)
Humid zone (537 m) – (Hypereutric Chromic Lixisols)									
A ₁ (0-8)	150	379	471	59.58	5.45	8.54	56.60	12211	89
A ₂ (8-18)	170	383	447	58.53	5.00	7.17	57.38	10819	91
AB (18-30)	180	414	406	11.97	4.70	5.50	68.80	10554	93
BA (30-46)	250	440	310	6.37	4.80	4.63	78.67	10416	94
Bt ₁ (46-64)	300	507	193	5.72	5.20	4.23	103.06	9542	97
Bt ₂ (64-84)	310	506	184	4.19	5.00	4.17	115.79	9259	98
Bt ₃ (84-135)	300	522	178	1.50	5.00	4.03	118.95	8127	98
BC (135-175)	260	569	171	3.66	5.00	3.82	112.79	9163	98
C (175-195+)	270	558	172	3.07	4.80	3.64	112.21	8717	98
R	-	-	-	-	-	-	-	4578	-
Sub-humid zone (695 m) – (Eutric Regosols)									
A (0-11)	50	290	660	45.27	5.15	9.12	12.30	5157	70
CA (11-17)	60	282	658	6.99	5.20	5.76	13.12	5572	71
C ₁ (17-46)	50	280	670	3.95	5.10	4.47	11.77	5566	70
C ₂ (46-70)	50	300	650	2.06	5.45	3.36	10.00	5145	68
C ₃ (70-78)	50	240	710	1.65	5.65	2.46	9.23	5349	64
Cr ₁ (78-148)	270	474	256	3.89	4.30	14.96	64.30	9645	93
Cr ₂ (148-185)	180	335	485	2.54	4.70	18.08	69.11	9301	87
Cr ₃ (185-200)	100	533	367	1.80	5.10	10.87	48.76	2428	79
R	-	-	-	-	-	-	-	7048	-
Dry zone (473 m) – (Eutric Regosols)									
A (0-3)	50	195	755	39.64	7.10	10.57	67.00	2994	56
CA (3-9)	80	304	616	11.29	6.85	10.83	54.98	5127	70
C ₁ (9-17)	100	321	579	7.09	6.00	7.49	43.92	5765	74
C ₂ (17-27)	110	308	582	4.97	5.50	8.17	42.17	6133	76
C ₃ (27-39)	120	326	554	4.08	5.10	7.96	38.42	5892	78
Cr ₁ (39-53)	130	358	512	3.19	4.80	8.85	30.56	6120	83
Cr ₂ (53-63+)	80	231	689	1.92	5.00	10.91	16.35	10325	75
R	-	-	-	-	-	-	-	4759	-

^a Total organic carbon; ^b Cation exchange capacity; ^c Total iron; ^d Chemical index of alteration.

Table 2. Selected chemical and physical characteristics of soil profiles derived from S-type granites along a climosequence in Pernambuco State, Brazil

Horizon/depth	Clay	Silt	Sand	TOC ^a	pH	CEC ^b	Fe _t ^c	Ti	CIA ^d
---------------	------	------	------	------------------	----	------------------	------------------------------	----	------------------

(cm)	(g kg ⁻¹)		(g kg ⁻¹)	(H ₂ O)	(cmolc kg ⁻¹)	(g kg ⁻¹)	(mg kg ⁻¹)	(%)	
Humid zone (348 m) – (Dystric Xanthic Ferralsols)									
A ₁ (0-9)	200	244	556	39.68	4.60	7.10	20.58	4898	91
A ₂ (9-20)	200	263	547	14.83	4.25	5.84	24.78	5416	94
AB (20-37)	200	361	439	9.01	4.20	4.58	29.95	5530	95
BA (37-50)	230	385	385	7.00	4.10	4.27	32.31	5488	95
Bo ₁ (50-69)	230	364	406	4.23	4.15	3.00	34.98	6036	96
Bo ₂ (69-89)	220	350	430	3.87	4.10	2.71	33.33	6380	95
Bo ₃ (89-109)	200	362	438	3.64	4.10	2.53	32.40	5651	95
Bo ₄ (109-147)	230	348	422	5.53	4.20	2.53	36.84	6169	96
Bo ₅ (147-165)	250	365	385	4.05	4.10	2.65	41.32	6060	96
R	-	-	-	-	-	-	-	2169	-
Sub-humid zone (738 m) – (Dystric Regosols)									
A (0-16)	50	90	860	4.44	4.30	4.10	4.97	1982	79
AC (16-34)	30	126	844	2.82	4.10	2.75	8.46	3361	83
CA (34-56)	60	139	801	3.31	3.75	2.80	10.16	3440	83
C ₁ (56-93)	70	139	791	3.58	3.70	2.96	12.08	3620	85
C ₂ (93-111)	80	137	783	2.60	3.90	3.24	8.18	2584	84
C ₃ (111-136)	70	166	764	1.29	3.75	2.80	8.86	2952	84
C ₄ (136-152)	60	161	779	1.44	4.00	2.32	10.79	3904	82
C ₅ (152-195)	70	183	747	1.16	4.20	2.28	9.90	3928	82
Cr (195-205)	50	161	789	0.31	4.35	1.30	6.95	3849	72
R	-	-	-	-	-	-	-	1145	-
Dry zone (389 m) – (Eutric Regosols)									
Ap (0-5)	40	51	909	4.57	6.00	2.75	4.70	1271	58
CA (5-17)	50	80	870	3.18	5.30	2.22	4.38	1373	61
C ₁ (17-26)	50	97	853	1.98	5.15	2.23	4.88	1572	62
C ₂ (26-40)	50	113	837	2.62	4.80	2.37	5.29	1494	62
C ₃ (40-48)	40	120	840	1.77	5.20	2.45	5.40	1741	61
Cr (48-59)	50	232	718	1.15	6.20	3.15	7.15	2392	62
R	-	-	-	-	-	-	-	1145	-

^a Total organic carbon; ^b Cation exchange capacity; ^c Total iron; ^d Chemical index of alteration.

2.3.2.2. Major element analyses

Powder samples were mechanically compressed to pellets for X-ray fluorescence analysis and the molecular proportions of major element oxides (SiO₂, TiO₂, Al₂O₃, Fe₂O₃, MgO, CaO, MnO, Na₂O, K₂O, and P₂O₅) were determined using an XRF spectrometry (S8 TIGER ECO – WDXRF-1KW). Loss on ignition was determined at 1,000 °C. The results were verified using international geochemical standard (SRM 2709, San Joaquin soil) (NIST, 2002). The recovery rates of major element (%) appeared in the following decreasing order: P (126) > Al (106) > Ca (105) > Ti (101) > Fe (100) > K (98) > Mg (96) > Si (89) > Mn (81) > Na (72). These results were considered satisfactory and warrant the quality of the XRF measurement.

2.3.2.3. Trace element analyses

For the trace elements measurement, 1 g of soil was digested in Teflon vessels with 6 mL of HNO₃, 3 mL of HF and 3 mL of HCl in a microwave oven (Mineralogical methods – SSSA, 2008). Analysis was performed only when the coefficient of determination (r^2) of the calibration curve was higher than 0.99; whenever more than 10% deviation was observed, the equipment was calibrated and samples analyzed again. All of the analyses were carried out in duplicate.

Concentrations of Cd, Pb, Zn, Cu, Ni, Cr, V, Ba, Co, Zr, Li and Ga were determined by inductively coupled plasma optical emission spectroscopy (ICP-OES/Optima DV7000, Perkin Elmer). To improve sensitivity to trace elements, we coupled a cyclonic spray chamber/nebulizer to the ICP-OES. The results were verified using international geochemical standard (SRM 2709, San Joaquin soil) (NIST, 2002). The recovery rates of trace element (%) appeared in the following decreasing order: Cu (109) > Zn (102) > Cr (92) > Ba (91) > V (89) > Cd (88) > Ni (86) > Pb (84) > Zr (81) > Co (79). These results were considered adequate and warrant the quality of the ICP-OES measurement. The reference values for Ga and Li have not been established for the certified sample (NIST 2002).

2.4. *Chemical weathering*

Major elements data were used to calculate the chemical index of alteration (CIA), following Nesbitt and Young (1982):

$$\text{CIA} = [\text{Al}_2\text{O}_3 / (\text{Al}_2\text{O}_3 + \text{Na}_2\text{O} + \text{CaO} + \text{K}_2\text{O})] \times 100.$$

This index is based on the ratio of a group of mobile elements to immobile ones assuming that Al is relatively immobile. It also assumes that feldspar to kaolin transformation is the predominant weathering process (Rasmussen et al. 2010). CIA was recently used to successfully evaluate the degree of chemical weathering of felsic rocks (Sanematsu et al. 2015).

2.5. *Enrichment factor (EF)*

Comparisons of soil profiles were performed using EF calculation (Blaser et al. 2000). The EF is a geochemical parameter widely used to assess the

pedogenetic processes influencing element distributions in soil profiles (Hu et al. 2013; Shi and Wang, 2013; Szolnoki et al. 2013). Classically, Ti and Zr are universally used for quantifying mass losses for major and trace elements in soils (Brimhall and Dietrich, 1987; Nesbitt, 1979). However, the use of Zr has been questioned by several workers because it is not always evenly distributed in samples (Nesbitt, 1979; Nesbitt and Markovics, 1997). Once the concentration of major and trace elements does not enable to track element gains/losses in tropical settings, the EF was calculated as:

$$EF = \frac{\left(\frac{E}{Z}\right)_{sample}}{\left(\frac{E}{Z}\right)_{background}}$$

Where:

EF = Enrichment factor;

E = Total content of the element considered;

Z = Total content of titanium;

EF < 1 indicates depletion, and EF > 1 indicates enrichment.

To compensate for the difference in the grain size and composition of samples, we employed geochemical normalization with Ti as a conservative element, as applied by several authors (Brimhall and Dietrich, 1987; Nesbitt, 1979). Ti concentrations in soil profiles and granite types are shown in Tables 1 and 2. Other elements could be used, such as Al, Li and Th (Braun et al. 1993, 1998), but they are not always evenly distributed in soil profiles of our work.

2.6. *Statistical analysis*

Results were assessed by descriptive statistics and discriminant analysis (DA). The discriminant analysis (DA) was performed using all major (Si, Ti, Al, Fe, Mg, Ca, Mn, Na, K, and P) and trace (Cd, Pb, Zn, Cu, Ni, Cr, V, Ba, Co, Zr, Li and Ga) elements as grouping variables. By analyzing several variables at a time the DA allowed the assessment of differences between the studied groups. Exploratory data treatments based on discriminant analysis were used to

identify the main factors which determine the variability among soils regarding parent material and climatic environment. The discriminant analysis defines the independent variables that are most important to distinguish the selected groups of data. For this study the groups were defined based on parent rock (I- and S-type granites) and climate condition (humid, sub-humid and dry zones). All statistical analyses were performed with XLSTAT statistical software (version 2014.5.03).

3. Results and Discussion

3.1. Mineralogy of I- and S-type granites

Overall, S-type granites showed fine to medium grains texture and light gray colors. These granites are mainly composed of quartz, feldspar and biotite evenly distributed and an absence of magnetic minerals (Figure 3a). The rocks showed gentle foliations outlined by mafic minerals. I-type granites have inequigranular, commonly porphyritic texture with medium to coarse K-feldspars, small amounts of gray quartz and black mafic minerals, commonly biotite (Figure 2a).

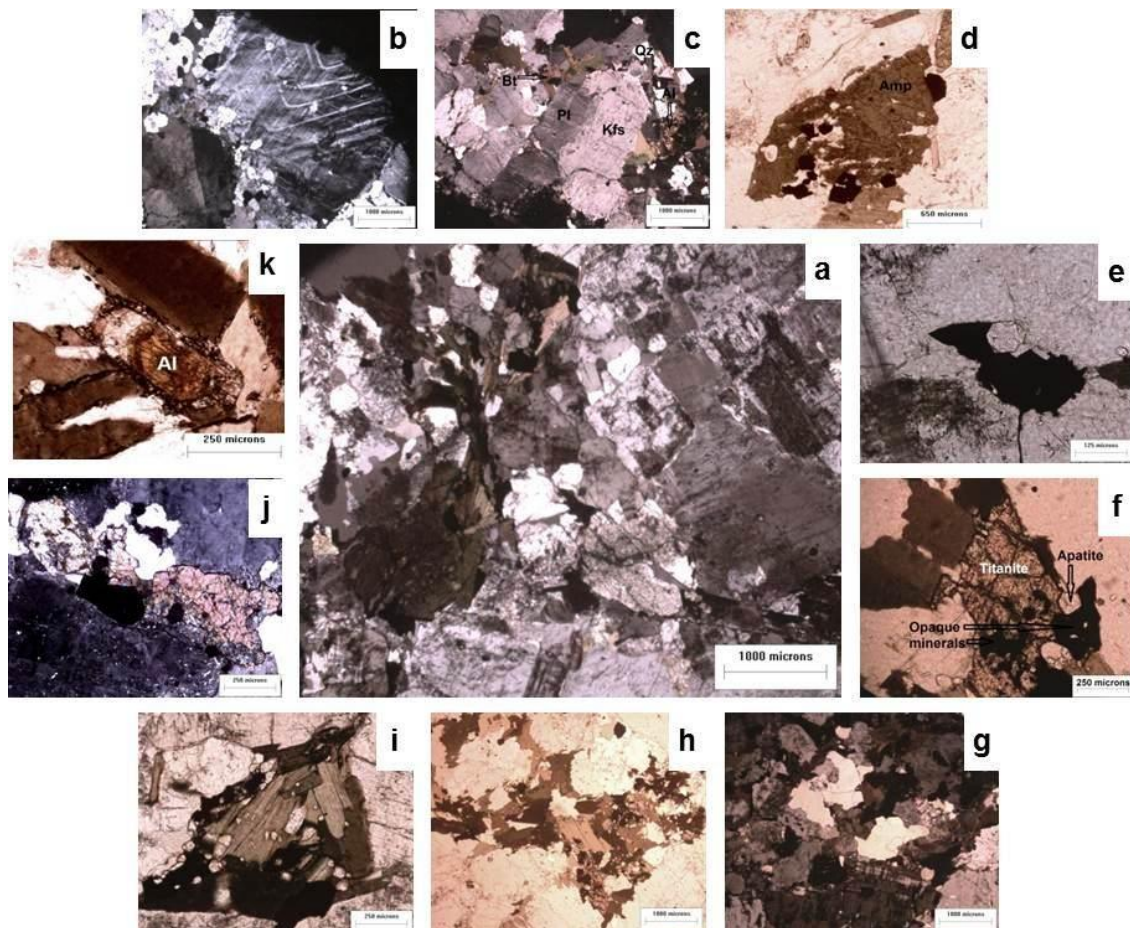


Figure 2. Petrographic characteristics of I-type granites. (a) General aspect; (b) K-feldspar; (c) Typical section, overview; (d) Amphibole; (e) Opaque mineral; (f) Titanite, apatite and opaque minerals; (g) Quartz; (h) Mafic phase minerals; (i) Apatites associated with mafic minerals; (j) Titanite; (k) Allanite.

Field measurements of fresh S-type granites with the hand-held magnetic susceptibility meter reveal only very low magnetic susceptibility ($0.01\text{-}0.02 \times 10^{-3}$ SI). Whereas, fresh I-type granites show elevated magnetic susceptibility ($3\text{-}20 \times 10^{-3}$ SI), likely caused by mafic and opaque minerals (i.e. magnetite) present in this type of granite. The magnetic susceptibility data are consistent with the findings of Ferreira et al. (1998).

K-feldspar, quartz, plagioclase and biotite are the dominant components, ranging from 85 to 90% and 87 to 93% of the total composition of the I- and S-type granites, respectively (Table 3). Quartz and plagioclase are more abundant in S-type granites whilst K-feldspars and opaque minerals were higher in I-type granites. Muscovite was observed only in S-types, ranging from 3 to 6% and exhibited several degrees of alteration, chiefly being replaced by sericite.

Amphibole, apatite and titanite were evidenced only in I-type granites (Table 3). Magnetic minerals and minor amounts of chlorite predominated in I-type granites.

Table 3. Mineralogical composition (%) of I- and S-type granites in Pernambuco State

Mineral	I-type granites			S-type granites		
	Humid	Sub-humid	Dry	Humid	Sub-humid	Dry
K-feldspar	61	55	65	45	37	23
Quartz	12	7	8	23	26	34
Plagioclase	7	12	7	5	22	28
Biotite	10	11	5	14	12	8
Amphibole	4	4	7	nd	nd	nd
Sericite / Muscovite	nd	nd	nd	6	3	6
Opaque mineral	2	4	4	4	<1	1
Allanite	3	2	< 1	3	<1	< 1
Apatite	1	2	3	nd	nd	nd
Titanite	nd	2	1	nd	nd	nd
Chlorite	< 1	< 1	nd	nd	nd	< 1
Total	100	100	100	100	100	100

nd – not detected.

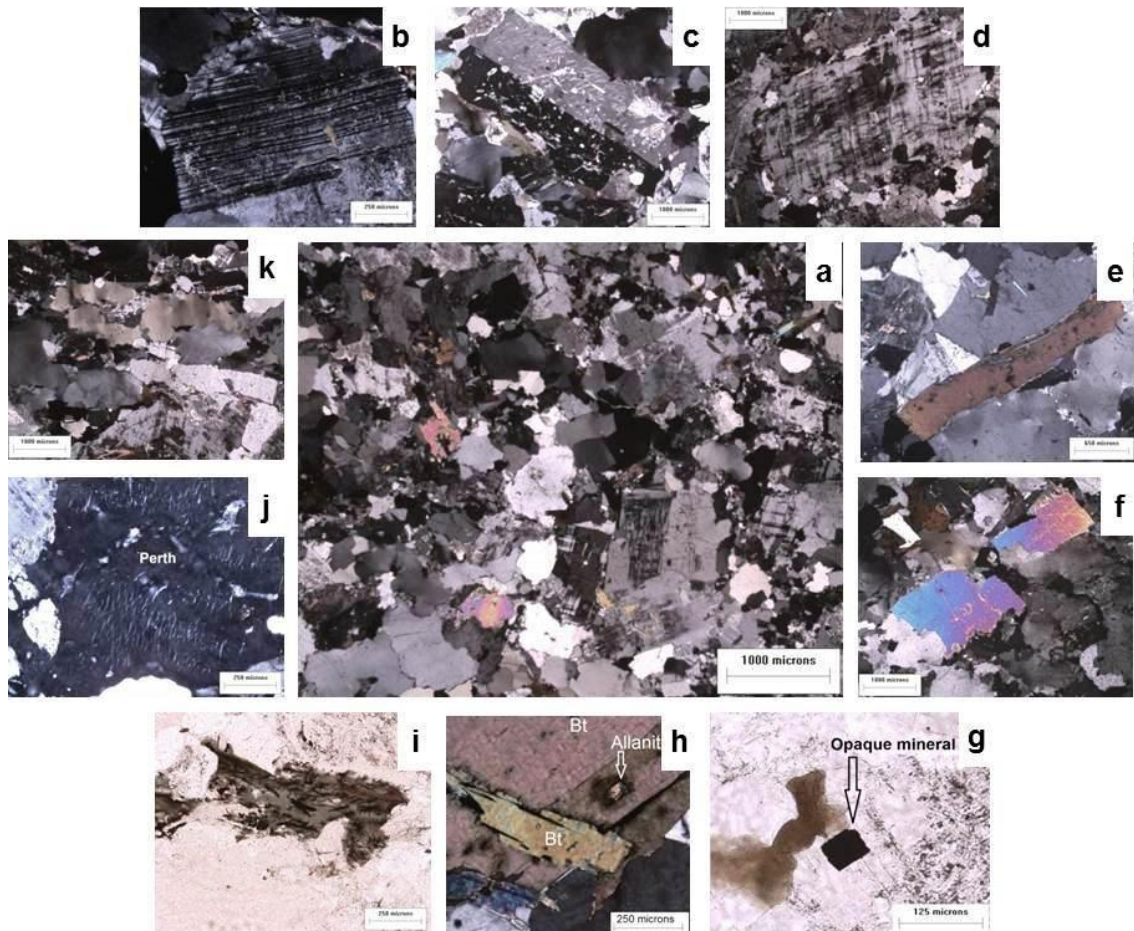


Figure 3. Petrographic characteristics of S-type granites. (a) General aspect; (b) Plagioclase; (c) Orthoclase; (d) Microcline; (e) Biotite; (f) Muscovite; (g) Opaque mineral; (h) Allanite; (i) Opaque minerals associated with chlorite; (j) Perthite; (k) Typical section, overview.

The mineral assemblage of I-type granites (Table 3) is consistent with the petrographic results of Chappell and White et al. (2001). Allanite and titanite tend to occur in I-type rather than S-type granites (Bea, 1996). Biotites are in the early alteration stage to chlorite. Feldspars are slightly altered to sericites. The K-feldspar crystals occur with cross-twinning, simple twinning and exsolution (perthites). These features occur in forms of small lamellae. The phosphate mineral apatite occurs in small crystals and is often associated with mafic minerals (Figure 2i). Apatite inclusions are common in biotite of I-type granites whereas they occur in larger discrete crystals in S-types (Chappell and White, 2001).

In the S-type granites, small amounts of biotite are changing in terms of composition to chlorite, with small inclusions of allanite with radioactive

elements in their composition (Figure 3h). Allanite disintegration is responsible for the spot formations of biotite. Plagioclases are sericitized usually forming lamellae of muscovite/sericite. K-feldspars are found as microcline (chess-board type and cross-hatch twinning) (Figure 3d) and orthoclase (simple twinning) (Figure 3c). The presence of flame perthites is a result of albite lamellae exsolution of the K-feldspar (Figure 3j).

3.2. *Geochemistry of major elements*

The geochemistry of major elements in I-type granites shows distinct pattern when compared to S-type granites (Figure 4). This was expected mainly because I-type granites are derived from igneous protolith, whereas S-type granites are derived from sedimentary rocks (Chappell and White, 1984). In general, the highest average concentrations of major elements (except for Si) were found in soil profiles derived from I-type granites under all climatic conditions (Figure 4).

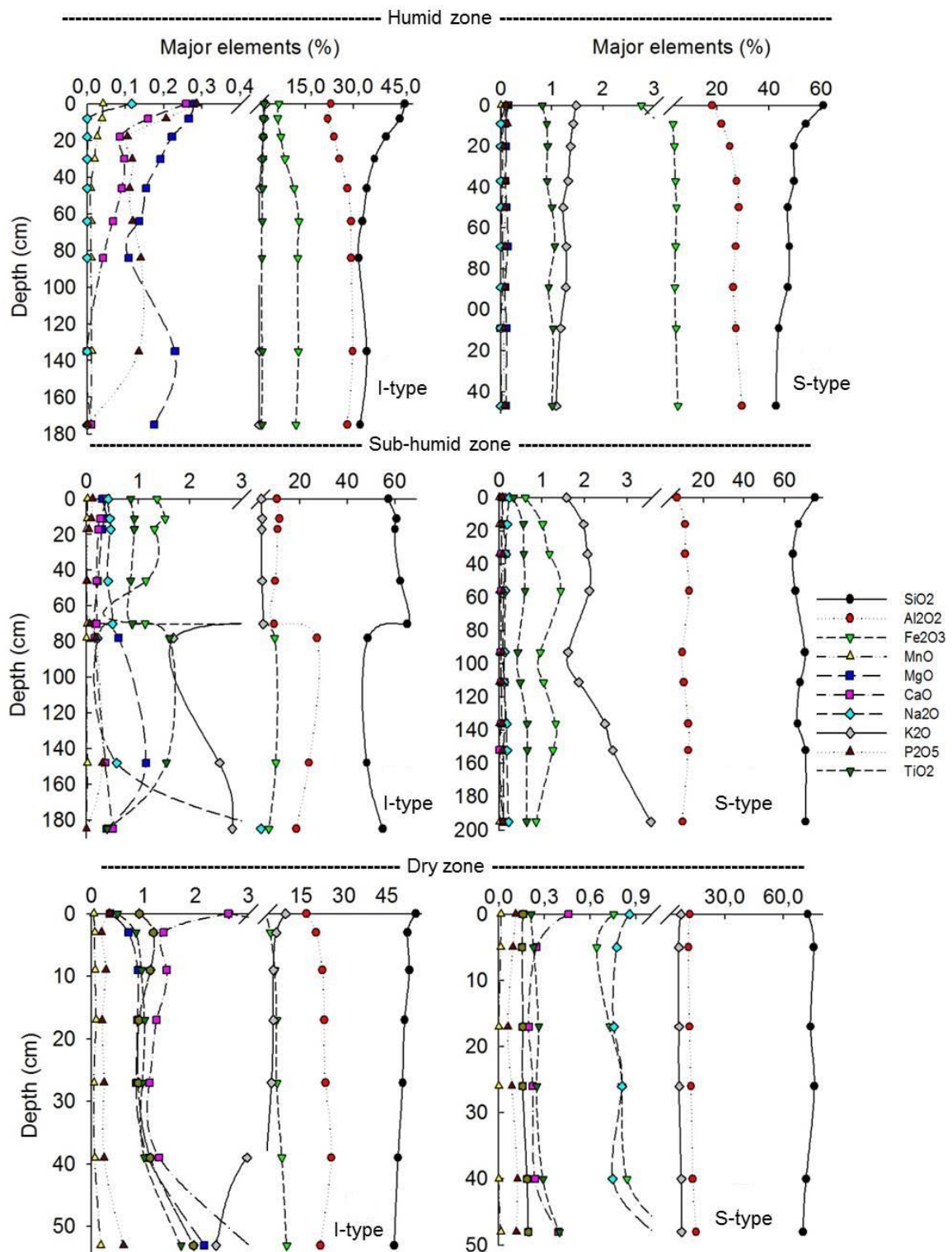


Figure 4. Concentration of major elements in soils derived from I- and S-type granites in three climatic zones of Pernambuco State, Northeast Brazil.

These results are clearly governed by their mineralogical characteristics (Table 3). For instance, the greater proportion of mafic, opaque and accessory minerals in I-type granites as well as the higher proportions of quartz and

muscovite in S-type granites (Table 3). The chemical compositions of some of these minerals in I-type granite are shown in Figure 5.

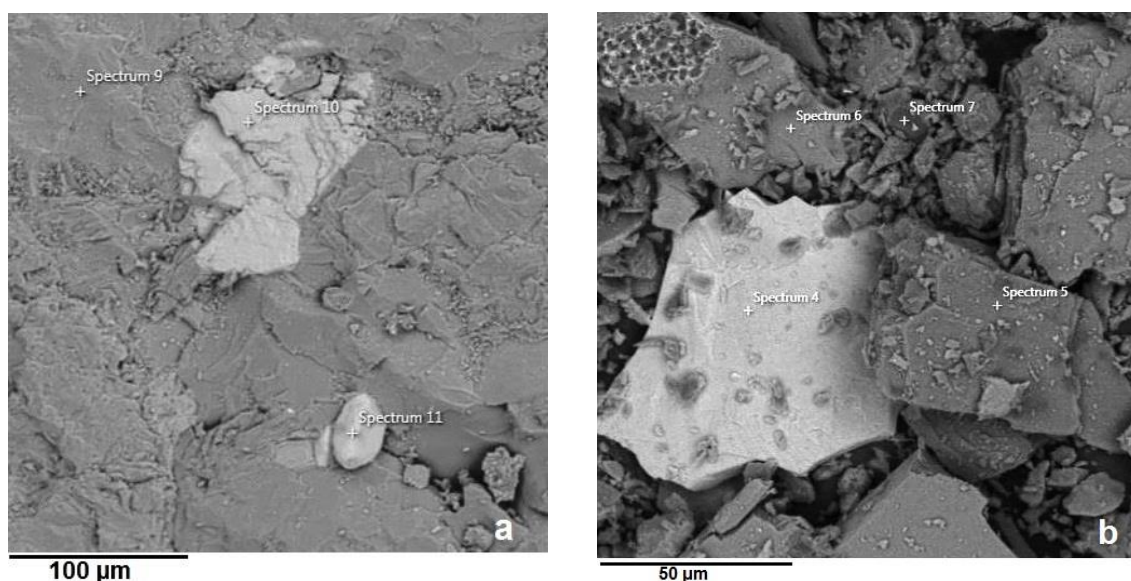


Figure 5. Scanning electron microscope (SEM) images captured from minerals in I-type granite and their respective elemental composition by energy dispersive X-ray spectrum (EDS). (a) Chemical composition of K-feldspar (Spectrum 9: Si – 56%, K -23%, Al – 17%, Fe – 2%, Na – 1%, Ba – 1%), magnetite (Spectrum 10: Fe – 97%, Si – 2%, Al – 1%), and zircon (Spectrum 11: Zr – 41%, Au – 23%, O - 17%, Si – 12%, C – 6.7%, Al – 0.3%), (b) Chemical composition of magnetite (Spectrum 4: Fe – 95%, Si – 3%, Al – 1%, K – 1%), plagioclase (Spectrum 5: Si – 60%, Al – 23%, Na – 10%, Ca – 7%), biotite (Spectrum 6: Si – 30%, Fe – 19%, Al – 14%, Mg – 13%, K – 12%, Au – 10%, Ti – 2%), and quartz (Spectrum 7: Si – 100%).

The average concentrations of major elements in soils derived from I- and S-type granites varied according to the climatic zones. Soil profiles over both granite types exhibited the following order for humid zone: Si > Al > Fe > Ti > K > Mg > Ca > P > Mn > Na (Figure 4a, d). This finding demonstrates cations leaching (Ca^{2+} , Na^+ and K^+) and conservation of relatively immobile elements (Al, Fe and Ti). These results are confirmed by the highest CIA values (95%) observed in both soil profiles (Tables 1, 2). These high CIA values indicate the almost complete removal of the labile major elements (Babechuk et al. 2014).

The higher Mg losses mainly at soils derived from I-type granites under sub-humid and humid zone are related to the presence of easily weatherable Fe–Mg phyllosilicates (Olsson and Melkerud, 2000). Strong losses of K and Na have also been observed in strongly acidified horizons, as a result of weathering of primary minerals (K-feldspar and plagioclase) combined with the fact that K or Na is adsorbed only to a smaller extent into secondary minerals (Egli et al. 2001).

Soils developed over I- and S-type granites located in the sub-humid zone exhibited, respectively, the following orders for elemental concentration: Si > Al > Fe > K > Ti > Mg > Ca > Na > P > Mn (Figure 4b) and Si > Al > K > Fe > Ti > Na > Mg > Ca > P > Mn (Figure 4e). Lower cation leaching was observed in this climatic zone compared to the humid zone. This can be attributed to the lower weathering intensity, as demonstrated by the mean CIA values of 74 and 81% for I- and S-types, respectively (Tables 1, 2). This CIA values indicates that the mineralogical compositions of these profiles not yet reached complete 'kaolinitisation' and still retain a considerable amount of the labile elements (K, Ca, Mg and Na) (Babechuk et al. 2014).

In the dry zone, major element concentrations decreased in the order Si > Al > Fe > K > Ca > Na > Ti > Mg > P > Mn for soil profile over I-type granite (Figure 4c) and Si > Al > K > Na > Fe > Ca > Ti > Mg > P > Mn for soil profile over S-type granite (Figure 4f). The highest Si and base contents, as well as the lowest Al and Fe concentrations are related to the lower weathering intensity evidenced in both soil profiles (over I- and S-type granites) as supported by the lowest CIA values (73% for I-type and 60% for S-type) (Tables 1, 2).

These CIA values suggest that physical weathering dominates in soil profiles under this climatic zone. The weathering intensity differences among soils derived from I- and S-type granites under similar climate rely on their mineralogical characteristics, such as higher proportion of resistant minerals in S-type granites (i.e. quartz and muscovite, Table 3) that leads to the lowest CIA values. According to Price and Velbel (2003), different CIA values may reflect variation in the chemistry of the unweathered parent rock rather than the degree of weathering.

The lower K losses than Na and Ca in all soil profiles developed from both granite types are related to the higher resistance of K-feldspar (major

source of K) as compared to plagioclase crystals (major source of Na and Ca), which is easily altered during the weathering processes (Yousefifard et al. 2012).

3.3. Geochemistry of trace elements

The average concentration of trace elements in soils derived from I- and S-type granites varied in accordance to the climatic zones. Soil profiles over I-type granites decreased in the order Ga > Zr > Ba > V > Pb > Th > Zn > Li > Co = Cr > Ni > Cu > Cd for the humid zone (Figure 6a); Ba > Zr > Ga > Pb > V > Li > Zn > Ni > Th > Cr > Co > Cu > Cd for the sub-humid zone (Figure 6b) and Zr > Ba > Ga > Pb > V > Zn > Li > Co > Ni = Cr > Th > Cu > Cd for the dry zone (Figure 6c). On the other hand, soils derived from S-types had the following decreasing order: Zr > Ga > Ba > Pb > V > Th > Zn > Cr = Li > Ni > Co > Cu > Cd for the humid zone (Figure 6d); Zr > Ba > Ga > Pb > V > Th > Ni > Cr > Zn = Li > Co > Cu > Cd for the sub-humid (Figure 6e) and Ba > Pb > Ga > Th > Ni > Li > V > Zr = Zn > Co > Cu > Cr > Cd for the dry zone (Figure 6f).

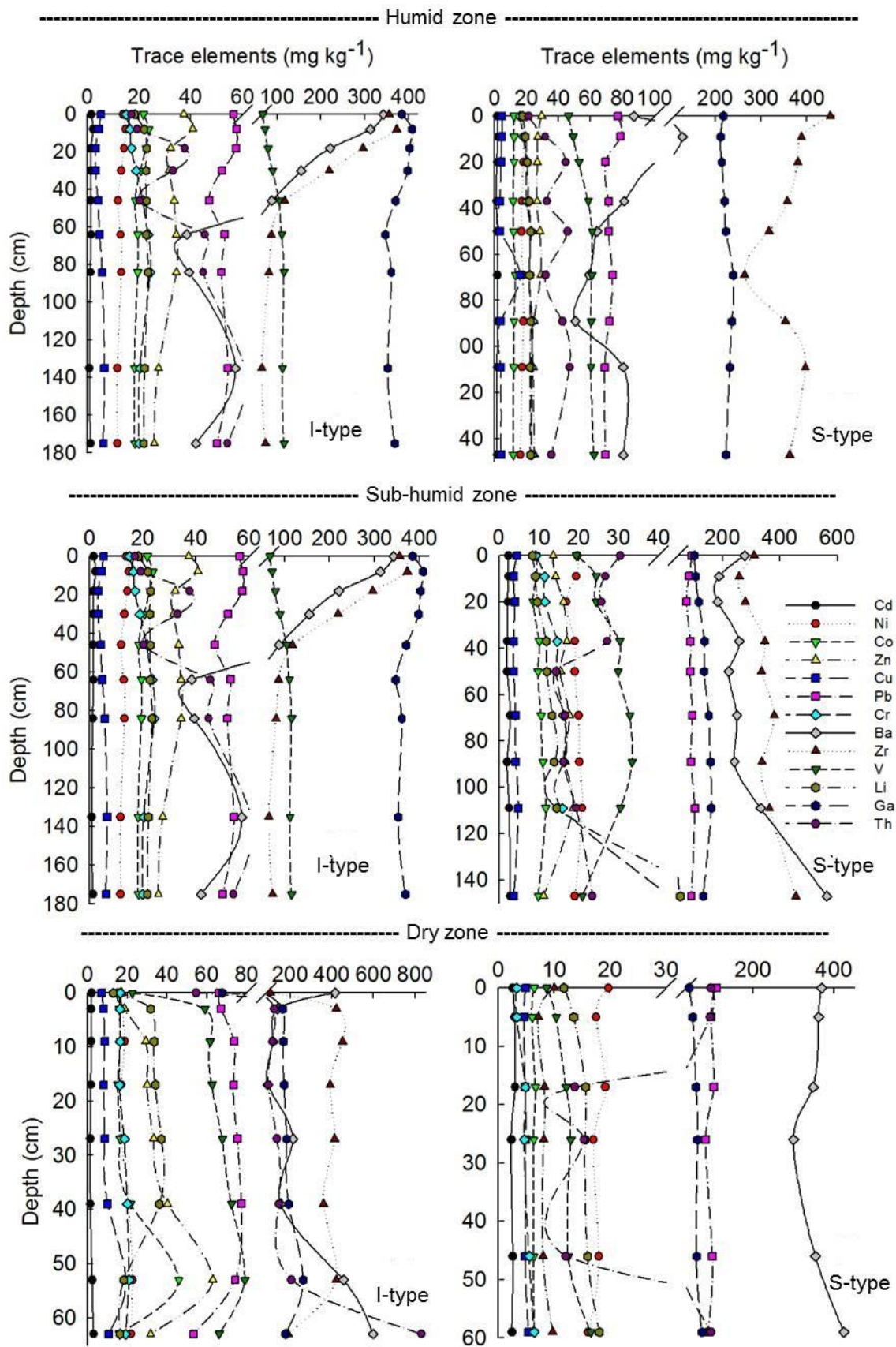


Figure 6. Concentration of trace elements in soils derived from I- and S-type granites in three climatic zones of Pernambuco State, Northeast Brazil.

In general, the aforementioned differences among soils derived from I- and S-type granites are related to parent material and element mobility across the climosequence. The higher average concentrations of trace elements in I-type granites soil profiles under all climatic conditions, except for Pb and Th, (Figure 6) are explained by the higher proportion of accessory minerals, chiefly ilmenite (Figure 7a), allanite, apatite, amphibole, and magnetite (Figure 7b).

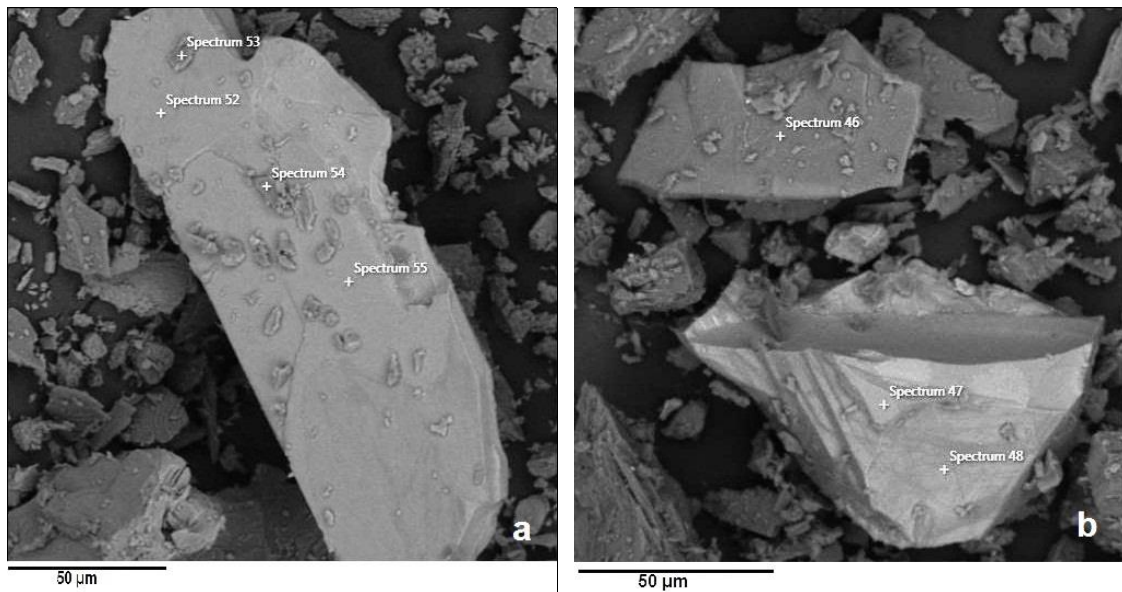


Figure 7. Scanning electron microscope (SEM) images captured from minerals in I-type granites and their respective elemental composition by energy dispersive X-ray spectrum (EDS). (a) Chemical composition of Ilmenite: spectrum 52 (Ti – 41%, Fe – 44%, Mn – 7%; Si – 4%, Ca – 2%, Al – 1.5%, K – 0.5%) and spectrum 55 (Fe – 48%, Ti – 43%, Mn – 7%, Si – 1%, Al – 1%) (b) Chemical composition of Plagioclase: spectrum 46 (Si – 57%, Al – 21%, Na – 9%, Ca – 8%, Fe – 3%, K – 2%), and magnetite: spectrum 47 (Fe – 96%, Al – 2%, Si – 2%) and spectrum 48 (Fe – 91%, Si – 4%, Al – 3%, Ti – 1%, Ca – 0.5%, K – 0.5%).

The study of soil geochemistry variation during weathering of I- and S-type granites indicated that major elements were easier leached than trace elements during weathering processes of both granite types.

The clear differences in soil geochemistry of trace and major elements according to granite types across a climosequence evidenced the importance of the geologic factor of soil formation to warrant the understanding of important environmental issues such as soil geochemistry. Thus, detailed characterization of the mineralogy and chemistry of the granite types cannot be neglected in climosequence studies.

3.4. Enrichment Factor of major elements

No enrichment of major elements was observed in soil profiles derived from S-type granites under all climatic zones, except for a slight enrichment of K in soil surface from dry zone (Table 5).

In contrast, Fe and Al enrichment in depth were evidenced in soils profiles developed on I-type granites under regions with higher weathering intensity (sub-humid and humid zones) (Table 4). The higher clay contents (Table 1) explain this enrichment. Al and Fe are usually enriched in the fine earth fraction (Hardy et al. 1999; Egli, 2001). Lower clay and total iron contents in soil subsurface derived from S-type granites (Table 2) explain the no Fe and Al enrichment in humid zone. In addition, slight Si and K enrichment were observed in soils derived from I-type granites under sub-humid and dry zones, especially in soil surfaces; Mn and Ca enrichment were verified only in topsoils from I-type granites under the dry zone (Table 4).

The highest major element enrichments were evidenced in I-type granite soil (Table 4). These results are clearly related to high clay contents (Table 1), probably in response to the ability of clay minerals in adsorb and accumulate major elements. The higher CEC, mainly in sub-humid and dry zones, would also drive the higher EF values in soils derived from I-type granites than in those originated from S-type granites. I-type granite soils presented the following ranges for major elements concentrations: 0.3 - 2.5 (Si), 0.5 - 3.2 (Al), 0.3 - 3.3 (Fe), 0.1 - 1.0 (Mg), 0.0 - 1.2 (Ca), 0.0 - 2.8 (Na), 0.04 - 2.8 (K), 0.0 - 1.1 (Mn), 0.0 - 0.8 (P). S-type granite soils exhibited EF ranges of 0.2 - 0.8 (Si), 0.2 - 0.8 (Al), 0.2 - 0.8 (Fe), 0.1 - 0.3 (Mg), 0.0 - 0.5 (Ca), 0.0 - 0.3 (Na), 0.1 - 1.2 (K), 0.0 - 0.4 (Mn), 0.1 - 0.8 (P) (Table 5).

The EF values mostly lower than 2 reflect the natural major elements concentration regarding parent material and climosequence since EF values ranging from 0.5 to 2 are attributed to the natural variability (Hernandez et al. 2003). The rare exceptions in saprolite derived from I-type granite under sub-humid zone (EF values > 3) do not characterize anthropogenic influence because the high values are found in the lowest soil profile horizons.

Table 4. Enrichment factor (EF) of major and trace elements with respect to the soils derived from I-type granites along a climosequence in Pernambuco State, Brazil

Horizon/Depth (cm)	EF																					
	Major elements									Trace elements												
	Si	Al	Fe	Mg	Ca	Na	K	Mn	P	Cd	Ni	Co	Zn	Cu	Pb	Cr	Ba	Zr	V	Li	Ga	Th
Humid zone (537 m) – (Hypereutric Chromic Lixisols)																						
A ₁ (0-8)	0.3	0.5	0.6	0.1	0.05	0.0	0.2	0.4	0.5	0.3	0.3	0.4	0.3	0.3	0.5	0.5	0.2	1.0	0.4	0.3	0.5	0.3
A ₂ (8-18)	0.3	0.6	0.6	0.2	0.03	0.0	0.2	0.4	0.4	0.4	0.4	0.5	0.3	0.3	0.6	0.6	0.2	1.2	0.5	0.4	0.6	0.3
AB (18-30)	0.3	0.7	0.7	0.1	0.02	0.0	0.1	0.3	0.2	0.3	0.4	0.5	0.3	0.2	0.6	0.7	0.2	1.0	0.6	0.4	0.6	0.7
BA (30-46)	0.2	0.7	0.9	0.1	0.02	0.0	0.1	0.2	0.2	0.3	0.3	0.5	0.3	0.2	0.6	0.8	0.1	0.7	0.6	0.4	0.6	0.6
Bt ₁ (46-64)	0.2	0.9	1.3	0.1	0.02	0.0	0.1	0.1	0.2	0.3	0.3	0.4	0.3	0.3	0.6	0.9	0.1	0.4	0.8	0.4	0.6	0.4
Bt ₂ (64-84)	0.2	0.9	1.5	0.1	0.02	0.0	0.04	0.1	0.3	0.3	0.4	0.5	0.3	0.4	0.6	1.1	0.03	0.3	0.9	0.4	0.6	0.9
Bt ₃ (84-135)	0.3	1.0	1.6	0.1	0.01	0.0	0.04	0.2	0.3	0.3	0.4	0.5	0.4	0.5	0.7	1.2	0.04	0.3	1.1	0.5	0.7	1.1
BC (135-175)	0.3	0.9	1.5	0.2	0.00	0.0	0.1	0.2	0.3	0.2	0.3	0.5	0.3	0.5	0.7	0.9	0.1	0.2	0.9	0.4	0.6	1.3
C (175-195)	0.2	0.9	1.5	0.1	0.00	0.0	0.1	0.1	0.0	0.3	0.4	0.5	0.3	0.5	0.6	1.0	0.0	0.3	1.0	0.4	0.7	1.2
Sub-humid zone (695 m) – (Eutric Regosols)																						
A (0-11)	1.2	0.8	0.3	0.4	0.2	0.2	1.0	0.4	0.3	1.2	1.0	1.7	1.3	0.9	1.2	1.3	3.3	3.0	2.5	1.4	3.0	0.3
CA (11-17)	1.2	0.8	0.3	0.4	0.1	0.2	1.0	0.3	0.2	1.0	0.9	1.6	1.2	0.5	1.2	1.3	2.5	2.8	2.4	1.2	2.8	0.3
C ₁ (17-46)	1.2	0.8	0.3	0.3	0.1	0.2	1.0	0.0	0.1	1.4	1.1	1.8	0.8	0.4	1.3	1.3	2.7	3.0	2.5	1.2	3.0	0.4
C ₂ (46-70)	1.3	0.8	0.3	0.3	0.1	0.2	1.1	0.3	0.1	1.7	1.2	1.8	0.7	2.3	1.6	1.3	2.2	3.1	2.5	1.1	3.0	0.4
C ₃ (70-78)	1.3	0.7	0.3	0.2	0.1	0.2	1.2	0.3	0.2	1.4	1.1	1.7	0.4	0.2	1.4	1.2	2.3	3.0	2.4	0.8	2.8	0.4
Cr ₁ (78-148)	0.6	1.2	1.2	0.4	0.04	0.04	0.3	0.0	0.3	0.4	0.6	1.1	0.9	0.7	0.6	2.6	0.3	0.5	2.1	1.0	1.9	1.1
Cr ₂ (148-185)	0.6	1.1	1.3	0.7	0.1	0.1	0.4	0.2	0.5	0.5	0.7	1.4	1.2	1.5	0.6	2.7	0.8	0.6	2.2	1.1	2.0	1.1
Cr ₃ (185-200)	2.5	3.2	3.3	1.0	0.5	2.8	1.7	0.1	0.5	2.4	2.4	2.3	1.9	3.2	2.6	4.4	1.9	0.9	4.2	1.8	2.9	3.1
Dry zone (473 m) – (Eutric Regosols)																						
A (0-3)	1.4	1.6	0.7	0.4	1.2	0.4	2.8	1.1	0.8	1.2	1.1	1.5	0.9	1.1	2.0	1.4	1.1	0.9	0.5	1.3	0.6	0.5
CA (3-9)	0.8	1.1	0.7	0.5	0.4	0.3	1.1	1.0	0.3	0.6	0.7	0.9	0.5	0.7	1.2	0.8	0.2	2.1	0.8	1.8	0.9	0.3
C ₁ (9-17)	0.7	1.1	0.8	0.5	0.3	0.2	0.8	0.9	0.3	0.5	0.7	0.9	0.8	0.7	1.1	0.7	0.2	2.0	0.8	1.7	0.8	0.3
C ₂ (17-27)	0.6	1.1	0.9	0.5	0.3	0.2	0.8	1.1	0.2	0.4	0.6	0.7	0.7	0.6	1.1	0.7	0.1	1.6	0.7	1.7	0.7	0.3
C ₃ (27-39)	0.7	1.1	0.9	0.5	0.3	0.2	0.7	0.6	0.3	0.4	0.6	0.8	0.8	0.6	1.2	0.8	0.3	1.8	0.8	1.9	0.8	0.4
Cr ₁ (39-53)	0.6	1.2	1.1	0.6	0.3	0.2	0.4	0.8	0.3	0.4	0.73	1.0	1.0	0.7	1.1	0.8	0.2	1.5	0.9	1.8	0.8	0.5
Cr ₂ (53-63)	0.4	0.6	0.8	0.7	0.4	0.2	0.2	1.3	0.4	0.4	0.47	1.3	0.9	0.8	0.6	0.5	0.4	1.0	0.6	0.5	0.7	0.3

3.5. Enrichment Factor of trace elements

The lowest EF mean values were observed in both soil profiles (soils over I- and S-type granite) located in humid zone (Tables 4, 5). Enrichment of trace elements was not observed in soil profiles derived from S-type in the humid zone ($EF < 1$), except for a slight enrichment of V, ranging from 1.0 to 1.2 (Table 5). In contrast, slight enrichment of Cr (0.5 – 1.2), V (0.4 – 1.1) and Th (0.3 – 1.3) in depth, as well as Zr (0.2 – 1.2) accumulation in surface were evidenced in soil profiles derived from I-type granite (Table 4). These results are clearly related to higher clay contents (Table 1) in soils originated from I-type granites, probably in response to the facility of clay minerals in adsorb and accumulate trace elements. The higher CEC, mainly in sub-humid and dry zones, would also drive the higher trace elements concentrations in soils derived from I-type granites than in those originated from S-type granites.

The highest enrichment of trace elements was observed in soil profiles over I-type granite under sub-humid zone (Table 4). All trace elements exhibited EF mean values higher than a unit, except for Th, decreasing in the order Ga (2.67) > V (2.58) > Zr (2.13) > Cr (2.0) > Ba (1.99) > Co (1.68) > Pb (1.32) > Cd (1.24) > Cu (1.22) > Li (1.20) > Ni (1.12) > Zn (1.04) > Th (0.88). Conversely, no enrichment was observed in soil profile over S-type granite under the same climatic zone, except for the enrichment of V ($EF = 1.48$) along the entire depths (Table 5).

Trace element enrichments among soils derived from I- and S-type granites were clearly different under the dry climate (Tables 4, 5). Soil profile derived from I-type granite showed Zr, Li and Pb enrichment at depth, and Cd, Ni, Co, Cr and Ba enrichment in soil surface. Nevertheless, only Pb enrichment in depth, and Cd, Cu and Th enrichment in topsoil were observed on soil profile originated from S-type granite. These differences are visibly ruled by their petrological, mineralogical and geochemical characteristics.

These patterns are regarded as enrichment signatures of the soil derived from both granite types in tropical settings. For instance, the climatic effects on trace and major elements enrichment are more evident in soils derived from I-types than S-type granites. These results may be mostly explained by mineral composition of both parent materials (Table 3) that develop soils with higher

clay contents and CEC values (Table 1), probably in response to the capacity of clay minerals to adsorb and accumulate trace elements. In addition, the V enrichment increasing from dry to humid zones, and conversely, the Pb enrichment increasing from humid to dry zones are visible enrichment signatures of soils derived from S-type granites. The lack of enrichment of other trace elements in soils from S-types is another tendency in tropical settings.

Despite of the use of Ti as immobile element during weathering processes has been questioned by several workers (e.g. Bern et al. 2011; Cornu et al. 1999; Kurtz et al. 2000; Tripathi and Rajamani, 2007), we have shown that this element was one of the most immobile and well distributed element in soil profiles derived from granites. Some authors have adopted Zr (Brimhall and Dietrich, 1987; Nesbitt, 1979) and Th (e.g. Braun et al., 1993, 1998) to track element gains/ losses in tropical settings. However, these elements were not always evenly distributed in soil originated from both granite types. Others authors also observed irregular Zr distribution in soil samples (Nesbitt, 1979; Nesbitt and Markovics, 1997). Thus, for analysis of major and trace elements mobility in soil derived from granites under tropical settings we recommended the use of Ti as tracer of pedogenic process.

Table 5. Enrichment factor (EF) of major and trace elements with respect to the soils derived from S-type granites along a climosequence in Pernambuco State, Brazil

Horizon/Depth (cm)	EF																					
	Major elements									Trace elements												
	Si	Al	Fe	Mg	Ca	Na	K	Mn	P	Cd	Ni	Co	Zn	Cu	Pb	Cr	Ba	Zr	V	Li	Ga	Th
Humid zone (348 m) – (Dystric Xanthic Ferralsols)																						
A ₁ (0-9)	0.4	0.6	0.5	0.1	0.1	0.0	0.1	0.2	0.7	0.3	0.4	0.7	0.9	0.4	0.7	0.4	0.2	1.1	1.1	0.1	0.3	0.4
A ₂ (9-20)	0.3	0.6	0.5	0.1	0.0	0.0	0.1	0.2	0.8	0.4	0.4	0.6	0.7	0.4	0.7	0.4	0.2	0.8	1.0	0.1	0.3	0.5
AB (20-37)	0.3	0.7	0.6	0.1	0.0	0.0	0.1	0.2	0.3	0.3	0.4	0.6	0.7	0.3	0.6	0.4	0.2	0.8	1.1	0.1	0.3	0.7
BA (37-50)	0.3	0.8	0.7	0.1	0.0	0.0	0.1	0.1	0.5	0.2	0.4	0.6	0.7	0.3	0.6	0.4	0.1	0.8	1.2	0.1	0.3	0.5
Bo ₁ (50-69)	0.2	0.7	0.7	0.1	0.0	0.0	0.1	0.2	0.5	0.3	0.3	0.5	0.7	0.3	0.6	0.4	0.1	0.6	1.2	0.1	0.3	0.6
Bo ₂ (69-89)	0.2	0.7	0.6	0.1	0.0	0.0	0.1	0.1	0.4	0.3	0.3	0.5	0.6	1.1	0.5	0.4	0.1	0.5	1.1	0.1	0.3	0.4
Bo ₃ (89-109)	0.3	0.7	0.6	0.1	0.0	0.0	0.1	0.0	0.5	0.3	0.4	0.6	0.6	0.3	0.6	0.5	0.1	0.7	1.2	0.1	0.3	0.6
Bo ₄ (109-147)	0.2	0.7	0.6	0.1	0.0	0.0	0.1	0.1	0.3	0.3	0.3	0.5	0.6	0.3	0.5	0.4	0.1	0.7	1.1	0.1	0.3	0.6
Bo ₅ (147-165)	0.2	0.7	0.8	0.1	0.0	0.0	0.1	0.1	0.4	0.2	0.3	0.5	0.6	0.3	0.5	0.4	0.1	0.7	1.2	0.1	0.3	0.5
Sub-humid zone (738 m) – (Dystric Regosols)																						
A (0-16)	0.5	0.3	0.2	0.1	0.1	0.0	0.2	0.0	0.3	0.5	0.7	0.9	0.8	0.5	1.0	0.4	0.6	1.2	1.7	0.1	0.4	0.9
AC (16-34)	0.3	0.2	0.2	0.1	0.0	0.0	0.1	0.0	0.1	0.3	0.4	0.5	0.5	0.2	0.6	0.3	0.2	0.6	1.3	0.1	0.2	0.5
CA (34-56)	0.3	0.2	0.3	0.1	0.0	0.0	0.1	0.0	0.2	0.3	0.3	0.5	0.5	0.3	0.5	0.3	0.2	0.6	1.2	0.1	0.2	0.4
C ₁ (56-93)	0.3	0.3	0.3	0.1	0.0	0.0	0.1	0.2	0.2	0.2	0.4	0.5	0.5	0.2	0.5	0.3	0.3	0.7	1.5	0.1	0.3	0.4
C ₂ (93-111)	0.4	0.3	0.3	0.1	0.0	0.0	0.1	0.0	0.3	0.3	0.5	0.7	0.7	0.3	0.7	0.4	0.4	1.0	2.0	0.1	0.4	0.3
C ₃ (111-136)	0.3	0.3	0.3	0.1	0.0	0.0	0.1	0.0	0.2	0.4	0.5	0.7	0.7	0.3	0.7	0.4	0.3	1.0	1.9	0.1	0.4	0.3
C ₄ (136-152)	0.2	0.2	0.3	0.1	0.0	0.0	0.1	0.0	0.2	0.2	0.3	0.5	0.5	0.2	0.5	0.3	0.3	0.6	1.5	0.1	0.3	0.2
C ₅ (152-195)	0.3	0.2	0.3	0.1	0.0	0.0	0.1	0.3	0.2	0.3	0.4	0.6	0.5	0.3	0.6	0.3	0.3	0.7	1.3	0.1	0.3	0.3
Cr (195-205)	0.3	0.2	0.2	0.1	0.0	0.0	0.2	0.2	0.2	0.3	0.3	0.5	0.3	0.2	0.5	0.9	0.6	0.9	0.9	0.3	0.2	0.3
Dry zone (389 m) – (Eutric Regosols)																						
Ap (0-5)	0.8	0.7	0.4	0.3	0.5	0.3	1.2	0.4	0.3	1.1	1.0	0.8	0.7	1.1	2.3	0.2	0.9	0.7	0.8	0.1	0.6	4.5
CA (5-17)	0.8	0.6	0.4	0.2	0.2	0.2	1.0	0.4	0.3	1.2	0.8	0.7	0.5	1.0	1.9	0.2	0.8	0.5	0.9	0.1	0.7	4.1
C ₁ (17-26)	0.7	0.5	0.3	0.2	0.2	0.2	0.9	0.0	0.2	1.0	0.8	0.7	0.5	0.9	1.7	0.2	0.7	0.5	0.9	0.1	0.7	0.5
C ₂ (26-40)	0.7	0.6	0.4	0.2	0.2	0.2	0.9	0.0	0.2	0.8	0.7	0.7	0.5	1.0	1.5	0.2	0.6	0.5	1.0	0.1	0.8	0.6
C ₃ (40-48)	0.6	0.6	0.4	0.2	0.2	0.2	0.9	0.0	0.3	0.8	0.7	0.6	0.4	0.8	1.5	0.2	0.6	0.4	0.8	0.1	0.7	0.4
Cr (48-59)	0.4	0.5	0.3	0.2	0.2	0.2	0.7	0.2	0.2	0.5	0.4	0.4	0.4	0.7	1.0	0.2	0.6	0.4	0.8	0.1	0.6	2.4

3.6. Geochemistry of soil derived from I- and S-type granites: a multivariate approach

Aiming to provide insights into the factors controlling the geochemistry of major and trace elements of soils originated from I- and S-type granites under tropical settings, we used the multivariate statistical technique (Discriminant Analysis - DA). The observed grouping pattern indicates clear geochemistry differences among soils developed on I- and S-types granites (Figure 8), varying in accordance with weathering contrast.

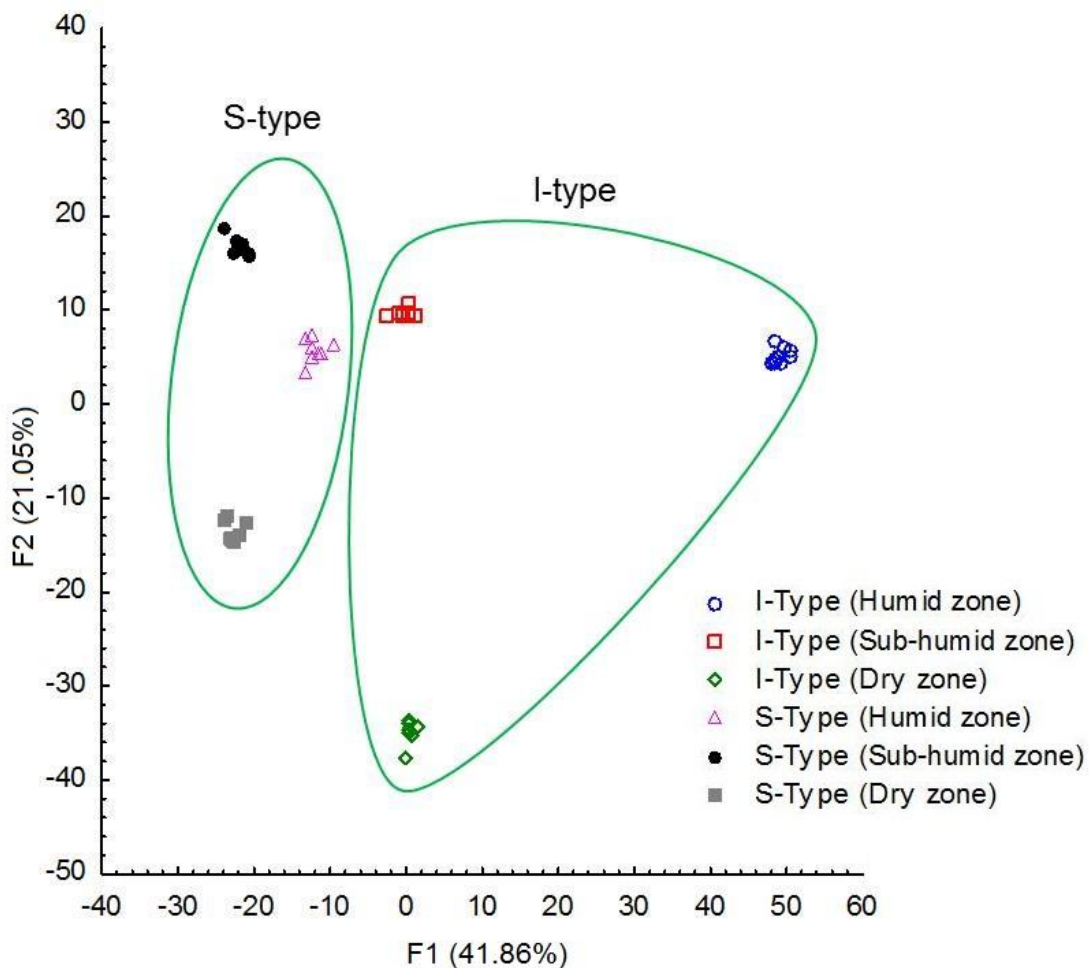


Figure 8. Discriminant analysis based on geochemistry of major and trace elements in soils developed on I- and S-type granites from dry to humid zones of Pernambuco State, Northeast Brazil.

In fact, the discriminant analysis clearly discriminated soil samples derived from I-type granites than those originated from S-type granites (Figure

8). Soil samples from I-type granites are chiefly concentrated on the positively “x” axis, with distribution pattern mostly conditioned by greater contents of clay, silt, TOC, and higher CEC and CIA values. Higher TOC in soil derived from I-type granite under humid zone are clearly related to the higher clay contents, probably in response to the facility of clay minerals in stabilizing and protecting organic matter from decomposition (Sorensen, 1981; Schmidt et al. 2011). Higher CEC in soils developed from I-type granites (especially those under the dry and sub-humid conditions) would also favor the higher contents of major and trace elements compared soils derived from S-type granites.

Soil samples from S-type granites are mainly concentrated on the negatively “x” axis (Figure 8), with distribution patterns mostly explained by contrasting mineral composition of both parent rocks (Table 3). Thus, the higher percentages of weathering resistant minerals in the S-type granites (i.e. quartz and muscovite) may have hindered higher weathering rates. On the other hand, more intense weathering rates in soils developed from I-type granites are justified by the higher percentages of less resistant minerals (i.e. Amphibole, opaque and other accessory minerals).

Two factors with eigenvalues higher than a unit explained roughly 69% (Figure 9) and 73% (Figure 10) of the geochemistry of major and trace elements in soils developed on I- and S-type granites, respectively. For soils derived from I-type granites, the F1 was negatively loaded for Si, Na, K, Ca, Cd, Ni, Pb, Ba and Zr (-0.55 to -0.94) plus sand (-0.96) and pH (-0.60), and positively loaded for Al, Fe, Ti, Cr, V, Ga and Th (0.63 to 0.92) plus CIA (0.98), clay (0.98) and silt (0.88); F2 positively loaded for Mn, Mg, P, Co, Zn and negatively loaded for Cu (-0.64 to -0.91) (Figure 9). This pattern of data distribution clearly differentiated the geochemical behavior of major and trace elements in accordance to the degree of weathering intensity. For instance, F1 visibly separated the relatively immobile elements (Al, Fe, Ti, Cr, V, Ga and Th), which accumulated in humid zone (Figure 9) from those that are leached (Si, Na, K, Ca, Cd, Ni, Pb, Ba and Zr) from soil profiles as a result of the highest weathering intensity. These results are supported by factor 2 and mean CIA values equal to 95%. These geochemical behaviors are also supported by EF values (Table 4).

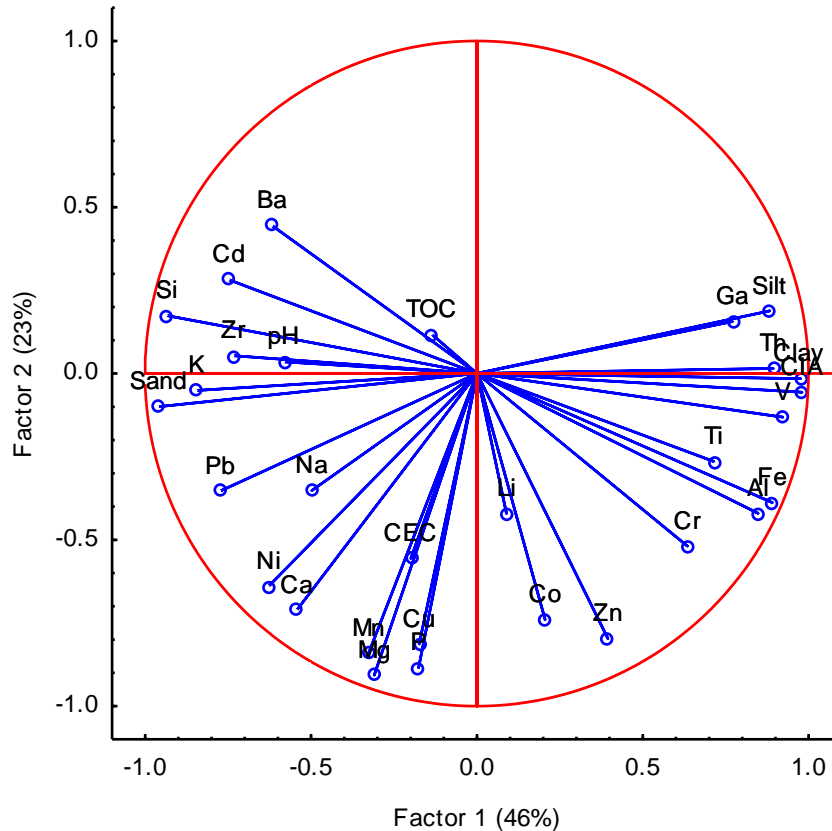


Figure 9. Loadings of major and trace elements on significant factors for soils derived from I-type granites in three climatic zones of Pernambuco State, Northeast Brazil.

For soils derived from S-type granites, F1 was negatively loaded on Si, K, Na, Ca, Cd, Pb, Ba (-0.75 to -0.93) plus sand (-0.92) and pH (-0.65), and positively loaded on Al, Fe, Ti, Co, Zn, Cr, Zr, V, Ga (0.69 to 0.98); F2 exhibited negative and positive loadings for Mn, Mg, P, Th (-0.55 to -0.68) and Ni (0.71), respectively (Figure 10). Similarly of soil samples derived from I-type granites, the pattern of data distribution originated from S-type granites clearly differentiated the geochemical behavior of major and trace elements according to the degree of weathering intensity (Figure 10). The relatively immobile elements concentrated on the positively “x” axis of F1, while the more mobile elements were concentrated on the negatively “x” axis.

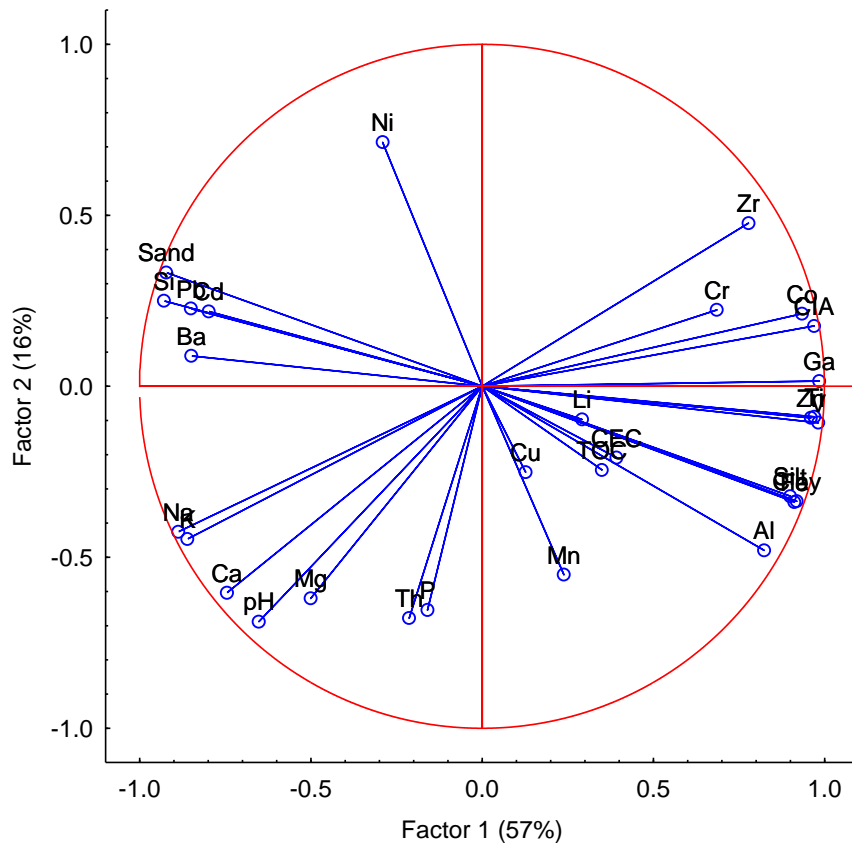


Figure 10. Loadings of major and trace elements on significant factors for soils derived from S-type granites in three climatic zones of Pernambuco State, northeast Brazil.

Regarding the soils formed from the I-type granite, a clear weathering gradient between the different climatic zones was also evidenced by the DA (Figure 8). Data grouping showed the following increasing weathering degree: humid zone > sub-humid zone > dry zone. The distribution of soil samples derived from I-type granites from the humid zone shows the stronger connection with higher CIA values.

Conversely, the climatic effects on major and trace elements geochemistry showed a less evident pattern on soils from S-type granites, probably owing to the highly resistant minerals in S-type granites, which hamper the expressiveness of climate action, especially under conditions with less aggressive chemical weathering (i.e. lower precipitation rates).

4. Conclusions

This paper reports a geochemical study on the major and trace elements found in soils derived from I- and S-type granites across a climosequence from semiarid to tropical zones. Highest major and trace element concentrations were found in soils developed from I-types than S-type granites, which reflect the petrological, mineralogical and geochemical signature of the underlying granites. The EF was a useful tool to observe enrichment signatures of soils derived from I- and S-type granites. Clearly, soils derived from S-types present V enrichment increasing from dry to humid zones while opposite enrichment pattern was observed for Pb. The highest EF values observed for I-type granite soils are mostly explained by their mineral composition which originates soils with higher clay contents and CEC values. Major elements were easier leached than trace elements during weathering processes of both granite types. The applications of multivariate statistical techniques are suitable tools to guide and support soil geochemistry management decisions not only to understand soils variability derived from different granite types but also to contribute to agriculture production and soil-related environmental issues. The data obtained are useful reference values for major and trace elements in soils developed from different granite types in a tropical environment. Additionally, this study shed some light on the complex interrelationship between climate, a major driving force in soil weathering, and granite types on governing soil geochemistry. The geologic factor of soil formation cannot be neglected in climosequence studies to warrant the understanding of important environmental issues such as soil geochemistry.

5. Reference

Almeida, M.E., Macambira, M.J.B., Oliveira, E.C., 2007. Geochemistry and zircon geochronology of the I-type high-K calc-alkaline and S-type granitoid rocks from southeastern Roraima, Brazil: Orosirian collisional magmatism evidence (1.97–1.96 Ga) in central portion of Guyana Shield. *Precambrian Research* 155, 69–97.

Babechuk, M.G., Widdowson, M., Kamber, B.S., 2014. Quantifying chemical weathering intensity and trace element release from two contrasting basalt profiles, Deccan Traps. *India Chemical Geology* 363, 56–75.

Bern, C.R., Chadwick, O.A., Hartshorn, A.S., Khomo, L.M., Chorover, J., 2011. A massbalance model to separate and quantify colloidal and solute redistributions in soil. *Chemical Geology* 282, 113–119.

Blaser, P., Zimmermann, S., Luster, J., Shotyk, W., 2000. Critical examination of trace element enrichments and depletions in soils: As, Cr, Cu, Ni, Pb, and Zn in Swiss forest soils. *Science of the Total Environment* 249, 257-280.

Braun, J.J., Pagel, M., Herbillon, A., Rosin, C., 1993. Mobilization and redistribution of REEs and thorium in a syenitic lateritic profile – a mass-balance study, *Geochimica et Cosmochimica Acta* 57, 4419–4434.

Braun, J.J., Viers, J., Dupré, B., Polve, M., Ndam, J., Muller, J.P., 1998. Solid/liquid REE fractionation in the lateritic system of Goyoum, East Cameroon: the implication for the present dynamics of the soil covers of the humid tropical regions. *Geochimica et Cosmochimica Acta* 62, 273–299.

Brazil. 2001. Mistério de Minas e Energia. *Geologia e recursos minerais do Estado de Pernambuco*. Serviço Geológico do Brasil e do Estado de Pernambuco, Recife, CPRM.

Brimhall, G.H., Dietrich, W.E., 1987. Constitutive mass balance relations between chemical composition, volume, density, porosity, and strain in metasomatic hydrochemical systems: results on weathering and pedogenesis. *Geochimica et Cosmochimica Acta* 51, 567–587.

Brito, L.T.L., Moura, M.S.B., Gama, G.F.B., 2007. Potencialidades da água de chuva no Semiárido brasileiro. Petrolina: Embrapa Semi-Árido. 181p.

Brito Neves, B. B. de. 1975. Regionalização geotectônica do Pré-cambriano nordestino. São Paulo. Tese de Doutorado. Instituto de Geociências, Universidade de São Paulo, Tese de Livre Docência. 198p.

Chappell, B.W., Bryant, C.J., Wyborn. D., 2012. Peraluminous I-type granites. *Lithos* 153, 142–153.

Chappell. B.W., White, A.J.R., 1984. I- and S- type granites in the Lachlan Fold Belt. southeastern Australia. In: Keqin. Xu.. Guangchi. Tu. (Eds.). *Geology of Granites and their Metallogenic Relation*: Beijing Science Press. 87–101pp.

Chappell, B.W., White, A.J.R., 1974. Two contrasting granite types. *Pacific Geology* 8, 173–174.

Chappell, B.W., White, A.J.R., 2001. Two contrasting granite types: 25 years later. *Australian Journal of Earth Science* 48, 489–499.

Clemens, J.D., 2003. S-type granitic magmas – petrogenetic issues, models and evidence. *Earth-Science Reviews* Rev. 61, 1–18.

Cornu, S., Lucas, Y., Lebon, E., Ambrosi, J.P., Luizão, F., Rouiller, J., Bonnay, M., Neal, C., 1999. Evidence of titanium mobility in soil profiles. Manaus, central Amazonia. *Geoderma* 91, 281–295.

Drumond, M.A., Santana, A.C., Antoniole, A., 2004. Recomendações para o usosustentável da biodiversidade no biomacaatinga. In: *Biodiversidade da Caatinga: Áreas e ações prioritárias para a conservação*. Brasília: MMA-UFRPE; Brasília, DF. 47-90pp.

Egli, M., Mirabella, A., Fitze, P., 2001. Weathering and evolution of soils formed on granitic, glacial deposits: results from chronosequences of Swiss alpine environments. *Catena* 45, 19–47.

Ferreira, V.P., Sial, A.N., Sá, E.F.J., 1998. Geochemical and isotopic signatures of Proterozoic granitoids in terranes of the Borborema structural

province, northeastern Brazil. *Journal of South American Earth Sciences* 5, 439-455.

Foden, J., Sossi, P.A., Wawryk, C.M., 2015. Fe isotopes and the contrasting petrogenesis of A-, I- and S-type granite. *Lithos* 212 (215), 32-44.

Frost, B.R., Barnes, C.G., Collins, W.J., Arculus, R.J., Ellis, D.J., Frost, C.D., 2001. A geochemical classification for granitic rocks. *Journal of Petrology* 42, 2033–2048.

Gee, G.W., Or, D., 2002. Particle size analysis. In: DANE, J.H.; TOPP, C.T. *Methods of soil analysis: physical methods. Cap II*, p.255-289, SSSA, Madison. 866p.

Guani, A.A., Searle, M., Robb, L., Chung, S.L., 2013. Transitional I S type characteristic in the Main Range Granite. Peninsular Malaysia. *Journal of Asian Earth Sciences* 76, 225-240.

Guan, Y., Yuan, C., Sun, M., Wilde, S., Long, X., Huang, X., Wang, Q., 2014. I-type granitoids in the eastern Yangtze Block: implications for the Early Paleozoic intracontinental orogeny in South China. *Lithos* 206 (207), 34-51.

Hardy, M., Jamagne, M., Elsass, F., Robert, M., Chesneau, D., 1999. Mineralogical development of the silt fractions of a Podzoluvisol on loess in the Paris Basin (France). *European Journal of Soil Science* 50, 443– 456.

Hernandez, L., Probst, A., Probst, J.L., Ulrich, E., 2003. Heavy metal distribution in some French forest soils: evidence for atmospheric contamination. *Science of the Total Environment* 312, 195-219.

Hu, Y., Liu, X., Bai, J., Shih, K., Zeng, E.Y., Cheng, H.H., 2013. Assessing heavy metal pollution in the surface soils of a region that had undergone three decades of intense industrialization and urbanization. *Environmental Science and Pollution Research* 20, 6150–6159.

INMET. 2015. Instituto Nacional de Meteorologia. Available in <http://www.inmet.gov.br/portal/index.php?r=clima/normaisclimatologicas>.

Accessed in: 16 de nov. de 2015.

IUSS Working Group WRB., 2014. World Reference Base for Soil Resources. World Soil Resources Report No. 106, FAO, Rome.

Koppen, W.P., 1931. Grundriss der Klimakunde. 2nd ed. Berlin: Walter de Gruyter. 388p.

Kurtz, A.C., Derry, L.A., Chadwick, O.A., Alfano, M.J., 2000. Refractory element mobility in volcanic soils. *Geology* 28, 683–686.

Mineralogical methods SSSA., 2008. Part 5 – Methods Of Soils Analysis – soil science society of America. Book Series 5. A.L. Ulery and L.R. Drees (Editors); Madison, USA, Wisconsin.

Murphy, C.P., 1986. Thin section preparation of soils and sediments. Berkhamsterd: Academic Publis. 145p.

NIST - National Institute of Standards and Technology, 2002. Standard Reference Materials -SRM 2709, 2710 and 2711 Addendum Issue Date: 18 January 2002.

Nesbitt, H.W., 1979. Mobility and fractionation of rare earth elements during weathering of a granodiorite. *Nature* 279, 206–210.

Nesbitt, H.W., Young, G.M., 1982. Early Proterozoic climates and plate motions inferred from major element chemistry of lutites. *Nature* 299 (5885), 715–717.

Nesbitt, H.W., Markovics, G., 1997. Weathering of granodioritic crust, long term storage of elements in weathering profiles, and petrogenesis of siliciclastic sediments. *Geochimica et Cosmochimica Acta* 61, 1653-1670.

Olsson, M.T., Melkerud, P.A., 2000. Weathering in three podzolized pedons on glacial deposits in northern Sweden and central Finland. *Geoderma* 94, 149–161.

Price, J.R., Velbel, M.A., 2003. Chemical weathering indices applied to weathering profiles developed on heterogeneous felsic metamorphic parent rocks. *Chemical Geology* 202, 397–416.

Rasmussen, C., Dahlgren, R.A., Southard, R.S., 2010. Basalt weathering and pedogenesis across an environmental gradient in the southern Cascade Range, California, USA. *Geoderma* 154, 473–485.

Sanematsu, K., Kon, Y., Imai, A., 2015. Influence of phosphate on mobility and adsorption of REEs during weathering of granites in Thailand. *Journal of Asian Earth Sciences* 111, 14–30.

Schmidt, M.W., Torn, M.S., Abiven, S., Dittmar, T., Guggenberger, G., Janssens, I. A., Nannipieri, P., 2011. Persistence of soil organic matter as an ecosystem property. *Nature* 478 (7367), 49-56.

Shi, X., Wang, J., 2013. Comparison of different methods for assessing heavy metal contamination in street dust of Xianyang City, NW China. *Environmental Earth Sciences* 68, 2409–2415.

Sorensen, L.H., 1981. Carbon-nitrogen relationships during the humification of cellulose in soils containing different amounts of clay. *Soil Biology and Biochemistry* 13(4), 313-321.

Souza, F.P., Ferreira, T.O., Mendonça, E.S., Romero, R.E., Oliveira, J.G.B., 2012. Carbon and nitrogen in degraded Brazilian semiarid soils undergoing desertification. *Agriculture Ecosystems and Environment* 148,11–21.

Szolnoki, Z., Farsang, A., Puskás, I., 2013. Cumulative impacts of human activities on urban garden soils: Origin and accumulation of metals. *Environmental Pollution* 177, 106-115.

Thomas, W.W., Carvalho, A.M.V., Amorim, A.M.A., Arbelaez, A.L., 1998. Plant endemism in two forests in southern Bahia, Brazil. *Biodiversity and Conservation* 7 (3): 311-322.

Tripathi, J.K., Rajamani, V., 2007. Geochemistry and origin of ferruginous nodules in weathered granodioritic gneisses, Mysore Plateau, Southern India. *Geochimica et Cosmochimica Acta* 71, 1674–1688.

Van Schmus, W.R., Oliveira E.P., Silva A.F.F., Toteu S.F., Penaye J., Guimarães I.P., 2008. Proterozoic links between the Borborema Province, NE Brazil, and the Central African Fold Belt. *Geological Society of London* 294, 69–99.

Vilalva, F.C.J., Vlach, S.R.F., Simonetti, A., 2016. Chemical and O-isotope compositions of amphiboles and clinopyroxenes from A-type granites of the Papanduva Pluton, South Brazil: Insights into late- to post-magmatic evolution of peralkaline systems. *Chemical Geology* 420, 186–199.

Wang, Z., Wang, J., Deng, Q., Du, Q., Zhou, X., Yang, F., Liu, H., 2015. Paleoproterozoic I-type granites and their implications for the Yangtze block position in the Columbia supercontinent: Evidence from the Lengshui Complex, South China. *Precambrian Research* 263, 157-173.

Yeomans, J.C., Bremner, J.M., 1988. A rapid and precise method for routine determination of organic carbon in soil. *Communications in Soil Science and Plant Analysis* 19,1467–1476.

Yousefifard, M., Ayoubi, A.J., Jalalian, A., Khademi, H., Makkizadeh, M.A., 2012. Mass Balance of Major Elements in Relation to Weathering in Soils Developed on Igneous Rocks in a Semiarid Region, Northwestern Iran. *Journal of Mountain Science* 9, 41–58.

Yusoff, Z.M., Ngwenya, B.T., Parsons, I., 2013. Mobility and fractionation of REEs during deep weathering of geochemically contrasting granites in a tropical setting, Malaysia. *Chemical Geology* 349, 71–86.

Zhao, X.F., Zhou, M.F., Li, J.W., Wu, F.Y., 2008. Association of Neoproterozoic A- and I-type granites in South China: Implications for generation of A-type granites in a subduction-related environment. *Chemical Geology* 257, 1–15.

CHAPTER III

**GEOCHEMISTRY OF REE IN I- AND S-TYPE GRANITES AND DERIVED
SOILS IN THREE CLIMATE ZONES OF NORTHEAST BRAZIL**

Geochemistry of REE in I- and S-type granites and derived soils in three climate zones of Northeast Brazil

Abstract

The Borborema Province, NE Brazil, represents the Western portion of the extensive geologic Brasiliano-Pan African orogenic system characterized by voluminous S- and I-type granites. In this study we compared the mineralogy and geochemistry of I- and S-type granites, their derived soils, and the rare earth elements (REEs) distribution in rocks and soils in three climatic zones of Pernambuco State, from semiarid to tropical settings. We measured total REEs, their relative mobility and Light REE/Heavy REE fractionation. The S-type granites are characterized by higher silicate contents, whereas I-type granites showed higher proportion of accessory minerals: allanite, titanite, apatite, amphibole and opaque minerals. The REE geochemistry of I-type granites are more differentiated than the S-type granites. This is largely due to the higher proportion of accessory minerals in I-type granites. Bastnaesite and monazite seems to be the major sources of REEs in soils derived from I- and S-type granites, respectively. According to the high La/Yb_N and LREE/HREE ratios, weathering processes showed significant impact on REE fractionation in soils derived from both granite types. In soils, the highest LREE/HREE fractionation is found in the humid zone, largely as a result of the dominance of kaolinites that have preferentially adsorbed LREEs. The highest chemical index of alteration (CIA) related to the highest LREE/HREE ratios suggest that LREE/HREE fractionation is a good indicator of the degree of granite weathering. Both, the granitic parent material composition and the weathering intensities related to climate are key factors to the understanding of REE distribution in soils in this environment.

Keywords: Rare earth elements; trace elements; chemical weathering; soil geochemistry

1. Introduction

The International Union of Pure and Applied Chemistry (Connelly et al. 2005) defines rare earth elements (REEs) as a group of 17 chemically similar metallic elements (Lanthanide series, plus scandium and yttrium). The latter two elements are included as REEs because they are chemically similar to the lanthanides (Jaireth et al. 2014). These elements have been commonly divided into two groups: light rare earth elements (LREEs: La-Eu) and heavy rare earth elements (HREEs: Gd-Lu) (Hu et al. 2006; Long et al. 2010; Sadeghi et al. 2013; Walters et al. 2010). The REEs are not as rare in nature as the name suggests. Cerium, 25th most abundant element in the crust, exhibits higher concentration in Earth's crust than copper and similar to Zn (Tyler 2004).

Rare earth elements have become strategically critical for developed and developing economies around the world owing to the wide application in many industrial key technologies (Gandois et al. 2014; Mihajlovic et al. 2014; Pagano et al. 2015). Nevertheless, the pedological behavior of REEs remains poorly understood (Chen et al. 2014). Recently, Laveuf and Cornu (2009) and Laveuf et al. (2012) recommended further study of the REE behavior in different pedological environments in order to quantify different geochemical behavior of REEs.

Granites are common igneous rock types of the continental crust. These rocks can be derived from different compositions and petrogenetic processes (Chappell and White 1984). Chappell and White (1974, 2001) simplified the classification of granites into I- and S-type granites. This classification, along with the use of A-type granites are widely used worldwide (Foden et al. 2015; Guani et al. 2013; Guan et al. 2014; Vilalva et al. 2016; Wang et al. 2015). Overall, I-type granites are derived from igneous protolith (infracrustal rocks), whereas S-type granites indicate derivation from sedimentary rock (supracrustal rocks) (Chappell and White 1984).

Although the REE geochemistry of soils derived from granites has been investigated (Aubert et al. 2001; Sanematzu et al. 2015), there has been no attempt to compare the REE geochemistry related to weathering along a climatic gradient (climosequence). In this study, soil profiles were sampled based on granite types (I- and S-types) in three distinct climatic zones (humid,

sub-humid and dry) from tropical to semiarid region of Pernambuco State, NE Brazil. We hypothesized that soils derived from I-type granites would show different geochemical and mineralogical signatures of REEs in comparison to those derived from S-type granites.

In this study, we address two fundamental questions. First, how do geochemical and mineralogical signatures of REEs differ from soils developed over I- and S-type granites along a climosequence from the semiarid to the humid zone? Second, are REEs mobilised during weathering of geochemically contrasting granites? Thus, our objectives are: (i) to describe the petrography and mineralogy of I- and S-type granites of the Borborema Province, Northeast Brazil; (ii) to investigate the source and geochemical behavior of REEs, and the controlling factors for their distribution; (iii) to evaluate the climosequence influence on geochemistry of REEs in soils from humid to semiarid climates. Our results can hopefully be used to understand the geochemistry of REEs in other parts of the tropics and sub-tropics which are underlain by S- and I-type granites.

2. Materials and methods

2.1. Study area

The study was carried out in the Borborema Province, Pernambuco State, NE Brazil. The Borborema Province represents the Western portion of the extensive geological Brasiliano-Pan African orogenic system formed by convergence of the West Africa/São Luis and San Francisco-Congo Cratons (Brito Neves, 1975). Geologically speaking, the Borborema Province comprises a mosaic of tectonic blocks including Paleoproterozoic basement and scattered Archean nuclei, Meso to Neoproterozoic supracrustal rocks, and voluminous intrusions of granites (Van Schmus et al. 2008).

The study region can be divided into three climatic zones according to Koppen classification (Koppen, 1931). The dry zone shows a semiarid climate (Bhs), characterized by negative water balance, as a result of the annual rainfall (< 800 mm) lower than evaporation (2.000 mm year⁻¹). Annual average air temperature ranges from 23 to 27 °C and relative humidity is about 50% (Brito

et al. 2007). In the sub-humid zone presents a climate classified as Aw, characterized by average air temperature is approximately 24 °C, the annual rainfall range from 800 to 1,000 mm. The humid zone represents a tropical climate (Am), warm and humid with annual rainfall ranging from 1,000 to 2,000 mm year⁻¹ (INMET 2015). The annual average air temperature equal to 27 °C shows thermal amplitude of about 5 °C and high relative humidity (> 50%).

There is a clear relationship between climatic conditions and the distribution of vegetation. The vegetation comprises the following units: (i) Primary evergreen forest (Atlantic rainforest) in humid zone; (ii) Semideciduous forest in sub-humid zone; (iii) Dry deciduous forest known as Caatinga in the dry zone. The Caatinga is an exclusively Brazilian biome and vulnerable to desertification (Souza et al. 2012).

2.2. Soil and Rock sampling

Soil profiles developed on I- and S-type granites from three climatic zones under native vegetation or with minimal anthropic influence were chosen based on geological maps and field local confirmation (Figure 1).

were classified according to the World Reference Base for Soil Resources (IUSS Working Group WRB 2014).

2.3. *Analytical methods*

2.3.1. *Granite analysis*

The I- and S-type granites and their modal mineral compositions were determined from fresh rock samples which were collected from an outcrop beside the soil profiles. The mineralogical identification was made from polished thin sections according to Murphy (1986) using a petrographic microscope.

The major element oxides (SiO_2 , TiO_2 , Al_2O_3 , Fe_2O_3 , MgO , CaO , MnO , Na_2O , K_2O , and P_2O_5) of whole-rock samples were determined by X-ray fluorescence (XRF) spectrometry (Rigaku, RIX 3000 model) using lithium tetraborate as a flux. Loss on ignition was determined at 1,000 °C. The results were verified using an international geochemical standard SRM 2709, San Joaquin soil (NIST 2002). The recovery rates of major element (%) appeared in the following decreasing order: P (126) > Al (106) > Ca (105) > Ti 101) > Fe (100) > K (98) > Mg (96) > Si (89) > Mn (81) > Na (72). These results were considered to be satisfactory and reflect the quality of the XRF measurement.

After optic microscope observation, granite samples were coated with a 20 nm gold layer (model Q150R - Quorum Technologie). Fine-grained minerals and their textures were observed using a TESCAN (model: VEGA-3 LMU) field emission SEM at an accelerating voltage of 15 kV. Afterwards, the energy dispersive X-ray spectrum (EDS; Oxford Instrument, model: 51-AD0007) coupled with SEM were used to analyze the semiquantitative characteristics of the mineral compositions.

2.3.2. *Soil analyses*

2.3.2.1. *Physical and chemical analyses*

Soil samples were collected from profiles over the various granites. The samples were collected from specific soil horizons at different depths. The particle size distribution was obtained according to the method of Gee and Or

(2002) using Calgon as chemical dispersion. All samples were submitted to pre-treatment with H₂O₂ to eliminate organic matter. Soil pH was determined using distilled water (1:2.5 soil:solution ratio). Exchangeable K and Na were extracted with Mehlich-1 procedures (1:10 soil:solution ratio). Calcium, Mg and Al were extracted with 1 mol L⁻¹ KCl (1:10 soil:solution ratio). All elements were determined by optical emission spectrometry (ICP-OES/Optima 7000, Perkin Elmer). Potential acidity (H⁺ + Al³⁺) was determined by calcium acetate method (0.5 mol L⁻¹, pH 7.0), and total organic carbon (TOC) according to Yeomans and Bremner (1988). The cation-exchange capacity (CEC) was calculated from the sum of the exchangeable cations and the total acidity. Physical and chemical analyses (Tables 1, 2) clearly demonstrate the large difference between soils derived from I- and S-type granites, as well as contrasts with respect to the environmental gradients.

Table 1. Selected chemical and physical attributes of soil profiles derived from I-type granites along a climosequence in Pernambuco State, Brazil

Horizon/depth (cm)	Clay	Silt	Sand	TOC ^a	pH	CEC ^b	Fe _t ^c	CIA ^d
	(g kg ⁻¹)			(g kg ⁻¹)	(H ₂ O)	(cmol _c kg ⁻¹)	(g kg ⁻¹)	(%)
Humid zone (537 m) – (Hypereutric Chromic Lixisols)								
A ₁ (0-8)	150	379	471	59.58	5.45	8.54	56.60	89
A ₂ (8-18)	170	383	447	58.53	5.00	7.17	57.38	91
AB (18-30)	180	414	406	11.97	4.70	5.50	68.80	93
BA (30-46)	250	440	310	6.37	4.80	4.63	78.67	94
Bt ₁ (46-64)	300	507	193	5.72	5.20	4.23	103.06	97
Bt ₂ (64-84)	310	506	184	4.19	5.00	4.17	115.79	98
Bt ₃ (84-135)	300	522	178	1.50	5.00	4.03	118.95	98
BC (135-175)	260	569	171	3.66	5.00	3.82	112.79	98
C (175-195+)	270	558	172	3.07	4.80	3.64	112.21	98
Sub-humid zone (695 m) – (Eutric Regosols)								
A (0-11)	50	290	660	45.27	5.15	9.12	12.30	70
CA (11-17)	60	282	658	6.99	5.20	5.76	13.12	71
C ₁ (17-46)	50	280	670	3.95	5.10	4.47	11.77	70
C ₂ (46-70)	50	300	650	2.06	5.45	3.36	10.00	68
C ₃ (70-78)	50	240	710	1.65	5.65	2.46	9.23	64
Cr ₁ (78-148)	270	474	256	3.89	4.30	14.96	64.30	93
Cr ₂ (148-185)	180	335	485	2.54	4.70	18.08	69.11	87
Cr ₃ (185-200)	100	533	367	1.80	5.10	10.87	48.76	79
Dry zone (473 m) – (Eutric Regosols)								
A (0-3)	50	195	755	39.64	7.10	10.57	67.00	56
CA (3-9)	80	304	616	11.29	6.85	10.83	54.98	70
C ₁ (9-17)	100	321	579	7.09	6.00	7.49	43.92	74
C ₂ (17-27)	110	308	582	4.97	5.50	8.17	42.17	76
C ₃ (27-39)	120	326	554	4.08	5.10	7.96	38.42	78
Cr ₁ (39-53)	130	358	512	3.19	4.80	8.85	30.56	83
Cr ₂ (53-63+)	80	231	689	1.92	5.00	10.91	16.35	75

^a Total organic carbon; ^b Cation exchange capacity; ^c Total Iron; ^d Chemical index of alteration.

Table 2. Selected chemical and physical attributes of soil profiles derived from S-type granites along a climosequence in Pernambuco State, Brazil

Horizon/depth (cm)	Clay (g kg ⁻¹)	Silt (g kg ⁻¹)	Sand (g kg ⁻¹)	TOC ^a (g kg ⁻¹)	pH (H ₂ O)	CEC ^b (cmolc kg ⁻¹)	Fe _t ^c (g kg ⁻¹)	CIA ^d (%)
Humid zone (348 m) – (Dystric Xanthic Ferralsols)								
A ₁ (0-9)	200	244	556	39.68	4.60	7.10	20.58	91
A ₂ (9-20)	200	263	547	14.83	4.25	5.84	24.78	94
AB (20-37)	200	361	439	9.01	4.20	4.58	29.95	95
BA (37-50)	230	385	385	7.00	4.10	4.27	32.31	95
Bo ₁ (50-69)	230	364	406	4.23	4.15	3.00	34.98	96
Bo ₂ (69-89)	220	350	430	3.87	4.10	2.71	33.33	95
Bo ₃ (89-109)	200	362	438	3.64	4.10	2.53	32.40	95
Bo ₄ (109-147)	230	348	422	5.53	4.20	2.53	36.84	96
Bo ₅ (147-165)	250	365	385	4.05	4.10	2.65	41.32	96
Sub-humid zone (738 m) – (Dystric Regosols)								
A (0-16)	50	90	860	4.44	4.30	4.10	4.97	79
AC (16-34)	30	126	844	2.82	4.10	2.75	8.46	83
CA (34-56)	60	139	801	3.31	3.75	2.80	10.16	83
C ₁ (56-93)	70	139	791	3.58	3.70	2.96	12.08	85
C ₂ (93-111)	80	137	783	2.60	3.90	3.24	8.18	84
C ₃ (111-136)	70	166	764	1.29	3.75	2.80	8.86	84
C ₄ (136-152)	60	161	779	1.44	4.00	2.32	10.79	82
C ₅ (152-195)	70	183	747	1.16	4.20	2.28	9.90	82
Cr (95-205)	50	161	789	0.31	4.35	1.30	6.95	72
Dry zone (389 m) – (Eutric Regosols)								
Ap (0-5)	40	51	909	4.57	6.00	2.75	4.70	58
CA (5-17)	50	80	870	3.18	5.30	2.22	4.38	61
C ₁ (17-26)	50	97	853	1.98	5.15	2.23	4.88	62
C ₂ (26-40)	50	113	837	2.62	4.80	2.37	5.29	62
C ₃ (40-48)	40	120	840	1.77	5.20	2.45	5.40	61
Cr (48-59)	50	232	718	1.15	6.20	3.15	7.15	62

^a Total organic carbon; ^b Cation exchange capacity; ^c Total iron; ^d Chemical index of alteration.

2.3.2.2. Rare earth elements analyses

For the REEs measurement, 1 g of soil was digested in Teflon vessels with 6 mL of HNO₃, 3 mL of HF and 3 mL of HCl in a microwave oven (Mineralogical methods – SSSA, 2008). We prepared a six-point calibration curve from a standard solution containing 1.000 mg L⁻¹ (Titrisol®, Merck) of each rare earth element. Analysis was performed only when the coefficient of determination (*r*²) of the calibration curve was higher than 0.99. Analytical data quality and standard operation procedures such as curve recalibration, analyses of blanks and standard reference material SRM 2709 San Joaquin soil (NIST 2002) were performed. Whenever more than 10% deviation was observed, the equipment was calibrated and samples analyzed again. All of the analyses were carried out in duplicate.

Concentrations of La, Ce, Pr, Nd, Sm, Eu, Gd, Tb, Dy, Ho, Er, Tm, Yb, Lu, Y, and Sc were determined by inductively coupled plasma optical emission spectroscopy (ICP-OES/Optima DV7000, Perkin Elmer). To improve sensitivity to REEs, we coupled a cyclonic spray chamber/nebulizer to the ICP-OES. Additionally, the high REE recovery rates obtained in the certified standard material used warrant the measurement accuracy. The recovery rates of REEs (%) in a certificated soil sample (SRM 2709, San Joaquin soil) appeared in the following decreasing order: Yb (92%) > Lu (83%) > Sm (81%) > Eu (78%) > Nd (77%) > Gd (75%) > La (66%) > Ce (61%) = Sc (61%).

The reference values for Pr, Dy, Er, Ho, Tm, Tb, and Y have not been established for the certified sample (NIST 2002). All results were considered to be satisfactory and reflect the quality of both the digestion method applied and our ICP-OES measurement. Mihajlovic et al. (2014), using aqua regia digestion and measuring REEs in ICP-MS, found similar recovery values varying from 64 to 98%.

REE concentrations were normalized to upper continental crust (UCC) as per Taylor and McLennan (1985). Moreover, we also quantified the fractionation between LREEs and HREEs according to the La/Yb ratio, and the Ce anomalies $[(Ce_N/(La_N * Pr_N))^{0.5}]$ and Eu anomalies $[(Eu_N/(Sm_N * Gd_N))^{0.5}]$ were calculated according to Compton et al. (2003), where N implies normalized values. A value below "1" (negative anomaly) represents depletion, a value above "1" (positive anomaly) enrichment compared to the UCC.

2.3.2.3. Clay mineralogy analysis

X-ray diffraction (XRD) analysis was performed on the clay fraction (< 2 μ m) of the soils - separated using standard sedimentation procedures - of the diagnostic horizon. A Shimadzu 6000 diffractometer fitted with a graphite monochromator set to select Cu K α radiation (30mA/40 kV) was used. The measurement range was 3° to 35°(2 θ), with steps of 0.02°2 θ at 1.2 s/step, except for treatment with ethylene glycol solvation (3-15°2 θ). Prior to analysis, the clay was submitted to the following standard treatments: organic matter elimination (15% hydrogen peroxide) and iron oxides elimination (dithionite-citrate-bicarbonate method).

Clays were oriented on glass slides with the following standard treatments: Mg saturation ($\text{MgCl}_2 - 1 \text{ mol L}^{-1}$), Mg saturation/glycerol solvation, K saturation ($\text{KCl} - 1 \text{ mol L}^{-1}$), and heat treatment of K-saturated samples, during three hours at 350 and 550 °C (Whittig and Allardice 1986). Clay mineral identification was based on criteria described by Jackson (1975); Brown and Brindley (1980); Moore and Reynolds (1997).

2.4. *Measurements of chemical weathering*

The sample powders were mechanically compressed to make pellets for X-ray fluorescence analysis. The molecular proportions of major element oxides were determined using XRF spectrometry (S8 TIGER ECO – WDXRF-1KW). Loss on ignition was determined at 1,000 °C. The results were verified using international geochemical standard (SRM 2709, San Joaquin soil), and used to calculate the chemical index of alteration (CIA), following Nesbitt and Young (1982). The formula for the CIA is as follows:

$$\text{CIA} = [\text{Al}_2\text{O}_3 / (\text{Al}_2\text{O}_3 + \text{Na}_2\text{O} + \text{CaO} + \text{K}_2\text{O})] \times 100.$$

This index increases with the loss of cations (Ca^{2+} , K^+ and Na^+). It is assumed that feldspar to kaolin transformation is the predominant weathering process and that Al is relatively immobile (Rasmussen et al. 2010). It is used as indicator specifically to evaluate the degree of chemical weathering of felsic rocks (Sanematsu et al. 2015).

2.5. *Statistical analysis*

Results were assessed by descriptive statistics and factor analysis (FA). The latter was applied to the correlation matrix of dataset in order to study REE geochemistry during granite weathering. To extract the significant factors while diminishing the contribution of variables with little importance, we employed Varimax rotation (Kaiser 1958).

3. Results

3.1. *Mineralogy of S- and I-type granites*

Overall, S-type granites showed texture with fine to medium crystals, with a light gray color (Figure 2c). The granites are mainly composed of quartz, feldspars and biotite evenly distributed; no magnetic minerals were observed (Figure 2d). These rock types showed gentle foliations outlined by mafic minerals. I-type granites have inequigranular, commonly porphyritic texture, with medium to coarse K-feldspars, small amounts of gray quartz and black mafic minerals, commonly biotite (Figure 2a). I-type granites are slightly magnetic due to magnetic minerals (i.e. magnetite).

K-feldspar, quartz, plagioclase and biotite are the dominant components, ranging from 85 to 90% and 87 to 93% of the total composition of the I- and S-type granites, respectively (Table 3). Quartz and plagioclase are more abundant in S-types whilst K-feldspars and opaque minerals were higher in I-types. Muscovite was observed only in S-types, ranging from 3 to 6% and exhibited some degree of alteration, chiefly being replaced by sericite. Amphibole (Figure 2i), apatite and titanite (Figure 2g) were evidenced only in I-type granites (Table 3).

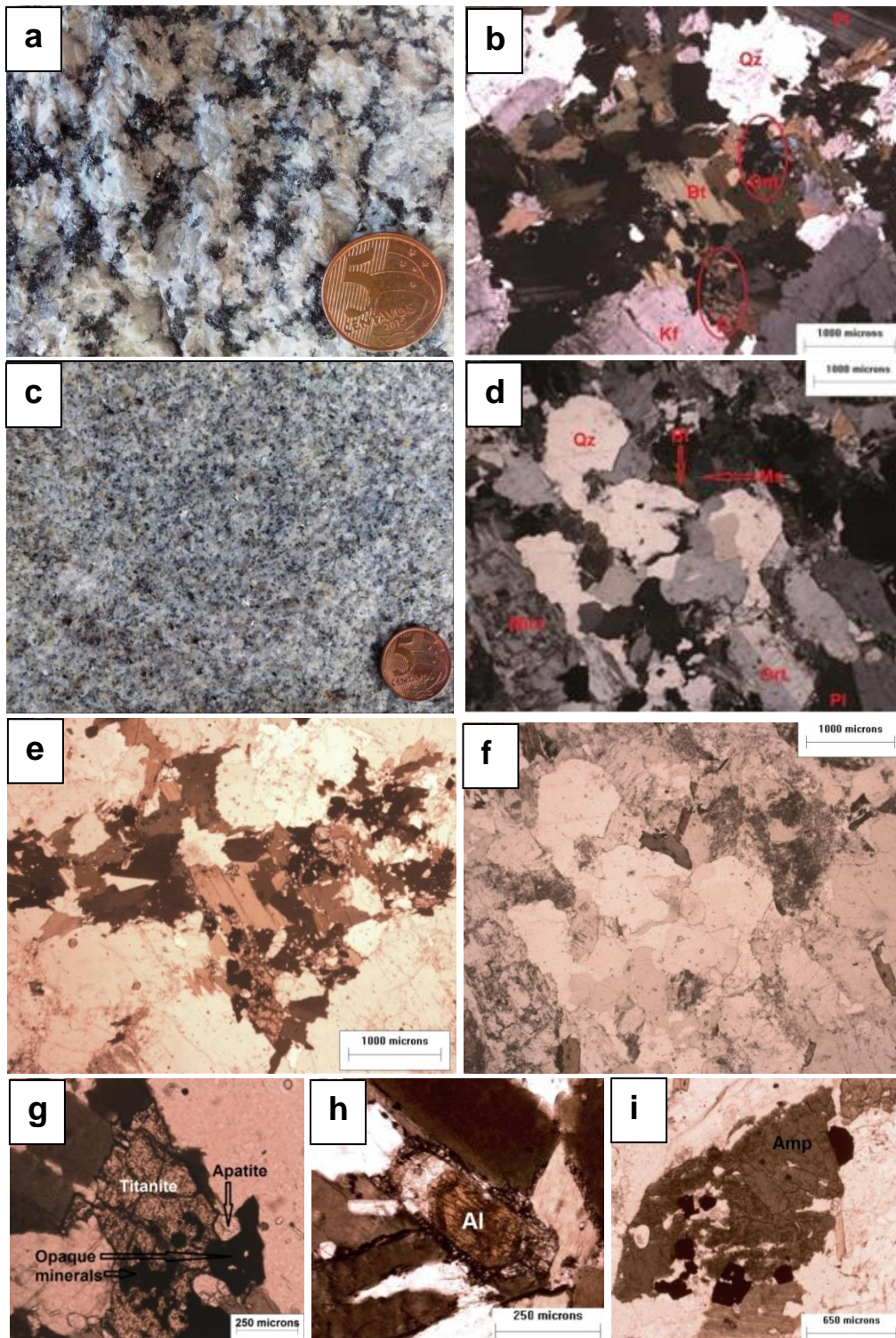


Figure 2. Macro-photograph of I- and S-type granites (a, c, respectively) and selected petrographic characteristics. General aspects (b, d, respectively). Mafic minerals of I- and S-type granites (e, f, respectively). Titanite, apatite and opaque minerals (g). Allanite (h). Amphibole (i) Qz – Quartz; Micr – Microcline; Ort – Orthoclase; Bt – Biotite; Pl – Plagioclase; Ms – Muscovite; Om – Opaque minerals; Ti – Titanite. Al – Allanite; Amp – Amphibole.

The mineral assemblage of I-type granites (Table 3) is consistent with the petrographical results of Chappell and White et al. (2001). Allanite and titanite tend to occur in I-type rather than S-type granites (Bea 1996). Biotites are in the early alteration stage to chlorite. Plagioclases are slightly altered to sericites. K-feldspars are found as microcline and orthoclase. The phosphate mineral apatite occurs in small crystals and is often associated with mafic minerals (Figure 2g). Apatite inclusions are common in biotite of I-type granites whereas they occur in larger discrete crystals in S-types (Chappell and White (2001).

Table 3. Mineralogical composition (%) of I- and S-type granites in Pernambuco State

Mineral	I-type granites			S-type granites		
	Humid	Sub-humid	Dry	Humid	Sub-humid	Dry
K-feldspar	61	55	65	45	37	23
Quartz	12	7	8	23	26	34
Plagioclase	7	12	7	5	22	28
Biotite	10	11	5	14	12	8
Amphibole	4	4	7	nd	nd	nd
Sericite / Muscovite	nd	nd	nd	6	3	6
Opaque mineral	2	4	4	4	<1	1
Allanite	3	2	< 1	3	<1	< 1
Apatite	1	2	3	nd	nd	nd
Titanite	nd	2	1	nd	nd	nd
Chlorite	< 1	< 1	nd	nd	nd	< 1
Total	100	100	100	100	100	100

nd – not detected.

In the S-type granites, small amounts of biotite are changing in terms of composition to chlorite. Small inclusions of allanite with radioactive elements in its composition are found in biotite (Figure 2d). The disintegration of allanite is responsible for the spot formations in biotites. Plagioclases are sericitized usually forming lamellae of muscovite/sericite. K-feldspars are found as microcline and orthoclase.

3.2. Clay mineralogy

Powder XRD of the clay fraction derived from I- and S-type granites revealed that kaolinite was the major phase in the samples, with minor amounts of quartz and feldspar (Figures 3). Greater expressions of primary minerals were identified in the dry zones, mainly in soils developed on S-type granites (Figure 3f). The humid zones originated typical kaolinitic soils (Figures 3a and 3d). The main differentiating pattern between these granites was the presence of 0.41 nm goethite peak, observed only in the clay fraction of the I-type granites (Figure 3a) in the sub-humid and humid zones.

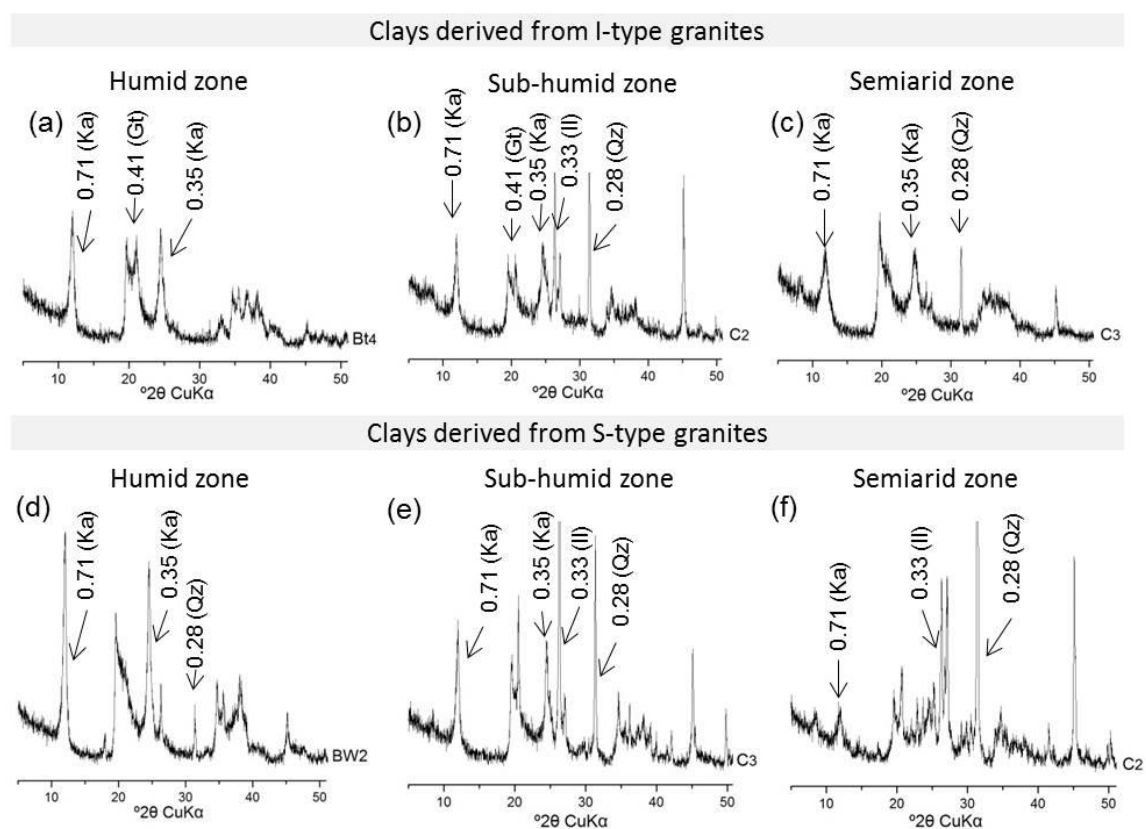


Figure 3. X-ray diffraction patterns for clays obtained from diagnostic horizons of soil profiles derived from I- and S-type granites in different climatic zones of Pernambuco State, Northeast Brazil. Humid zone (a, d); Sub-humid zone (b, e); Dry zone (c, f). Ka – Kaolinite; Gt – Goethite; Il – Illite; Qz – Quartz.

The presence of kaolinite, illite, Interstratified illite-vermiculite and gibbsite were observed through the oriented aggregates (Figure 4). Kaolinite was recognized by its 001 and 002 peak reflections of 0.71 and 0.35 nm, respectively. The disappearance of these peaks upon 550°C heat treatment

confirms its presence, as well as the absence of chlorite in all samples. The mica peak (1.0 nm) – not very sharp – indicates illite formation as the first mica weathering product (Yousefifard et al. 2015). The persistence of this peak after ethylene glycol solvation treatment confirms its existence.

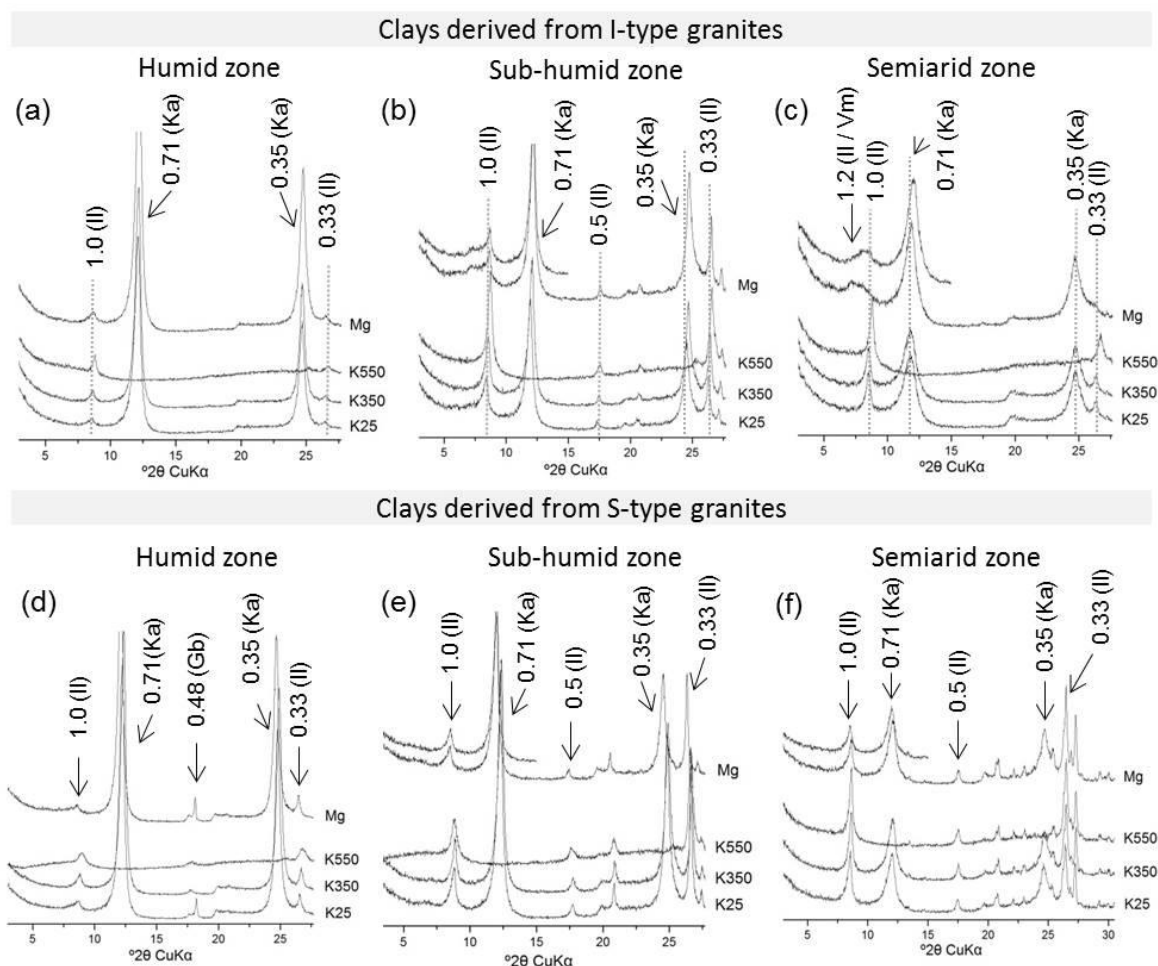


Figure 4. X-ray diffraction patterns for various clay treatments obtained from diagnostic horizons of soil profiles derived from I- and S-type granites in different climatic zones of Pernambuco State, Northeast Brazil. Humid zone (a, d); Sub-humid zone (b, e); Dry zone (c, f). Ka – Kaolinite; Gb – Gibbsite; Il – Illite; Qz – Quartz; Il / Vm - Interstratified illite-vermiculite.

In the dry zone, the 1.2 nm peak (Figure 4c) corresponds to different minerals, likely illite-vermiculite. This finding was only observed in soil profiles derived from I-type granites. Nevertheless, S-type granite exhibited predominantly monosalitization process (kaolinite – 0.7 nm), with coexistence

of illite (0.1, 0.5, 0.33 nm) and no evidence of interstratified illite-vermiculite (Figure 4f).

Soils of both granite types, from the dry to the humid zone, are mainly kaolinitic soils, with minor amounts of illite (Figures 4a and 4d). A gibbsite peak (0.48 nm) was found only in soil derived from S-type granite (Figure 4d) based on its disappearance after the 300 °C treatment.

3.3. *Geochemistry of REEs in soil profiles*

Regardless of the climatic zone, the average REE concentrations in soils derived from S-type granites exhibited the following order: Ce > La > Nd/Pr > Y > Sm > Er > Dy > Sc > Eu > Gd > Yb > Lu > Tb/Ho/Tm, except for the larger concentration of Gd in sub-humid and dry zones, ranging from 0.6 to 3.0 mg kg⁻¹ and 0.8 to 1.7 mg kg⁻¹, respectively, higher than Eu and Sc (Figure 4). Soils derived from I-type granites showed the following order: Ce > La > Pr > Nd > Sm > Er > Y > Sc > Eu > Lu > Gd > Dy > Yb > Tb/ Ho/Tm for humid zone; and Ce > La > Pr > Nd > Y > Sm > Er > Dy > Sc > Eu > Gd > Yb > Lu > Tb/Ho/Tm for sub-humid and dry zones (Figure 5). The HREEs geochemistry is more influenced by the environmental gradient in comparison to the LREEs for all soil types (Figures 5, 6). The Lu accumulation in depth was more pronounced in soil derived from I-type granite (Figure 5b).

Soils derived from I-type granites exhibited higher total REE contents than those derived from S-types, ranging from 58.8 to 305.3 mg kg⁻¹, 55.0 to 683.7 mg kg⁻¹ and 83.75 to 749.2 mg kg⁻¹ for humid, sub-humid and dry zones, respectively (Table 4). The high to low average sequence of REEs values is Dry > Sub-humid > Humid zone. These data are within the ΣREE concentration range likely to occur in soils (Hu et al. 2006; Laveuf and Cornu 2009; Liang et al. 2005; Tyler 2004).

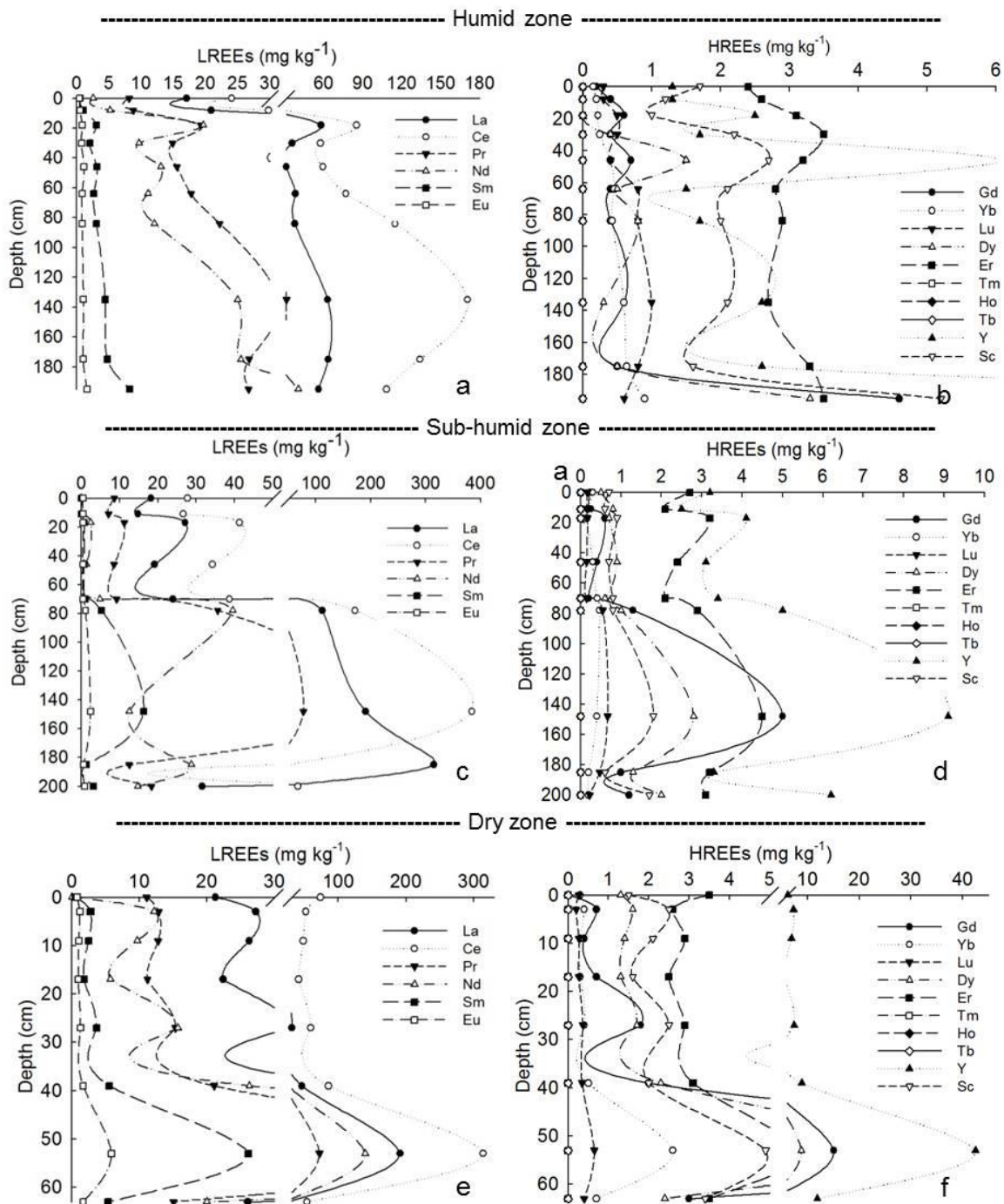


Figure 5. Concentration of REEs in soils derived from I-type granites in three climatic zones of Pernambuco State, Northeast Brazil. Hypereutric Chromic Lixisols (a and b); Eutric Regosols (c and d); Eutric Regosols (e and f).

Soils developed over I-type granites contain large amounts of Σ LREE compared to those derived from S-types, ranging from 53.1 to 296.0 mg kg^{-1} for the humid zone, 49.0 to 683.7 mg kg^{-1} for the sub-humid zone and 83.75 to 749.2 mg kg^{-1} for the dry zone (Figure 5). Clearly, their concentration increased

from dry to humid zones. This finding suggests that LREE concentration is higher where weathering is more intense (Table 4).

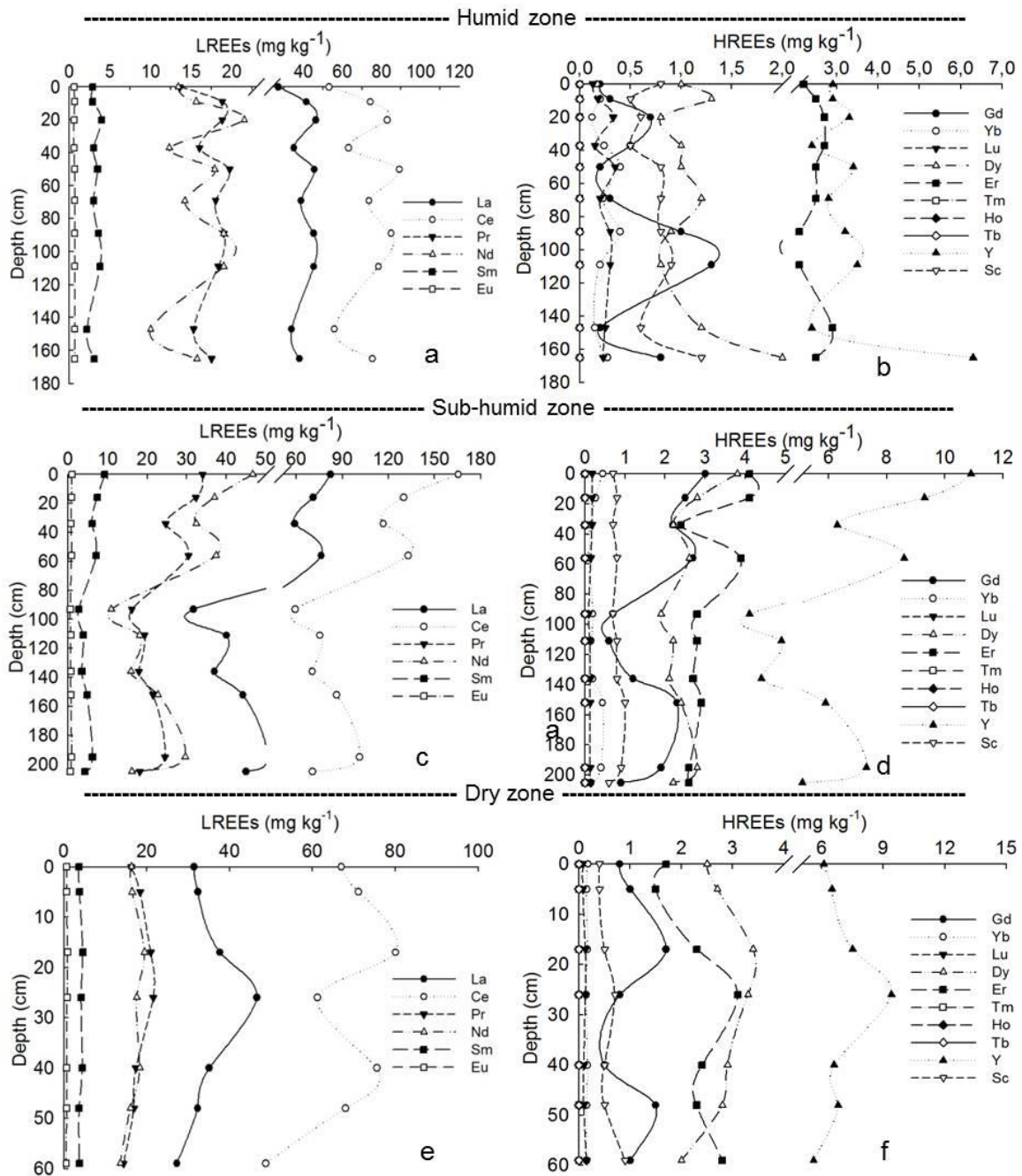


Figure 6. Concentrations of REEs in soils derived from S-type granites in three climatic zones of Pernambuco State, Northeast Brazil. Dystric Xanthic Ferralsols (a and b); Dystric Regosols (c and d); Eutric Regosols (e and f).

Overall, the Σ REE concentrations in soils derived from I- and S-type granites were lower than the values reported from the Upper Continental Crust

(UCC) except for saprolites derived from I-type granites (Table 4). Both LREEs and HREEs in saprolites originating from I-types showed the largest enrichment in relation to the UCC, with values reaching 305.3, 707.57 and 829.45 mg kg⁻¹ for humid, sub-humid and dry zones, respectively, reflecting differences in fractionation associated with the formation of both granite types.

4. Discussion

4.1. Geochemistry of REEs in I- and S-type granites

The geochemistry of REEs in I-type granites shows distinct pattern when compared to S-type granites (Table 5). This was expected mainly because I-types are derived from igneous protolith whereas S-types are derived from sedimentary rocks (Chappell and White 1984). As a result, distinct mineralogy and geochemistry of REEs have been observed (Clemens 2003; Yusoff et al. 2013).

Table 5. Geochemistry of REEs in I- and S-type granites in Pernambuco State, Brazil

Climatic zone	La	Ce	Pr	Nd	Sm	Eu	Gd	Yb	Lu	Dy	Er	Y	Sc
I-type granite (mg kg ⁻¹)													
Humid	56.0	108.3	26.7	40.4	8.3	1.7	4.6	0.9	0.6	3.3	3.5	18.3	5.2
Sub-humid	31.6	67.6	18.3	14.7	3.2	0.9	1.2	0.2	0.2	2.0	3.1	6.2	1.7
Dry	26.1	54.1	15.1	20.0	5.4	1.7	3.0	0.7	0.4	2.4	3.5	11.9	3.4
Mean	37.9	76.6	20.0	25.0	5.6	1.4	2.9	0.6	0.4	2.6	3.4	12.1	3.4
S-type Granite (mg kg ⁻¹)													
Humid	37.9	75.4	17.5	15.7	3.1	0.7	0.8	0.3	0.2	2.0	2.5	6.3	1.2
Sub-humid	45.0	70.6	18.1	16.1	4.3	0.6	0.9	0.2	0.2	2.2	2.6	5.1	0.6
Dry	27.3	48.8	14.4	13.6	3.8	0.6	1.0	0.2	0.2	2.0	2.8	5.6	0.9
Mean	36.7	64.9	16.7	15.1	3.7	0.6	0.9	0.2	0.2	2.1	2.6	5.7	0.9

The mean concentrations of REEs in I- and S-type granites were normalized to the UCC (Taylor and McLennan 1985) to investigate distribution patterns. The majority of REEs in S-type granites exhibited depletion compared with the UCC, except for La, Ce, Pr and Er (Figure 7). Conversely, the majority of REEs in I-type granites exhibited enrichment compared with the UCC, except for Gd, Yb, Dy and Sc. These results reflect the fractionation between LREEs and HREEs in soils derived from I- and S-type granites (Table 4).

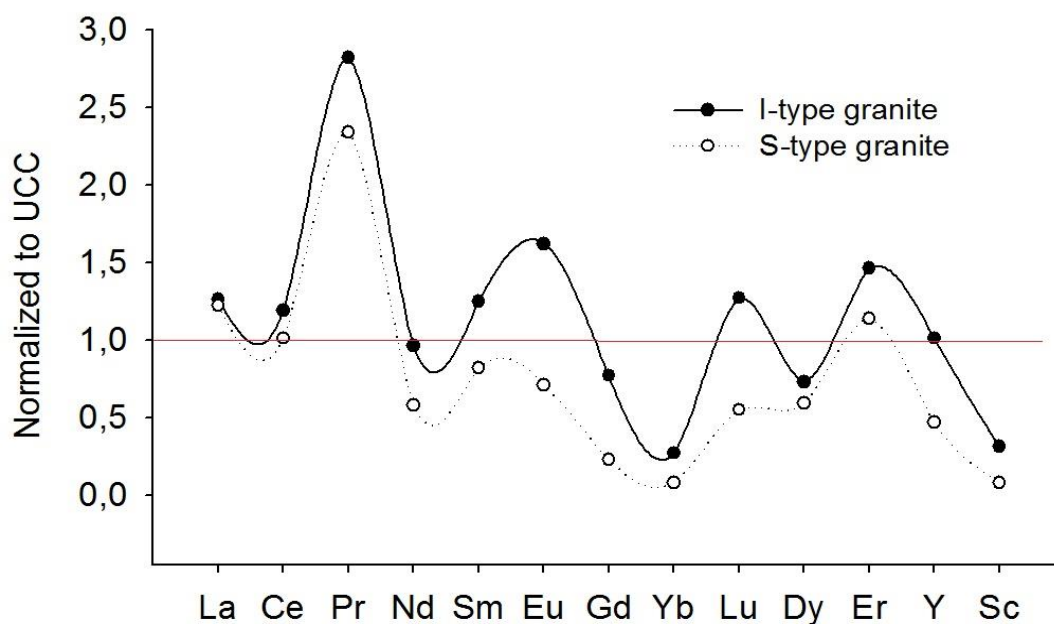


Figure 7. Rare earth elements in I- and S-type granites normalized to Upper Continental Crust (UCC). UCC values used (Taylor and McLennan 1985) (mg kg^{-1}) La: 30; Ce: 64; Pr: 7.1; Nd: 26; Sm: 4.5; Eu: 0.88; Gd: 3.8; Yb: 2.2; Lu: 0.32; Dy: 3.5; Er: 2.3; Ho: 0.8; Tb: 0.64; Tm: 0.33; Y: 22; Sc: 11.

The larger REE contents in I-types in comparison to S-type granites are explained by the higher proportion of mafic and accessory minerals, chiefly bastnaesite, titanite, allanite, apatite, amphibole and opaque minerals (Table 3). Titanite is moderately enriched in LREEs because of their relatively-high partition coefficients between titanite and melts (Green and Pearson 1986; Prowatke and Klemme 2005). Allanite contains REEs as major compositions and is rich in LREEs relative to HREEs (Gieré and Sorensen 2004; Tyler 2004) due to its large co-ordination polyhedral. It may contain more than 20% of REEs (Braun et al. 1993; Ercit 2002). Likewise, apatite is usually enriched in LREEs (Henderson 1984). Amphibole is also enriched in REEs (Sm, Eu, Gd and Dy) (Rollinson 1993). The higher proportion of mafic minerals in I-type granites explains the larger Sc contents in comparison to S-type granites. Moreover, Sc is more concentrated in basic rocks than in felsic rocks (Taylor and McLennan 1985). Biotite from I-type granite is enriched in LREEs due to inclusions of bastnaesite (Figure 8, spectrum 34). This mineral seems to be the major source of REEs in soils derived from I-type granites.

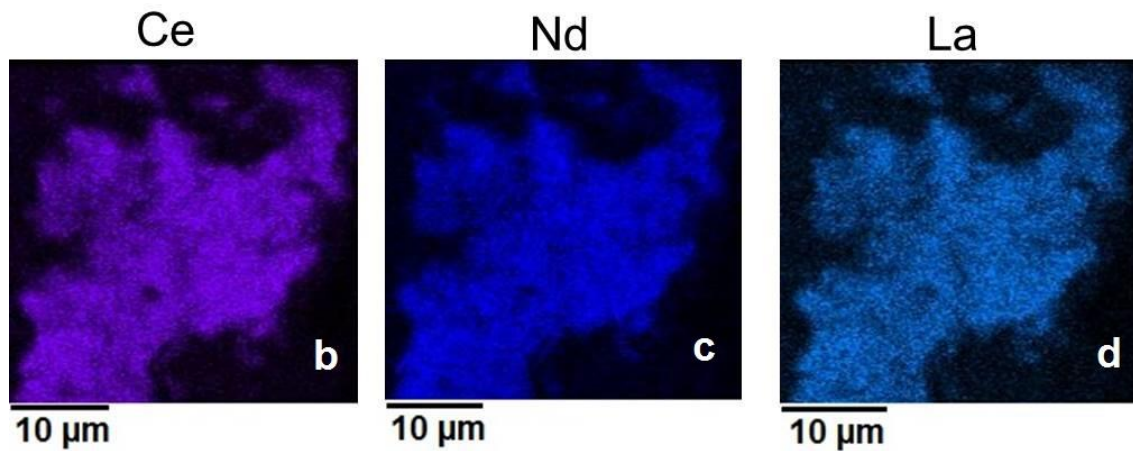
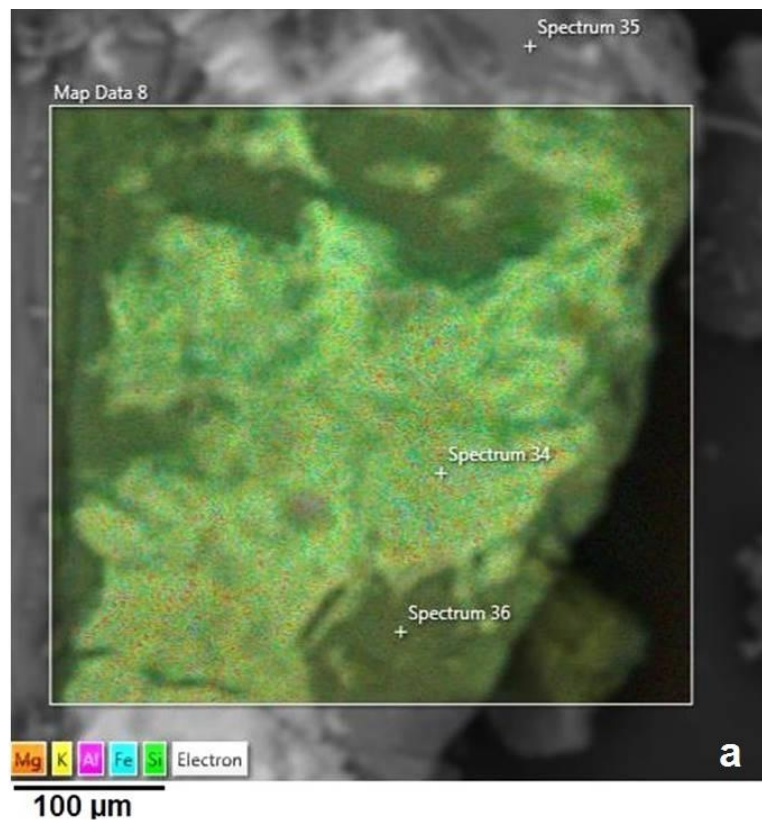


Figure 8. Cross-section of biotite with inclusion of bastnaesite using scanning electron microscope with energy-dispersive X-ray spectroscopy attached facilities (SEM-EDS) (a): Spectrum 34 (Bastnaesite, Ce – 32%, La – 20%, F – 13%, Nd – 9%, Ca – 8%, Si, Fe – 5%, Pr – 3%, Al, K – 2%, Mg – 1%), spectrum 35 (Biotite, Si – 32%, Fe – 29%, Al – 15%, K – 14%, Mg – 8%, Ti – 1.8%, Mn – 0.2%), spectrum 36 (Biotite, Si – 33%, Fe – 28%, Al – 16%, K – 13%, Mg – 8%, Ti – 2%). Semiquantitative elemental map (b, c, d) from a cross-section of biotite with inclusion of bastnaesite using scanning electron microscope with energy-dispersive X-ray spectroscopy attached facilities (SEM-EDS).

Muscovite derived from granites shows high abundance of all REEs, with means of 235 mg kg⁻¹ and 19 mg kg⁻¹ for LREEs and HREEs, respectively (Taylor and McLennan 1985). Quartz does not contain REEs (Compton et al. 2003). Feldspars contain negligible amounts of REEs, except Eu (Condie et al. 1995). In comparison to other REEs, this specific behaviour for Eu is related to the substitution of Eu²⁺ by Ca²⁺, Sr²⁺ or Na⁺ (Gromet and Silver 1983; Panahi et al. 2000). Apatite from S-type granite is enriched in LREEs due to inclusions of monazite (Figure 9, spectrum 90). This mineral seems to be the major source of REEs in soils derived from S-type granites.

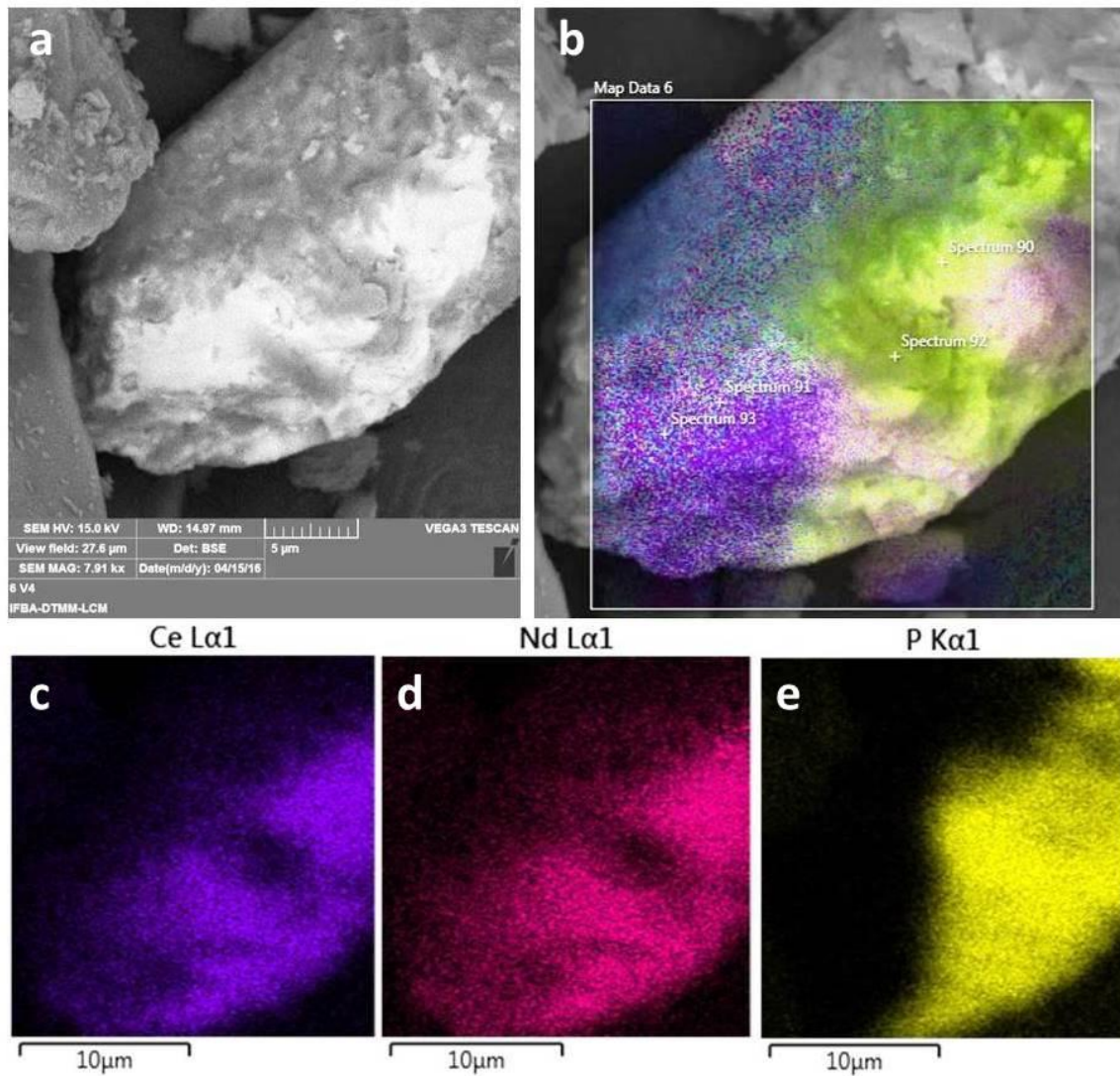


Figure 9. Scanning electron microscope (SEM) image captured from apatite with inclusion of monazite in S-type granite (a) and respective elemental

composition by energy dispersive X-ray spectrum (EDS). (b) Cross-section of apatite with inclusion of monazite: spectrum 90 (apatite plus monazite, Ca – 28%, P – 20%, Ce – 15%, Si – 11%, La – 7%, Nd – 5%, Al, K, Th – 4%, Pr – 2%), spectrum 91 (Monazite Ce – 35%, Nd – 19%, La – 15%, Si – 7%, Pr – 6%, Sm – 5%, Al – 3%, K -2%, Ca, Cd - 1%), spectrum 92 (Apatite, Ca – 54%, P – 31%, Ce – 5%, Si, La, Nd – 3%, Al – 1%), spectrum 93 (Monazite, Ce – 33%, Nd – 19%, La – 13%, Si – 9%, Sm, Gd – 7%, Pr – 6%, Al – 3%, K,Th – 2%) (b). Semiquantitative Ce (c), Nd (d) and P (e) maps from a cross-section of apatite with inclusion of monazite using scanning electron microscope with energy-dispersive X-ray spectroscopy attached facilities (SEM-EDS).

4.2. Enrichment /depletion of REEs during granite weathering

The REE concentrations in soils were normalized to the UCC (Taylor and McLennan 1985) to investigate distribution patterns. The REEs show large variations compared to UCC (Figure 10). In general, soils derived from I- and S-type granites are enriched (values are higher than unity) in LREEs, mainly La, Ce and Pr and depleted in HREEs, except for Er of all environmental conditions and soil types and Lu at the lower part of the weathering profiles originated from I-type granites.

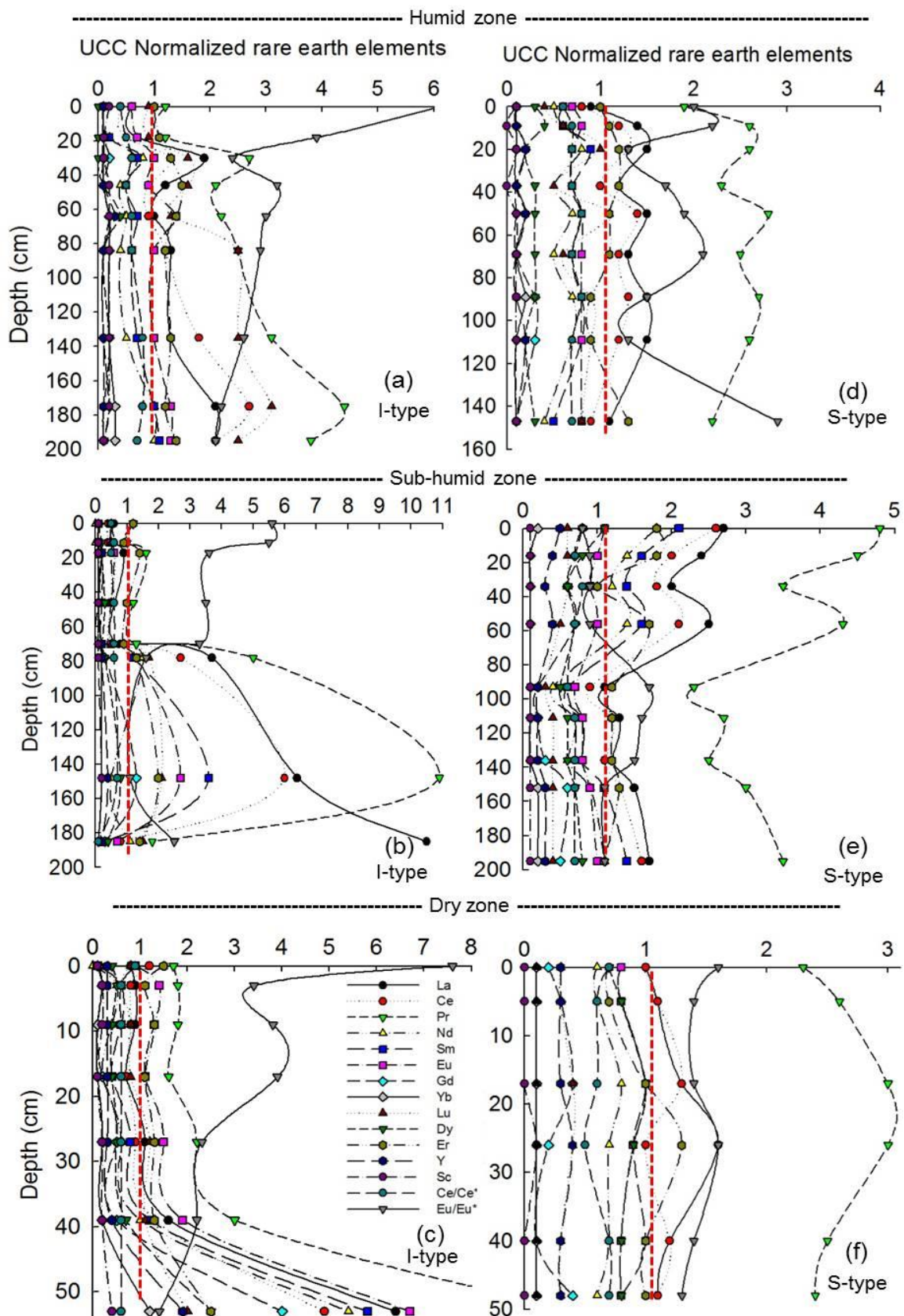


Figure 10. Concentration of REEs in soils profiles derived from I- and S-type granites in three climatic zones of Pernambuco State (Northeast Brazil) relative to the concentration of the upper continental crust. UCC values used (Taylor

and McLennan 1985) (mg kg^{-1}) La: 30; Ce: 64; Pr: 7.1; Nd: 26; Sm: 4.5; Eu: 0.88; Gd: 3.8; Yb: 2.2; Lu: 0.32; Dy: 3.5; Er: 2.3; Ho: 0.8; Tb: 0.64; Tm: 0.33; Y: 22; Sc: 11.

The LREEs were depleted from the upper layers of soils derived from I-type granites and accumulated in the lower part (saprolites) of the profiles (Figure 10). Soil profiles over S-type granites exhibited enrichment of La, Ce and Pr not only in soil surface but also in the subsurface and depletion of Nd, Sm and Eu, except for the upper part of soil profile in sub-humid zone were observed (Figure 10).

The negative Ce anomalies in soils derived from I- and S-type granites, ranging from 0.1 to 0.9 and 0.5 to 0.8 (Figure 10), respectively, reflect the relative enrichment of La and Pr, being indicative of Ce depletion, mainly in surface as also observed by Yusoff et al. (2013). Despite of the strong Ce accumulation in saprolites developed over I-type granites, no positive Ce anomalies have been observed as a result of high La and Pr enrichment.

Strong positive Eu anomalies were evidenced on soil surfaces derived from I-type granites, with values reaching 6.1, 5.6 and 7.6 for humid, sub-humid and dry zones, respectively, decreasing with depth (Figure 10). The deepest soil layers (saprolites) exhibited only slightly positive Eu anomalies, with values reaching 1.3 for humid, 1.1 for sub-humid and 1.4 for dry zone. This can be explained by the higher depletion of Sm and Gd leading to accumulation in saprolites as well as by their redox-sensitive. In other words, when Eu is reduced to the divalent oxidation, it can partition into plagioclase and be replaced by Sr^{2+} , leading to positive Eu anomalies in the feldspar (Aubert et al. 2001; Compton et al. 2003). In contrast, lower positive Eu anomalies were observed in soils develop over S-type granites, ranging from 1.1 to 2.9, except for the first four horizons located in the sub-humid zone that exhibited weak negative Eu anomalies (0.8 to 0.9) (Figure 10).

The LREE/HREE fractionation based on La/Yb_N ratios in soils derived from I-type granites ranged from 4.6 to 19.3 for the humid zone, 4.3 to 17.46 for the sub-humid zone, except for saprolite with values reaching 115.6, and 2.7 to 6.8 for dry zone (Figure 10). On the other hand, La/Yb_N ratios in soils derived from S-type granites ranged from 8.3 to 28.3, 7.4 to 50.8 and 12.8 to 24.4 for

humid, sub-humid and dry zones, respectively (Figure 10). The REEs were mobilized during granite weathering. It is clear that weathering processes influenced the REE fractionation. With increasing intensity of chemical weathering there is greater fractionation of REE. The higher La/Yb_N ratios from dry to humid zones are a result of both LREEs accumulation and HREEs depletion resulting from weathering.

4.3. *Geochemical signatures of REEs: Climate vs. Parent material*

Mobility and fractionation of REEs during weathering are widely controlled by climate and the stability of primary REE minerals. Several studies have demonstrated the influence of both factors. Weathering processes commonly result in REEs depletion from the upper part of soil profiles and accumulation in the lower parts (Aubert et al. 2001; Nesbitt and Markovics 1997). The different composition of primary minerals between I- and S-type granites seems to produce different mobilization patterns of REEs during weathering. Strong fractionation of REEs was observed in soils primarily derived from I-type granites.

Weathering of silicate minerals are chiefly responsible for the formation of clay minerals. The composition, mobilization and adsorption of REEs in soils depend largely on the type of clay mineral formed (Galán et al. 2007; Henderson 1984). Kaolinite, the most dominant clay mineral in soils derived from granites, seems to be the most important adsorbent for REEs. Moreover, kaolinite preferentially adsorbs LREE over HREE (Yusoff et al. 2013). Kaolinite is most common in humid weathering environments, so its abundance in soils decreases from humid to the dry climates. Conversely, illite abundance tends to increase from soils in the humid to the dry zone. Vermiculite was detected only in clay fraction of I-type located in dry zone (Figure 4c). These clay minerals are enriched in LREEs (Laveuf and Cornu 2009). Goethite and gibbsite was found only in soil derived from I- and S-type granites located in humid zone, respectively (Figure 4d). These oxides also contain REEs (Palumbo et al. 2001).

Aiming to provide more insights into the factors controlling REE behavior during weathering, we used the additional technique of factor analysis. Three

factors with eigenvalues higher than a unit explained roughly 84 and 83% of the REE distribution in I- and S-type granites, respectively (Table 6). For soils derived from I- type granites the F1 was positively loaded for La, Ce, Pr, Nd, Sm, Eu, Gd, Yb, Dy, Er, Y, and Sc (0.68-0.98); F2 positively loaded for Lu, clay, silt, Fe, and CIA (0.85-0.96) and negatively loaded for sand (-0.98) and pH (-0.60), and F3 showed high loading of CEC (0.80). For soils derived from S-type granites F1 was positively loaded on La, Ce, Pr, Nd, Sm, Eu, Gd, and Er (0.81-0.97); F2 positively and negatively loaded on Lu, clay, silt, Fe, and CIA (0.85-0.94) and Dy, Y, sand and pH (-0.92 to -0.64), respectively, and F3 exhibited negative loadings for TOC (-0.89) and CEC (-0.94).

Table 6. Factors controlling REEs behavior during weathering process in three climatic zones of Pernambuco, Brazil

	I type granites			S type granites		
	F1	F2	F3	F1	F2	F3
La	0,77	0,21	0,42	0,97	0,03	0,04
Ce	0,68	0,27	0,58	0,95	-0,06	0,06
Pr	0,74	0,23	0,57	0,96	-0,17	0,09
Nd	0,94	0,08	0,07	0,96	-0,18	0,03
Sm	0,92	0,07	0,35	0,93	-0,31	0,07
Eu	0,98	-0,01	0,15	0,81	-0,35	0,24
Gd	0,96	-0,12	0,20	0,83	-0,33	0,20
Yb	0,97	0,00	-0,06	0,42	0,27	0,30
Lu	0,36	0,85	0,14	0,15	0,85	0,12
Dy	0,95	-0,22	0,11	0,41	-0,86	0,20
Er	0,84	0,07	0,33	0,81	0,04	-0,08
Y	0,96	-0,24	0,04	0,59	-0,70	0,16
Sc	0,84	0,16	-0,27	0,46	0,44	0,20
Clay	-0,01	0,96	-0,01	-0,30	0,89	-0,21
Silt	-0,16	0,94	-0,02	-0,26	0,91	-0,02
Sand	0,10	-0,98	0,02	0,29	-0,92	0,10
TOC	-0,25	-0,30	0,00	-0,16	0,13	-0,89
pH	-0,11	-0,59	-0,36	-0,44	-0,64	0,02
CEC	0,25	-0,22	0,80	-0,06	0,24	-0,94
Fe	-0,06	0,87	-0,09	-0,23	0,93	-0,05
CIA	0,00	0,95	0,05	0,12	0,94	-0,22
Eigenvalue	10,40	5,95	1,39	10,26	5,49	1,78
EV (%)	49,55	28,34	6,62	48,85	26,15	8,48
Cumulative(%)	49,55	77,89	84,51	48,85	75,00	83,48

The LREEs in soils derived from I-type granites tend to be concentrated in the deeper layers as shown by F1 (Table 6) and Table 4; also, HREEs showed a slight enrichment. As might be expected, the highest degree of LREEs depletion is related to the highest concentrations of minerals that dissolve easily, such as allanite and apatite, titanite (Ma et al. 2011; Yusoff et

al. 2013). These results suggest that LREEs represented by F1 were predominantly derived from primary minerals. Not surprisingly, sand and pH were inversely correlated with CIA and Fe. In other words, the higher the quartz concentrations (Table 3) the higher the dilution effect in REE and trace element concentrations (Hardy and Cornu 2006). As seen from F3 (Table 6), the TOC and CEC did not influence REE geochemistry during granite weathering. For soils derived from S-type granites, the F1 (Table 6) also showed high positive loads for LREEs not because subsurface accumulation but due to surface enrichment. It might be related to the lowest concentrations of easily weatherable minerals (Table 3). The high geochemical association of HREEs (e.g. Lu, Dy, Y) with Fe-oxyhydroxides, clay concentration might be related to preferential adsorption of the HREEs to pedogenic minerals, (Brioschi et al. 2013; Laveuf and Cornu 2009; Pédrot et al. 2015).

4.4. REEs as indicator of weathering intensity

Despite of the behavior of REEs during weathering has been extensively studied (Condie et al. 1995; Ma et al. 2011; Mihajlovic et al. 2014; Panahi 2000), the question of whether REE mobility and fractionation may be used as a proxy of the degree of weathering remains debatable (Ma et al. 2007; Malpas et al. 2001;). Specifically, when it comes to the weathering of different granites (Yusoff et al. 2013).

To shed more light on this issue, we compared the fractionation patterns with the degree of weathering, using the chemical index of alteration (CIA) (Nesbitt and Young 1982) - a general indicator of the degree of chemical weathering of felsic rocks (Sanematsu et al. 2015). The weathering degree of I- and S-type granites (Tables 1, 2) as well as the LREE/HREE ratios (Table 4) varied systematically with contrasting climates. Overall, the weathering intensity and the LREE/HREE ratios decreased in the following order: humid zone > sub-humid zone > dry zone. The CIA in humid zones was higher than 90%. These findings demonstrate leaching effects, loss of cations, and predominance of kaolinite in the mineral assemblage (Rasmussen et al. 2010). These results are well related to the clay mineralogy composition in each soil profile, which exhibited dominance of monosialitization process in this climatic zone (Figure

4a and 4d). The positive correlation of CIA values with high LREE/HREE ratios ($r= 0.3$; $n= 48$; $p < 0.0001$) suggests that LREE/HREE ratios are good indicators of the degree of granite weathering.

5. Conclusions

This study explores the effects of mineralogy and geochemistry of I- and S-type granites, their derived soils, and the rare earth elements (REEs) distribution in rocks and soils across a climosequence from semiarid to tropical settings. S-type granites are characterized by higher silicate contents, whereas I-type granites show higher proportion of mafic and accessory minerals: allanite, titanite, apatite, amphibole and opaque minerals. Bastnaesite and monazite seems to be the major sources of REEs in soils derived from I- and S-type granites, respectively. According to the high La/Yb_N and LREE/HREE ratios, weathering processes showed significant correlation on REE fractionation in soils derived from both granite types. The higher LREE/HREE fractionation in soils in the humid zone is explained by the dominance of kaolinites that have preferentially retained LREEs over HREEs. In general, both granite types show a similar REE signature, with an enrichment of LREEs over HREEs, a negative Ce-anomaly and positive Eu anomaly. The highest CIA values are related to the highest LREE/HREE ratios and suggest that LREE/HREE fractionation is a good indicator of the degree of granite weathering. The differences in the composition of primary minerals between I- and S-type granites, as well as in the degree of weathering resulted in different mobilization of REEs during granite weathering. Thus, both climate and parent material composition are key factors for the understanding of REE mobility during weathering.

6. References

- Aubert, D., Stille, P., & Probst, A. (2001). REE fractionation during granite weathering and removal by waters and suspended loads: Sr and Nd isotopic evidence. *Geochimica et Cosmochimica Acta*, 65, 387–406.
- Bao, Z., & Zhao, Z. (2008). Geochemistry of mineralization with exchangeable REY in the weathering crusts of granitic rocks in South China. *Ore Geology Reviews*, 33, 519–535.
- Bea, F. (1996). Residence of REE, Y, Th and U in granites and crustal protoliths: implication for the chemistry of crustal melts. *Journal of Petrology*, 37, 521–552.
- Beyala, V. K. K., Onana, V. L., Priso, E. N. E., Parisot, J. C., & Ekodeck, G. E. (2009). Behaviour of REE and mass balance calculations in a lateritic profile over chlorite schists in South Cameroon. *Chemie der Erde-Geochemistry*, 69, 61–73.
- Braun, J. J., Pagel, M., Herbilln, A., & Rosin, C. (1993). Mobilization and redistribution of REEs and thorium in a syenitic lateritic profile: a mass balance study. *Geochimica et Cosmochimica Acta*, 57, 4419–4434.
- Brazil. 2001. Mistério de Minas e Energia. Geologia e recursos minerais do Estado de Pernambuco. Serviço Geológico do Brasil e do Estado de Pernambuco, Recife, CPRM.
- Brioschi, L., Steinmann, M., Lucot, E., Pierret, M. C., Stille, P., Prunier, J., & Badot, P. M. (2013). Transfer of rare earth elements (REE) from natural soil to plant systems: implications for the environmental availability of anthropogenic REE. *Plant and Soil*, 366, 143–163.
- Brito, L. T. L., Moura, M. S. B., & Gama, G. F. B. (2007). Potencialidades da água de chuva no Semiárido brasileiro. *Petrolina: Embrapa Semi-Árido*. 181p.

Brito Neves, B. B. de. 1975. Regionalização geotectônica do Pré-cambriano nordestino. São Paulo. Tese de Doutorado. Instituto de Geociências, Universidade de São Paulo, Tese de Livre Docência. 198p.

Brown, G., & Brindley, G. W. (1980). X-ray Diffraction procedures for clay mineral identification. In: Brindley, G.W., Brown, G. (Eds) *London: Mineralogical Society*, 5, 305-360.

Chappell, B. W., & White, A. J. R. (1984). I- and S- type granites in the Lachlan Fold Belt, southeastern Australia. In: Keqin, Xu., Guangchi, Tu. (Eds.). *Geology of Granites and their Metallogenic Relation: Beijing Science Press*. pp.87–101.

Chappell, B. W., & White, A. J. R. (1974). Two contrasting granite types. *Pacific Geology*, 8, 173–174.

Chappell, B. W., & White, A. J. R. (2001). Two contrasting granite types: 25 years later. *Australian Journal of Earth Sciences*, 48, 489–499.

Chen, L. M., Zhang, G. L., & Jin, Z. D. (2014). Rare earth elements of a 1000-year paddy soil chronosequence: Implications for sediment provenances. Parent material uniformity and pedological changes. *Geoderma*, 230, 274–279.

Clemens, J. D. (2003). S-type granitic magmas – petrogenetic issues, models and evidence. *Earth-Science Reviews*, 61, 1–18.

Compton, J. S., White, R. A., & Smith, M. (2003). Rare earth element behavior in soils and salt pan sediments of a semiarid granitic terrain in the Western Cape, South Africa. *Chemical Geology* 201, (3–4), 239–255.

Condie, K. C., Dengate, J., & Cullers, R. L. (1995). Behavior of rare earth elements in a paleoweathering profile on granodiorite in the Front Range, Colorado, USA. *Geochimica et Cosmochimica Acta*, 59, 279–294.

Connelly, N. G., Damhus, T., Hartshorn, R. M., & Hutton, A. T. (2005). Nomenclature of inorganic chemistry. IUPAC Recommendations 2005, International Union of Pure and Applied Chemistry, The Royal Society of Chemistry, Cambridge.

Ercit, T. S. (2002). The mess that is “allanite”. *Canadian Mineralogist*, 40, 1411–1419.

Feng, D., Chen, D., Peckmann, J., & Bohrmann, G. (2010). Authigenic carbonates from methane seeps of the northern Congo fan: microbial formation mechanism. *Marine and Petroleum Geology*, 27, 748–756.

Foden, J., Sossi, P. A., & Wawryk, C. M. (2015). Fe isotopes and the contrasting petrogenesis of A-, I- and S-type granite. *Lithos*, 212-215, 32-44.

Galán, E., Fernández-Caliani, J. C., Miras, A., Aparicio, P., & Márquez, M. G. (2007). Residence and fractionation of rare earth elements during kaolinization of alkaline peraluminous granites in NW Spain. *Clay Minerals*, 42, 341–352.

Gandois, L., Agnan, Y., Leblond, S., Delmas, N. S., Roux, G. L., & Probst, A. (2014). Use of geochemical signatures, including rare earth elements in mosses and lichens to assess spatial integration and the influence of forest environment. *Atmospheric Environment*, 95, 96-104.

Gee, G. W., & Or, D. (2002). Particle size analysis. In: Dane, J.H., & Topp, C.T. (Eds.) *Methods of soil analysis: physical methods*. Cap II, SSSA, Madison, p.255-289.

Gieré, R., & Sorensen, S. S. (2004). Allanite and other REE-rich epidote-group minerals. *Reviews in Mineralogy and Geochemistry*, 56, 431–493.

Green, T. H., & Pearson, N. J. (1986). Rare earth element partitioning between sphene and coexisting silicate liquid at high pressure and temperature. *Chemical Geology* 55,105–119.

Gromet, P. L., & Silver, L. T. (1983). Rare earth element distributions among minerals in a granodiorite and their petrogenetic implications. *Geochimica et Cosmochimica Acta*, 47 (5), 925–939.

Guani, A. A., Searle, M., Robb, L., & Chung, S. L. (2013). Transitional I S type characteristic in the Main Range Granite. Peninsular Malaysia. *Journal of Asian Earth Sciences*, 76, 225-240.

Guan, Y., Yuan, C., Sun, M., Wilde, S., Long, X., Huang, X., & Wang, Q. (2014). I-type granitoids in the eastern Yangtze Block: implications for the Early Paleozoic intracontinental orogeny in South China. *Lithos*, 206-207, 34-51.

Hardy, M., & Cornu, S. (2006). Location of natural trace elements in silty soils using particlesize fractionation. *Geoderma*, 133 (3–4), 295–308.

Henderson, P. (1984). General geochemical properties and abundances of the rare earth elements. In: Henderson, P. (Ed.), *Rare earth Element Geochemistry: Developments in Geochemistry*, vol 2. Elsevier Science Publishers, Amsterdam.

Hu, Z., Haneklaus, S., Sparovek, G., & Schnug, E. (2006). Rare earth elements in soils. *Commun. Soil Science and Plant Nutrition*, 37, 1381–1420.

INMET. 2015. Instituto Nacional de Meteorologia. Available in <http://www.inmet.gov.br/portal/index.php?r=clima/normaisclimatologicas>.

Accessed in: 16 de nov. de 2015.

IUSS- Working Group WRB. (2014). *World Reference Base for Soil Resources 2014*. World Soil Resources Report No. 106, FAO, Rome.

Jackson, M. L. (1975). *Soil chemical analysis: advanced course*. 29ed. Madison, University of Wisconsin, 895p.

Jaireth, S., Hoatson, D. M., & Mieziotis, Y. (2014). Geological setting and resources of the major rare-earth-element deposits in Australia. *Ore Geology Reviews* 62, 72–128.

Kaiser, H. F. (1958). The Varimax criterion for analytic rotation in factor analysis. *Psychometrika*, 23, 187–200.

Koppen, W.P. (1931). *Grundriss der Klimakunde*. 2nd ed. Berlin: Walter de Gruyter. 388p.

Laveuf, C., Cornu, S., Guillerme, L. R. G., & Juillot, F. (2012). The impact of redox conditions on the rare earth element signature of redoximorphic features in a soil sequence developed from limestone. *Geoderma*, 170, 25-38.

Laveuf, C., & Cornu, S. (2009). A review on the potentiality of Rare Earth Elements to trace pedogenetic processes. *Geoderma*, 154, 1–12.

Liang, T., Zhang, S., Wang, L., Kung, H. T., Wang, Y., Hu, A., et al. (2005). Environmental biogeochemical behaviors of rare earth elements in soil–plant systems. *Environmental Geochemistry and Health*, 27 (4), 301–311.

Long, K. R., Van Gosen, B. S., Foley, N. K., & Cordier, D. (2010). The principal rare earth deposits of the United States—a summary of domestic deposits and a global perspective. *United States Geological Survey Scientific Investigations Report*, 5220, 96.

Ma, J., Wei, G., Xu, Y., Long, W., & Sun, W. (2007). Mobilization and re-distribution of major and trace elements during extreme weathering of basalt in Hainan Island. South China: *Geochimica et Cosmochimica Acta*, 71, 3223–3237.

Ma, L., Jin, L., & Brantley, S. L. (2011). How mineralogy and slope aspect affect REE release and fractionation during shale weathering in the Susquehanna/Shale Hills Critical Zone Observatory. *Chemical Geology*, 290, 31–49.

Malpas, J., Duzgoren-Aydin, N. S., & Aydin, A. (2001). Behaviour of chemical elements during weathering of pyroclastic rocks, Hong Kong. *Environment International*, 26, 359–368.

Mihajlovic, J., Stärk, H. J., & Rinklebe, J. (2014). Geochemical fractions of rare earth elements in two floodplain soil profiles at the Wupper River, Germany. *Geoderma*, 228–229, 160–172.

Mineralogical methods - SSSA., 2008. Part 5 – Methods Of Soils Analysis – soil science society of America. Book Series 5. A.L. Ulery and L.R. Drees (Editors); Madison, USA, Wisconsin.

Moore, D. M., & Reynolds, R. C. (1997). Identification of mixed-layered clay minerals. X-Ray diffraction and the identification and analysis of clay minerals. Ed.2. New York: Oxford University Press, 378p.

Murphy, C.P. (1986). Thin section preparation of soils and sediments. *Berkhamsterd: Academic Publishing.*, 145p.

National Institute of Standards and Technology - NIST. Standard Reference Materials -SRM 2709, 2710 and 2711 Addendum Issue Date: 18 January 2002.

Nesbitt, H. W., & Markovics, G. (1997). Weathering of granodiorite crust, long-term storage of elements in weathering profiles and petrogenesis of siliciclastic sediments. *Geochimica et Cosmochimica Acta*, 61, 1653–1670.

Nesbitt, H.W., & Young, G.M. (1982). Early Proterozoic climates and plate motions inferred from major element chemistry of lutites. *Nature* 299 (5885), 715–717.

Pagano, G., Guida, M., Tommasi, F., & Oral, R. (2015). Health effects and toxicity mechanisms of rare Earth elements—Knowledge gaps and research prospects. *Ecotoxicology and Environmental Safety*, 115, 40–48.

Panahi, A., Young, G. M., & Rainbird, R. H. (2000). Behavior of major and trace elements (including REE) during Paleoproterozoic pedogenesis and diagenetic alteration of an Archaean granite near Ville Marie, Quebec, Canada. *Geochimica et Cosmochimica Acta*, 64 (13), 2199–2220.

Pédrot, M., Dia, A., Davranche, M., & Gruau, G. (2015). Upper soil horizons control the rare earth element patterns in shallow groundwater. *Geoderma*, 239–240, 84–96.

Prowatke, S., & Klemme, S. (2005). Effect of melt composition on the partitioning of trace elements between titanite and silicate melt. *Geochimica et Cosmochimica Acta*, 69, 695–709.

Rasmussen, C., Dahlgren, R. A., & Southard, R. S. (2010). Basalt weathering and pedogenesis across an environmental gradient in the southern Cascade Range, California, USA. *Geoderma*, 154, 473–485.

Rollinson, H. R. (1993). *Using Geochemical Data; Evaluation, Presentation, Interpretation*. Longman, Harlow, 352 p.

Sadeghi, M., Morris, G. A., Carranza, E. J. M., Ladenberger, A., & Andersson, M. (2013). Rare earth element distribution and mineralization in Sweden: An application of principal component analysis to FOREGS soil geochemistry. *Journal of Geochemical Exploration*, 133, 160–175.

Sanematsu, K., Kon, Y., & Imai, A. (2015). Influence of phosphate on mobility and adsorption of REEs during weathering of granites in Thailand. *Journal of Asian Earth Sciences*, 111, 14–30.

Souza, F. P., Ferreira, T. O., Mendonça, E. S., Romero, R. E., & Oliveira, J. G. B. (2012). Carbon and nitrogen in degraded Brazilian semiarid soils undergoing desertification. *Agriculture Ecosystems and Environment*, 148, 11–21.

Taylor, S. R., & McLennan, S. M. (1985). *The continental crust: its composition and evolution. An examination of the geochemical record preserved in sedimentary rocks*. Blackwell, Oxford.

Tyler, G., & Olsson, T. (2002). Conditions related to solubility of rare and minor elements in forest soils. *Journal of Plant Nutrition and Soil Science*, 165, 594–601.

Tyler, G. (2004). Rare earth elements in soil and plant systems—a review. *Plant and Soil*, 267 (1–2), 191–206.

Van Schmus, W. R., Oliveira, E. P., da Silva Filho, A. F., Toteu, S. F., Penaye J., & Guimarães, I. P. (2008). Proterozoic links between the Borborema Province, NE Brazil, and the Central African Fold Belt. *Geological Society, London, Special Publications*, 294, 69–99.

Vilalva, F. C. J., Vlach, S. R. F., & Simonetti, A. (2016). Chemical and O-isotope compositions of amphiboles and clinopyroxenes from A-type granites of the Papanduva Pluton, South Brazil: Insights into late- to post-magmatic evolution of peralkaline systems. *Chemical Geology*, 420, 186–199.

Walters, A., Lusty, P., Chetwyn, C., & Hill, A. (2010). Rare earth elements. Mineral Profile Series British Geological Survey. United Kingdom, 45 p.

Wang, Z., Wang, J., Deng, Q., Du, Q., Zhou, X., Yang, F., et al. (2015). Paleoproterozoic I-type granites and their implications for the Yangtze block position in the Columbia supercontinent: Evidence from the Lengshui Complex, South China. *Precambrian Research*, 263, 157-173.

Wei, F. S., Zheng, C. J., Chen, J. S., & Wu, Y. Y. (1991). Study on the background contents on 61 elements of soils in China. *Chinese Journal of Environmental Science*, 12, 12–20.

Whittig, L. D., & Allardice, W. R. (1986). X-ray diffraction techniques. In: Klute, A. (Ed.), *Methods of Soil Analysis — Part I. Physical and Mineralogical Methods*. *Soil Science Society of America*, Madison, WI, pp. 331–362.

Yeomans, J. C., & Bremner, J. M. (1988). A rapid and precise method for routine determination of organic carbon in soil. *Commun. Soil Science and Plant Nutrition*, 19, 1467-1476.

Yousefifard, M., Ayoubi, S., Poch, R. M., Jalalian, A., Khademi, H., & Khormali, F., (2015). Clay transformation and pedogenic calcite formation on a lithosequence of igneous rocks in northwestern Iran. *Catena*, 133, 186–197.

Yusoff, Z. M., Ngwenya, B. T., & Parsons, I. (2013). Mobility and fractionation of REEs during deep weathering of geochemically contrasting granites in a tropical setting, Malaysia. *Chemical Geology*, 349, 71–86.

CHAPTER IV

**EFFECT OF I AND S TYPE GRANITE PARENT MATERIAL MINERALOGY
AND GEOCHEMISTRY ON SOIL FERTILITY: A MULTIVARIATE
STATISTICAL AND GIS-BASED APPROACH**

Effect of I- and S-type granite parent material mineralogy and geochemistry on soil fertility: a multivariate statistical and gis-based approach

Abstract

This study provides new insights into the effects of parent material on inherent soil fertility. We describe the mineralogy and geochemistry of I- and S-type granites and their effect on soil fertility under similar environmental conditions in the Borborema Province, NE Brazil using standard mineralogical, geochemical and soil analysis as well as multivariate analysis and geographic information system approaches. We hypothesized that soils derived from I-type granites will derive higher natural fertility than those derived from S-type granites. The mineralogy and chemistry of two different granitic parent materials have a profound effect on soil fertility. S-type and I-type granites have different mineralogical compositions whereby S-type granites have higher concentrations of silica and I-type granites contain larger concentration of mafic and accessory minerals, mainly amphibole and apatite. Geophysical field measurements show different magnetic susceptibilities, whereby I-type granites have substantial higher magnetic properties than S-type granites. Soils derived from I-type granites have higher natural fertility than soils derived from S-type granites. The application of principal component, cluster and discriminant analysis (95% accuracy) were effective tools to discriminate soils developed from different granites. Spatial distribution maps are suitable soil fertility management tools to guide and support soil fertility management decisions for improved soil and crop specific fertilization. These findings have wider implications in large parts of the tropics (S-America, sub-Saharan Africa, India, SE and East Asia, Australia) which are underlain by igneous and metamorphic rock types including S- and I-type granites and where effective management tools are needed to increase nutrient use efficiencies for increased productivity of food, fodder and energy crops.

Keywords: Granite; parent material; mineralogy; geochemistry of soils; inherent soil fertility.

1. Introduction

Parent material is one of the five major factors that influence soil formation and is regarded the initial state of the soil system (Jenny, 1941). The mineralogical and chemical nature of the parent material plays a major role on soil fertility (Van Straaten, 2007). Granitic rocks are abundant in the Earth's upper continental crust underlying large expanses of agricultural land in the tropics and in areas with temperate climates. In Pernambuco State alone, granites cover approximately 1/3 of the whole land area (Brazil, 2001). However, granites are generally regarded as nutrient poor parent materials in the formation of soils, although they differ widely in chemical and mineralogical compositions. Chappell and White (1974, 2001) simplified the classification of granites into I- and S-type granites. This classification, along with the use of A-type granites is widely used (Foden et al., 2015; Guan et al., 2014; Guani et al., 2013; Litvinovsky et al., 2015; Vilalva et al., 2016; Wang et al., 2014; Wang et al., 2015; Zhao et al., 2008).

In general, the S- and I-type granites are derived from melting of meta-sedimentary sources and melt products of meta-igneous source rocks, respectively (Chappell and White, 1984; Chappell et al., 2012). The genesis and geochemical signature of I- and S-type granites has been widely studied (Almeida et al., 2007; Antunes et al., 2008; Antunes et al., 2009; Chappell and White, 1974, 2001; Chappel et al., 2012; Clemens, 2003; Foden et al., 2015; Guan et al., 2014; Guani et al., 2013). So far however, no attempts have been made to study the specific influence of the mineralogy and geochemistry of I- and S-type granites on soil fertility.

One of the most effective tools to study environmental and agricultural issues is the use of multivariate statistical techniques (Chen et al., 2008; Gielar et al., 2012; Templ et al., 2008). Principal component analysis (PCA) and cluster analysis (CA) have been used for multivariate analysis in soil science (Franco-Uria et al., 2009; Li et al., 2009; Silva et al., 2015) and have been mainly applied for source identification. The use of integrated methods such as multivariate statistical techniques and GIS approaches (Facchinelli et al., 2001; Li et al., 2004; Manta et al., 2002; Micó et al., 2006; Sun et al., 2013; Thuong et

al., 2013; Varol, 2011) have rarely been used as tool to identify natural soil fertility derived from different parent material.

The objectives of this study were: (i) to describe the petrography and mineralogy of I- and S-type granites of the Borborema Province, Pernambuco State, Northeast Brazil; (ii) to address the effect of I- and S-type granites on soil fertility using geochemical and mineralogical methodologies supported by multivariate analyses as well as geographic information system (GIS) mapping techniques.

2. Materials and methods

2.1. Site setting and sampling

The study was carried out in the Borborema Province, Pernambuco State, northeastern Brazil. Geologically speaking the Borborema Province is the western part of a major Late Neoproterozoic mobile belt (Brasiliano-Pan-African) that extends from Brazil into Africa in pre-drift reconstructions (Van Schmus et al., 2008). Petrographic and geochemical details of Borborema Province can be found in a number of previous studies (Cruz et al., 2014; Da Silva Filho et al., 2014; Ferreira et al., 1998; Santos and Medeiros, 1999).

For this study, two geological granite zones were selected in eastern Pernambuco State (Figure 1). Soil sampling along two transects (A and B) was carried out in areas with minimal anthropogenic disruption and similar climatic conditions. A total of 15 sites each were selected from the two transects with site intervals varying from 500 m to 1 km. Slight variations in these sampling distances were necessitated by absence of native vegetation or presence of other rock types at the sampling site. Composite soil samples consisting of three subsamples were taken from the sampling sites at 0–20 and 20–40 cm depths.

The A-transect is characterized by soils derived from S-type granites and cover an area from 08°41'03.5" to 08°39'56.4"S and 036°18'37.7" to 036°05'49.3"W, between 609 and 764 m elevation with gentle slope morphologies. The B-transect encompassed soils developed over I-type granites (08°42'15.7" to 08°37'48.2"S and 036°01'33.0" to 036°00'46.9"N)

between 450 and 693 m elevation with relatively steep slope morphologies. Soils derived from I- and S-type granites are classified as Eutric Regosols and Dystric Regosols, respectively (IUSS Working Group WRB, 2014). (IUSS Working Group WRB, 2014).

The climate, according to the Koppen classification (Koppen, 1931), is semiarid (Bsh). It is characterized by average air temperature of approximately 24 °C, annual rainfall ranges from 800 to 1,000 mm. The study area is located on the Borborema Plateau (400-800 m). The vegetation is composed of semi-deciduous tropical forest and dry deciduous forest (Caatinga), the unique biome that is exclusively Brazilian and one of the sites most vulnerable to desertification (Souza et al., 2012). They are thorny brushes that inhabit in arid and semiarid regions of Northeast Brazil. This vegetation type occupies approximately 5/6 of Pernambuco's surface area (Araújo Filho et al., 2000).

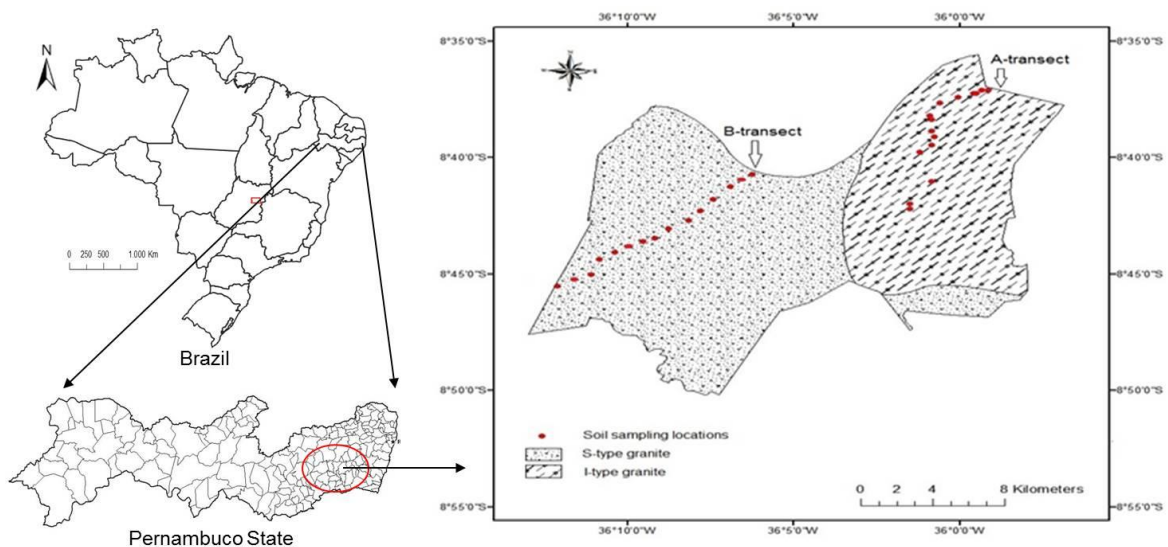


Figure 1. Distribution of soil sampling location over I- and S-type granites from the Borborema Province, Pernambuco State, northeastern Brazil.

2.2. Granite analysis

The I- and S-type granites and their modal mineral compositions were determined from fresh rock samples which were collected from each transect. The mineralogical identification was made from polished thin sections according to Murphy (1986) using a petrographic microscope.

The major-element oxides (SiO_2 , TiO_2 , Al_2O_3 , Fe_2O_3 , MgO , CaO , MnO , Na_2O , K_2O , and P_2O_5) of whole-rock samples were determined by with X-ray fluorescence (XRF) spectrometry (S8 Tiger model-1KW). Loss on ignition was determined at 1000 °C. The two granite types were also analyzed for their magnetic properties, using a handheld magnetic susceptibility meter (KT-10, Terraplus).

After optic microscope observation, granite samples were coated with a 20 nm gold layer (model Q150R - Quorum Technologie). Fine-grained minerals and their textures were observed using a TESCAN (model: VEGA-3 LMU) field emission SEM at an accelerating voltage of 15 kV. Afterwards, the energy dispersive X-ray spectrum (EDS; Oxford Instrument, model: 51-AD0007) coupled with SEM were used to analyze the semiquantitative characteristics of the mineral compositions.

2.3. Soil analysis

The particle size distribution was obtained according to Gee and Or (2002), using Calgon as chemical dispersant. All samples were pre-treated by hydrogen peroxide (H_2O_2) to eliminate organic matter. Soil pH was measured in distilled water (1:2.5 soil:solution ratio). Potassium, Na, P, Co, Cu, Fe, Mn, Mo, Ni and Zn were extracted using Mehlich-1 procedures (1:10 soil:solution ratio). Calcium, Mg and Al were extracted with 1 mol L^{-1} KCl (1:10 soil:solution ratio). All elements were determined by optical emission spectrometry (ICP-OES/Optima 7000, Perkin Elmer). Then, the sum of the bases, cation exchange capacity and aluminum saturation percentage were calculated. Potential acidity ($\text{H}^+ + \text{Al}^{3+}$) was determined by calcium acetate method (0.5 mol L^{-1} , pH 7.0), and total organic carbon (TOC) according to Yeomans and Bremner (1988).

X-ray diffraction (XRD) was performed on the clay fraction ($< 2 \mu\text{m}$) - separated using standard sedimentation procedures - of the topsoil horizon using a Shimadzu 7000 diffractometer fitted with a graphite monochromator set to select Cu $\text{K}\alpha$ radiation (30mA/40 kV). The measurement range was 3° to 35° (2θ), with steps of $0.02^\circ 2\theta$ at 1.2 s/step, except for treatment with ethylene glycol solvation ($3\text{-}15^\circ 2\theta$). Prior to analysis, the clay was submitted to the following standard treatments: organic matter elimination (15% H_2O_2) and iron

oxides elimination (dithionite-citrate-bicarbonate method).

Clays were oriented on glass slides with the following standard treatments: Mg saturation ($\text{MgCl}_2 - 1 \text{ mol L}^{-1}$), Mg saturation/glycerol solvation, K saturation ($\text{KCl} - 1 \text{ mol L}^{-1}$), and heat treatment of K-saturated samples, during three hours at 350 and 550 °C (Whittig and Allardice, 1986). Clay mineral identification was based on criteria described by Brown and Brindley (1980); Jackson (1975); Moore and Reynolds (1997). The major-element oxides were determined by pressed pellet with X-ray fluorescence (XRF) spectrometry (S8 Tiger model-1KW). Loss on ignition was determined at 1000 °C.

2.4. Quality assurance and quality control

Optical emission spectrometry analysis was performed only when the coefficient of determination (r^2) of the calibration curve was higher than 0.99. Analytical data quality and standard operation procedures such as curve recalibration, analyses of blanks were performed. Calibration was carried out every ten samples. Whenever more than 10% deviation was observed, the equipment was calibrated and samples analyzed again. All analyses were carried out in duplicate. The accuracy of the geochemical data by XRF was assessed according to international geochemical standards (SRM 2709, San Joaquin soil). The recovery rates of major element (%) appeared in the following decreasing order: P (126) > Al (106) > Ca (105) > Ti (101) > Fe (100) > K (98) > Mg (96) > Si (89) > Mn (81) > Na (72). These results were considered to be satisfactory and reflect the quality of the XRF measurement.

2.5. Statistical and geographic information system

Results were assessed by descriptive and multivariate statistical analyses. Normality tests of the raw and transformed data were performed using STATISTICA 10 software. Principal component analysis (PCA) was used to select the key variables responsible for distinguishing the granite types. To extract the significant principal components while diminishing the contribution of variables with little importance, we employed Varimax rotation (Kaiser, 1958). We used the Kaiser method for choosing the appropriate number of factors

(only factors with eigenvalues > 1 were selected).

To classify soil samples into groups with similar soil fertility characteristics, cluster analysis were carried out according to the method of Ward (Ward, 1963) and Euclidean distance as a measure of similarity. Moreover, discriminant analysis was carried out to verify the representative characteristics of the groups and to understand how a combination of variables can be used to predict S- and I-type granites occurrences and subsequently contribute to soil fertility assessments.

Spatial variability analysis of the essential elements was performed by GIS through the deterministic interpolation techniques - based on the extent of similarity (Inverse Distance Weighted - IDW). All maps were produced using ArcGIS 10.2 software.

3. Results and discussion

3.1. Mineralogy of S- and I-type granites

S-type granites are light grey, slightly foliated granites with fine to medium crystal size. They are mainly composed of quartz, feldspar, biotite and muscovite/sericite evenly distributed (Figure 2a). They do not contain magnetic minerals. The mineralogical composition of S-type granites is as follows: microcline (30%) > quartz (26%) > plagioclase (Albite - 22%) > biotite (12%) > orthoclase (7%) > sericite / muscovite (3%) > opaque minerals (< 1%) > allanite (< 1%) (Figure 2b). Small amounts of biotite are changing composition to chlorite, with small inclusions of radioactive allanite (Figure 2c) that is responsible for the spot formations in biotites. The plagioclases are sericitized usually forming lamellae of muscovite/sericite. K-feldspars are found as microcline (chess-board type and cross-hatch twinning) (Figure 2d) and orthoclase (simple twinning). The presence of flame perthites is a result of albite lamellae exsolution of the K-feldspar (Figure 2e).

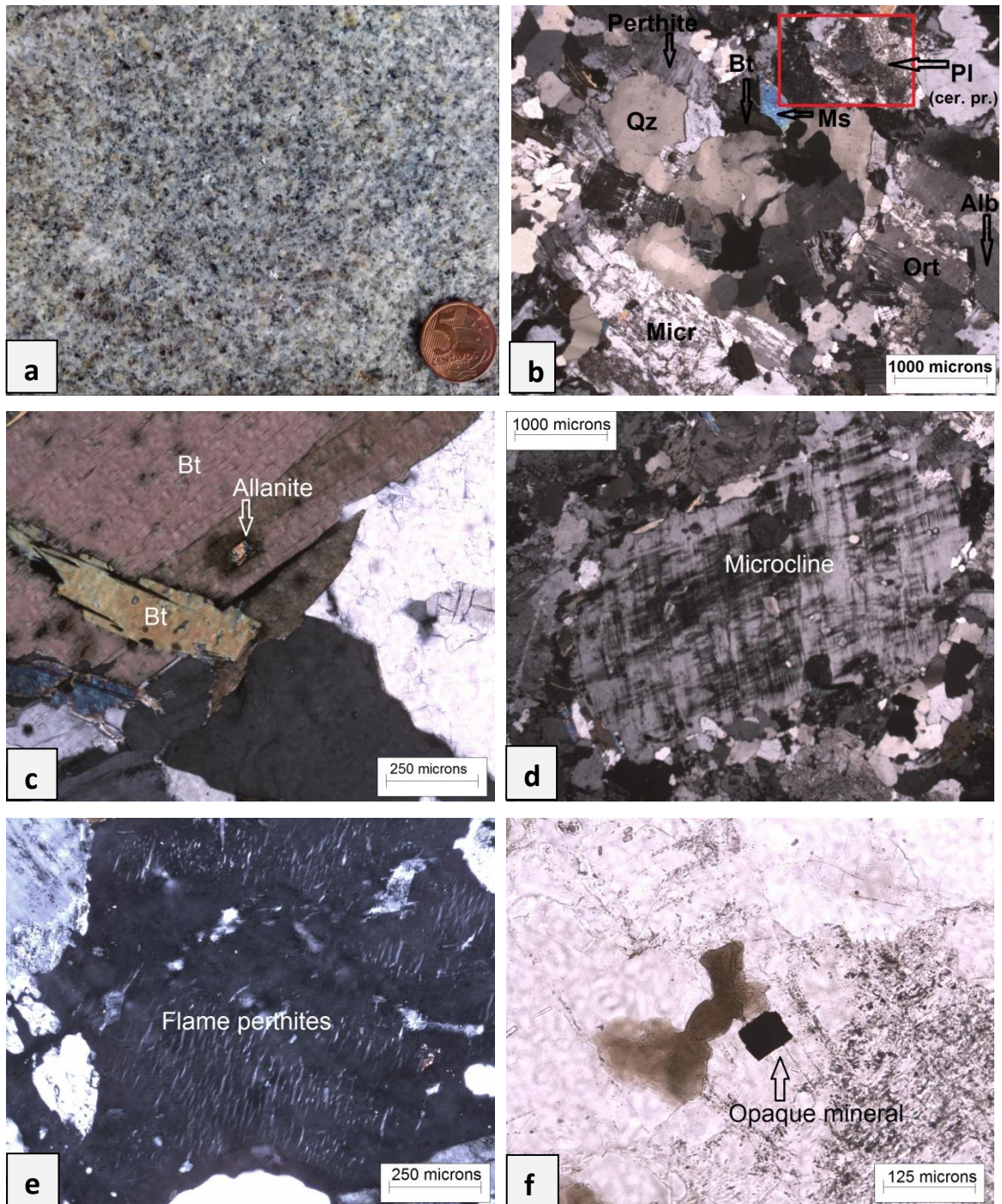
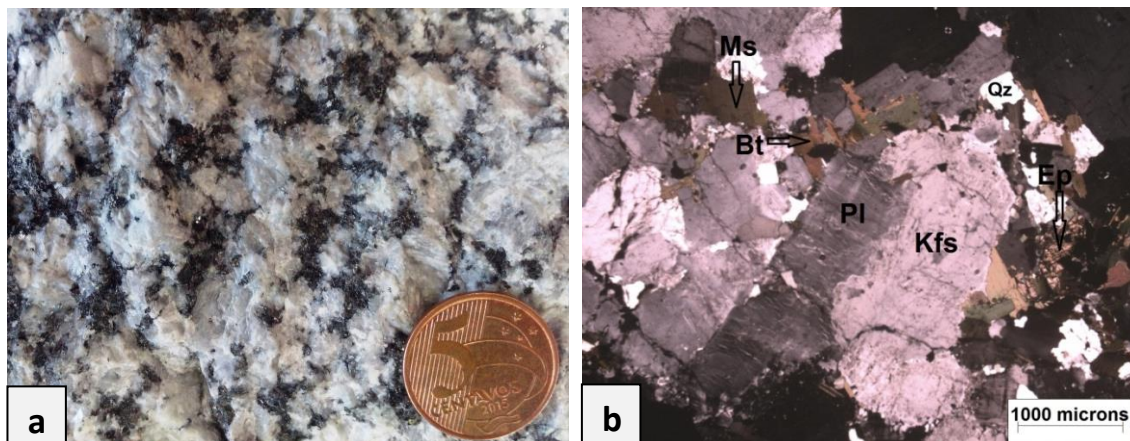


Figure 2. (a) Macrophotograph (b) and microphotographs of a typical S-type granite, (c) inclusion of allanite in biotite, (d) microcline, (e) flame perthites, (f) opaque mineral. Bt – Biotite; Qz – Quartz; Micr – Microcline; Ort – Orthoclase; Pl – Plagioclase; Ms – Muscovite; Alb – Albite.

Field measurements of fresh S-type granites with the hand-held magnetic susceptibility meter reveal only very low magnetic susceptibility ($0.01- 0.02 \times 10^{-3}$ SI).

In contrast to the S-type granites, I-type granites have inequigranular, commonly porphyritic texture, with medium to coarse K-feldspars, small amounts of gray quartz and black mafic minerals, commonly biotite (Figure 2b). I-type granites are slightly magnetic due to magnetic minerals (i.e. magnetite).

The mineralogical composition of I-type granites follows the order: Microcline (55%) > plagioclase (12%) > biotite (11%) > quartz (7%) > amphibole (4%) > opaque minerals (4%) > apatite (2%) > allanite (2%) > titanite (2%) > orthoclase (< 1%) > chlorite (< 1%) (Figure 3b). I-type granites clearly exhibit higher proportions of accessory minerals (Figure 2f) than S-type granites (Figure 3c). Biotites are in the early alteration stage to chlorite. Feldspars are slightly altered to sericites. The K-feldspar crystals occur with cross-twinning, simple twinning and exsolution (perthites). These occur in forms of small lamellae. The phosphate mineral apatite occurs in small crystals and is commonly associated with mafic minerals (Figure 3d). Apatite inclusions are common in biotite of I-type granites (Chappell and White, 2001).



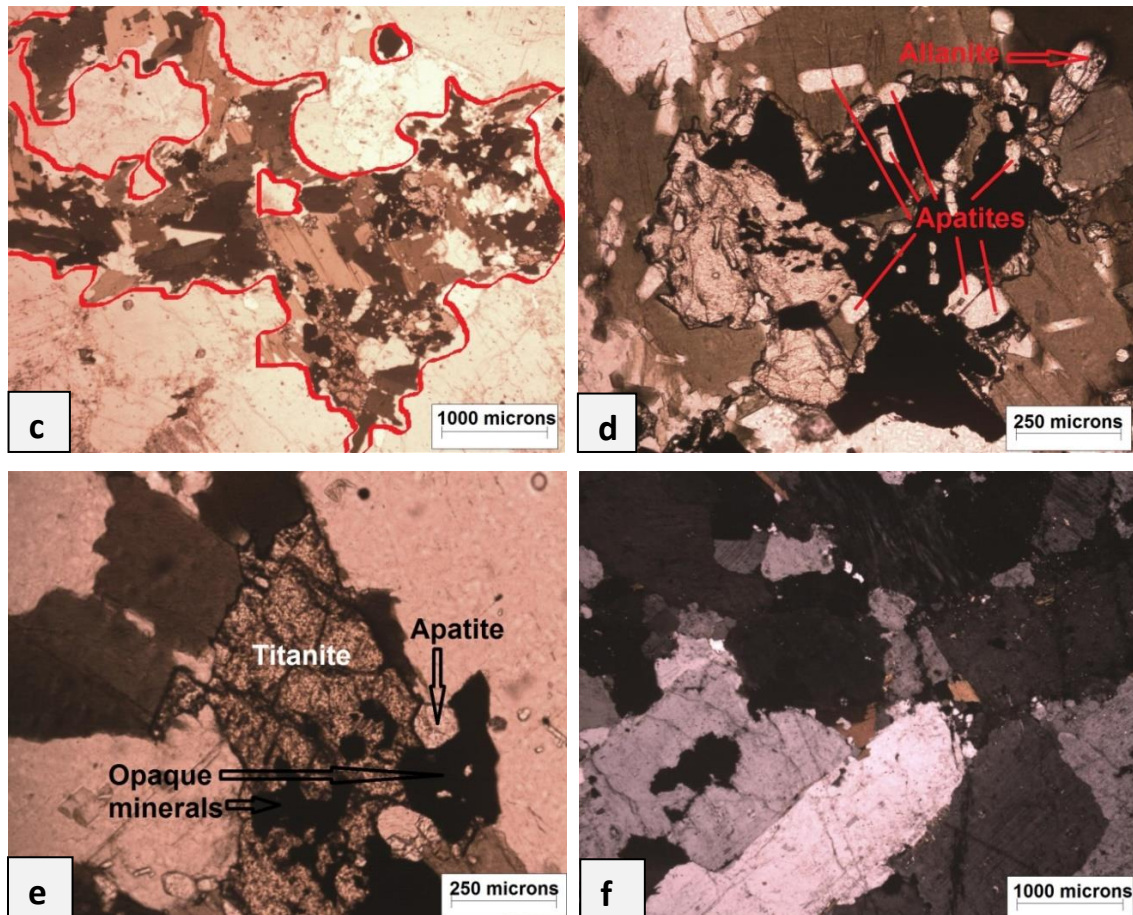


Figure 3. (a) Macro-photograph and (b) Micro-photographs of a typical I-type granite. (c) Mafic phase minerals (d) Apatites associated with mafic minerals. (e) Titanite, apatite and opaque mineral phases, (f) Typical section, overview. Bt – Biotite; Qz – Quartz; Pl – Plagioclase; Ms – Muscovite; Kfs - K-feldspar; Ep - Epidote.

Field measurements of fresh I-type granites with the hand-held magnetic susceptibility meter show elevated magnetic susceptibility ($3-20 \times 10^{-3}$ SI), likely caused by mafic minerals present in this type of granite. The magnetic susceptibility data are consistent with the findings of Ferreira et al. (1998).

3.2. Geochemistry of I- and S-type granites and corresponding topsoils

Differences observed in the mineralogical properties of I- and S-type granites (Figures 2, 3) explain their distinct chemical compositions in rocks and topsoils (Table 1). Chemically, the S-type granite contains large amounts of

SiO₂ (75%), typical for S-types (Chappell and White, 1984). Sodium had a relatively higher concentrations in I-type granites (Na₂O > 3.2%) than in S-type granites (Na₂O < 3.2%). Both granites contain approximately 5% of K₂O in accordance with the chemical properties of both granite types described by Chappell and White (1974).

Table 1. Total chemical composition of I- and S-type granites and topsoils overlying both granite types in sub-humid zone of Pernambuco State, Brazil

	SiO ₂	Al ₂ O ₃	Fe ₂ O ₃	MnO	MgO	CaO	Na ₂ O	K ₂ O	TiO ₂	P ₂ O ₅
	Granites (%)									
I-type	63.59	16.8	5.79	0.06	1.2	2.78	3.64	4.76	1.17	0.47
S-type	75.67	15.0	1.41	0.01	0.4	0.72	2.60	5.50	0.19	0.11
	Topsoils (%)									
I-type	54.08	8.89	1.76	0.02	0.25	0.45	0.31	3.86	1.02	0.11
S-type	71.10	6.22	0.71	0.00	0.06	0.08	0.19	1.60	0.36	0.06

I-type granites exhibited higher CaO, Na₂O, Fe₂O₃, MnO, MgO, P₂O₅ contents compared to S-types. CaO and Na₂O contents in S-types are likely lost in solution when feldspars are weathered to clay minerals (Chappell and White, 2001). The slightly higher K₂O content in S-type granites in comparison to I-type granites is likely related to the incorporation of K into clay minerals during chemical weathering (Chappell and White, 2001). Thus higher K₂O/Na₂O ratio are usually observed in S-type granites. The sum of Na₂O + K₂O + CaO is higher in I-type granites than in S-type granites.

The presence of titanite (Figure 3e) associated with high contents of Fe₂O₃ (Table 2), in I-type granite, suggests that the last crystallization was from a relatively oxidized magma (Guani et al., 2013). The higher CaO, MgO, Fe₂O₃ and MnO contents in I-type granites (Table 1) are related to the larger proportion of accessory minerals, such as apatite, magnetite, zircon and mafic minerals (Figure 4). The P₂O₅ content four times greater in soils developed over I-type granites is explained by the presence of apatite (Figure 4a, spectrum 20). It can be concluded that the geochemistry of the topsoil samples largely reflect the composition of the underlying granite type.

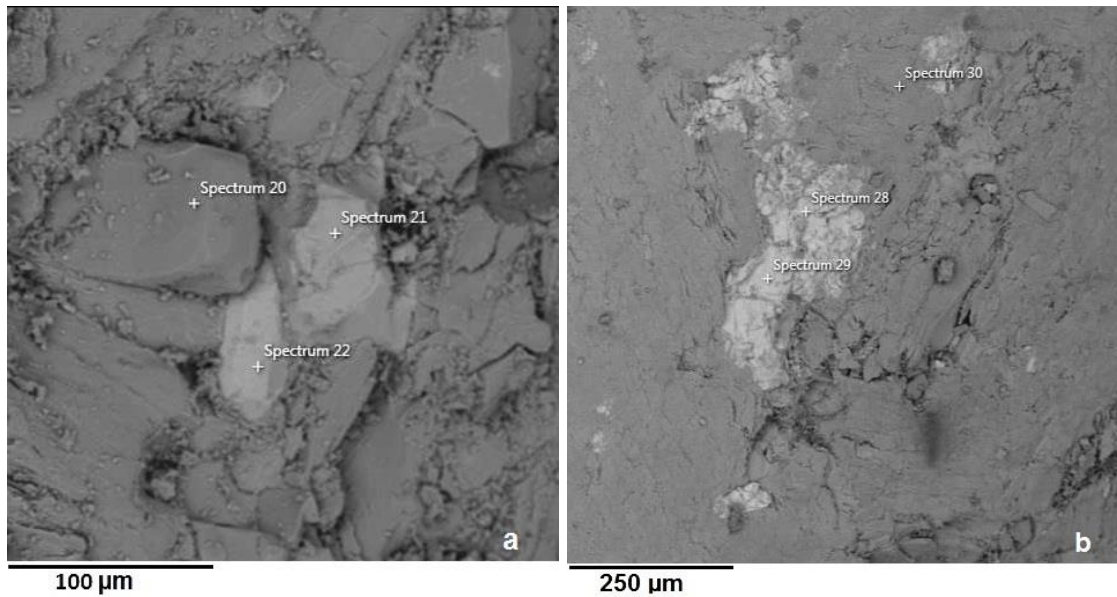


Figure 4. Scanning electron microscope (SEM) image captured from I-type granites and their respective elemental composition by energy dispersive X-ray spectrum (EDS). (a) Chemical composition of apatite (Spectrum 20: Ca – 67%, P – 29%, Fe – 1%, Si – 1%, Al – 1% K – 1%), magnetite (Spectrum 21: Fe – 98%, Si, Al, Ca – 1%), and zircon (Spectrum 22: Zr – 78%, Si – 20%, Fe – 2%). (b) Chemical composition of magnetite: spectrum 28 (Fe – 98%, Si, Al – 1%) and spectrum 29 (Fe – 98%, Si, Al – 1%); and biotite (Spectrum 30 Si – 33%, Fe – 25%, Al – 16%, K – 13%, Mg 11%, Ti – 2%).

In general, the mineralogical assembly of the clay fractions of the topsoils overlying both S- and I- type granites are similar. They are composed of mica, illite, kaolinite and quartz (Figures 5a, 5b). However, there is a clear distinction between two samples in terms of mica. Soils formed over I-type granite exhibited biotite in clay fraction. It was identified by the relative peak intensity at plane 002 (0.5 nm) – much less than half the intensity of the diffraction peak in the plane 001 (1.0 nm), this is characteristic of trioctahedral mica (biotite). On the other hand, soils originated from S-type granites showed muscovite in clay fraction, identified by the half of relative peak intensity at plane 002 (0.5 nm) compared to the intensity of the diffraction peak in the plan 001 (1.0 nm), which is typical of dioctahedral mica (muscovite) (Moore and Reynolds, 1997). These results are very well related to the mineralogical composition of each granite (Figures 2, 3), as well as to the lithology and sub-humid climate conditions

where these soils are being formed.

Kaolinite occurs at 0.71 and 0.35 nm spacings in the reflections 001 and 002. In addition, the absence of the kaolinite peak when subjected to heat treatment of 550° C confirms the presence of this clay mineral. Quartz occurs at 0.42 and 0.33 nm in 001 reflection, while the peaks of 1.01 and 0.5 nm, persistent across all treatments, are characteristic of illite.

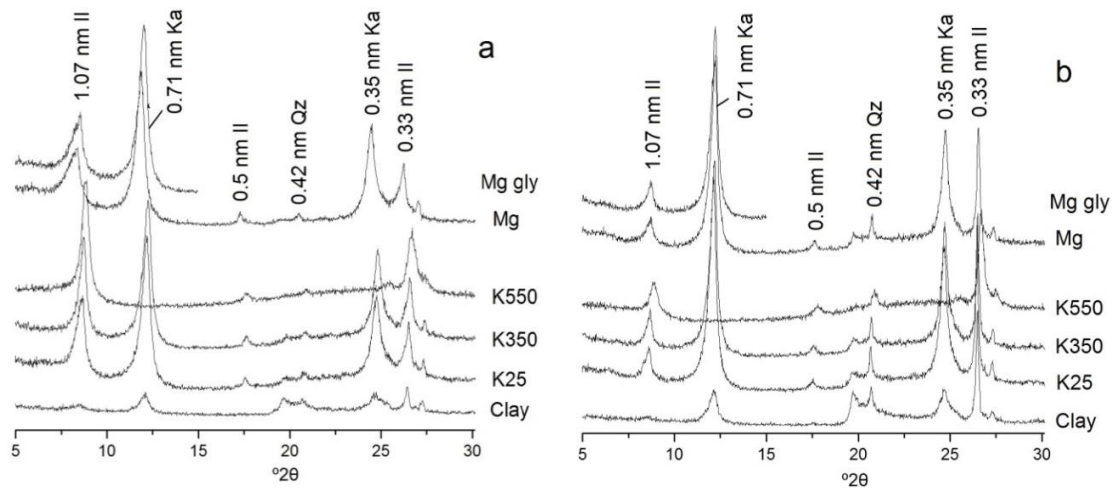


Figure 5. Representative X-ray diffraction patterns (Cu K α -radiation) obtained from the two soil types: (a) Topsoil derived from I-type granite, (b) Topsoil derived from S-type granite. Il: illite; Ka: kaolinite. Qz: quartz; Mg gly: Mg glyconated.

3.3. Physico-chemical properties and soil fertility

In the study area, the particle size distribution in soils reflects the underlying granite composition. Soils originated from S-type granites showed the highest concentration of sand size particles, ranging from 78 to 89% and 76 to 87% for surface (0-20 cm) and subsurface (20-40 cm) horizons, respectively. Conversely, soils derived from I-type granites exhibited higher silt contents, ranging from 24 to 35% and 25 to 32% for surface (0-20 cm) and subsurface (20-40 cm) horizons, respectively (Table 2).

Clay contents were slightly greater in soils developed from I-type granites. These results can be explained by contrasting mineral composition of the parent rocks. Thus, the higher percentages of weathering resistant minerals in

the S-type granites (i.e. quartz and muscovite) have likely hindered higher weathering rates. In contrast, the higher proportion of easily weatherable minerals in I-type granites favored the genesis of soils with higher silt and clay contents.

In terms of the soil pH, soils formed from I-type granites exhibited lower acidity (pH 5.2), higher base saturation (BS > 50%), lower Al saturation values (< 50%) and higher CEC ($5.2 \text{ cmol}_c \text{ kg}^{-1}$) than soils developed over S-type granites. As expected, the organic matter contents were always higher in surface horizons (Table 2).

The higher organic matter accumulation in soils derived from I-type granites than those developed from S-types are probably related to the larger surface area in soils developed over I-type granites, which promote higher stabilization of soil organic carbon than sandy soils, forming stable organo-mineral complexes (Six et al. 2002). In addition, the higher CEC in soils over I-type granites would also favor a more intimate interaction between the organic and mineral fractions and, thus, further promote soil carbon protection (Lehmann and Kleber, 2015). Thus, soil developed from I-type granites can play a more important role in ecosystems services such as agriculture production, carbon sequestration and mitigation of soil degradation than soils originating from S-types granites.

The soil analyses showed that most nutrient element concentrations in soils overlying I-type granites are higher than in soils overlying S-type granites. These results can be explained by the higher proportions of mafic, opaque and accessory minerals that, upon weathering, would release more nutrients for plants. The greatest difference in extractable concentrations of nutrient elements in I-type granites compared to S-type granites are found in the following order: $\text{Co} > \text{Ni} > \text{Ca} > \text{P} > \text{Mg} > \text{Mn} > \text{Fe} > \text{K} > \text{Zn} > \text{Cu} > \text{Al} > \text{Mo} > \text{Na}$ (Table 2). Differences observed in the mineralogical and geochemical properties of I- and S-type granites (Figures 2, 3) explain their distinct soil fertility differences. Imbalances among Ca and Mg (low Ca/Mg ratio) in both soil types may lead to Ca deficiencies. Liming materials (calcite – CaCO_3) can be used to reverse this trend on agricultural land (Van Straaten, 2007).

Despite being moderately acidic and show low water retention capacity, regosols are widely used for crop production owing to its favorable topographic conditions (gently sloping sites) and easy management in this region (Brazil, 2000). The major agricultural uses of these soils are corn, beans, palm, cassava and cotton productions (Brazil, 2000). Our results have wide application to improve the soil management for these crops.

Using the criteria for soil fertilizer recommendations for the State of Pernambuco (IPA, 2008), the inherent natural soil fertility of the regosols developed from S-type granites is very low. In contrast, those for regosols derived from I-type granites are moderate. The results of the soil analyses over different granite parent materials have practical management implications. Soils derived from S-type granites need to receive large amounts of mineral fertilizers to support crop development and management, while soils derived from I-type granites need only modest fertilizer inputs. For instance, soils developed from S-types are recommended to receive 60 kg ha^{-1} of P in order to grow beans and corn, the most cultivated crops in this region. On the other hand, soils derived from I-type granites demand less than a half of that rate to cultivate the same crops. In addition, liming requirement for soils derived from S-type granites should be twofold higher than those originating from I-type granites (IPA, 2008).

These results can be used to develop general fertilizer recommendations making better use of fertilizer-based nutrient resources not only to the study area but also to soils worldwide developed under similar geological backgrounds, such as Australia (Chappell et al. 2012; Foden et al. 2015), China (Zhao et al. 2008; Guan et al. 2014), Saudi Arabia (Robinson et al. 2015), Spain (Canosa et al. 2012), Brazil (Almeida et al. 2007), so long as all other soil-forming factors are also considered.

Table 2. Mean, maximum and minimum nutrient concentrations, and standard deviation of selected chemical and physical characteristics of soils derived from I- and S-type granites in sub-humid zone of Pernambuco, Brazil

	Depth (cm)	I-type granite				S-type granite			
		Mean	Max ^a	Min ^b	Stand Dev ^c	Mean	Max	Min	Stand Dev
----- mg kg ⁻¹ -----									
pH (H ₂ O)	0-20	5.2	6.0	4.0	0.5	4.9	5.0	4.0	0.6
	20-40	5.2	6.0	4.0	0.5	4.9	5.0	4.0	0.2
Ca (cmolc kg ⁻¹)	0-20	0.3	0.5	0.1	0.1	0.1	0.1	0.0	0.0
	20-40	0.2	0.5	0.1	0.1	0.1	0.1	0.0	0.0
Mg (cmolc kg ⁻¹)	0-20	1.4	4.3	0.5	0.8	0.3	0.7	0.1	0.2
	20-40	1.7	4.7	0.5	1.0	0.3	0.7	0.1	0.0
K (cmolc kg ⁻¹)	0-20	0.2	0.4	0.1	0.1	0.1	0.2	0.0	0.0
	20-40	0.2	0.6	0.07	0.1	0.1	0.2	0.0	0.0
P (mg kg ⁻¹)	0-20	14.6	68	0.8	10	2.9	9.7	0.8	1.7
	20-40	19.5	84	1.4	17	3.0	5.0	0.9	1.3
Na (cmolc kg ⁻¹)	0-20	0.4	1.1	0.2	0.1	0.4	0.7	0.2	0.1
	20-40	0.4	1.0	0.2	0.2	0.4	0.7	0.2	0.1
Al (cmolc kg ⁻¹)	0-20	0.5	1.0	0.0	0.3	0.4	0.8	0.0	0.2
	20-40	0.5	1.4	0.1	0.3	0.4	0.7	0.0	0.2
Fe (mg kg ⁻¹)	0-20	83	217	15	6.7	42	124	7.5	20
	20-40	71	145	11	44	37	70	7.7	14
Mn (mg kg ⁻¹)	0-20	11	34	2.2	5.3	3.2	8.8	0.7	1.9
	20-40	10	21	1.8	4.3	4.1	8.8	1.2	2.4
Zn (mg kg ⁻¹)	0-20	1.6	2.8	0.9	0.5	1.0	1.9	0.7	0.3
	20-40	1.6	2.0	1.1	0.3	1.0	1.6	0.6	0.2
Cu (mg kg ⁻¹)	0-20	0.2	0.5	0.0	0.1	0.1	0.6	0.0	0.1
	20-40	0.2	0.4	0.0	0.1	0.1	0.6	0.1	0.1
Ni (mg kg ⁻¹)	0-20	0.2	0.6	0.1	0.1	0.04	0.2	0.0	0.0
	20-40	0.3	0.6	0.1	0.1	0.04	0.2	0.0	0.02
Co (mg kg ⁻¹)	0-20	0.2	0.5	0.0	0.1	0.01	0.1	0.0	0.0
	20-40	0.2	0.6	0.0	0.1	0.01	0.1	0.0	0.02
Mo (mg kg ⁻¹)	0-20	0.01	0.01	0.0	0.0	0.0	0.0	0.0	0.0
	20-40	0.01	0.02	0.0	0.01	0.0	0.0	0.0	0.0
CEC ^d (cmolc kg ⁻¹)	0-20	5.2	9.5	2.7	1.9	2.6	4.4	1.3	0.5
	20-40	4.2	8.8	2.6	0.8	2.9	4.2	1.2	0.4
BS ^e (%)	0-20	54	68	42	5.4	37	41	21	6.6
	20-40	58	71	44	6.5	32	39	22	5.7
Al sat ^f (%)	0-20	19	53	0.0	14	33	81	0.0	19
	20-40	23	61	1.5	12	34	77	0.0	17
TOC ^g (g kg ⁻¹)	0-20	23.7	48.7	9.4	9.8	5.8	8.7	2.1	0.9
	20-40	5.4	21.2	3.5	8.5	3.3	6.9	1.7	0.8
Clay (g kg ⁻¹)	0-20	60	110	30	8.1	50	80	30	11.5
	20-40	70	130	40	7.4	60	90	30	10.3
Silt (g kg ⁻¹)	0-20	284	315	241	18.1	95	137	72	22
	20-40	277	328	253	20.6	126	142	94	24.7

Sand	0-20	656	737	575	23.7	855	898	783	26.4
(g kg ⁻¹)	20-40	653	719	542	21.1	814	876	768	23.3

^a Maximum; ^b Minimum; ^c Standard deviation; ^d Cation Exchange capacity; ^e Base saturation; ^f Aluminum saturation; ^g Total organic carbon.

In order to provide further information regarding the fertility status of granite-derived soils, multivariate statistical techniques (PCA, CA and DA) and a GIS approach were used. Due to the high similarity of soil fertility values between the two depths, only the data from the topsoil horizon were used.

3.4. Multivariate statistical analyses

Using PCA we select the key variables that explain the differences in soil fertility according to the granite type. The selection was carried out based on strong positive correlation among the variables and their multivariate normal distribution. Variables with poor correlations were eliminated. Following the criteria of eigenvalues greater than 1, two independent extracted factors explained 81% of the total variance among soils over granites of different compositions. Both factors show that Mg, Ca, Ni, Co, P, Zn, and Mn are best suited to differentiate between the soil fertilities derived from the underlying I- and S-type granites.

The first PC (eigenvalue = 4.7) was responsible for 68% of the total variance between the two soils over different types of granites and was best represented by Mg (0.83), Ca (0.68), Ni (0.67), Co (0.65) and P (0.57). In addition, 12.9% of the total variance was explained by PC 2 (eigenvalue = 1.04) with Zn (0.77) and Mn (0.69) providing the most contributions. These components allow for distinguishing the soil fertility owing to the higher proportion of accessory minerals found in I-type granite.

The results of cluster analysis confirmed those of PCA (Figure 6). Cluster 1 and 2 were entirely formed by soils developed over I- and S-type granites, respectively; cluster 3 comprises soils predominantly derived from I-type granites, excepted for two soil samples derived from S-type granites. Cluster 1 and 3 showed higher Mg, Ca, Ni, Co, P, Zn, and Mn concentrations in comparison to cluster 2. This finding was also supported by the petrography and geochemistry of the two types of granites – a greater presence of

accessory minerals in the I-type granite (Figures 3c, d, e) and higher concentrations of nutrient elements in their chemical composition (Table 1).

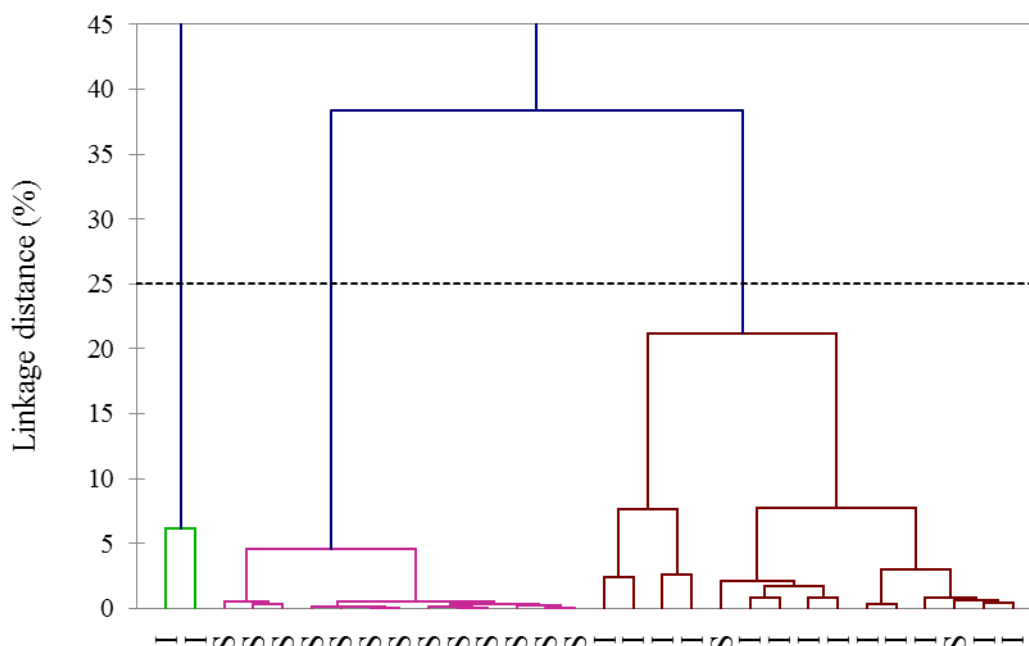


Figure 6. Cluster analyses of soils derived from I- and S-type granites in similar climatic zone of Pernambuco State, Northeast Brazil.

The use of combined tools provide a greater insight to discriminate soils developed from different granites. To confirm the misclassification of two soil samples, we used the additional technique of discriminant analysis (Figure 7) that showed no reclassification error for cluster 1 and 2 (left to right from Figure 6), but 15% for the cluster 3 (i.e. two samples). The statistically significant results also show a high percentage of correct classification, ranging from 85% to 100%. The Wilks' lambda statistics confirm that the differences among the soils overlying different granite types is significant at $P = 0.05$. In fact, both misclassified samples were located at transition zone between the I- and S-type granites; also these samples are far from their centroid (group mean) in group B, showing the dimensions along which both samples may differ in relation to soils derived from I-type granites (Figure 7).

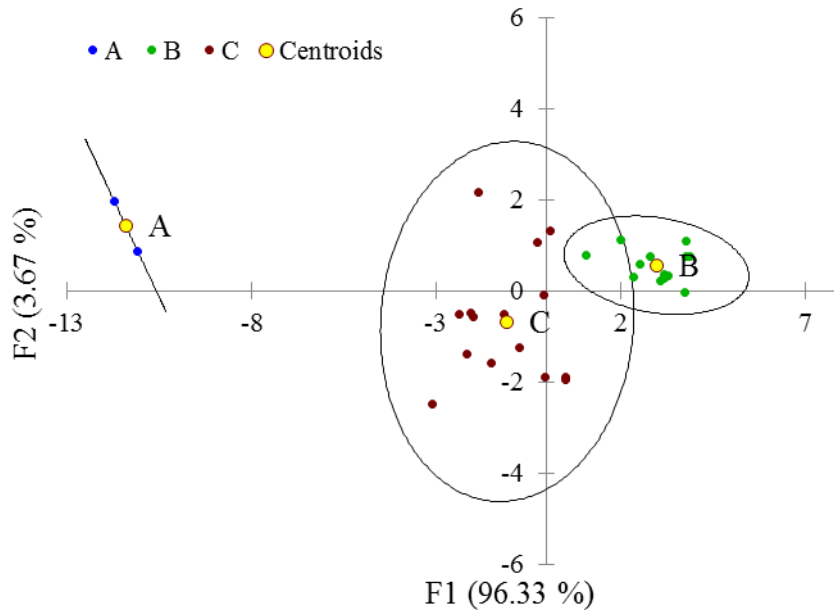


Figure 7. Discriminant analysis of the groups formed in cluster analysis.

The following canonical discriminant functions: $D1 = -0.082Ca + 0.54Mg + 0.36P - 0.31Mn - 0.83Co - 0.92Ni - 0.74Zn$ and $D2 = -0.99Ca + 0.35Mg - 1.03P - 0.01Mn + 1.63Co - 0.62Ni - 0.22Zn$ can be used to discriminate other soils derived from I- and S-type granites within the same region or under similar encountered conditions. The first function provides the best discrimination between soils derived from I- and S-type granites (96%). These methods show that both discriminant functions can correctly classify soils derived from I- and S-type granites.

3.5. Spatial distribution patterns of soil fertility

The GIS mapping technique was used to outline the spatial distribution of seven essential elements (Mg, Ca, Ni, Co, P, Zn, and Mn) previously selected by PCA. To develop element distribution patterns, the spatial interpolation method of inverse distance weighted (IDW) was applied with 12 neighbouring samples used to estimate each grid point. Appropriate spatial patterns for all elements were obtained (Figure 8). All elements showed much higher concentrations of nutrient elements in soils derived from the I-type granites than soils underlain by S-type granites. Thus, the spatial distribution maps of soil fertility, based on I-

and S-type granites, are important tools for agricultural management decisions, such as delineating soil zones that are suitable for specific crop nutritional requirements.

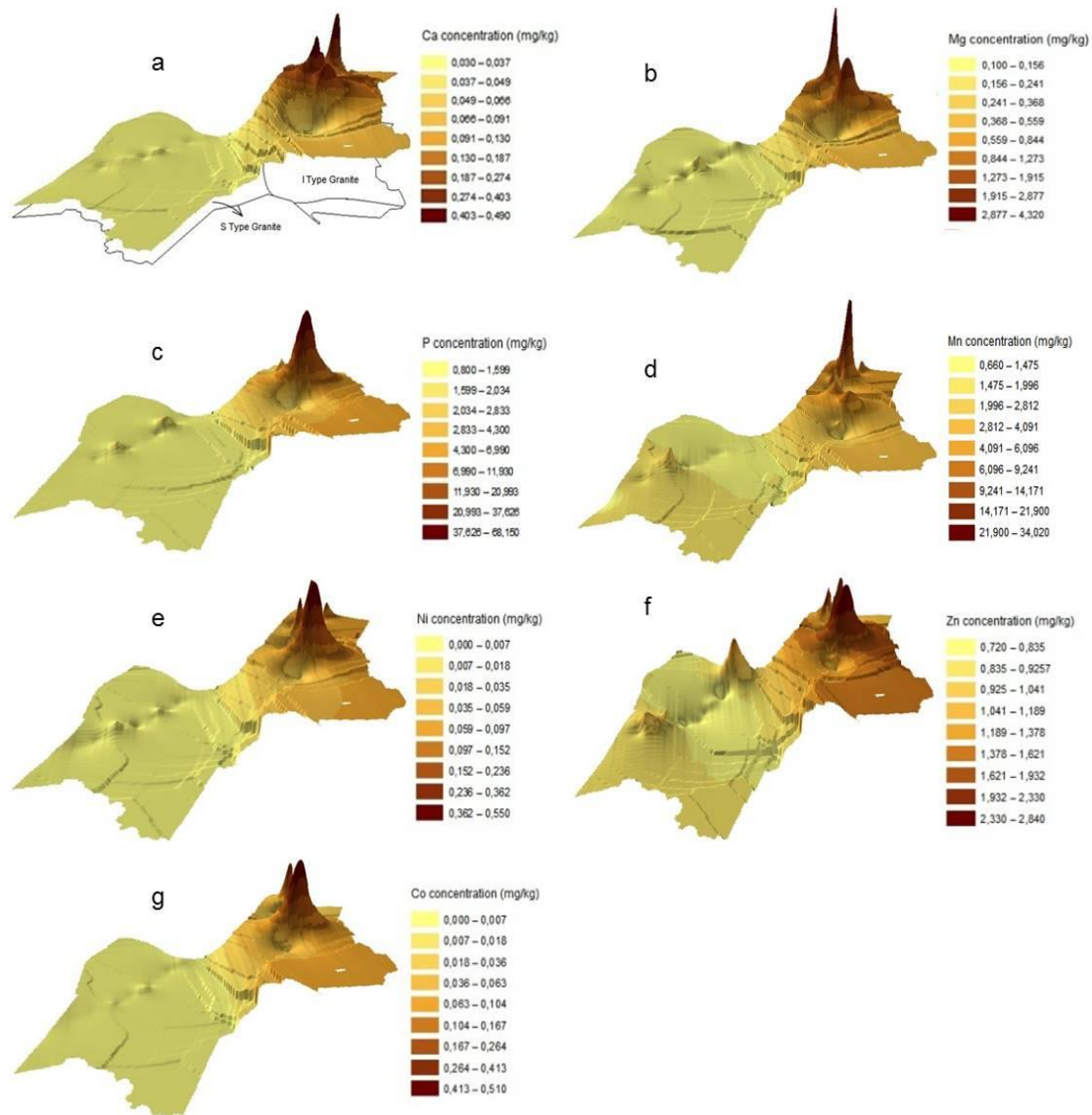


Figure 8. Digital Terrain Model for available contents of Ca (a), Mg (b), P (c), Mn (d), Ni (f) and Co (g) in soils derived from I- and S-type granites in similar climatic zone of Pernambuco State., Northeast Brazil.

4. Conclusions

The mineralogy and chemistry of two different granitic parent materials have a profound effect on soil fertility. S-type and I-type granites have different mineralogical compositions whereby S-type granites have higher concentrations of silica and I-type granites contain larger concentration of mafic and accessory minerals, mainly amphibole and apatite. The chemical composition of the two granites reflects their different respective mineralogical compositions. Geophysical field measurements of the two different granites show different magnetic susceptibilities, whereby I-type granites have substantial higher magnetic properties than S-type granites. Soil fertility analyses showed that soils derived from these two types of granites exhibit different soil fertilities. Soils overlying I-type granites showed higher natural fertility than soils derived from S-type granites. According to the Soil Fertilizer Recommendations for the State of Pernambuco, the inherent natural soil fertility of the soils developed from S-type granites is very low. In contrast, those for soils derived from I-type granites have moderate soil fertility status. Principal Component Analyses identified Ca, Mg, P, Mn, Zn, Co and Ni as key variables to discriminate soils derived from I- and S-type granites. The application of principal component, cluster and discriminant analysis (95% accuracy) were effective tools to discriminate soils developed from different granites. Spatial distribution maps are suitable soil fertility management tools to guide and support soil fertility management decisions for improved soil and crop specific fertilization. These findings have wider implications in large parts of the tropics (S-America, sub-Saharan Africa, India, SE and East Asia, Australia) which are underlain by igneous and metamorphic rock types including S- and I-type granites and where effective management tools are needed to increase nutrient use efficiencies for increased productivity of food, fodder and energy crops.

5. References

- Almeida, M.E., Macambira, M.J.B., Oliveira, E.C., 2007. Geochemistry and zircon geochronology of the I-type high-K calc-alkaline and S-type granitoid rocks from southeastern Roraima, Brazil: Orosirian collisional magmatism evidence (1.97–1.96 Ga) in central portion of Guyana Shield. *Precam. Res.* 155, 69–97.
- Antunes, I.M.H.R., Neiva, A.M.R., Silva, M.M.V.G., Corfu, F., 2008. Geochemistry of S-type granitic rocks from the reversely zoned Castelo Branco pluton (central Portugal). *Lithos* 103, 445–465.
- Antunes, I.M.H.R., Neiva, A.M.R., Silva, M.M.V.G., Corfu F., 2009. The genesis of I- and S-type granitoid rocks of the Early Ordovician Oledo pluton, Central Iberian Zone (central Portugal). *Lithos* 111, 168–185.
- Araújo Filho, J.C, Burgos, N., Lopes, O.F., Silva, F.H.B.B., Medeiros, L.A.R., Melo Filho, H.F.R. et al., 2000. Levantamento de reconhecimento de baixa e média intensidade dos solos do Estado de Pernambuco. Rio de Janeiro: Embrapa Solos p. 53-54. (Embrapa Solos, Boletim de Pesquisa; 11).
- Brazil., 2000. Ministry of Agriculture. Recognition Survey of low and medium intensity of soils from Pernambuco State. Research Bulletin. n. 11. (In Portuguese).
- Brazil. Ministério de Minas e Energia. Geologia e recursos minerais do Estado de Pernambuco. Serviço Geológico do Brasil e do Estado de Pernambuco, Recife, CPRM, 2001.
- Brown, G., Brindley, G.W., 1980. X-ray Diffraction procedures for clay mineral identification. In: Brindley, G.W., Brown, G. London: Mineralogical Society 5, 305-360.
- Canosa, F., Izard, A.M., Fuente, M.F., 2012. Evolved granitic systems as a source of rare-element deposits: The Ponte Segade case (Galicia, NW Spain). *Lithos* 153, 165–176.

Chappell, B.W., White, A.J.R., 1974. Two contrasting granite types. *Pacific Geology* 8, 173–174.

Chappell, B.W., White, A.J.R., 1984. I- and S- type granites in the Lachlan Fold Belt, southeastern Australia. In: Keqin, Xu., Guangchi, Tu. (Eds.). *Geology of Granites and their Metallogenic Relation*: Beijing Science Press. pp.87–101.

Chappell, B.W., White, A.J.R., 2001. Two contrasting granite types: 25 years later. *Australian J. Earth Sci.* 48, 489–499.

Chappell, B.W., Bryant, C.J., Wyborn, D., 2012. Peraluminous I-type granites. *Lithos* 153, 142–153.

Chen, T., Liu, X.M., Zhu, M.Z., Zhao, K.L., Wu, J.J., Xu, J.M., Huang, P.M., 2008. Identification of trace element sources and associated risk assessment in vegetable soils of the urban-rural transitional area of Hangzhou, China. *Environ. Pollut.* 15, 67–78.

Clemens, J.D., 2003. S-type granitic magmas – petrogenetic issues, models and evidence. *Earth Sci. Rev.* 61, 1–18.

Cruz, R.F., Pimentel, M.M., Accioly, A.C.A., Rodrigues, J.B., 2014. Geological and isotopic characteristics of granites from the Western Pernambuco-Alagoas Domain: implications for the crustal evolution of the Neoproterozoic Borborema Province. *Braz. J. Geol.* 44 (4), 627-652.

Da Silva Filho, A.F., Guimarães, I.P., Van Schmus, W.R., Armstrong, R.A., Rangel da Silva, J.M., Osako, L.S., Cocentino, L.M., 2014. Shrimp U–Pb zircon geochronology and Nd signatures of supracrustal sequences and orthogneisses constrain the Neoproterozoic evolution of the Pernambuco–Alagoas domain, southern part of Borborema Province, NE Brazil. *Int. J. Earth Sci.* 103, 2155–2190.

Facchinelli, A., Sacchi, E., and L. Mallen., 2001. Multivariate statistical and GISbased approach to identify heavy metal sources in soils. *Environ. Pollut.* 114, 313-324.

Ferreira, V.P., Sial, A.N., Sá, E.F.J., 1998. Geochemical and isotopic signatures of Proterozoic granitoids in terranes of the Borborema structural province, northeastern Brazil. *J. South Am. Earth Sci.* 5, 439-455.

Foden, J., Sossi, P.A., WAWRYK, C.M., 2015. Fe isotopes and the contrasting petrogenesis of A-, I- and S-type granite. *Lithos* 212-215, 32-44.

Franco-Uria, A., Lopez-Mateo, C., Roca, E., Fernandez- Marcos, M.L., 2009. Source identification of heavy metals in pastureland by multivariate analysis in NW Spain. *J. Hazard Mater.* 165, 1008–1015.

Gee, G.W., OR, D., 2002. Particle size analysis. In: DANE, J.H.; TOPP, C.T. *Methods of soil analysis: physical methods*. Cap II, p.255-289, SSSA, Madison, 866p.

Gieler, A., Rybicka, E.H., Moller, S., Einax, J.W., 2012. Multivariate analysis of sediment data from the upper and middle Odra River (Poland). *Appl. Geochem.* 27, 1540–1545.

Guan, Y., Yuan, C., Sun, M., Wilde, S., Long, X., Huang, X., Wang, Q., 2014. I-type granitoids in the eastern Yangtze Block: implications for the Early Paleozoic intracontinental orogeny in South China. *Lithos* 206-207, 34-51.

Guani, A.A., Searle, M., Robb, L., Chung, S.L., 2013. Transitional I S type characteristic in the Main Range Granite. Peninsular Malaysia. *J. Asian Earth Sci.* 76, 225-240.

Instituto Agronômico de Pernambuco - IPA., 2008. Fertilizer recommendations for Pernambuco State: 2nd approach, 3.ed. revised – Recife, 212p. (In Portuguese).

IUSS Working Group WRB., 2014. World Reference Base for Soil Resources 2014. World Soil Resources Report No. 106, FAO, Rome.

Jackson, M.L., 1975. *Soil chemical analysis: advanced course*. 29.ed. Madison, University of Wisconsin, 895p.

Jenny, H., 1941. Factors of soil formation: A system of quantitative pedology. McGraw-Hill, New York.

Kaiser, H.F., 1958. The Varimax criterion for analytic rotation in factor analysis. *Psychometrika* 23, 187–200.

Koppen, W.P., 1931. *Grundriss der Klimakunde*. 2nd ed. Berlin: Walter de Gruyter. 388p.

Lehmann, J., Kleber, M., 2015. The contentious nature of soil organic matter. *Nature* 528(7580), 60-68.

Li, J.L., He, M., Han, W., Gu, Y.F., 2009. Analysis and assessment on heavy metal sources in the costal soils developed from alluvial deposits using multivariate statistical methods. *J. Hazard Mater.* 164, 976–981.

Li, X.D., Lee, S.L., Wong, S.C., Shi, W.Z., Thornton, I., 2004. The study of metal contamination in urban soils of Hong Kong using a GIS-based approach. *Environ. Pollut.* 129, 113-124.

Litvinovsky, B.A., Jahn, B.M., Eyal, M., 2015. Mantle-derived sources of syenites from the A-type igneous suites — New approach to the provenance of alkaline silicic magmas. *Lithos* 232, 242–265.

Manta, D.S., Angelone, M., Bellanca, A., Neri, R., Sprovieria, M., 2002. Heavy metals in urban soils: a case study from the city of Palermo (Sicily), Italy. *Sci. Total Environ.* 300 (1-3), 229-243.

Micó, C., Recatalá, L., Peris, M., Sánchez, J., 2006. Assessing heavy metal sources in agricultural soils of an european mediterranean area by multivariate analysis. *Chemosphere* 65, 863–872.

Moore, D.M., Reynolds, R.C., 1997. Identification of mixed-layered clay minerals. X-Ray diffraction and the identification and analysis of clay minerals. Ed.2. New York: Oxford University Press, 378p.

Murphy, C.P., 1986. Thin section preparation of soils and sediments. Berkhamsterd: Academic Publis. 145p.

Robinson, F.A., Foden, J.D., Collins, A.S., 2015. Geochemical and isotopic constraints on island arc, synorogenic, post-orogenic and anorogenic granitoids in the Arabian Shield, Saudi Arabia. *Lithos* 220 (223), 97–115.

Santos, E.J., Medeiros, V.C., 1999. Constraints from granitic plutonism on proterozoic crustal growth of the transverse zone, Borborema Province, NE Brazil. *Revista Brasileira de Geociências* 29, 73-84.

Silva, Y.J.A.B., Nascimento, C.W.A., Cantalice, J.R.B., Silva, Y.J.A.B., Cruz, C.M.C.A., 2015. Watershed-scale assessment of background concentrations and guidance values for heavy metals in soils from a semiarid and coastal zone of Brazil. *Environ. Monit. Assess.* 187,558-568.

Six, J., Conant, R.T., Paul, E.A., Paustian, K., 2002. Stabilization mechanisms of organic matter: implications for C-saturation of soils. *Plant Soil* 241, 155–176.

Souza, F.P., Ferreira, T.O., Mendonça, E.S., Romero, R.E., Oliveira, J.G.B., 2012. Carbon and nitrogen in degraded Brazilian semiarid soils undergoing desertification. *Agr. Ecosyst. Environ.* 148, 11–21.

Sun, C., Liu, J., Wang, Y., Sun, L., Yu, H., 2013. Multivariate and geostatistical analyses of the spatial distribution and sources of heavy metals in agricultural soil in Dehui, Northeast China. *Chemosphere* 92 (5), 517-23.

Templ, M., Filzmoser, P., Reimann, C., 2008. Cluster analysis applied to regional geochemical data: Problems and possibilities. *Appl. Geochem.* 23, 2198–2213.

Thuong, N.T., Yoneda, M., Ikegami, Takakura, M., 2013. Source discrimination of heavy metals in sediment and water of to lich river in hanoi city using multivariate statistical approaches. *Environ. Monit. Assess.* 185, 8065–8075.

Van Schmus, W.R., Oliveira, E.P., da Silva Filho, A.F., Toteu, S.F., Penaye J. Guimarães, I.P., 2008. Proterozoic links between the Borborema Province, NE Brazil, and the Central African Fold Belt. *Geological Society*, London, Special Publications 294, 69-99.

Van Straaten, P., 2007. *Agrogeology: The use of rocks for crops*. Enviroquest, Cambridge, Ontario, Canada, 426p.

Varol, M., 2011. Assessment of heavy metal contamination in sediments of the Tigris River (Turkey) using pollution indices and multivariate statistical techniques. *J. Hazard Mater.* 195, 355–364.

Vilalva, F.C.J., Vlach, S.R.F., Simonetti, A., 2016. Chemical and O-isotope compositions of amphiboles and clinopyroxenes from A-type granites of the Papanduva Pluton, South Brazil: Insights into late- to post-magmatic evolution of peralkaline systems. *Chem. Geol.* 420, 186–199.

Wang, X.S., Hu, R.Z., Bi, X.W., Leng, C.B., Panl, C., Zhu, J.J., Chen, Y.W., 2014. Petrogenesis of Late Cretaceous I-type granites in the southern Yidun Terrane: New constraints on the Late Mesozoic tectonic evolution of the eastern Tibetan Plateau. *Lithos* 208-209, 202-219.

Wang, Z., Wang, J., Deng, Q., Du, Q., Zhou, X., Yang, F., Liu, H., 2015. Paleoproterozoic I-type granites and their implications for the Yangtze block position in the Columbia supercontinent: Evidence from the Lengshui Complex, South China. *Precam. Res.* 263, 157-173.

Ward, J.H., 1963. Hierarchical grouping to optimize an objective function. *Journal of the American Statistical Association* 58, 236-244.

Whittig, L.D., Allardice, W.R., 1986. X-ray diffraction techniques. In: Klute, A. (Ed.), *Methods of Soil Analysis — Part I. Physical and Mineralogical Methods*. Soil Science Society of America, Madison, WI, pp. 331–362.

Yeomans, J.C., Bremmer, J.M., 1988. A rapid and precise method for routine determination of organic carbon in soil. *Commun. Soil Sci. Plan.* 19, 1467-1476.

Zhao, X.F., Zhou, M.F., Li, J.W., Wu, F.Y., 2008. Association of Neoproterozoic A- and I-type granites in South China: Implications for generation of A-type granites in a subduction-related environment. *Chem. Geol.* 257, 1–15.

